

INFORMATION TO USERS

This manuscript has been reproduced from the microfilm master. UMI films the text directly from the original or copy submitted. Thus, some thesis and dissertation copies are in typewriter face, while others may be from any type of computer printer.

The quality of this reproduction is dependent upon the quality of the copy submitted. Broken or indistinct print, colored or poor quality illustrations and photographs, print bleedthrough, substandard margins, and improper alignment can adversely affect reproduction.

In the unlikely event that the author did not send UMI a complete manuscript and there are missing pages, these will be noted. Also, if unauthorized copyright material had to be removed, a note will indicate the deletion.

Oversize materials (e.g., maps, drawings, charts) are reproduced by sectioning the original, beginning at the upper left-hand corner and continuing from left to right in equal sections with small overlaps. Each original is also photographed in one exposure and is included in reduced form at the back of the book.

Photographs included in the original manuscript have been reproduced xerographically in this copy. Higher quality 6" x 9" black and white photographic prints are available for any photographs or illustrations appearing in this copy for an additional charge. Contact UMI directly to order.

UMI

A Bell & Howell Information Company
300 North Zeeb Road, Ann Arbor, MI 48106-1346 USA
313/761-4700 800/521-0600

**DEVELOPMENT OF FOURIER SERIES AND ARTIFICIAL NEURAL
NETWORK APPROACHES TO MODEL HOURLY ENERGY USE IN
COMMERCIAL BUILDINGS**

A Dissertation

by

AMITAVA DHAR

Submitted to the Office of Graduate Studies of
Texas A&M University
in partial fulfillment of the requirements for the degree of

DOCTOR OF PHILOSOPHY

May 1995

Major Subject: Mechanical Engineering

UMI Number: 9534327

UMI Microform 9534327
Copyright 1995, by UMI Company. All rights reserved.

This microform edition is protected against unauthorized
copying under Title 17, United States Code.

UMI

300 North Zeeb Road
Ann Arbor, MI 48103

**DEVELOPMENT OF FOURIER SERIES AND ARTIFICIAL NEURAL
NETWORK APPROACHES TO MODEL HOURLY ENERGY USE IN
COMMERCIAL BUILDINGS**

A Dissertation

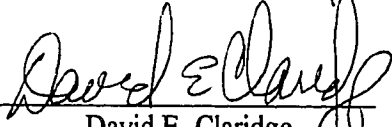
by

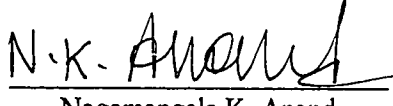
AMITAVA DHAR

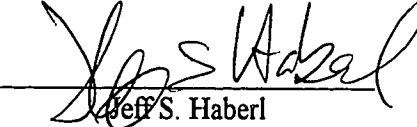
Submitted to the Office of Graduate Studies of
Texas A&M University
in partial fulfillment of the requirements for the degree of

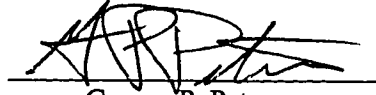
DOCTOR OF PHILOSOPHY

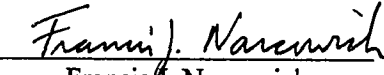
Approved as to style and content by:


David E. Claridge
(Chair of Committee)


Nagamangala K. Anand
(Member)


Jeff S. Haberl
(Member)


George P. Peterson
(Head of Department)


Francis J. Narcowich
(Member)

May 1995

Major Subject: Mechanical Engineering

ABSTRACT

Development of Fourier Series and Artificial Neural Network Approaches to Model
Hourly Energy Use in Commercial Buildings.

(May, 1995)

Amitava Dhar,

B.M.E., Jadavpur University;

M.Tech., Indian Institute of Technology at Kharagpur

Chair of Advisory Committee: Dr. David E. Claridge

This dissertation develops Fourier series and Artificial Neural Network (ANN) approaches to model hourly energy use in commercial buildings and illustrates application to data-screening.

The procedure for modeling hourly energy use has two steps: (i) Day-typing and (ii) Model development. The mean diurnal energy use and the diurnal profile may be different during working weekdays, weekends, holidays and Christmas due to major changes in mode of operation. The first step, known as day-typing, is important for removing such effects. The second step is to develop models for each day-type.

Fourier series analysis is eminently suitable for modeling strongly periodic data. Energy use in commercial buildings being strongly periodic, is appropriate for Fourier series treatment. Generalized Fourier Series (GFS) model equations, developed for both weather independent and weather dependent energy use, give a set of parameters involving time and/or weather variables. Stepwise regression is performed to select the important parameters and a final model for each day-type is developed using the selected parameters.

There are situations when only temperature data is available. A Temperature based Fourier Series (TFS) equation for modeling heating and cooling energy use has been developed to deal with such cases. Two important advantages of TFS are that it (i)

represents nonlinear variation of energy use in a linearized functional form and (ii) can indirectly account for humidity and solar effect in the cooling energy use.

ANNs with back propagation algorithms give high prediction accuracy and has been applied by many researchers to model hourly energy use in commercial buildings. However, the training of Back Propagation Network (BPN) algorithms is a long, uncertain process. ANNs with local basis functions require significantly shorter training times than conventional BPNs. A methodology has been developed to model heating and cooling energy use in commercial buildings using a one-hidden-layer ANN with two dimensional wavelet basis functions derived from cubic splines.

A suitable prediction interval can be generated and used to perform data-screening. Application of the TFS approach to data-screening is illustrated with monitored data.

To my parents,
my brother Prabir, sister Didimoni, my son Gora and
all my friends.

ACKNOWLEDGMENTS

This dissertation is a result of guidance, encouragement and support from my professors, colleagues, friends and family. I can name only a few here, however, my deep regards will always be there for all of them.

My first two years at Texas A&M were probably the most critical years in my life. My wife had a cardiac problem and passed away eighteen days after my son Gora was born. A year after her demise, my father breathed his last. Many a time, I was not sure of completing my Ph.D. First, I would like to thank Dr. Claridge; he has been more than an advisor to me during all these days; my Ph.D. would not have been possible without him.

Dr. Reddy is the source of many good ideas that finally shaped this dissertation. He has been a guide and a friend at the same time. I always felt free to talk about any problem with him. I am grateful for his guidance and friendship.

Dr. Haberl has always been encouraging to my work. He gave me many interesting papers and reports on analysis of building energy use and related subjects. Those materials were extremely helpful for this research. Dr. Srinivas Katipamula and Dr. Kelly Kissock helped me improve my knowledge of building HVAC systems and modeling energy use and my computer skill. Dr. Dave Ruch has been extremely helpful in clearing doubts on mathematical matters. Useful discussions with Sabaratnam Thamilseran, Jingrong Wang and Dr. Liu Minsheng cannot be forgotten.

I am forever grateful to my parents, my brother Prabir, sister Didimoni and my son Gora. They are my constant inspiration. My first wife dreamt with me of my Ph.D. and that is why I am here. I am unfortunate not to be able to have her with me today.

I gratefully acknowledge support for this research from the Texas State Energy Conservation Office of the Intergovernmental Division of the General Services Commission (State Agencies Program) as part of the LoanSTAR Monitoring and Analysis Program. Finally, I am thankful to all my committee members for their time and patience in correcting and improving the content of this dissertation.

TABLE OF CONTENTS

	Page
ABSTRACT	iii
DEDICATION	v
ACKNOWLEDGMENTS	vi
TABLE OF CONTENTS	vii
LIST OF FIGURES	xii
LIST OF TABLES	xx
NOMENCLATURE	xxiii
CHAPTER	
I INTRODUCTION	1
Motivation	1
Objectives	2
Description of the Following Chapters	3
II LITERATURE REVIEW	4
Introduction	4
The Objectives of Energy Conservation Programs	4
Steady State Inverse Models - Regression Approaches	5
Single Variable Regression Models	6
Multivariable Regression Models	7
Fourier Series Approach	9
Artificial Neural Network - A Dynamic Modeling Approach	9
Back Propagation Networks (BPN)	11
Recurrent Networks	14
Kohonen Self Organizing Networks	15
Counter Propagation Networks (CPN)	16
Adaptive Resonance Theory (ART) Networks	18
ANNs with Localized Training Algorithm	20

CHAPTER	Page
Global and Local Basis Functions	20
Network Optimization Techniques	21
RBFN: ANN with Radial Basis Function	24
Radial Basis Function	24
RBFN Architecture	25
RBFN Optimization	25
Wave-Net: ANN with Wavelet Basis Function	26
Calibrated Simulation Modeling - A Hybrid Approach	27
Calibration Time Periods	28
Sensitivity Analysis	28
Indoor Temperature Calibration	29
Day-typing	29
Summary	29
III SUITABILITY OF FOURIER SERIES ANALYSIS	
OF HOURLY ENERGY USE IN COMMERCIAL	
BUILDINGS	31
Introduction	31
Periodicity in the Data	32
Fourier Series Modeling	34
Summary	41
IV MODELING WEATHER INDEPENDENT ENERGY USE	44
Introduction	44
Modeling Procedure	44
Day-typing	44
Modeling	45
Model Development from Short Data Sets	49
Application to Monitored Data	50
Day-typing	50

CHAPTER	Page
Model Development	51
Identifying Important Frequencies	56
Summary	64
V GENERALIZED FOURIER SERIES (GFS) MODELING OF WEATHER DEPENDENT ENERGY USE	65
Introduction	65
Model Equation	65
Modeling Procedure	70
Application to Monitored Data	70
Cooling Energy Use	71
Heating Energy Use	73
Results from Several Buildings	73
Effect of Short Data Sets	73
Summary	81
VI TEMPERATURE BASED FOURIER SERIES MODELING OF HEATING AND COOLING ENERGY USE	83
Introduction	83
Model Concept	83
Application to Monitored Data	89
Cooling Energy Use	89
Heating Energy Use	90
Comparison with GFS Approach	93
Summary	95
VII AN ARTIFICIAL NEURAL NETWORK WITH WAVELET BASIS FUNCTIONS TO PREDICT HOURLY HEATING AND COOLING ENERGY USE	96
Introduction	96
Wavelets	97

CHAPTER	Page
Multiresolution Analysis	98
Two Dimensional Cubic Spline Wavelets	100
Wave-Net Modeling of Heating and Cooling Energy Use	104
Application to Monitored Data	105
Cooling Energy Use	107
Heating Energy Use	108
Comparison With Conventional BPN	110
Predictive Ability of Wave-Net	112
Model Results	114
Prediction Results	114
Summary	115
VIII DATA-SCREENING	118
Introduction	118
Data-screening Procedure	118
Unusual and Bad Data	119
Reliability and Length of Data Set	119
Choice of Modeling Approach	121
Screening Outdoor Temperature Data	123
Prediction Interval of a Multivariate Model	128
Application to Monitored Data	129
Summary	130
X CONCLUSIONS AND FUTURE DIRECTIONS	137
Introduction	137
GFS Approach	137
TFS Approach	138
ANN with Wavelet Basis Functions - Wave-Net	138
Data-screening	139
REFERENCES	140

APPENDIX	Page
A FOURIER SERIES APPROXIMATION AND WAVELETS - AN INTRODUCTION	149
B A SAMPLE PROGRAM FOR FOURIER SERIES MODELING	163
C ANSI C PROGRAM FOR ARTIFICIAL NEURAL NETWORK WITH BACK PROPAGATION ALGORITHM	166
D SAS PROGRAM FOR ARTIFICIAL NEURAL NETWORK WITH WAVELET BASIS FUNCTIONS	183
E A SAMPLE PROGRAM FOR PERFORMING DATA-SCREENING OF ENERGY USE IN COMMERCIAL BUILDINGS	194
VITA	207

LIST OF FIGURES

Figure	Page	
2.1	1-P (a), 2-P (b), 3-P (c and d) and 4-P (e and f) model representation of hourly weather independent and weather dependent energy use in commercial buildings	8
2.2	Backpropagation network architecture with functional details of each node	12
2.3	A conventional recurrent network architecture with one hidden layer (adapted from Parthasarathi et al., 1992)	14
2.4	An example of Kohonen self-organizing network architecture (adapted from Beale and Jackson, 1990)	16
2.5	A counterpropagation network architecture (adapted from Beale and Jackson, 1990)	17
2.6	Adaptive Resonance Theory (ART) architecture (adapted from Beale and Jackson, 1990)	19
2.7	Sigmoid function	22
2.8	Hyperbolic tangent function	22
2.9	A one dimensional Gaussian function	22
2.10	One dimensional cubic B-spline scaling function (a Gaussian approximation has been used)	23
2.11	Wavelet corresponding to one dimensional cubic B-spline scaling function	23
3.1	Whole building electricity use in the Zachry Engineering Center in 1992. The plot shows presence of seasonal effect on energy use	33
3.2	Lighting energy use in the Business building of the University of Texas at Arlington in 1992. The plot shows the presence of the seasonal effect on energy use	33

Figure	Page
3.3 Cooling energy use for the Zachry Engineering Center in 1992. The plot shows the presence of the seasonal effect on energy use	35
3.4 Cooling energy use for the Business Building in University of Texas at Arlington in 1992. The plot shows presence of the seasonal effect on energy use	35
3.5 Heating energy use in the Burdine Building at UT Austin in 1992. The plot shows the presence of the seasonal effect on energy use	36
3.6 Heating energy use in the P.C. Library at UT Austin in 1992. The plot shows the presence of the seasonal effect on energy use	36
3.7 A time series plot of whole building electricity use for September 1992 and October 1992 in the Zachry Engineering Center that shows diurnal periodicity	37
3.8 A time series plot of lighting energy use in the Business Building at UT Arlington for September 1992 and October 1992 that shows diurnal periodicity	37
3.9 A time series plot of cooling energy use during September 1992 and October 1992 of the Zachry Engineering Center which shows diurnal periodicity	38
3.10 A time series plot of cooling energy use in the Business Building at UT Arlington during September 1992 and October 1992 which shows diurnal periodicity	38
3.11 A time series plot of heating energy use in the Burdine Building at UT Austin during November 1992 and December 1992 which shows diurnal periodicity	39
3.12 A time series plot of heating energy use in the P.C. Library at UT Austin during November 1992 and December 1992 which shows diurnal periodicity	39

Figure	Page
3.13	Illustrative load profile for $E_{h,d} = X$ with $X = 1 - \cos\left(\frac{2\pi}{24} h\right)$ showing a periodic load shape with constant mean and amplitude 42
3.14	Illustrative load profile for $E_{h,d} = X + Y$ with $Y = 1 - \cos\left(\frac{2\pi}{24} d\right)$ showing a periodic load shape with variable mean but constant amplitude 42
3.15	Illustrative load profile for $E_{h,d} = X + Y + Z$ with $Z = XY$ showing a periodic load shape with variable mean and amplitude 42
4.1a	Stage I of a day-typing procedure used in conjunction with Fourier series approach to model hourly energy use in educational buildings. Primary day-types are created from data at this stage 46
4.1b	Stage II (final stage) of a day-typing procedure used in conjunction with Fourier series approach to model hourly energy use in educational buildings. Final day-types are determined from primary day-types at this stage 47
4.2	The procedure adopted in the present Fourier series approach to model hourly energy use in commercial buildings 48
4.3	Frequency distribution of mean whole building electric energy use for working weekday group in ZEC during 1992 53
4.4	Frequency distribution of first cosine frequency of whole building electric energy use for working weekday group in ZEC during 1992 53
4.5	Time series plots of measured and residual whole building electricity use in ZEC for (a) January-June 1992, (b) July-December 1992 and (c) May 1992 58
4.6	Individual contribution of sine (a) and cosine (b) frequencies of the Fourier series model of E_{wbc} in ZEC during weekdays 59

Figure	Page
4.7 Cumulative contribution of sine (a) and cosine (b) frequencies of the Fourier series model of E_{wbc} in ZEC during weekdays	60
4.8 Plots of normalized (divided by model intercept, i.e., mean energy use) Fourier coefficients of weather independent energy use models at eighteen sites. Note that SH1, CH1, CH2 and SH4 are common to nearly all models	62
4.9 The plot shows how fourth sine frequency modifies the diurnal profile to model the dip in energy use around noon	63
4.10 Cumulative frequency plot of the Fourier series model for E_{wbc} in ZEC during weekdays	63
5.1 A plot illustrating how (i) the normalized coefficients (intercept (a), temperature slope (b), humidity slope (c) and solar slope (d)) in equation 5.1 vary from hour to hour of the day when regressions are performed for each hour of the day separately. Data chosen is the cooling energy use in ZEC from 1st September 1989 to 22nd December 1989 (working weekdays only)	67
5.2 A plot illustrating how (i) the normalized coefficients (intercept (a), temperature slope (b), and solar slope (c)) in equation 5.1 vary from hour to hour of the day when regressions are performed for each hour of the day separately. Data chosen is the heating energy use in ZEC from 1st September 1989 to 22nd December 1989 (working weekdays only)	68
5.3 R-square and C.V. plots of individual hourly models of cooling energy use (a) and heating energy use (b) in ZEC during September 01, 1989 to December 22, 1989 (working weekdays only)	68
5.4 Time series plots of cooling energy use in ZEC during January 1992 to June 1992 (a) and May 1992 (b)	74

Figure	Page
5.5 Time series plots of heating energy use in BUR during January 1992 to June 1992 (a) and March 1992 (b)	75
5.6 Bar chart of C.V.s for all the months of 1992 using prediction by five models developed from data of January, February-March, April-May, June-September and twelve months' data. This site is ZEC	80
5.7 Bar chart of C.V.s for all the months of 1992 using prediction by five models developed from data of January, February-March, April-May, June-September and twelve months' data. The site is BUS	80
6.1 Plots of 2-P (a), 4-P with low slope change (b), 4-P with high slope change (c) and 6-P (d) equations and the corresponding n-P Fourier model fit	87
6.2 Time series plots of measured and residual cooling energy use in ZEC from January to June in 1992 when the TFS model is used	92
6.3 A three dimensional plot of cooling energy use versus hour of day and ambient temperature during working weekdays of January to June 1992 in ZEC	92
6.4 Time series plots of measured heating energy use from January to June, 1992 in BUR. The residual plot after modeling with equation 6.9 is also shown. Note the relatively higher negative residual values from the end of January to mid February which identified the unusual valve operation of the heating system during that period	94
6.5 A three dimensional plot of heating energy use versus hour of day and ambient temperature during working weekdays of January to June 1992 in BUR	94
7.1a Scaling function $\phi_{000}(x, y)$	102
7.1b Wavelet $\psi^1_{000}(x, y)$	102
7.1c Wavelet $\psi^2_{000}(x, y)$	103
7.1d Wavelet $\psi^3_{000}(x, y)$	103

Figure	Page	
7.2	A two dimensional grid for locating the scaling function and wavelets. One scaling function and three wavelets are located (centered) at each point marked with a filled circle for $m = 4$, while three wavelets are located at each grid point at finer scales ($1 \leq m \leq 3$)	106
7.3	A schematic two dimensional Wave-Net to model heating and cooling energy use in commercial buildings	106
7.4	Time series plots of measured and residual cooling energy use in ZEC during January through June, 1992	109
7.5	Time series plots of measured and residual heating energy use in BUR during January through June, 1992	109
7.6	The plot shows how the approximation of measured heating energy use in BUR on January 09, 1992 improved at each stage of Wave-Net modeling. The first approximation is with linear model only (eq. (7.14)) while the second and final approximations are made by subsequently adding scaling functions and wavelets at scale = 4 and 3 respectively (also see Table 7.1)	111
7.7	Cooling energy use and residuals of continuous prediction months in ZEC in 1992	116
7.8	Cooling energy use and residuals of alternate prediction months in ZEC in 1992	116
7.9	Heating energy use and residuals of continuous prediction months in BUR in 1992	117
7.10	Heating energy use and residuals of alternate prediction months in BUR in 1992	117
8.1	Data-screening procedure for weather independent and weather dependent energy use in commercial buildings	120

Figure	Page
8.2 Drybulb temperature at Zachry Engineering Center versus drybulb temperature measured by National Weather Services (NWS) at Easterwood Airport in College Station for 1992. The straight line shows a single variable linear regression fit ($R^2 = 0.88$, C.V. = 13.3%) to the data	124
8.3 The drybulb temperature at S. F. Austin Building versus drybulb temperature measured by National Weather Service (NWS) at Austin in 1992. The straight line shows a single variable linear regression fit ($R^2 = 0.74$, C.V. = 19 %) to the data	125
8.4 Drybulb temperature at the University Hall Building at UT Arlington versus drybulb temperature measured by National Weather Service (NWS) at Dallas - Fort Worth Airport in 1992. The straight line shows a single variable linear regression fit ($R^2 = 0.87$, C.V. = 15.3 %) to the data	126
8.5 Drybulb temperature at TSTC, Harlingen versus drybulb temperature measured by National Weather Service (NWS) at Harlingen in 1992. The straight line shows a single variable linear regression fit ($R^2 = 0.92$, C.V. = 6.3 %) to the data	127
8.6 Measured temperature data from the Zachry Engineering Center versus NWS temperature with the model and prediction interval is shown for the data from January 1, 1992 through June 30, 1992	131
8.7 Measured temperature data and the prediction interval for the period from July 1, 1992 through December 31, 1992 shows that a few points fall outside the prediction limit. Such observations are replaced by model predicted values	132

Figure	Page
8.8 Scatter plot of measured cooling energy use versus screened outdoor temperature data during July 1, 1992 thru December 31, 1992 (weekdays only) in ZEC. The “plus” symbols denote normal energy use while the “square box” symbols denote the unusual data points	133
8.9 Time series plot of measured cooling energy use data during July 1, 1992 thru December 31, 1992 (weekdays only) in ZEC. The variable “group” is the indicator variable plotted on the secondary y - axis and is used to indicate the unusual or bad data. A “0” value indicates that the data is normal while a “1” value indicates unusual energy consumption or bad data	134
8.10 Scatter plot of measured cooling energy use versus screened outdoor temperature data from July 1, 1992 thru December 31, 1992 (weekends only) in ZEC. The “plus” symbols denote normal energy use while the “square box” symbols denote the unusual data points	135
8.11 Time series plot of measured cooling energy use data during July 1, 1992 thru December 31, 1992 (weekends only) in ZEC. The variable “group” is the indicator variable plotted on the secondary y - axis and is used to indicate the unusual or bad data. A “0” value indicates that the data is normal while a “1” value indicates unusual energy consumption or bad data	136

LIST OF TABLES

Table	Page
3.1	Comparison of R-square and C.V. of various hourly Fourier series models using (a) month, (b) week and (c) day respectively as the time variable which captures annual periodicity of whole building electricity use data 43
4.1	Results of Duncan's multiple range test performed to identify primary day-types for whole building electric energy use in ZEC in 1992 52
4.2	Results of Duncan's multiple range test performed to identify final day-types for whole building electric energy use in ZEC in 1992 52
4.3	Summary of the forward selection procedure for whole building electricity use during working weekdays in ZEC. Data period covers the calendar year 1992. Standard errors of all variables are statistically insignificant (less than $F = 0.0001$). CH_i (& SH_i) and CD_i (& SD_i) represent the i th frequency of the cosine (and sine) terms of the diurnal cycle and of the annual cycle respectively 55
4.4	Fourier model results of weather independent energy use at four educational buildings in Texas 56
4.5	Key descriptors of Texas buildings whose monitored data were analyzed during this study 61
5.1	Results of Duncan's multiple range test performed on the cooling energy use residuals in ZEC in 1992 72
5.2	Summary of Fourier series modeling for hourly cooling energy use in ZEC (calendar year 1992) and TCOM (June 1993 to August 1993) 72
5.3	Summary of Fourier series modeling for hourly heating energy use in the Burdine building during January 1992 to June 1992 76

Table	Page
5.4 Generalized Fourier Series (GFS) models of hourly energy use at various buildings in Texas	76
5.5a Results of Duncan's multiple range test used for grouping outdoor drybulb temperature data of Zachry Engineering Center at College Station, Texas in 1992	78
5.5b Results of Duncan's multiple range test used for grouping outdoor drybulb temperature data of Business Building at UT Arlington, Texas in 1992	79
6.1 Results of equation (6.5) fitted to data generated by equation (6.6a) through equation (6.6d). ST_i and CT_i are the i th sine temperature frequencies and cosine temperature frequencies respectively	86
6.2 Contribution of Fourier frequencies to the TFS model for heating and cooling energy use at two sites during January 01 to June 30, 1992. SH_i and CH_i are Fourier sine and cosine time frequencies, whereas ST_i and CT_i are Fourier sine and cosine temperature frequencies respectively	91
6.3 Comparison of R-square and C.V. values of Generalized Fourier Series (GFS) and Temperature based Fourier Series (TFS) models of weather dependent energy use in several buildings	93
7.1 Location and basis function of various scaling function and wavelet nodes	107
7.2 Improvement of model C.V. (%) with addition of nodes at different scales in Wave-Net	110
7.3 Comparison of C.V.s (%) of Back Propagation Network (BPN) and Wave-Net models for different sites in Texas	113
7.4 Comparison of optimization speed of Back Propagation Network (BPN) and Wave-Net for different sites in Texas	113

Table		Page
7.5	Summary of results obtained from the prediction tests conducted on yearlong data of heating and cooling energy use in four sites in Texas ..	114
8.1	Comparison of C.V. (%) of four different modeling approaches applied to eight data channels from five sites in Texas. The shaded boxes indicate the lowest C.V. values among the temperature based modeling approaches (TFS, BPN and Wave-Net)	122

NOMENCLATURE

A	Projection operator
a	Weights of Spline-Net
C	Weight matrix
c	Coefficients
CD _i	<i>i</i> th frequency of the cosine term of the Fourier series for seasonal cycle
CH _i	<i>i</i> th frequency of the cosine term of the Fourier series for diurnal cycle
CT _i	<i>i</i> th cosine frequency of Fourier temperature series
C(p)	Mallow's coefficient of parameters
C. V.	Coefficient of Variation (%) based on root mean square error
d	Day of year in Fourier series model equations; dimension of vectors in one-hidden-layer Artificial Neural Network
d ₁ , d ₂	Distance
e	Exponential function; error
exp	Exponential function
E	Hourly energy use
f	Function; elements of matrix F
F	Function; Hidden unit response matrix
g	Gaussian function
H	Hidden unit response matrix
h	Hour of day
I	Global solar radiation on a unit horizontal surface; Input vector matrix in back propagation network
j	Frequency of a Fourier series representation
K	Output vector of Kohonen layer
k	Elements of matrix K; Frequency of a Fourier series representation; location of a basis function in multiresolution analysis; An index denoting

	series corresponding to internal load or weather variables
M	Number of output nodes in Adaptive Resonance Theory (ART) network
MAX	A function that determines the maximum value from a set of elements
m	Scale in a multiresolution analysis; Fourier frequency of temperature series
n	Fourier frequency of time series
N	Number of input nodes in Adaptive Resonance Theory (ART) network
N_p	p th order B-spline
n_{\max}	Number of hidden layers in a back propagation network
O	Output vector in a back propagation network
P	Penalty function
p	Number of parameters of a linear model
P_k	Period of a Fourier series representation with frequency k
P_j	Time period of a Fourier series representation with frequency j
q	A quantity denoting the range of support of a wavelet
R	Set of real numbers
R^2	Model goodness-of-fit
RMSE	Root mean square error
SD _i	i th frequency of the sine term of the Fourier series for annual cycle
SH _i	i th frequency of the sine term of the Fourier series for diurnal cycle
ST _i	i th sine frequency of Fourier temperature series
T	Outdoor dry bulb temperature; Feedback weight vector in Adaptive Resonance Theory (ART) network
T_{\max}	Maximum ambient temperature at a particular location
T_{\min}	Minimum ambient temperature at a particular location
t	time; elements of matrix T
V	Grossberg weight matrix; Vector space
v	Elements of matrix V

W	Specific humidity and electricity used by air handlers; Weight matrix in a neural network; Vector space obtained by taking orthogonal projection of vector space V in multiresolution analysis
w	Weight elements of matrix W
X	Fourier series representation for the diurnal cycle; Input Vector for Adaptive Resonance Theory (ART) network
x	Any independent variable; input to a node in back propagation network; elements of matrix X
Y	Fourier series representation for the seasonal cycle; Output vector of Grossberg layer in CPN
y	Any dependent variable; elements of matrix Y
Z	Interaction terms of diurnal and seasonal cycle; Set of integers in wavelet analysis
z	Optimizing parameter of radial basis function network

Subscripts

cw	Chilled water
d	Day of year
h	Hour of day
hw	Hot water or steam
le	Lighting and equipment
i, j, k	Integers
m	Integer; temperature frequency
n	Number of hidden layers in back propagation network; time frequency
wbe	Whole building electricity

Superscript

T	Transposed matrix
----------	-------------------

Greek Letters

α	Coefficient of Fourier series sine frequencies; Scaling function and wavelet coefficients
γ, ϕ, η	Coefficient of Fourier series sine frequencies
β	Learning rate in Artificial Neural Network; Coefficient of Fourier series cosine frequencies
δ	Scaling function and wavelet coefficients; Coefficient of Fourier series cosine frequencies
ζ	Coefficient of Fourier series cosine frequencies
γ', δ'	Coefficients of Fourier time series
ε	Random error of a linear model
$\mu(h)$	A function of hour of day
θ	Phase angle
ϕ	Coefficient of Fourier series sine frequencies; scaling function in a multiresolution analysis
ψ	Coefficient of Fourier series cosine frequencies; one dimensional wavelet
$\psi^1, \psi^2, \psi^3,$	First, second and third component of two dimensional wavelet
μ	Weighted sum of input vectors in Adaptive Resonance Theory network
η	Learning rate in a BPN or Kohonen network
σ	Standard deviation
ρ	Vigilance factor

CHAPTER I

INTRODUCTION

This chapter (i) describes the motivation and objectives of the work presented in this dissertation and (ii) gives a brief description of the contents of different chapters that follow.

Motivation

Energy use in commercial buildings accounts for about 13% of the total energy use in the U.S.A. (EIA, 1986). Energy retrofits of 1700 buildings in the U.S.A. are reported to have a median annual energy savings of 18% of the whole building energy usage, with a median payback time of 3.1 years (Greely et al., 1990). Energy conservation in commercial buildings is important for reducing not only energy consumption but also carbon dioxide emissions and other harmful environmental effects of energy use.

A successful building energy retrofit monitoring and analysis program includes several important aspects: (i) collection of monitored building energy data, (ii) screening the data, (iii) determining retrofit savings, (iv) fault diagnosis of the building systems, and (v) optimization of building energy use by improving operation and maintenance practices. Modeling of energy use is needed for the latter four aspects mentioned above. While modeling at lower resolutions of data (at the daily and monthly level) is often suitable for determining retrofit savings (Kissock, 1993), modeling at higher resolution (at the hourly level) is important for performing data-screening, fault diagnosis and optimization of building energy use. Existing approaches for data-driven (or inverse) modeling (Rabl, 1988) of hourly energy use in commercial buildings may be broadly classified into three groups: (i) steady-state inverse models (i.e., regression models), (ii) dynamic inverse models (i.e., Artificial Neural Networks or ANNs) and (iii) hybrid

Journal model is *ASME Journal of Solar Energy Engineering*.

models (i.e., calibrated simulation models). Regression techniques being simple and easy to implement, are suitable for application when a large number of channels are monitored. Two, three and four parameter regression models can be used for determining retrofit savings when monitored data are available (Kissock, 1993). However, these model equations cannot represent the time-dependence of the energy use due to scheduling effects. The effect of scheduling needs to be accounted for by performing rigorous day-typing (Katipamula and Haberl, 1991). Calibrated simulation models require detailed information on the actual building systems and need many adjustments to achieve an acceptable prediction accuracy. These methods have been found useful when little or no monitored baseline data is available (Katipamula and Claridge, 1992) and for diagnosing operating problems (Liu et. al, 1994). Artificial neural networks such as Back Propagation Networks (BPN) and Recurrent Networks have been used in many fields of engineering for predicting time series data. Although these techniques give high prediction accuracy, they require enormous training time (Anstett et al., 1992) and do not provide physically based models. Also, convergence of the training process is not guaranteed (Bakshi and Stephanopolos, 1993). Development of modeling techniques that (i) account for scheduling and/or weather effects, (ii) offer required prediction accuracy, (iii) are easy to develop and (iv) have modest computational requirement is, therefore, necessary.

Objectives

As pointed out in the previous section, development of accurate models for hourly energy use in commercial buildings has important ramifications for (i) retrofit savings analysis, (ii) diagnostics, (iii) optimization of building energy use and (iv) acquiring physical insights into the operating patterns of the buildings. Patterns of energy use being different in different buildings, one particular approach may not be suitable for modeling energy use in commercial buildings in general. This necessitates development and adoption of multiple techniques to address the issue.

The objective of the research reported in this dissertation was to develop advanced modeling approaches using Fourier series and Artificial Neural Networks (ANN). The suitability of these approaches was verified and limitations investigated by applying to the monitored data from several buildings in Texas. Finally, the use of hourly models to perform data-screening was investigated.

Description of the Following Chapters

This dissertation is presented in nine chapters, references, five appendices and a vita. The topic is introduced and the background work is described in Chapters I and II. The suitability of Fourier series to model energy use in commercial buildings is explained in Chapter III and the Generalized Fourier Series (GFS) approaches to model weather independent and weather dependent energy use are described and illustrated in Chapter IV and Chapter V respectively. Use of the Fourier series approach with outdoor temperature as the only variable to model heating and cooling energy use (Temperature based Fourier Series or TFS approach) is described and illustrated in Chapter VI. The development and application of an Artificial Neural Network (ANN) with two dimensional wavelet basis functions derived from a cubic spline is presented in Chapter VII. A comparison between GFS, TFS, conventional Back Propagation Network (BPN) and the ANN with wavelet basis functions (Wave-Net) in terms of prediction accuracy is presented and a procedure for data-screening is described in Chapter VIII. A summary of the present work and possible future directions are presented in Chapter IX. Fundamentals of Fourier series and wavelet approximation is described in appendix A and the programs that were written for implementing the modeling procedures are included in appendices B C, D and E.

CHAPTER II

LITERATURE REVIEW

Introduction

As mentioned in the previous chapter, a successful building energy conservation program includes several aspects which require modeling energy use at the daily and hourly level. The focus of the research reported here was on the development of modeling methodologies at the hourly level. Literature on existing regression techniques, Artificial Neural Network (ANN) approaches and calibrated modeling methodologies were reviewed to identify the areas of interest. Fourier series was found to be an effective tool, but not yet used to model hourly energy use in commercial buildings. ANN was found to be a powerful and widely used technique for modeling time series data. In particular, ANNs with local basis functions were found to be more attractive than back propagation networks and were yet to be applied to model hourly energy use in commercial buildings. This chapter presents the objectives of energy conservation programs and the literature review on regression, ANN and calibrated modeling approaches.

The Objectives of Energy Conservation Programs

An energy conservation program for reducing energy use in commercial buildings may have macro or micro objectives. The macro objectives of a program are to implement retrofits in a large number of buildings, determine overall savings and report the results in a suitable form to the sponsoring utility. This calls for defining populations to sample, collecting and processing weather data and utility bills and analyzing data to determine savings. Energy conservation programs conducted by utilities and state Public Utility Commissions (PUC) are typically macro objective oriented. Monthly consumption data is normally used to determine energy savings. Three modeling approaches that are often adopted to do this are (i) difference and ratio estimation, (ii)

statistically adjusted engineering estimation and (iii) multivariate modeling (Hirst and Reed, 1991).

The objectives of energy conservation programs at the micro level are to determine savings for individual buildings, study diurnal load profiles, detect possible operation and maintenance problems and optimize building energy use. These require careful monitoring and analysis of energy use at the daily and hourly level for each building. An example of energy conservation at the micro level is the Texas LoanSTAR Monitoring and Analysis Program (MAP) (Claridge et al., 1991).

A micro level energy conservation program needs emphasis on selection and development of analysis techniques at the individual building and building system level. Retrofit savings can be determined by analyzing the data at lower resolutions (at the monthly and daily level) whereas data-screening, fault diagnosis and optimization of building energy use need models at the hourly or fifteen-minute level. As mentioned in Chapter I, the existing techniques for modeling hourly energy use can be broadly classified into three groups: (i) steady-state inverse modeling or regression modeling approaches, (ii) Dynamic modeling approaches, for example, Artificial Neural Network (ANN) (Krieder and Wang, 1991) approaches and (iii) hybrid approaches such as calibrated simulation modeling approaches (Katipamula and Claridge, 1992). We will briefly describe these approaches in the following sub-sections.

Steady State Inverse Models - Regression Approaches

Model development using regression is attractive because it, in general, requires less effort and less user-expertise than calibrated simulation and ANN approaches. Also, regression approaches give reasonably good prediction accuracy. Considerable effort has, therefore, been made to develop and adopt regression modeling techniques under the Texas LoanSTAR Monitoring and Analysis Program (MAP) (Claridge et al., 1991). Single and multivariable regression models will be discussed briefly in the following sub-sections.

Single Variable Regression Models. A regression model with a single variable, for example, outdoor temperature is preferred to a multivariable regression model because metering outdoor temperature is easier and more reliable than metering other variables, for example, humidity and solar radiation. One parameter (1-P), two parameter (2-P) (Kissock, 1993), three parameter (3-P) (Fels, 1986) and four parameter (4-P) (Ruch and Claridge, 1992; Kissock et al., 1992) techniques are available for modeling energy use in commercial buildings. These steady state inverse modeling techniques have been so far used to model energy use at daily and monthly level, because the dynamic behavior of the building is insignificant at these levels of resolution. However, one can also use these equations to develop individual hourly models. Time-dependence of energy use due to systematic scheduling may be accounted for by binning the data of each day-type (Katipamula and Haberl, 1991) into twenty-four hourly groups and developing separate models for each hour of the day. A 1-P mean model for each hour of day may be used to model weather independent energy use, for example, a 1-P model for lighting and equipment loads at the hourly level can be expressed as:

$$E_h = \beta_{0,h} \quad (2.1)$$

where the subscript h stands for the hour of day. 2-P, 3-P and 4-P models may be used to model weather dependent energy use in commercial buildings with outdoor temperature as the only variable:

$$E_h = \left. \begin{array}{l} \beta_{0,h} + \beta_{1,h} T, \\ \beta_{0,h} + \beta_{1,h} (T - \beta_{3,h})^- + \beta_{2,h} (T - \beta_{3,h})^+ \end{array} \right\} \begin{array}{l} 2 - P \text{ model} \\ 4 - P \text{ model} \end{array} \quad (2.2)$$

where the symbols $()^-$ and $()^+$ indicate that these quantities are set to zero when negative and positive respectively. Clearly, constraining either $\beta_{1,h}$ or $\beta_{2,h}$ in the 4-P model equation for energy use to zero makes it a 3-P or PRISM model (Fels, 1986). 3-P

models are, therefore, special cases of 4-P models. These models may be appropriate for modeling energy use in Constant Air Volume (CAV) systems with economizer cycles or hot deck reset schedules, and Variable Air Volume (VAV) systems (Reddy et al., 1994). Six examples of these models are shown in Figure 2.1.

Multivariable Regression Models. Single variable regression models use outdoor temperature as the only variable. However, weather dependent energy use such as cooling energy use depends on outdoor temperature, specific humidity, solar radiation and the type of HVAC system in the building. Suitable multivariable regression models can be developed by incorporating the engineering principles that govern the HVAC system operation (Forrester and Wepfer, 1984). A simplified multivariable regression model based on engineering principles is of the following form (Katipamula et al., 1994):

$$E = a + b + cI + dIT_0 + eIT_{dp} + fq_{sol} + gq_i \quad (2.3)$$

where a, b, c, d, e, f and g are the coefficients, T is the temperature, q is the heat gain and I is an indicator variable that accounts for change in slope due to the effect of outdoor temperature at higher range of values. Subscripts 0, dp, sol and i stand for outdoor drybulb temperature, dewpoint temperature, horizontal solar flux and internal load respectively.

As noted earlier, the energy consumption data of each day-type can be binned into twenty-four hourly groups and single variable or multivariable regression models can be developed for each hour of the day in order to account for the effect of time dependent systematic scheduling. However, this leads to a large number of final model equations for each day-type and, as a result, gaining insight into the operating pattern of the building systems becomes difficult. A single model equation for each day-type can be obtained when techniques like the Fourier series approach or Artificial Neural Networks are adopted for model development. These will be discussed in the sections that follow.

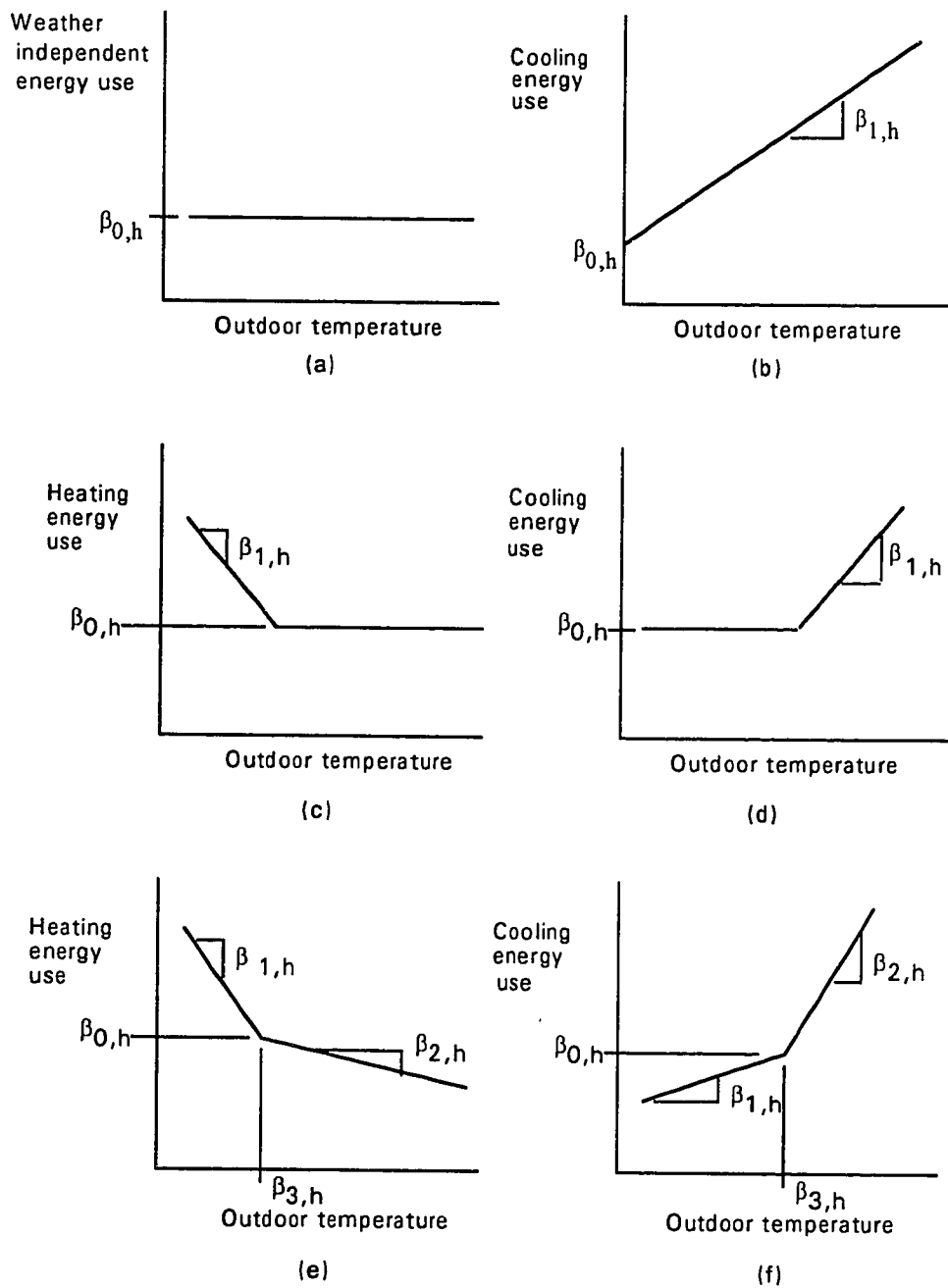


Figure 2.1 1-P (a), 2-P (b), 3-P (c and d) and 4-P (e and f) model representation of hourly weather independent and weather dependent energy use in commercial buildings.

Fourier Series Approach

Energy use in commercial buildings is strongly periodic due to systematic scheduling effects under which the building systems operate. Adopting the Fourier series model equation, therefore, may be a convenient approach to model hourly data. Climatic data (i.e., solar radiation and outdoor temperature) are periodic and have been analyzed using Fourier series by several researchers (Philips, 1984; Hittle and Pederson, 1981). Trigonometric models with hour of day as the primary variable have been proposed in the classical literature (Pandit and Wu, 1983). Attempts at Fourier series modeling of hourly energy use in commercial buildings are relatively few, the most important being perhaps that by Seem and Braun (1991) who chose a week as the maximum period of the Fourier series. The regression fit was poor, however, partly because of the choice of maximum period. Commercial buildings undergo major operating changes from weekdays to weekends and choosing an appropriate period is crucial.

Artificial Neural Networks - A Dynamic Modeling Approach

An Artificial Neural Network (ANN) approach with the incorporation of known physical parameters that govern the phenomenon into the network structure is very appealing for modeling time series data (Willis et al., 1991). Comparative studies of neural networks and regression approaches have been conducted by several researchers (Miller and Seem, 1991; Parthasarathy et al., 1992; Curtiss et al., 1993). These studies showed that an ANN approach provides a better fit and thus is more suitable for application to modeling and control. Refenes et al. (1993) compared the ANN approach with multiple linear regression for predicting future stock ranking time series data and found that the ANN approach offers much higher prediction accuracy. Clearly, there is a need for a thorough understanding of the currently available ANN techniques as well as how to modify and adopt such techniques for modeling hourly energy use in commercial buildings.

Early research in the field of ANNs was restricted to developing computational techniques that can resemble human intelligence. However, the current direction has been more towards performing the elementary functions that a biological neuron can do (Wasserman, 1989); the computational steps adopted in an ANN may or may not be the same as those inside the anatomy of a human brain. McClelland and Rumelhart (1991) have given a broad definition of ANN which has been summarized further by Bakshi and Stephanopolos (1993). An ANN is defined to have (i) a set of processing units, (ii) a state of activation, (iii) an output function for each processing unit, (iv) a pattern of connectivity among the processing units, (v) a propagating rule for propagating patterns of activities through the network of connectivities, (vi) an activating rule for combining the inputs impinging on a unit to produce a new level of activation for the unit, (vii) a learning rule whereby patterns of connectivity are modified by experience and (viii) an environment within which the system must operate.

Broadly, neural networks that were available till the late 1980s (Beale and Jackson, 1990) for pattern recognition or modeling are varieties of multilayered perceptron networks. Some examples are Back Propagation Networks (BPN), Recurrent networks, Counter Propagation Networks (CPN), Kohonen self-organizing networks, Hopfield networks, Adaptive Resonance Theory (ART) networks and networks using Bi-directional Associative Memories (BAM). All these networks have complex architectures that give little or no understanding of the inside processing. In addition, design of these networks is largely based on heuristics or rules of thumb. The prediction accuracy is, however, acceptable for many applications. In other words, ANNs are complex nonlinear regression models whose structures are determined empirically (Leonard and Kramer, 1991).

Recent understanding of neural nets confirms that computation in the frame work of an ANN is similar to the mathematical approximation of a multidimensional function over a space by any activation function (Poggio and Girosi, 1989):

$$E = \sum_{i=1}^m c_i \phi_i(t) \quad (2.4)$$

Such an understanding has opened the direction of research towards development of simplified networks with the flexibility of selecting application-specific local activation functions, suitable for providing (i) high prediction accuracy (ii) less computational complexity and (iii) some physical understanding. Examples of such modern networks are (i) Radial Basis Function Networks (RBFN) (Moody and Darken, 1989; Stokbro et al., 1990; Holcomb and Morari, 1991; Lee and Kil, 1991), (ii) ANNs with ellipsoidal activation functions (Vankatasubramaniam and Kavuri, 1991), (iii) Wave-net: An ANN with wavelet basis functions (Bakshi and Stephanopolis, 1993) and many more.

Back Propagation Networks (BPN). The architecture of a back propagation network consists of an input layer which is fed with all the input variables, one or more hidden layers within which mathematical processing of the inputs takes place and an output layer that processes information received from a hidden layer and gives the predicted value of the dependent variables as the outputs (Figure 2.2). Hidden layers and the output layer of the network may have several nodes or perceptrons within which the weighted sum of inputs is activated by an activation function. Networks of this type may be able to predict one or more dependent variables simultaneously. The processing of input data for determining the approximation is expressed mathematically as follows (Adum Blum, 1991):

$$H_1 = F(IW_1), \quad H_n = F(H_{n-1}W_n) \quad \text{and} \quad O = F(H_n W_{n+1}) \quad (2.5)$$

where I is the input vector, H and O are output vectors of the hidden layers and output layers respectively, n is the number of hidden layers and W_n is the weight vector between $(n-1)^{\text{th}}$ and n^{th} layers.

The function $F(x)$ in eq. 2.5 determines response of the network to input data and is known as the activation function. The sigmoid and hyperbolic tangent are two commonly used activation functions for modeling time series data.

$$\text{Sigmoid: } F(x) = \frac{1}{1 + e^{-x}}, \quad \text{Hyperbolic tangent: } F(x) = \frac{e^x - e^{-x}}{e^x + e^{-x}} \quad (2.6)$$

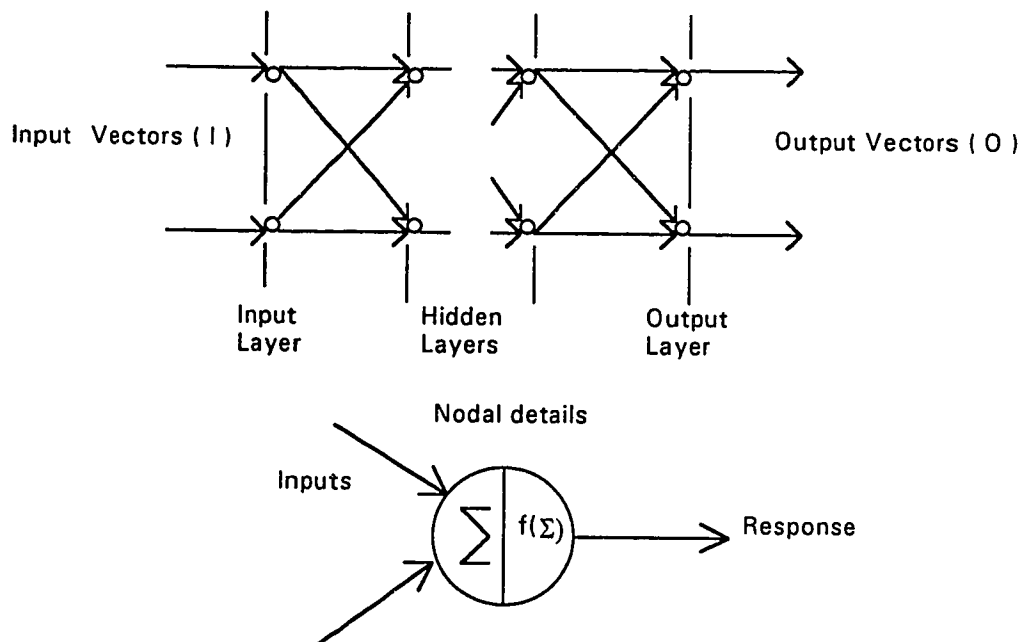


Figure 2.2 Backpropagation network architecture with functional details of each node.

Training of a network essentially means determination of the weight vectors W in eq. 2.5. The optimization technique that is adopted for training a conventional BPN is the gradient descent method (McClelland and Rumelhart, 1991). The weight of an incoming

signal at any node is initialized with random values and is adjusted by the negative of the partial derivative of the error (the difference between the approximated value and desired value) with respect to the net input to that node. The partial derivative is, however, multiplied by a factor known as the learning rate (which typically varies between 0.01 and 1.0) before doing the adjustment. Learning rate is an important parameter. A high learning rate will accelerate the training but the training process may get stuck at local minima on the error surface. On the other hand, a low learning rate may improve the optimization but the speed of training will be extremely low (Sejnowski and Rosenberg, 1987).

The adjustment described above starts from the output layer and proceeds backward until weights between the input layer and the first hidden layer are modified. This process needs to be repeated a large number of times (also known as epochs) to minimize the error. As a result, the training procedure becomes computationally intensive. The learning technique is also termed a supervised learning technique, in the sense that the weights of the network are optimized by comparing the approximated values with the target outputs. An explicit derivatation of the formula for training weights in the hidden layers and output layer is available in Beale and Jackson(1990).

In order to achieve a faster convergence of the optimization process described above, a bias may be added to the response of each neuron. Adding a bias (bias is a constant added in a particular form in the function to shift the response along one of the axes) in the range of ± 0.5 can reduce training time by an average of 30% to 50% (Stornetta and Huberman, 1987). Another way of improving the training time is to introduce momentum (Rumelhart and Mclelland, 1989). The weights are adjusted in each epoch by a factor of previous corresponding weight change (e.g., 1.5 times the previous change), in addition to the adjustment described before.

Zhou and Dobrivoje (1993) suggested some modifications to the generalized back propagation algorithm and introduced a new training method with adaptive selection of learning rate. They compared network performances with and without the new learning method by applying the method to a simulated data set and showed that the

modified network learns much more efficiently. Loh and Fong (1993) considered training a BPN using the method of least squares instead of the gradient descent rule. Application to a simulated data set from a nonlinear dynamical system showed that the new algorithm had a rapid rate of convergence compared to the conventional back propagation algorithm.

Recurrent Networks. A recurrent network has the same architecture as a BPN except that both feedback and feedforward connections are present (Figure 2.3). Recurrent networks have been modified and improved to model time series data by many researchers in recent years (Parthasarathy et al., 1992; Rao and Ramanurthi, 1993; Puskorius and Feldkamp, 1993; Chen et al., 1993).

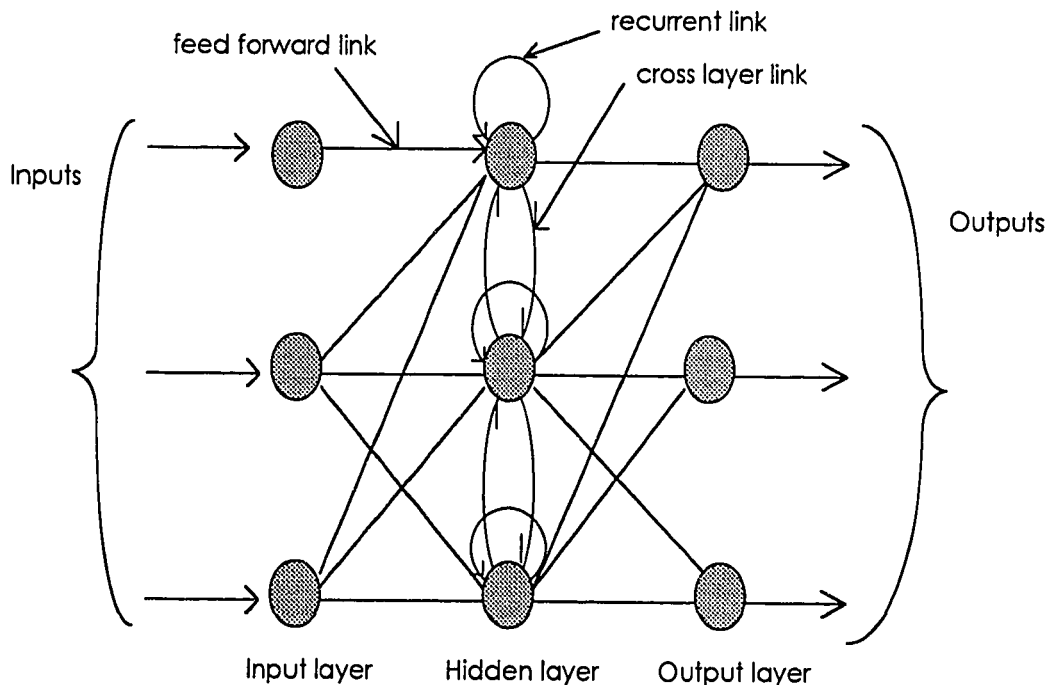


Figure 2.3 A conventional recurrent network architecture with one hidden layer (adapted from Parthasarathi et al., 1992).

Parthasarathy et al. (1992) used a four layer recurrent network (two hidden layers) for self-tuning adaptive control of complex process plants. The nodes within each hidden layer (i) use feedback of their own and (ii) share information among themselves (cross talk). These properties make this type of network suitable for modeling highly nonlinear processes. A modified gradient descent algorithm is used for training the network. Rao and Ramamurthi (1993) proposed some modifications in the network learning algorithm for enhancing network performance. They suggested the use of a combination of Fahlman's quickprop algorithm and the real time recurrent network learning algorithm for network training to achieve faster convergence. Sterzing and Schurmann (1993) presented a study on recurrent networks and proposed modifications towards application to time series data. Puskorius and Feldkamp (1992a, 1992b and 1993) have proposed use of a decoupled extended Kalman filtering (DEKF) technique for training a recurrent network algorithm to achieve a better network optimization. Chen et al. (1993) presented a preliminary approach to modify the learning algorithm of recurrent networks to minimize the size of the network for a particular problem. Dodier et al. (1993) initiated application of recurrent networks for predicting time series data of energy use in commercial buildings.

Kohonen Self-Organizing Networks. Unlike the BPN and the recurrent network, the Kohonen self-organizing network (Kohonen, 1990) does not rely on an external training response (the desired response of the network, i.e., the target values) being available for each input from the target data set. It has an input layer of nodes and a two dimensional flat grid of nodes (Figure 2.4). Feedback is restricted within the nodes inside the flat grid and each of the nodes in the flat grid is itself an output node.

The training algorithm of a Kohonen network aims to optimize the number of lateral layer nodes. The sum of squares of differences between the weights from input node i to grid node j (d_j) at time t ($w_{ij}(t)$) and input $x_i(t)$ over $i = 1$ to n , where n is the number of inputs, is determined for each output node. An initially large lateral grid is

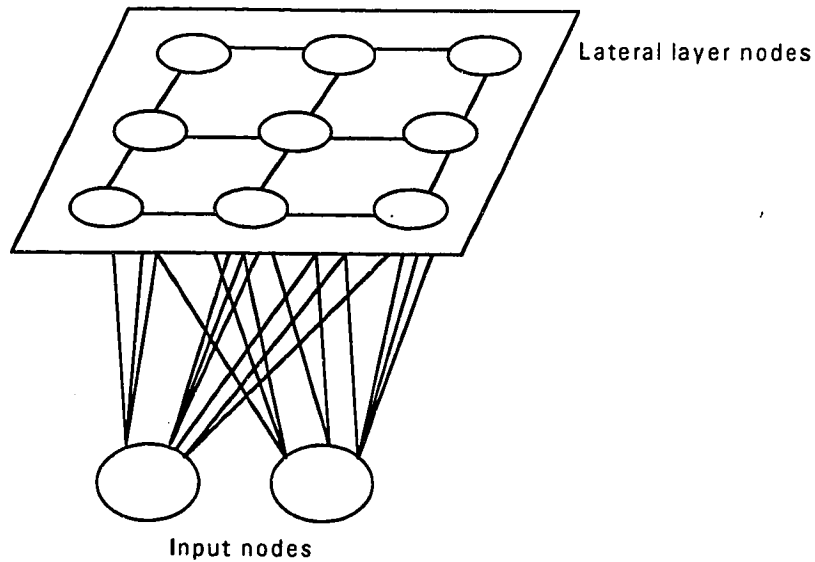


Figure 2.4 An example of Kohonen self-organizing network architecture (adapted from Beale and Jackson, 1990).

gradually reduced by selecting the neighborhood around the node with minimum d_j (area of maximum activity) and adjusting w_{ij} s by using the following formula:

$$w_{ij}(t+1) = w_{ij}(t) + \eta(t)\{x_i(t) - w_{ij}(t)\} \quad (2.7)$$

where $\eta(t)$ is the learning rate at time t . Clearly, the process is repetitive until an optimum localization of the area of maximum activity is achieved. The activation function for this type of network could be a Mexican hat function. For more details on this network, Kohonen (1990) or Beale and Jackson (1990) may be consulted.

Counter Propagation Networks (CPN). The counter propagation network is actually a combination of a Kohonen network (Kohonen, 1990) and a Grossberg layer

(Grossberg, 1969). The network consists of an input layer, one Kohonen layer and one Grossberg layer (Figure 2.5). If the net output of an optimized Kohonen layer is denoted

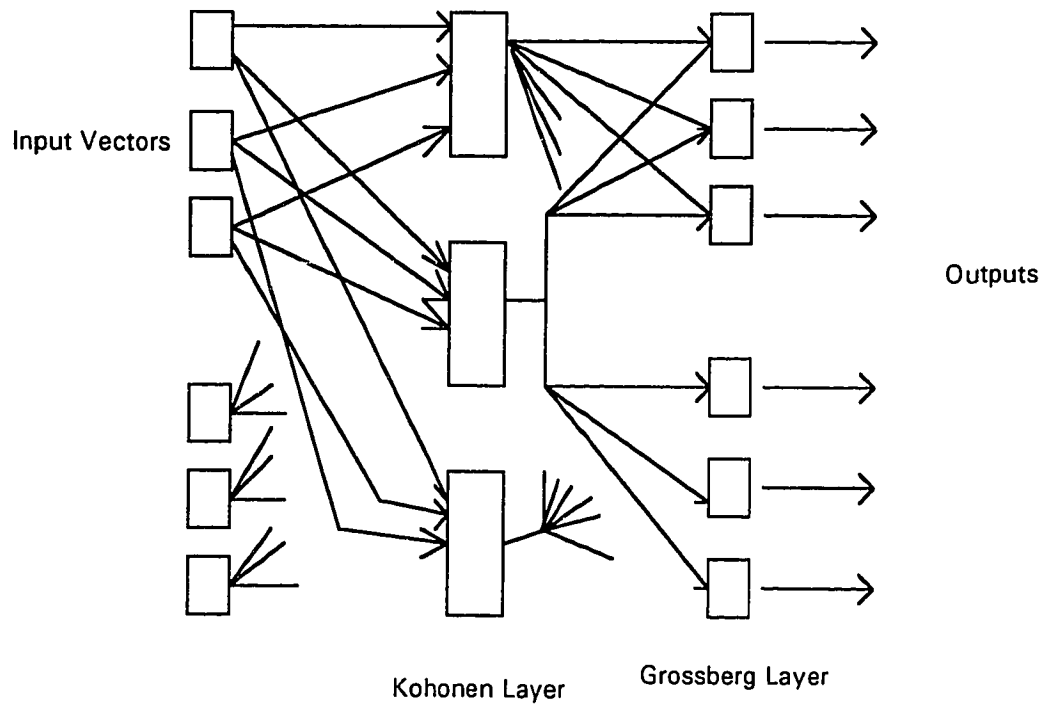


Figure 2.5 A counterpropagation network architecture (adapted from Beale and Jackson, 1990).

by vector K , then the net Grossberg layer output vector Y is determined as follows:

$$Y = KV \quad (2.8)$$

where V is the Grossberg layer weight matrix. The training of a Kohonen layer is similar to that described earlier whereas a Grossberg layer is trained by using the following formula:

$$v_{ij\text{new}} = v_{ij\text{old}} + \beta (y_j - v_{ij\text{old}})k_i \quad (2.9)$$

where β is the variable learning rate that gradually reduces during the training process and v , y , and k are the elements of matrices V , Y and K respectively. Subscripts i and j stand for i^{th} Kohonen layer node and j^{th} Grossberg layer node.

The prediction accuracy that can be achieved by a CPN is less than a BPN but a CPN trains itself much faster than a BPN, reducing the computation time substantially. CPN, therefore, may be a suitable choice for the applications that can not afford to have slow computation (Hecth-Nielsen, 1987). The evaluation of potential by applying this methodology to measured energy use in buildings may be an interesting future issue.

Adaptive Resonance Theory (ART) Networks. The BPN, Kohonen network and CPN all suffer from their inability to learn new information on top of the old (stability-plasticity dilemma). ART is a self-organizing network, based on cognitive and behavioral models and has the feature of solving the stability-plasticity dilemma (Carpenter and Grossberg, 1988). The network relies on the details of architecture more than any other ANN. It consists of two layers: an input/comparison layer and an output/recognition layer. These layers are connected with extensive use of feedback (Figure 2.6). It has feed-forward weight vectors (W) from the input layer to output layer and feedback weight vectors (T) from output layer to input layer. For M output nodes and N input nodes, the weight vectors are initialized as follows:

$$t_{ij}(0) = 1, \quad w_{ij}(0) = \frac{1}{1 + N} \quad (2.10)$$

where $0 \leq i \leq N - 1$ and $0 \leq j \leq M - 1$

For each output node, the weighted sum (μ_j) of input vectors is determined. The feedback vector elements (t_{ij}) corresponding to the maximum μ_j are determined to satisfy the condition

$$\frac{\|T \bullet X\|}{\|X\|} > \rho \quad (2.11)$$

where ρ is the vigilance factor, generally fixed between 0 and 1;

$$\|X\| = \sum_{i=0}^{N-1} x_i \quad \text{and} \quad \|T \bullet X\| = \sum_{i=0}^{N-1} t_{ij^*}(t)x_i, \quad t_{ij^*} \text{ is the } t_{ij} \text{ corresponding to}$$

$$\text{Max} \left[\sum_{i=0}^{N-1} w_{ij}(t)x_i \right], \quad 0 \leq j \leq M-1.$$

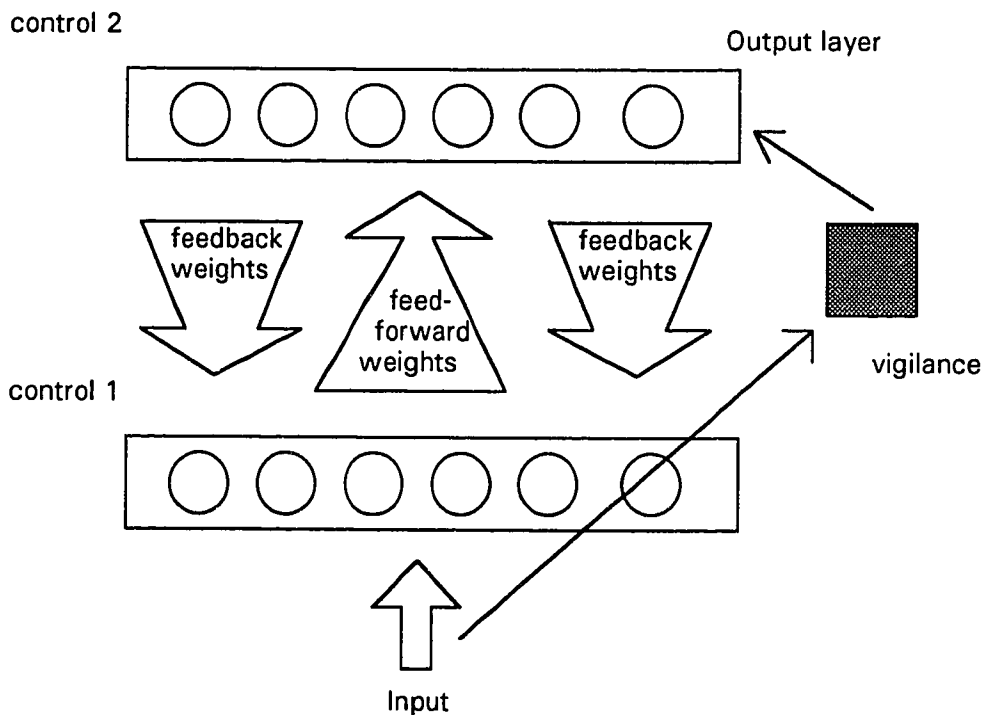


Figure 2.6 Adaptive Resonance Theory (ART) architecture (adapted from Beale and Jackson, 1990).

If the test fails, the output of the corresponding output node is set to zero (disabled) and the test is continued. The process is repeated until all the weights are optimized and the disabled node is enabled at the beginning of each epoch.

The first version of ART (ART1) has been described above; however, ART2 and ART3 versions are also available. ART has some attractive features like (i) the training process is stable and (ii) convergence is guaranteed. The application of ART to modeling time series data is yet to be tested.

There are many other networks available, for example, Hopfield nets (Hopfield, 1984), Bi-directional Associative Memory (BAM) networks (Kosko 1987a and 1987b), etc. However, the suitability of these networks to represent time series data is yet to be known.

ANNs with Localized Training Algorithm. Back Propagation Networks (BPN) and Recurrent networks are probably the most widely used networks for time series data. BPN has been applied to predict weather independent and weather dependent energy use in commercial buildings (Kreider and Wang, 1991; Wang and Kreider, 1992; Anstett and Kreider, 1993). Curtiss et al. (1993) applied BPN for adaptive control of HVAC processes.

ANNs with a localized training algorithm may offer high prediction accuracy with less processing time than BPNs and recurrent networks. These techniques may also provide better physical insight into the actual process (Moody and Darken, 1989; Holcomb and Morari, 1991; Bakshi and Stephanopolis, 1993). These networks have only one hidden layer and the number of hidden-layer-nodes may be determined by using a suitable statistical criterion. Thus, the problem of apparent arbitrariness in determining the network architecture is avoided. In order to provide a clearer picture, we will first discuss factors influencing the choice of activation functions and the optimization techniques which are the two most important aspects of neural network approximation.

Global and Local Basis Functions. Any function $\phi(x)$ that is active (has non zero real values) over a large range of x and provides a global approximation of empirical data is known as global functions. Examples of global functions are step functions, sigmoid functions (Figure 2.7), trigonometric functions like sines, cosines, hyperbolic tangents

(Figure 2.8), etc. Figures 2.7 and 2.8 show that these functions are active over a large range of input values. A network that uses any of these global functions for activation, suffers from several shortcomings. Each node of the network influences the output over a large range of input values. In addition, if the same global function is used for all the nodes as in a BPN, the nodes will start interacting with each other. Correction of the network output for a given input, therefore, will require modification of parameters influenced by all the interacting nodes (Bakshi and Stephanopolos, 1993).

On the other hand, local functions have finite support; they are active only in the immediate vicinity of a given input value. The Gaussian function (Figure 2.9), splines and corresponding wavelets (Figures 2.10 and 2.11) are examples of local functions. Local functions, when used for activation in a network, offer important advantages in terms of choosing improved optimization algorithms. We will discuss global and local optimization techniques in the next section.

Network Optimization Techniques. Nonlinear global optimization techniques involve long, uncertain training processes. During the network training, the weights of the network may assume large values where the derivative of the activation is very small. This makes the convergence extremely slow (network paralysis). Moreover, the error surface of a complex network like a BPN is highly convoluted, and the process may stop at a local minimum (Wasserman, 1989).

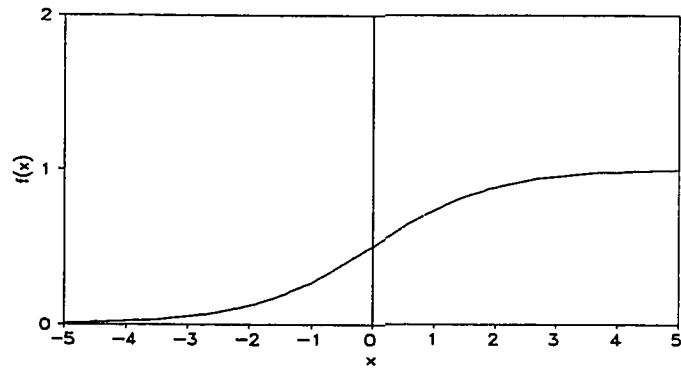


Figure 2.7 Sigmoid function.

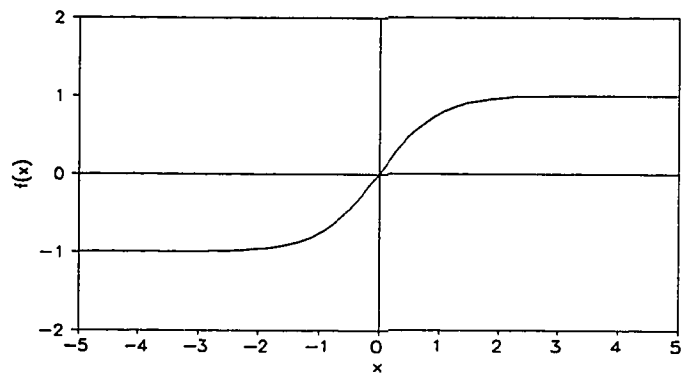


Figure 2.8 Hyperbolic tangent function.

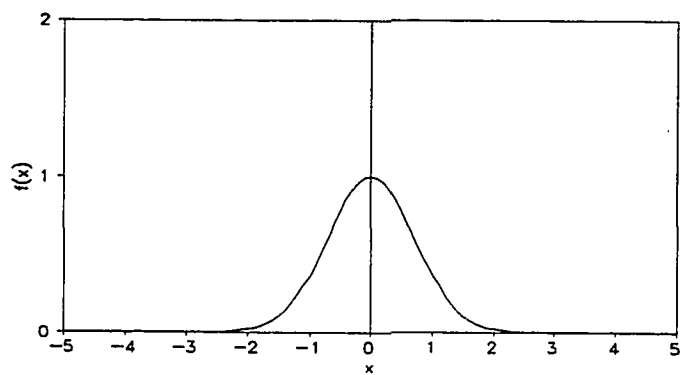


Figure 2.9 A one dimensional Gaussian function.

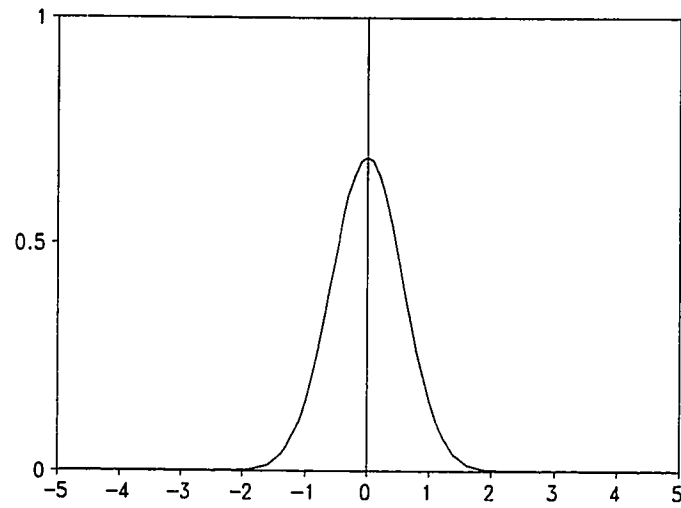


Figure 2.10 One dimensional cubic B-spline scaling function (a Gaussian approximation has been used).

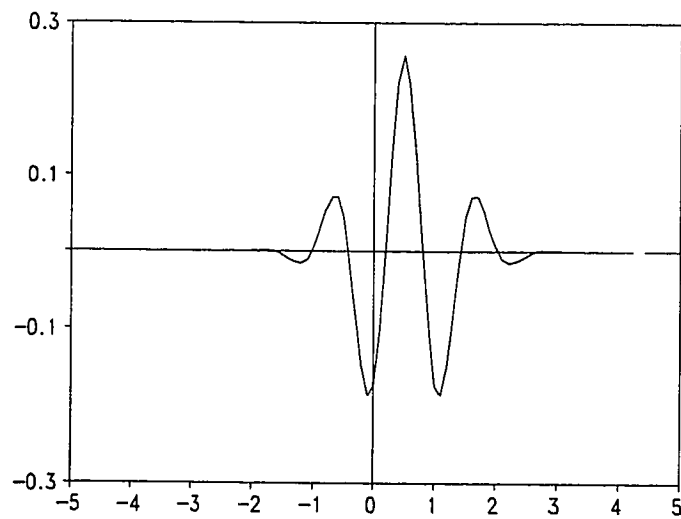


Figure 2.11 Wavelet corresponding to a one dimensional cubic B-spline scaling function.

Localized training approaches eliminate the disadvantages discussed above. Faster optimization is possible, both local and global errors can be controlled and reliability of the output based on training data density can be measured (Leonard and Kramer, 1991). We will present the details of two networks that use localized training algorithms: (i) RBFN: an ANN with radial basis functions (Moody and Darken, 1989; Holcomb and Morari, 1991) and (ii) Wave-Net: an ANN with wavelet basis functions (Bakshi and Stephanopolos, 1993).

RBFN: ANN With Radial Basis Function. RBFN, a one-hidden-layer ANN, uses radial basis functions for activation and the training of the network is accomplished by a localized training algorithm. In order to present the concept systematically, we will first discuss radial basis functions. This will be followed by description of the network architecture and training algorithm.

Radial Basis Function. A radial basis function $g_i(x)$ is defined as follows:

$$g_i(x) = g(\|\hat{x} - \hat{x}_i\|_w) \quad (2.12)$$

where \hat{x} and \hat{x}_i are the input and fixed vectors (columnar), $\|\cdot\|_w$ is the weighted Euclidean norm of weight matrix W and g is a scalar, monotonic function $(0, \infty)$ (Poggio and Girosi, 1989). The Gaussian function is a common form of radial basis function:

$$g_i(x) = \exp\left(-\frac{\|x - x_i\|^2}{2\sigma_i^2}\right), \quad x \in \mathbf{R} \text{ (} x \text{ is any real number)} \quad (2.13)$$

$$g_i(\hat{x}; W_i, \hat{x}_i) = \frac{|W_i|}{\pi^{d/2}} \exp\left[-\frac{1}{2}(\hat{x} - \hat{x}_i)^T W_i^2 (\hat{x} - \hat{x}_i)\right], \quad x \in \mathbf{R} \quad (2.14)$$

Equation 2.13 is the one dimensional Gaussian whereas equation 2.14 represents a multivariable Gaussian for d dimensions. W_j is a $d \times d$ symmetric, nonsingular weight matrix and becomes simply the inverse of standard deviation for one dimensional case. The superscript T stands for the transpose of the matrix.

RBFN Architecture. A RBFN consists of an input layer, a hidden layer and an output layer. A conventional RBFN designed by Moody and Darken (1989) assumes the weights between input layer and hidden layer to be unity while the weights between the hidden units and output units are determined by RBFN optimization. Hidden layer response to the inputs is governed by the radial basis functions described by equation 2.13 or equation 2.14.

RBFN Optimization. Moody and Darken proposed a training method (optimization) for RBFN which, although uses heuristics for determining the hidden layer architecture, is faster than the speed advantage compared to any nonlinear global optimization technique like gradient descent method. The algorithm uses the following modified form of equation 2.13 as the activation function :

$$g_i(\hat{x}) = \exp\left(\frac{\|\hat{x} - \hat{x}_i\|}{\sigma_i^2}\right) \quad (2.15)$$

where σ_i is analogous to the standard deviation and is determined as:

$$\sigma_i = \sqrt{d_1 d_2} \quad (2.16)$$

where d_1 and d_2 are the Euclidean distances from the i^{th} center to the two nearest centers. The centers are fixed at points with $i = 1$ to h , based on heuristic judgment. The weights c_j s of the equation

$$y = \sum_{i=1}^h c_i g_i(x) \quad (2.17)$$

are determined by the standard least squares regression of y against $g_i(x)$.

A problem with the above algorithm is that the set of Gaussian basis functions is nonorthogonal which results in the overlapping of the response of individual Gaussians. Holcomb and Morari (1991) proposed a modified RBFN algorithm to solve this problem. They introduced a function, which is called penalty function to overcome the problem of overlapping. The physical explanation of penalty function was, however, not provided.

Many other researchers are continuing their work on RBFNs. Chakraborty et al. (1993) proposed an algorithm to arrive at near optimum initial configuration of the network very quickly. Also, the number of hidden layer units is determined mathematically. Koffman and Meckl (1993) are continuing their research on evaluating performances of different types of RBFNs. They are using different types of radial basis functions (Hyperbolic paraboloid, Mexican hat function, etc.) and comparing their learning speed. Chen and Lin (1993) conducted a study of the existing RBFN training methods and suggested a modified gradient algorithm that ensures correct optimization of the weight vectors.

Wave-Net: ANN with Wavelet Basis Function. A complete functional representation of input-output relationship in a back propagation type of neural network with multiple hidden layers does not help in understanding the physical aspect of the process being modeled. However, a better understanding of the relationship of energy use with an independent variable, for example, outdoor drybulb temperature, is possible when a simpler functional form is used. In addition, unlike BPN, the use of local basis functions may provide a more accurate prediction and a significantly faster optimization because a linear optimization technique such as the method of least squares can be

adopted. A one-hidden-layer neural network of RBFN type corresponds to a simpler input-output relationship and, therefore, can serve the purpose of gaining physical understanding of the process. Also, the optimization is faster than the gradient descent method which is used to train a conventional BPN. Wave-Net, like RBFN, is a one-hidden-layer ANN with wavelet basis functions. However, Wave-Net is superior to an RBFN in the sense that the wavelet basis functions have better localization characteristics. Moreover, the number of hidden nodes (or the basis functions) can be optimized by retaining only the statistically significant smoothing components (known as scaling functions) and detailed components (also known as wavelets). This results in a more compact network architecture. The advantage is even more when an orthonormal set of scaling functions and wavelets are chosen as the bases (Meyer, 1985) because orthonormality allows completely localized training. Boubez and Peskin (1993) described an ANN that uses wavelets as the basis functions and learns by the rule of multiresolution analysis (Mallat, 1989b). They used D4 wavelets developed by Daubechies (1988) and adopted analytical solution technique for determining the weights (the wavelet coefficients). Bakshi and Stephanopolos (1993) developed the same network separately but pointed out that the weights can be determined by using the standard least squares regression method and the choice of wavelet basis will depend on the type of application. A detailed description on wavelet analysis and Wave-Net algorithm developed for modeling hourly energy use in commercial buildings is included in Chapter VII.

Calibrated Simulation Modeling - A Hybrid Approach

There are situations when a little or no pre-retrofit data are available. A calibrated modeling approach may be an appropriate choice for estimating energy use in such cases (Katipamula and Claridge, 1992). The model is developed based on engineering equations and the prediction is calibrated by adjusting system parameters. Calibration can be improved in several ways (Bou-Saada, 1994), for example, (i) suitable time period may be chosen for performing calibrations, (ii) sensitivity analysis can be

performed to identify the parameters that are the most sensitive to a simulation and such parameters may be adjusted to improve the model fit, (iii) indoor temperature calibration may be adopted and (iv) a suitable day-typing technique may be adopted to remove the effect of major changes in operating schedule of the building systems. The calibrated modeling approach has also been used to identify operational improvements in buildings (Liu and Claridge, 1995).

Calibration Time Periods. Testing and modifying the simulation models by using long-term data sets are expensive and time-consuming. An alternative to this is to choose short-term data sets that cover all the seasons of the year. A cold weather month, a hot weather month and a moderate weather month can be used to tune simulation models (Kaplan et al., 1990a). Kaplan pointed out that a cold weather period and a hot weather period may be sufficient to calibrate models for stable weather patterns.

The other method of calibrating models by using short data sets is the Short-Term Energy Monitoring (STEM) method (Subbarao et al., 1990; Balcomb et al., 1993; 1994). STEM essentially uses Primary and Secondary Terms Analysis and Renormalization (PSTAR) method in a building. PSTAR is based on analysis in the frequency domain and allows one to separately determine the building loss coefficient, the building mass and the solar gain area without one factor interfering with the other.

Sensitivity Analysis. The usefulness of sensitivity analysis lies in the fact that it reduces the amount of work needed to finalize the model. This is achieved by (i) identifying the most sensitive parameters from among all those that affect building energy use and (ii) tuning such sensitive parameters to improve the model fit. The first run of simulation is performed to establish a base case reference point and then several runs are performed with extreme value of each parameter that affects the model prediction. The results of these simulations are used to determine the most sensitive parameters. Details

of studies on sensitivity analysis applied to calibration of simulation models may be found in Hsieh et al. (1989), Mahone et al. (1992) and Griffiths and Anderson (1994).

Indoor Temperature Calibration. Calibration of simulation models can be accomplished by matching simulated indoor temperatures to measured indoor temperatures. Hsieh (1988) compared DOE-2 predicted temperatures with measured temperatures to help identify the discrepancy between actual and model predicted energy use. Clarke et al. (1993) conducted a similar test under PASSYS program. Haberl and Komor (1990) used minimum and maximum zone temperatures to verify HVAC system operation.

Day-typing. Energy use in commercial buildings are affected in a major way by the systematic scheduling of the building systems; separating the data set based on major operational changes prior to model development is an important step. The day-typing of energy data may involve either a simple data sorting based on the calendar or a complex statistical analysis. Katipamula and Haberl (1991) proposed a day-typing methodology to identify diurnal load shapes using monitored end-use data. According to this technique, the day-types are generated based on a univariate statistical analysis that assumes any final day-type not to have more than 10% Coefficient of Variance (C.V.-STD). The resulting load shapes were used in DOE-2 calibration (Bronson 1992). A detailed day-typing technique proposed by Dhar et. al (1994b) involves primary day-typing using Duncan's multiple range test (Ott, 1988) and univariate analysis of energy data of each primary day-type in the frequency domain. The key difference between these two approaches is that the earlier considers the standard deviation of the data at each individual hour while the latter considers mean energy use and overall diurnal load shape to identify the final day-types.

Bou-saada (1994) proposed use of graphical indices developed by Abbas (1993) to identify day-types and calibrate DOE-2 simulated prediction with measured data. Use

of C.V. rmse instead of percentage difference for calibration was also proposed. The procedure was illustrated by using the data from USDOE Forrestal building.

In general, the method of developing calibrated simulation models is elaborate and time consuming. The methodology may not be suitable when adequate data are available for developing regression or ANN models (Reddy et al., 1994a).

Summary

In this chapter, a brief description of the literature reviewed on modeling hourly energy use in commercial buildings was presented. Three existing techniques, e.g., regression techniques, ANN approaches and calibrated modeling approaches were reviewed and the development of Fourier series approaches and Artificial Neural Network techniques were identified as the topics of current interest. This is because these two methodologies have the potential to offer high prediction accuracy and are supposed to take less training time than a calibrated modeling approach. Calibrated modeling approaches are, however, superior to regression and ANN approaches for purposes like evaluating the effect of a particular parameter, for example, cold deck temperature of a building HVAC system on the building energy use. The development and application of Fourier series and ANN approaches to model hourly building energy use will be presented in the following chapters.

CHAPTER III
SUITABILITY OF FOURIER SERIES ANALYSIS OF HOURLY
ENERGY USE IN COMMERCIAL BUILDINGS

Introduction

Fourier analysis is one of the most important tools of mathematics and mathematical physics. It originally arose from the problems involving vibrating cords that were being studied by Leonard Euler and Daniel Bernoulli in the 18th century. The subject was named after Jean-Baptist-Joseph Fourier, whose work on the representation of mathematical functions was published in his *Theorie analytique de la chaleur* (The Analytical Theory of Heat) in 1822 (Fourier, 1878).

The present application is the analysis of hourly energy use such as lighting and equipment energy use, electricity use by air handling units, cooling energy use, heating energy use, etc., in commercial buildings; these uses are inherently periodic in nature. The profiles of energy uses repeat themselves in the diurnal cycle due to fixed scheduling, as well as over the annual cycle due to seasonal variation. These energy uses are, therefore, well-suited for Fourier series treatment.

A Fourier series representation of a continuous function is as follows:

$$F(x) = \frac{a_0}{2} + \sum_{k=1}^{\infty} [a_k \sin kx + b_k \cos kx] \quad (3.1)$$

However, when a function needs to be approximated in the form of a Fourier series from a finite number of measured data points in a particular interval, the Fourier series described in eq. 3.1 need to be modified to a finite Fourier series. If $2n+1$ data points are available, then the finite Fourier series takes the following form (Graybill, 1976):

$$F(x) = \frac{a_0}{2} + \sum_{k=1}^n [a_k \sin kx + b_k \cos kx] \quad (3.2)$$

The finite sum from $k = 1$ to n of the weighted trigonometric terms is also called a trigonometric polynomial of order n (or less, if both a_n and b_n are zero). In other words, a trigonometric polynomial of order n has $2n+1$ coefficients $a_1, b_1, \dots, a_n, b_n$ and it can be shown that if $2n+1$ distinct points are fixed in the interval $0 \leq x \leq 2\pi$, there is always a unique trigonometric polynomial of order n or less that takes prescribed values at these points. This idea led to the development of Fourier series modeling of hourly energy use in commercial buildings.

In this chapter, the presence of periodicity in the energy use is illustrated with examples and the theory of Fourier series is discussed. We will start with the discussion of the annual and diurnal periodicity present in the data in the next section.

Periodicity in the Data

As mentioned in the previous section, both weather independent and weather dependent energy use in commercial buildings show periodicity. The daily mean energy use may vary over a year in a building. For example, in educational buildings, energy use is different during spring, summer and fall semesters, semester breaks, Christmas, etc. In addition, the energy use often increases slowly from the beginning of a semester and decreases gradually towards the end. This primarily occurs in the lighting and equipment (LE) energy use or whole building electric (WBE) energy use, which (internal load) in turn affects cooling and heating energy use. Such effects, referred to here as seasonal effect, leads to the presence of periodicity in the annual pattern of energy use. Figure 3.1 shows a time series plot of WBE energy use during 1992 in a large university building (Zachry Engineering Center) on the Texas A&M University campus, while Figure 3.2 shows LE energy use during 1992 in the Business Building of the University of Texas at Arlington (UTA). We note in both plots the increases in energy consumption at the beginning of spring (January), summer (late May) and fall semesters (late August) and drops in energy use at the semester ends. Energy use also drops during spring break and Christmas at these sites. These two examples illustrate the presence of seasonal periodicity in weather independent energy use.

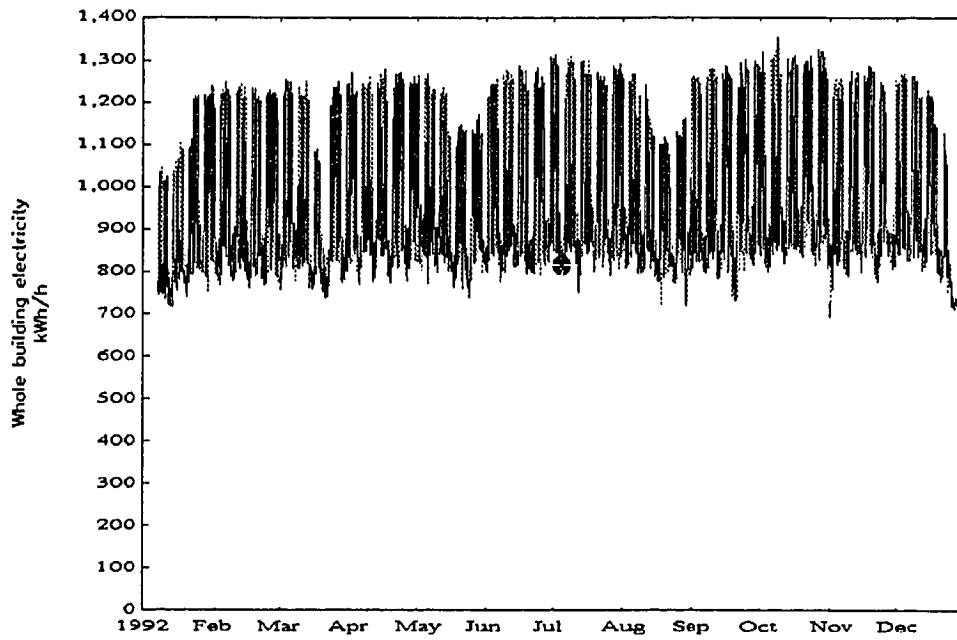


Figure 3.1 Whole building electricity use in the Zachry Engineering Center in 1992. The plot shows the presence of the seasonal effect on energy use.

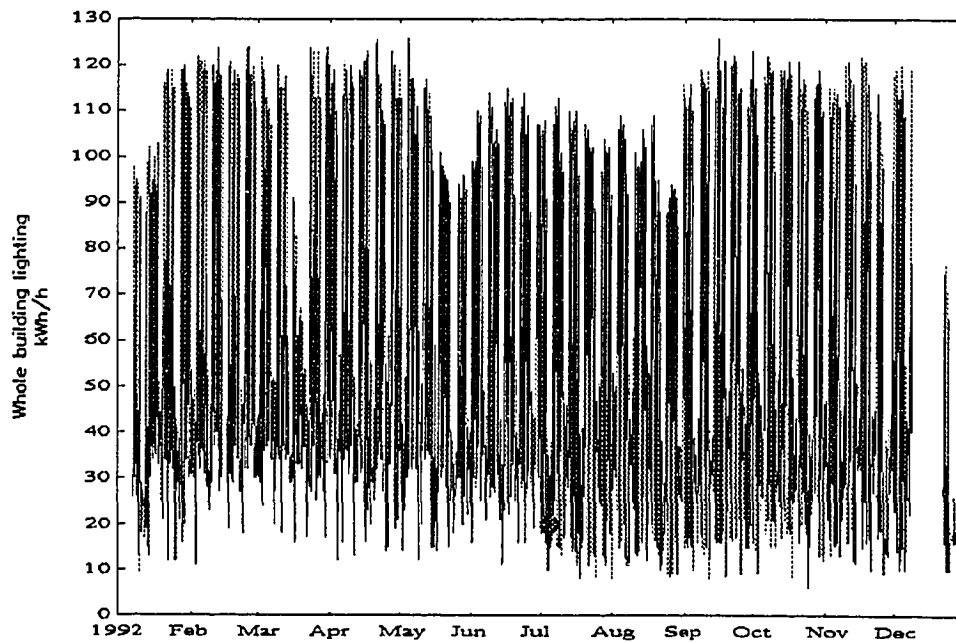


Figure 3.2 Lighting energy use in the Business building of the University of Texas at Arlington in 1992. The plot shows the presence of the seasonal effect on energy use.

Time series plots of cooling energy use in the Zachry Engineering Center and in the Business Building are shown in Figure 3.3 and Figure 3.4 respectively. Although cooling energy use is largely weather dependent, the seasonal effect is observable in these time series plots. The seasonal effect is obvious from the time series plots of heating energy use in Burdine and P. C. Library buildings, both located in University of Texas at Austin (UT) (Figure 3.5 and Figure 3.6).

Apart from the annual periodicity discussed in the preceding paragraph, the pattern of weather independent energy use such as the internal load in a building repeats itself over a day due to the fixed operating schedule of the building. This diurnal periodicity is illustrated by the time series plots of the weather independent energy use during September 1992 and October 1992 in the Zachry Engineering Center and the Business Building (Figure 3.7 and Figure 3.8). It is observed that during the weekdays, energy use starts increasing at around 8 a.m., drops a little during lunch time and again drops sharply in the evening. However, the patterns are different during weekdays and weekends. This is accounted for by day-typing which is discussed in Chapter IV. Time series plots of cooling energy use during September 1992 and October 1992 are shown in Figures 3.9 and 3.10, whereas the time series plots of heating energy use in November 1992 and December 1992 in Burdine building and P.C. Library are shown in Figures 3.11 and 3.12 respectively. As mentioned previously, these energy uses are weather dependent and the plots in Figures 3.9 through 3.12 show diurnal periodicity with varying amplitude due to the weather effect as well as systematic scheduling.

The following section describes how annual and diurnal periodicities can be accounted for in the Fourier series model of energy use in commercial buildings.

Fourier Series Modeling

A general representation of a linear model of energy use is as follows:

$$E = \mu(h) + \varepsilon \quad (3.3)$$

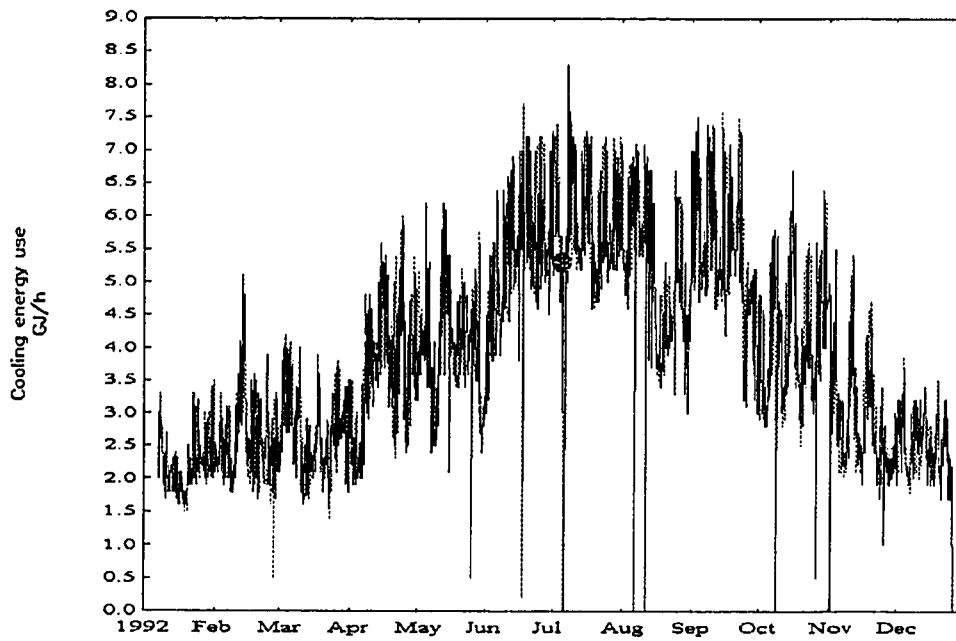


Figure 3.3 Cooling energy use for the Zachry Engineering Center in 1992. The plot shows the presence of the seasonal effect on energy use.

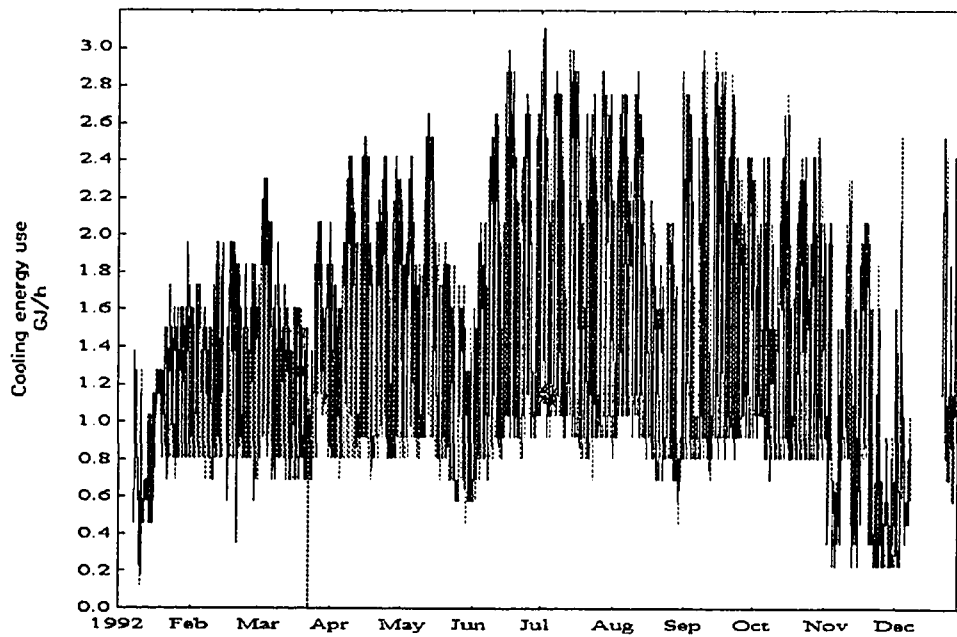


Figure 3.4 Cooling energy use for the Business Building in University of Texas at Arlington in 1992. The plot shows presence of the seasonal effect on energy use.

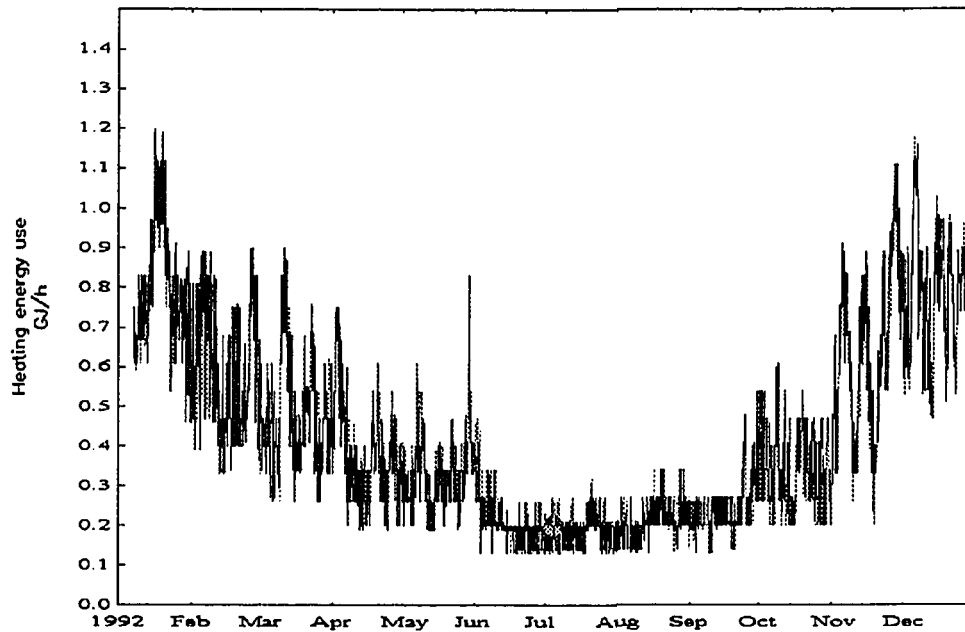


Figure 3.5 Heating energy use in the Burdine Building at UT Austin in 1992. The plot shows the presence of the seasonal effect on energy use.

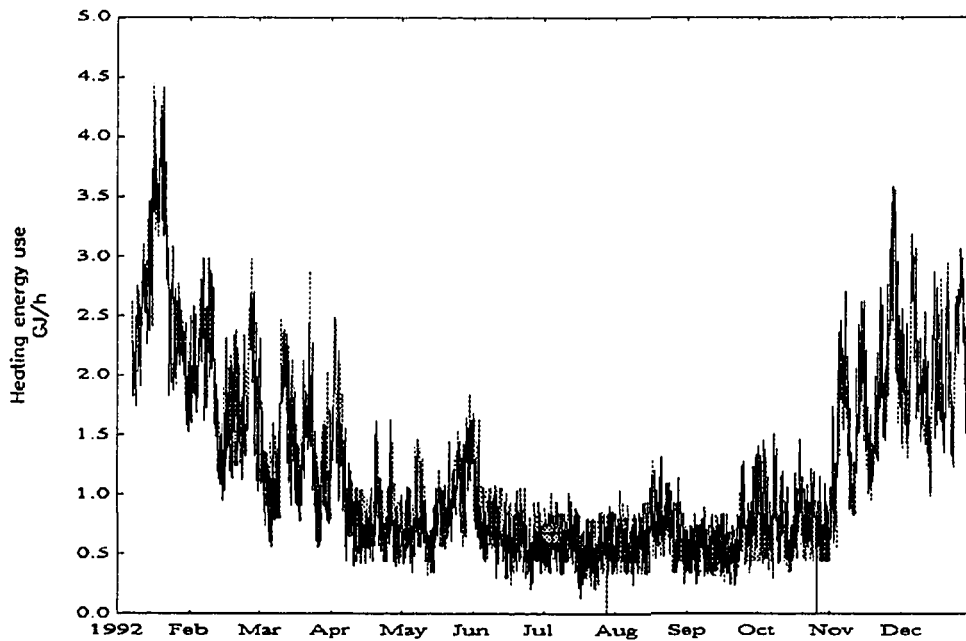


Figure 3.6 Heating energy use in the P.C. Library at UT Austin in 1992. The plot shows the presence of the seasonal effect on energy use.

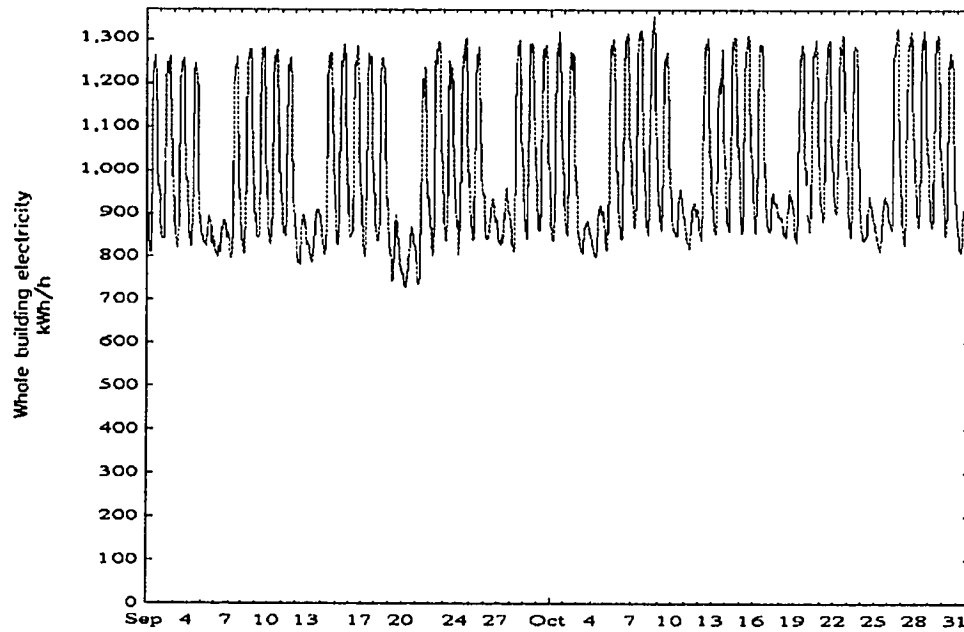


Figure 3.7 A time series plot of whole building electricity use for September 1992 and October 1992 in the Zachry Engineering Center that shows diurnal periodicity.

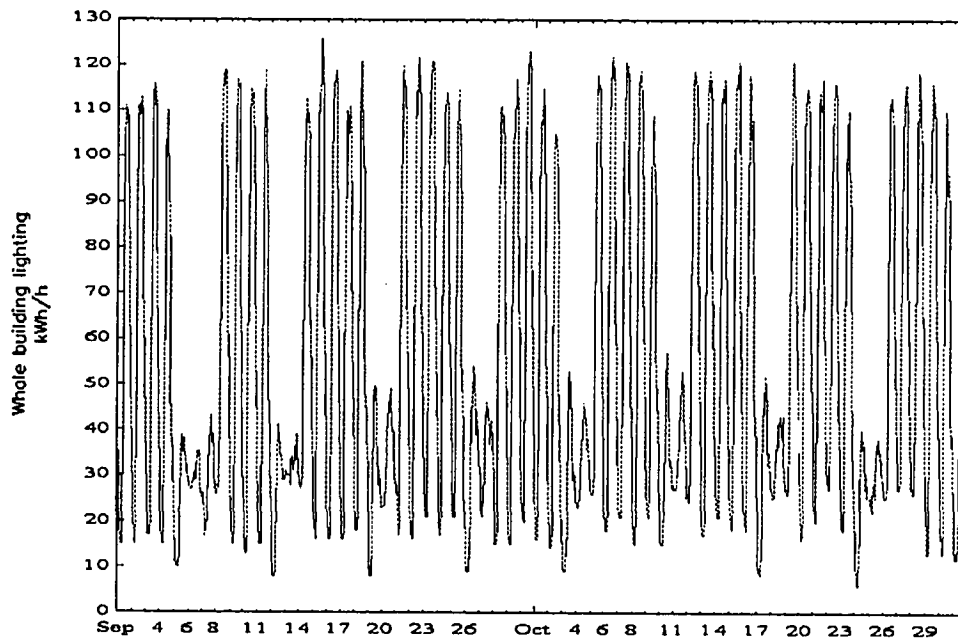


Figure 3.8 A time series plot of lighting energy use in the Business Building at UT Arlington for September 1992 and October 1992 that shows diurnal periodicity.

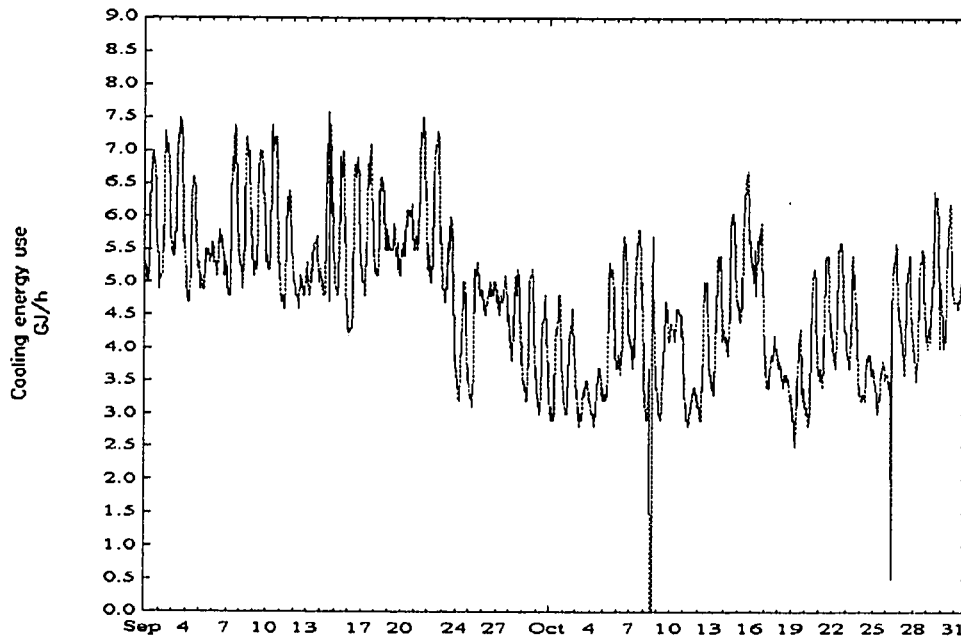


Figure 3.9 A time series plot of cooling energy use during September 1992 and October 1992 of the Zachry Engineering Center which shows diurnal periodicity.

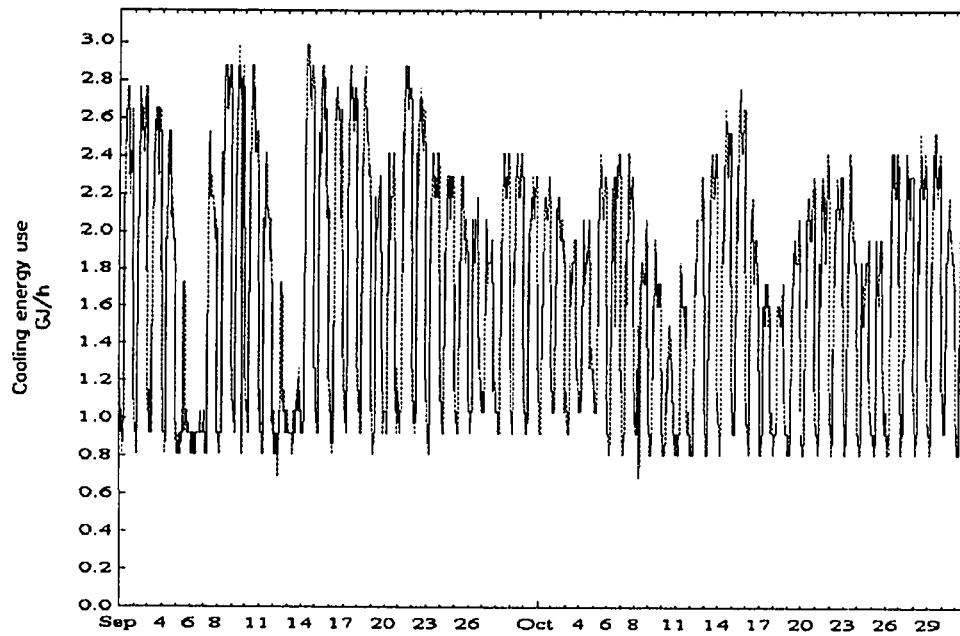


Figure 3.10 A time series plot of cooling energy use in the Business Building at UT Arlington during September 1992 and October 1992 which shows diurnal periodicity.

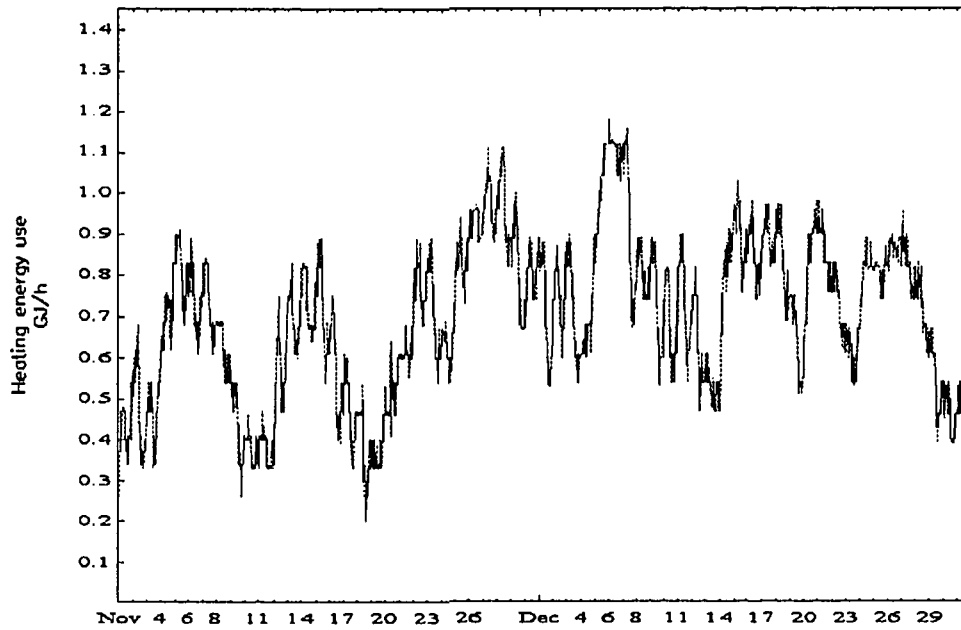


Figure 3.11 A time series plot of heating energy use in the Burdine Building at UT Austin during November 1992 and December 1992 which shows diurnal periodicity.

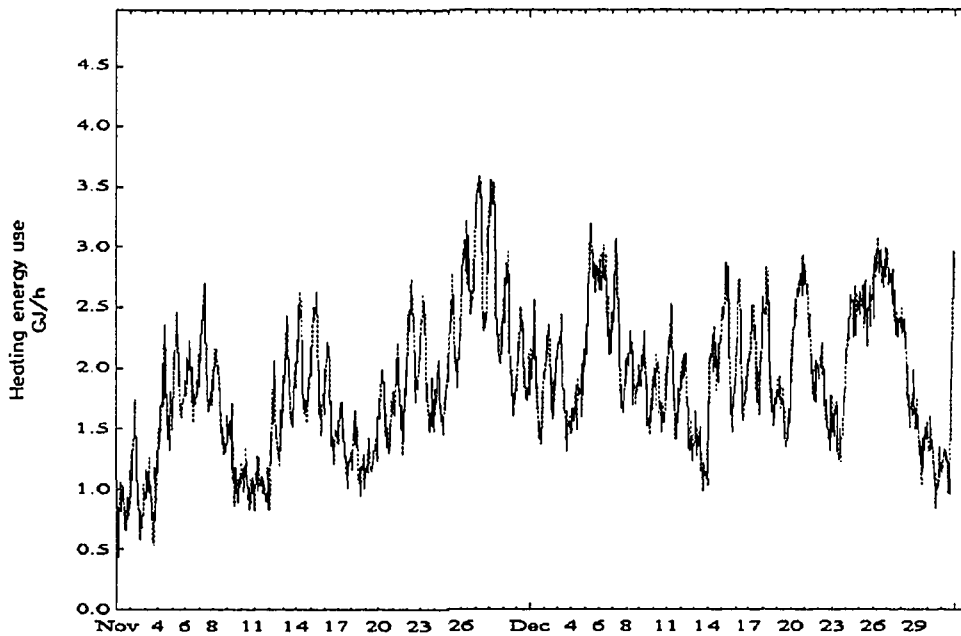


Figure 3.12 A time series plot of heating energy use in the P.C. Library at UT Austin during November 1992 and December 1992 which shows diurnal periodicity.

where E is the energy use, h is the independent variable and ε is the random error. If the variation of E with h is periodic, the function $\mu(h)$ can be represented by a Fourier series (Graybill, 1976).

$$E_h = \beta_0 + \sum_{j=1}^{j_{\max}} \left[\alpha_j \sin \frac{2\pi}{P_j} h + \beta_j \cos \frac{2\pi}{P_j} h \right] + \varepsilon_h, \quad -\infty < h < +\infty \quad (3.4)$$

where E_h is the energy use at hour h , α_j and β_j are the coefficients of the j^{th} sine and cosine frequencies and P_j is the period of the j^{th} frequency. An upper limit on the number of frequencies that can be chosen is $j_{\max} < (h/2)$ since otherwise, the number of parameters will be greater than the number of hours (or measured data points for the data used here) in a day. A model such as equation 3.3 is restrictive in that it does not allow the mean (β_0) and amplitude (combination of α_j and β_j) to vary seasonally. Since the energy use patterns shown in Figures 3.1 and 3.2 do exhibit such variations, a more generalized model would be of the form:

$$E_{d,h} = X(d) + Y(h) + Z(d,h) + \varepsilon_{d,h}, \quad (3.5)$$

$$\text{where } X = \sum_{k=0}^k \left[\gamma_k \sin \frac{2\pi}{P_k} d + \delta_k \cos \frac{2\pi}{P_k} d \right], \quad Y = \sum_{j=0}^{j_{\max}} \left[\alpha_j \sin \frac{2\pi}{P_j} h + \beta_j \cos \frac{2\pi}{P_j} h \right]$$

$$\text{and } Z = \sum_{k=0}^k \sum_{j=0}^{j_{\max}} \left[\phi_k \sin \frac{2\pi}{P_k} d + \psi_k \cos \frac{2\pi}{P_k} d \right] \cdot \left[\eta_j \sin \frac{2\pi}{P_j} h + \zeta_j \cos \frac{2\pi}{P_j} h \right]$$

Note that X and Y represent seasonal and diurnal periodicities respectively, while Z accounts for the interaction between the two. In other words, Y alone will represent a load shape of constant mean and amplitude (a simple sinusoid is shown in Fig. 3.13). When X is added to the expression, variation in mean energy use can also be treated (Fig. 3.14). Addition of Z enables the model equation to represent load shapes with varying mean and varying amplitude (Fig. 3.15). Note that seasonal variation in equation

3.5 is modeled with daily energy data. We have also investigated whether this choice is most appropriate. For example, weekly-mean daily or monthly-mean daily values of energy use could have given "smoother" seasonal variation patterns. Using daily data to represent seasonal variation is logically the best of all three options because it provides analysis at the highest resolution. However, analysis of data from two buildings (results summarized in Table 3.1) has revealed that the choice of the variable for the annual cycle does not make any significant difference.

The annual frequency terms in eq. 3.5 can model the seasonal pattern substantially, as described above. However, the model fit can be improved further by performing suitable day-typing prior to modeling and developing separate model equation for each day-type. A day-typing technique has been described in detail in Chapter IV.

As already mentioned, the hour of day h is the independent variable to represent the diurnal cycle. Since there are 24 hours in a day, one needs to choose the frequencies from the first twelve frequencies. Similarly, a maximum of the first 183 frequencies can be used to account for the annual periodicity. The variable d for the annual cycle is the day of year having value 1 on January 01 and 365 on December 31. In a leap year, however, the longest period of the annual cycle changes to 366.

In addition to modeling weather independent energy use, finite Fourier series representation of a function can be used to model weather dependent energy use such as cooling and heating energy use. The weather variables such as outdoor drybulb temperature, outdoor humidity and horizontal solar flux can be combined with a Fourier series to model weather dependent energy use. These will be discussed in detail in Chapter V and Chapter VI.

Summary

In this chapter, we pointed out that Fourier series is a powerful tool for analyzing periodic data and both weather independent and weather dependent energy use in commercial buildings can be modeled by the Fourier series approach. The presence of

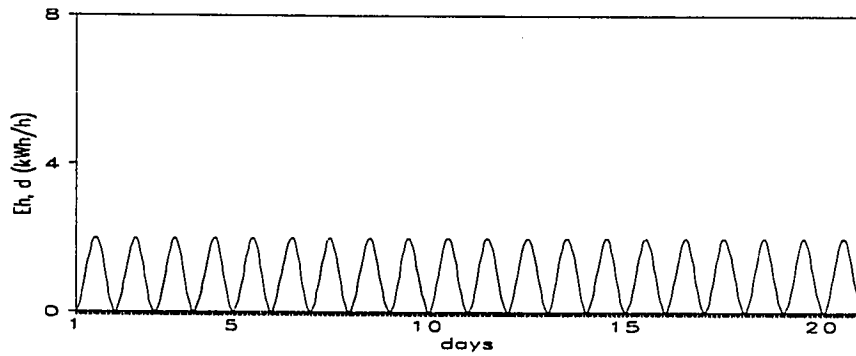


Figure 3.13 Illustrative load profile for $E_{h,d} = X$ with $X = 1 - \cos\left(\frac{2\pi}{24}h\right)$ showing a periodic load shape with constant mean and amplitude.

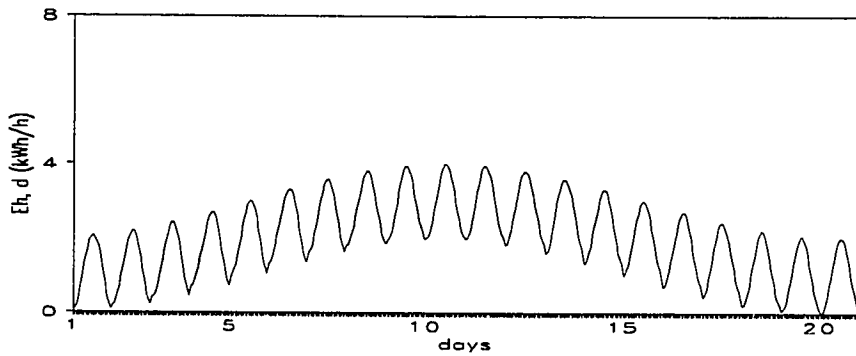


Figure 3.14 Illustrative load profile for $E_{h,d} = X + Y$ with $Y = 1 - \cos\left(\frac{2\pi}{24}d\right)$ showing a periodic load shape with variable mean but constant amplitude.

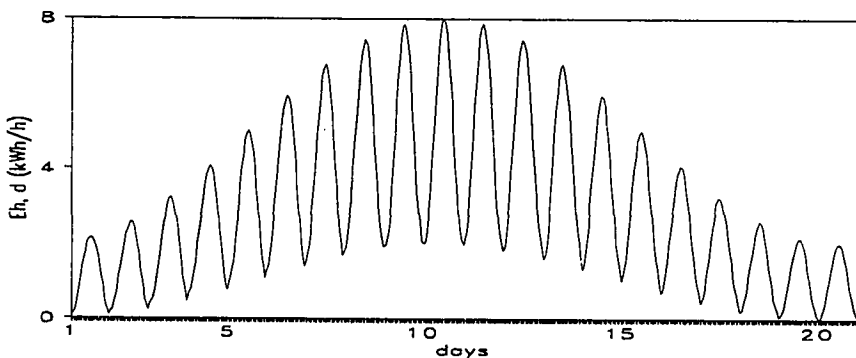


Figure 3.15 Illustrative load profile for $E_{h,d} = X + Y + Z$ with $Z = XY$ showing a periodic load shape with variable mean and amplitude.

Table 3.1 Comparison of R-square and C.V. of various hourly Fourier series models using (a) month, (b) week and (c) day respectively as the time variable which captures annual periodicity of whole building electricity use data.

Site	Time Variable	Day-type	R ²	C. V. (%)
ZEC	day	weekdays	0.93	4.24
		weekends	0.63	3.36
	week	weekdays	0.93	4.25
		weekends	0.63	3.35
	month	weekdays	0.92	4.39
		weekends	0.57	3.59
BUS	day	weekdays	0.83	14.74
		weekends	0.65	16.06
	week	weekdays	0.83	14.81
		weekends	0.65	16.04
	month	weekdays	0.81	15.62
		weekends	0.62	16.90

annual periodicity due to the seasonal effect, and diurnal periodicity due to the fixed operating schedule have been illustrated with monitored data from several buildings. The hour of the day and the day of the year are chosen as the independent variables for the diurnal and annual cycles respectively in the Fourier series functional form. In the end, the usefulness of day-typing in improving the model fit is pointed out.

In the following chapters, the modeling procedure for weather independent and weather dependent energy use in commercial buildings will be described and illustrated with examples.

CHAPTER IV

MODELING WEATHER INDEPENDENT ENERGY USE

Introduction

The previous chapter discussed (i) the presence of periodicity in energy consumption data and (ii) the theory and basis of Fourier series modeling. This chapter presents a Fourier series modeling approach for weather independent energy use and illustrates the same with application to monitored data from several buildings.

Modeling Procedure

The load profile of weather independent energy use depends on the mode of operation of the building systems. Prior to model development, the data set needs to be divided into groups (or day-typed) based on differences in operating schedule of the building systems. A model equation for each day-type is then developed using a statistical procedure which will be described later.

Day-typing. The method of day-typing adopted here involves dividing the data set into primary day groups based on the calendar (weekdays, weekends, holidays and Christmas). Duncan's multiple range test (Ott, 1988) which is a mean comparison test for multiple groups of data, (it considers both mean and standard deviation of the groups to be compared) is then performed and the day-groups with statistically insignificant differences in mean energy consumption are aggregated together. The day-types thus achieved are the primary day-types. Univariate analysis of each important frequency that appears in the model of energy use is then performed separately for each primary day-type to further divide the data into multiple day-types. The important frequency are those which appear consistently in a particular type of building. It will be shown later on in this chapter that the following frequencies consistently appear for weather independent load shapes:

$$\sin \frac{2\pi}{24}h, \cos \frac{2\pi}{24}h, \cos \frac{4\pi}{24}h \text{ and } \sin \frac{8\pi}{24}h.$$

The above terms correspond to the sine and cosine terms for the frequencies with 24-hour, 12-hour and 6-hour periods respectively. A histogram of the amplitude for each frequency is developed and checked for multimodal distribution behavior. Only if (i) the histogram is multimodal and (ii) a physical reason can be attributed to such a distribution, is it recommended that the particular primary day-type be divided into groups. The last step of day-typing is to repeat the Duncan test and aggregate the day-types with statistically insignificant differences in mean energy consumption. The day-typing procedure described above is illustrated further in the flow charts in Figures 4.1a and 4.1b.

Modeling. The modeling procedure for weather independent energy use in commercial buildings is shown in Figure 4.2. To start with, the model equation 3.5 is rewritten as follows:

$$E_{d,h} = X(d) + Y(h) + Z(d,h) + \varepsilon_{d,h}, \quad (4.1)$$

$$\text{where } X = \sum_{k=0}^{k_{\max}} \left[\gamma_k \sin \frac{2\pi k}{365}d + \delta_k \cos \frac{2\pi k}{365}d \right], \quad Y = \sum_{j=0}^{j_{\max}} \left[\alpha_j \sin \frac{2\pi j}{24}h + \beta_j \cos \frac{2\pi j}{24}h \right]$$

$$\text{and } Z = \sum_{k=0}^{k_{\max}} \sum_{j=0}^{j_{\max}} \left[\phi_k \sin \frac{2\pi k}{365}d + \psi_k \cos \frac{2\pi k}{365}d \right] \bullet \left[\eta_j \sin \frac{2\pi j}{24}h + \zeta_j \cos \frac{2\pi j}{24}h \right]$$

We note from the above equation that the right hand side has a large number of terms. However, while modeling actual energy use in commercial buildings, the data will generally support only a few terms in the final model equation. This will be illustrated later in this chapter.

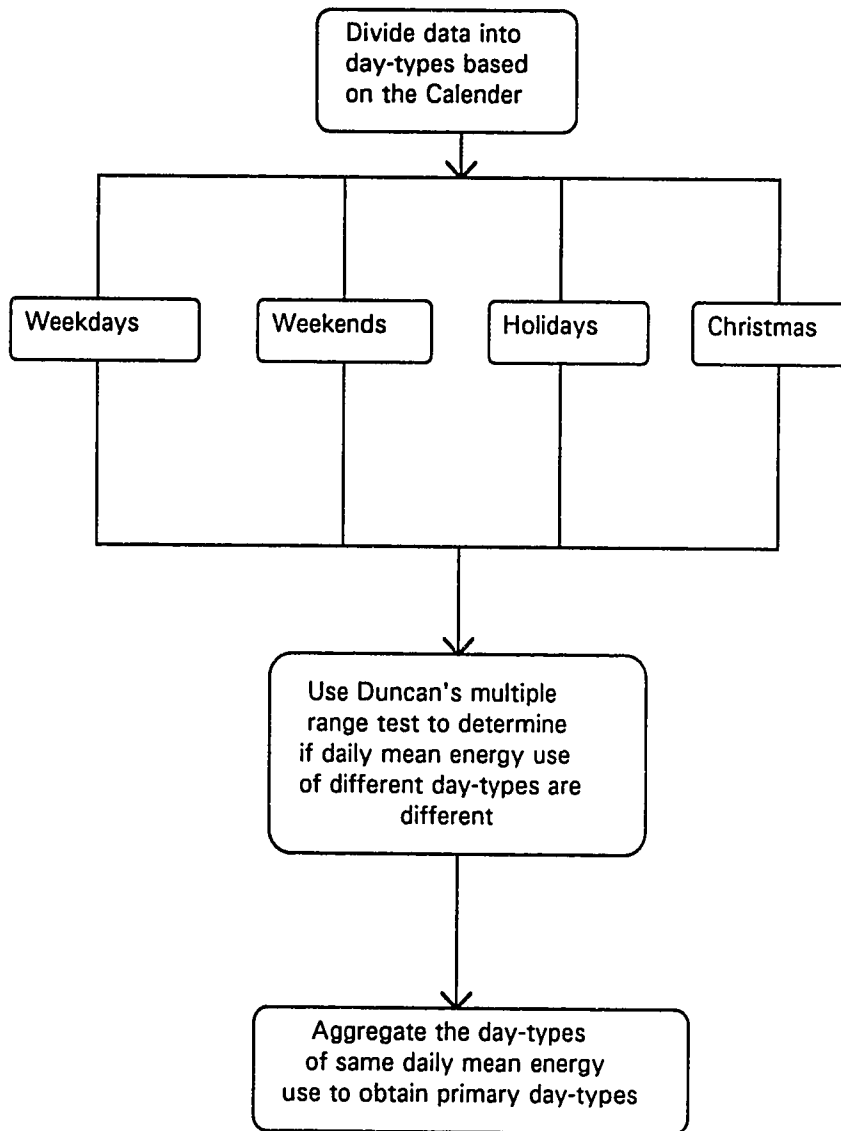


Figure 4.1a Stage I of a day-typing procedure used in conjunction with Fourier series approach to model hourly energy use in educational buildings. Primary day-types are created from data at this stage.

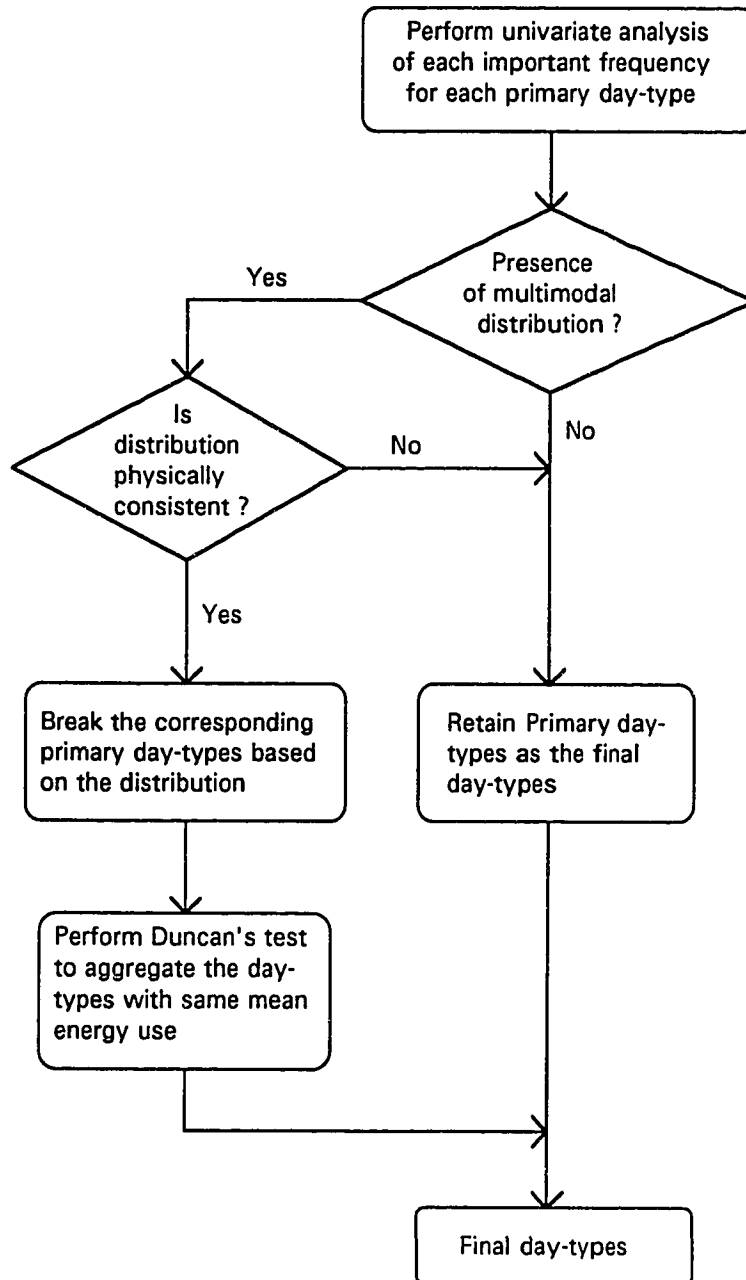


Figure 4.1b Stage II (final stage) of a day-typing procedure used in conjunction with the Fourier series approach to model hourly energy use in educational buildings. Final day-types are determined from primary day-types at this stage.

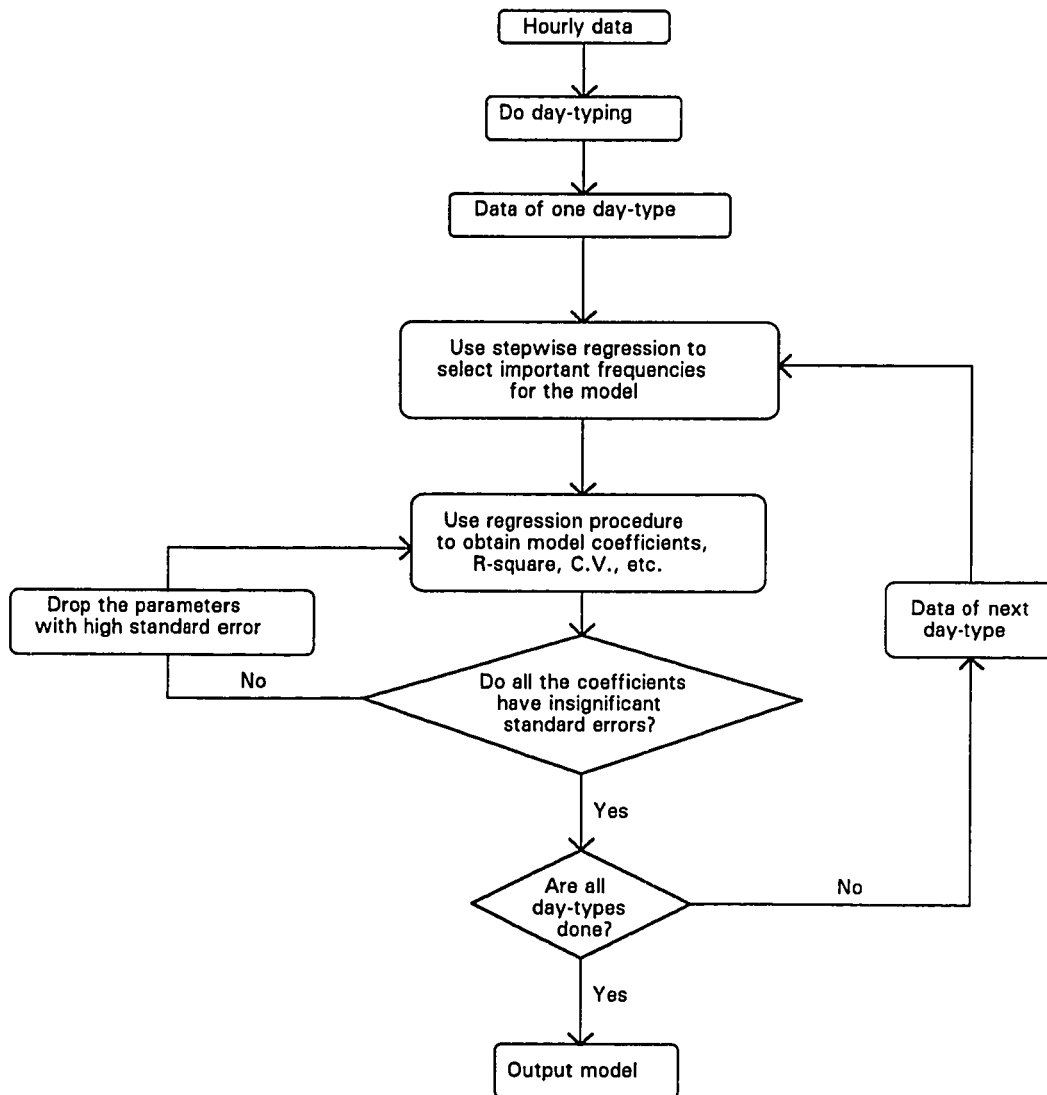


Figure 4.2 The procedure adopted in the present Fourier series approach to model hourly energy use in commercial buildings.

Equation 4.1 is the Generalized Fourier Series (GFS) model equation for weather independent energy use in commercial buildings. For a particular day-type, hourly data is used and stepwise forward selection performed to select the significant independent variables from the set of Fourier frequencies. Mallows's $C(p) \approx p$ for minimum p , the number of independent parameters including the intercept, is used as the criteria for such selection (Ott, 1988). The $C(p)$ statistic is defined as follows:

$$C(p) = \frac{SSE_p}{s_e^2} - n + 2p$$

where SSE_p is the sum of squares of error from a model with p parameters including the intercept, s_e is the mean square error of the regression with largest possible number of independent variables and n is the number of observations.

Once the parameters of the models are selected using $C(p)$ criteria, regression is performed using the selected frequencies. However, the model may contain parameters with significant standard error. In that case, a suitable level of significance (say, 10%) may be used as the criteria to drop the parameters with significant standard error. The procedure is repeated for all the day types and finally, a set of model equations for all day types is obtained.

The above procedure, when applied to measured energy use, often identifies a large number of terms for the final model equations. Higher frequency terms sometimes may have negligible partial R-square and may improve model fit marginally. A reasonable cut-off criteria of partial R-square (0.005) may be used to retain only the important frequency terms in the final model equations.

Model Development from Short Data Sets

A year-long data set contains all possible day-types and model equations for all the day-types may be developed by applying the procedure described in the previous sections. However, if data is available for only a short period prior to retrofitting, model equations for all the day-types can not be developed directly. In such cases, model equations for the day-types for which data is unavailable may be developed by using

post-retrofit data. For example, if there are some data for working weekdays but no data for Christmas during the pre-retrofit period, then the data for the Christmas period is generated from the working weekday model by using a factor F_h , which is the ratio of the mean energy use at a particular hour during Christmas to the mean energy use of the corresponding hour during working weekdays in the post-retrofit condition. The data generated for Christmas can then be used to develop the Fourier series model for the pre-retrofit Christmas period. However, it may be noted that this method does not work if the retrofit involves a schedule change.

$$F_h = \frac{\bar{E}_{h, \text{post, Christmas}}}{\bar{E}_{h, \text{post, working weekdays}}}, \quad (4.2)$$

$$E_{h, \text{pre, Christmas}} = F_h \times E_{h, \text{pre, working weekdays}}$$

Application to Monitored Data

The Fourier series approach has been applied to model monitored data collected from various LoanSTAR sites. A detailed study of one example (whole building electric energy use in the Zachry Engineering Center, ZEC) is presented and the results of several other examples are discussed in this section.

ZEC, a large educational building, contains class rooms, labs, offices and computer facilities. The seasonal and diurnal variation of whole building electric energy use (E_{wbe}) can be observed in the time series plots shown in Figures 3.1 and 3.7 in the previous chapter. Cooling and heating energy in this building is supplied from a central plant and, therefore, E_{wbe} shows insignificant weather (primarily outdoor drybulb temperature) dependence.

Day-typing. The one-year data (1992) of E_{wbe} is grouped by using the calendar and the following groups are obtained: (i) working weekdays, (ii) weekends, (iii) holidays (1st January, spring break: 16th March to 20th March, 3rd July, Thanksgiving: 26th and 29th November), referred to as holiday group and (iv) 23rd to 31st December,

referred to as Christmas group. The primary day-types are then identified by performing Duncan's multiple range test the results of which are summarized in Table 4.1. The test indicated insignificant difference between the weekend and the holiday group. Weekend and holiday groups were, therefore, aggregated together and three primary day-types were obtained.

The next step is to convert the hourly energy consumption data to daily frequency content information. This essentially enables one to store the diurnal profile information in a concise way. The histograms for each of the frequencies of each day-type are then developed and inspected for the presence of multiple modes. Although the histogram of the daily-mean hourly energy use (which is the intercept or zeroth frequency term in a Fourier series model) did not show any clear presence of multiple modes (Figure 4.3), the histogram of the first cosine frequency of working weekday group had a bimodal distribution (Figure 4.4). When the data of working weekday group was divided based on the histogram shown in Figure 4.4, days during the semester breaks were separated out. Note that the analysis mentioned here enables one to compare both mean energy use and overall diurnal profile and fix the final day-types accordingly. Duncan's test was performed again (the results are summarized in Table 4.2) on four day-types which suggested that the four groups be accepted as the final day-types: (i) weekdays school-in-session, (ii) weekends, (iii) semester break weekdays and (iv) Christmas.

Model Development. The generalized functional form suggested by equation 4.1 is used to regress hourly data of each day-type using stepwise regression with the forward selection procedure. A widely used criteria to select the optimum number of significant frequencies is the Mallows's $C(p) \approx p$ criteria (Ott, 1988). The above procedure, when applied to model energy use, often retains a large number of terms in the final model.

Table 4.1 Results of Duncan's multiple range test performed to identify primary day-types for whole building electric energy use in ZEC in 1992.

Analysis of Variance Procedure				
Duncan's Multiple Range Test for variable: WBELEC				
Alpha= 0.1 df= 8607 MSE= 18920.47				
Harmonic Mean of cell sizes= 417.2411				
Number of Means 2 3 4				
Critical Range 18.92 19.89 20.52				
Means with the same letter are not significantly different.				
Duncan Grouping	Mean	N	DAYTYPE	
A	1008.279	5756	1	working weekdays
B	847.467	192	3	holidays
B	838.736	2399	2	weekends
C	792.687	264	4	Christmas

Table 4.2 Results of Duncan's multiple range test performed to identify final day-types for whole building electric energy use in ZEC in 1992.

Analysis of Variance Procedure				
Duncan's Multiple Range Test for variable: WBELEC				
Alpha= 0.1 df= 8607 MSE= 17579.29				
Harmonic Mean of cell sizes= 467.727				
Number of Means 2 3 4				
Critical Range 14.40 15.22 15.80				
Means with the same letter are not significantly different.				
Duncan Grouping	Mean	N	DAYTYPE	
A	1028.016	4821	1	working weekdays
B	906.513	935	4	semester break weekdays
C	839.383	2591	2	weekends, holidays
D	792.687	264	3	Christmas

Stem Leaf	Frequency
109 2	1
108 0013379	7
107 0033456	7
106 01122347889	11
105 00001122344566799	17
104 011112223344444566667788899999	30
103 0112233444555556666777789	24
102 011111111112233444444445556666777888999	38
101 000112446777778888899999999	29
100 0111222246789	13
99 11234467789	11
98 112345667888	12
97 4569	4
96 0378	4
95 13558999	8
94 4	1
93 257889	6
92 000199	6
91 2288	4
90	
89	
88 89	2
87	
86 16	2
85 56	2

Multiply Stem.Leaf by 10, e.g., 109 2 means $109.2 = 1092$ (frequency = 1).

Figure 4.3 Frequency distribution of mean whole building electric energy use for working weekday group in ZEC during 1992.

Stem Leaf	Frequency
-11 86	2
-12 2	1
-12 66	2
-13 433322111100	12
-13 9888766555	10
-14 4432100	7
-14 998	3
-15 444321100	9
-15 99987666	8
-16 4333221110	10
-16 999888887665555555	19
-17 44444333333332210000000	24
-17 999999888877777666666655555555	35
-18 44444333322221111100000	25
-18 999988777776666665555555	27
-19 444443332222222211100	23
-19 99998886655	12
-20 3000	4
-20 655	3
-21 3	1

Multiply Stem.Leaf by 10, e.g., -11 86 means $-11.8 \times 10 = -118$ and $-11.6 \times 10 = -116$ (frequency = 2).

Figure 4.4 Frequency distribution of first cosine frequency of whole building electric energy use for working weekday group in ZEC during 1992.

This is seen in Table 4.3 where 29 parameters (the mean or intercept term needs to be included as well) are suggested by the criteria $C(p) \approx p$.

A last refinement to the selection process is to drop the higher frequency terms that have negligible partial R-squares. Thus, if we choose an arbitrary but reasonable cut-off of 0.005 in partial R-square, then only the first 7 parameters need be retained in the model, yielding a model R-square of 0.9427 as against 0.9611 when all 29 terms are included. However, the stepwise regression results show that Z terms (equation 4.1) were insignificant in this case, meaning that energy use during weekdays with school-in-session has load shapes with fairly constant amplitude.

Table 4.4 presents results of applying the above procedure to monitored data for lights and electricity use (E_{le}) and whole building electricity use (E_{wbe}) for ZEC, E_{wbe} for Medical School Building (MSB) in Houston and E_{wbe} for two educational buildings in UT Austin (WEL and PAI). Model results for both pre-retrofit and post-retrofit conditions in ZEC and MSB are presented. The regression R-squares are excellent for the working weekday group which contains the largest number of days, while the R-squares are generally poorer for the other groups. This is partly because of the way R-square is computed:

$$R^2 = \left[1 - \frac{\sum_n (E - \hat{E})^2}{\sum_n (E - \bar{E})^2} \right], \quad n = \text{number of hourly observations in a day-type.} \quad (4.3)$$

where E , \hat{E} and \bar{E} are the measured, predicted and mean energy use respectively. Since R-square is a statistic which depends on the degree to which data scatter about the mean as explained by the model, a model fitted to data that have less scatter is likely to have a poorer R-square value. Consequently, one should also look at the Coefficient of Variation (C.V.) of the Root Mean Square Error (RMSE) in order to get a complete evaluation of the fit. We note that C.V.s are low enough (all the C.V.s in Table 4.4 are

Table 4.3 Summary of the forward selection procedure for whole building electricity use during working weekdays in ZEC. Data period covers the calendar year 1992. Standard errors of all variables are statistically insignificant (less than $F = 0.0001$). CH_i (& SH_i) and CD_i (& SD_i) represent the i th frequency of the cosine (and sine) terms of the diurnal cycle and of the annual cycle respectively.

No. of parameters	Variable entered	Partial R^2	Model R^2	C(p)
2	CH1	0.6092	0.6092	43582.1
3	SH1	0.2670	0.8762	10497.9
4	CH2	0.0413	0.9175	5388.0
5	SH4	0.0123	0.9298	3863.5
6	SH3	0.0068	0.9366	3024.4
7	SD1	0.0061	0.9427	2274.2
8	CH3	0.0034	0.9461	1852.8
9	SD2	0.0031	0.9492	1469.0
10	SH2	0.0024	0.9516	1177.1
11	CH4	0.0022	0.9538	907.5
12	CD4	0.0016	0.9554	708.2
13	SD5	0.0016	0.9570	509.2
14	SD4	0.0011	0.9581	375.0
15	CH1*SD1	0.0005	0.9586	320.7
16	SH1*SD1	0.0004	0.9590	269.4
17	CH1*SD2	0.0004	0.9594	225.6
18	CD3	0.0003	0.9597	186.4
19	CH5	0.0003	0.9599	157.2
20	SH5	0.0002	0.9602	131.7
21	CD2	0.0002	0.9603	111.9
22	SH2*SD1	0.0002	0.9605	95.2
23	CD1	0.0001	0.9606	83.7
24	SH1*SD3	0.0001	0.9607	72.3
25	CH1*SD3	0.0001	0.9608	62.0
26	CH1*CD1	0.0001	0.9609	51.3
27	SH1*CD4	0.0001	0.9610	42.2
28	SH1*SD4	0.0001	0.9611	33.0
29	CH1*SD4	0.0000	0.9611	29.3
30	SH3*SD1	0.0000	0.9611	25.6

Table 4.4 Fourier model results of weather independent energy use at four educational buildings in Texas.

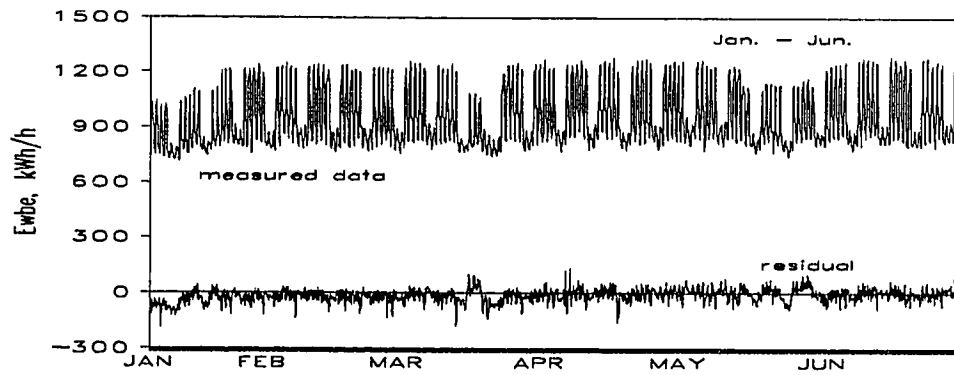
Building name	Energy use	Period	Data length	Day-type	R ²	C.V. (%)
ZEC	E _{le}	Pre-retrofit	9/1/89 - 12/31/89 (4 months)	Weekdays school-in-session	0.96	4.1
				Weekends	0.64	5.1
				Christmas	0.87	8.4
ZEC	E _{wbe}	Post-retrofit	1/1/92 - 12/31/92 (12 months)	Weekdays school-in-session	0.94	3.8
				Weekends	0.41	4.4
				Semester break weekdays	0.84	9.5
				Christmas	0.33	4.7
MSB	E _{wbe}	Pre-retrofit	9/1/91 - 8/6/93 (35 months)	Weekdays	0.95	3.3
				Weekends	0.36	4.5
MSB	E _{wbe}	Post-retrofit	8/7/93 - 11/30/94 (16 months)	Weekdays	0.93	4.5
				Weekends	0.61	4.6
				Christmas	0.70	7.8
WEL	E _{wbe}	Post-retrofit	1/1/93 - 12/31/93 (12 months)	Weekdays school-in-session	0.90	5.0
				Weekends	0.68	5.3
				Semester break weekdays	0.73	7.1
				Christmas	0.79	5.2
PAI	E _{wbe}	Post-retrofit	1/1/93 - 12/31/93 (12 months)	Weekdays school-in-session	0.82	6.9
				Weekends	0.27	6.8
				Semester break weekdays	0.44	9.6
				Christmas	0.34	5.7

below 10%) in all the cases for the models to be deemed satisfactory. The accuracy of the model fit is illustrated in Figures 4.5 where time series plots of measured energy use and of the residuals (i.e., the difference between measured and model predicted values) for ZEC in 1992 are shown during different periods of the year.

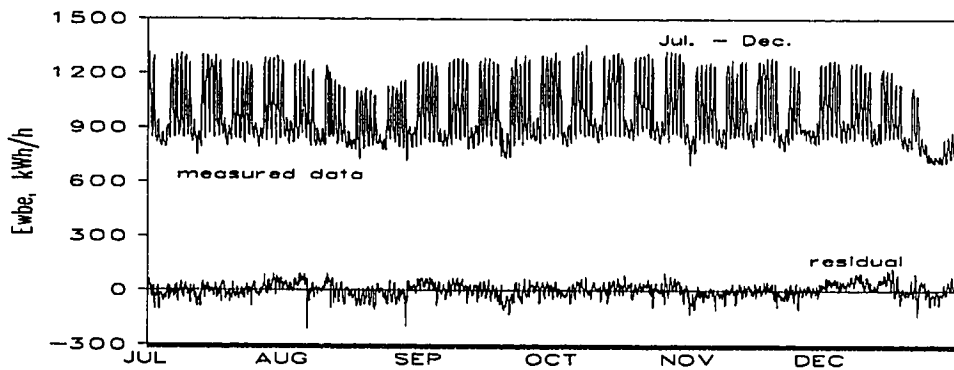
Identifying Important Frequencies

The objective of this section is to detect the common scheduling patterns under which different educational buildings operate. This is easily done by studying the Fourier frequencies retained by a stepwise regression to monitored E_{wbe} data. For most of the buildings, we have found the number of model terms to be between seven and twelve.

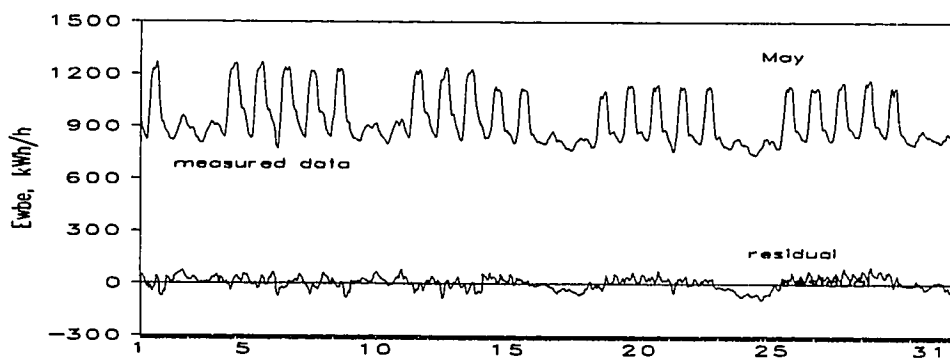
However, it is observed that the first four or five frequencies explain most of the variation (see the partial R^2 values in Table 4.3). This is also illustrated in Figures 4.6 and 4.7 which show individual and cumulative contributions of successive sine and cosine frequencies. Hence, it is more convenient to compare just these terms across buildings. Data from eighteen buildings described in Table 4.5 are used for this purpose. Three months' continuous data (working weekdays only) was chosen based on the availability of clean data for these eighteen buildings. Fourier series models were developed and the frequencies that have significant partial R-square (greater than 0.005) were selected. Once the models were developed, all the Fourier coefficients of the independent variables were normalized by dividing by the mean energy use (i.e., the model intercept). These coefficients are plotted in Figure 4.8 for 18 sites. Other than SIM (which is an elementary school) and DMS (which is a middle school), TDH (which is an office building) and PCL (which is a university library), all other sites are university buildings. We observe that for most of the university buildings, four frequencies that consistently appear are CH1, SH1, CH2 and SH4. Frequencies SH5, CH7 and SH7 were never selected while SH2, CH3, SH3, CH6 and SH6 appeared only in models of some buildings whose load profiles were distinctly different from the others because of operational differences. An important conclusion is that most of the university buildings, though operated in different campuses, seem to be operated in like fashion, with the same four frequencies (CH1, SH1, CH2 and SH4) appearing consistently. CH1 and SH1 are the strongest and represent the overall diurnal behavior. CH2 is the 12-hour frequency and is due to the fact that institutional buildings are occupied roughly 12 hours and unoccupied during the remaining 12 hours. SH4, the 6-hour frequency, is picked up by the model due to the dip in energy use around noon when lunch breaks are taken (Figure 4.9). The contribution of first, second, third and fourth frequencies can also be noted in Figure 4.10.



(a)

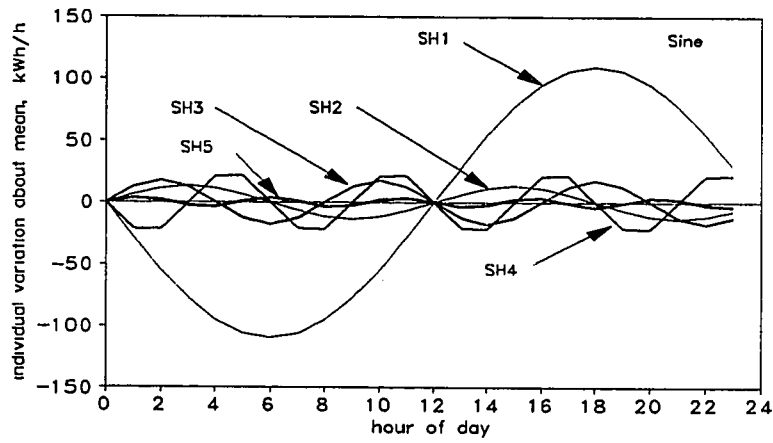


(b)

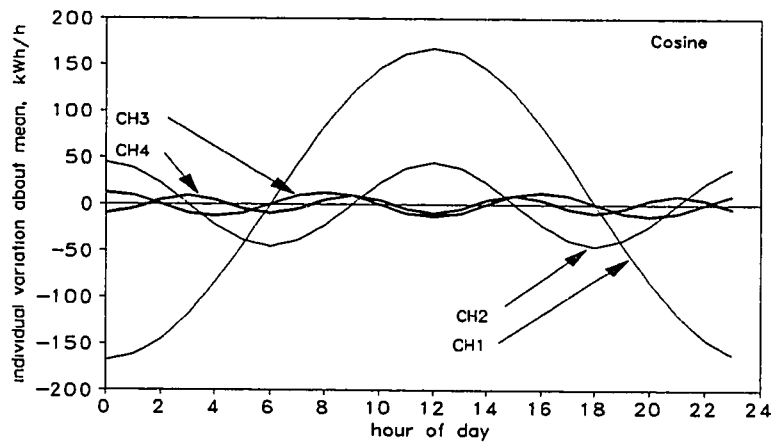


(c)

Figure 4.5 Time series plots of measured and residual whole building electricity use in ZEC for (a) January-June 1992, (b) July-December 1992 and (c) May 1992.

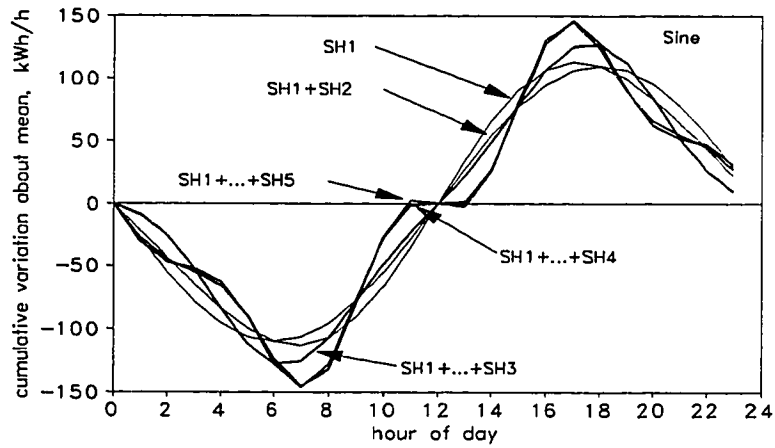


(a)

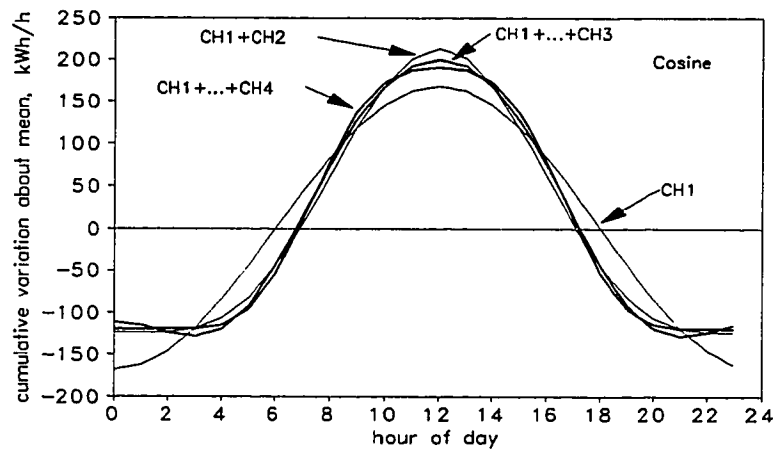


(b)

Figure 4.6 Individual contribution of sine (a) and cosine (b) frequencies of the Fourier series model of E_{wbc} in ZEC during weekdays.



(a)



(b)

Figure 4.7 Cumulative contribution of sine (a) and cosine (b) frequencies of the Fourier series model of E_{wbc} in ZEC during weekdays.

Table 4.5 Key descriptors of Texas buildings whose monitored data were analyzed during this study.

Sl. No.	Build- ing	Location	Type of building	Area (m ²)
1	EDB	Austin	Class rooms, offices	23,340
2	UTC	Austin	Class rooms	14,190
3	PCL	Austin	Library	44,970
4	GAR	Austin	Class rooms, offices, auditorium	5,020
5	GEA	Austin	Class rooms, offices, labs	5,670
6	WAG	Austin	Class rooms, offices, labs	5,350
7	WEL	Austin	Class rooms, offices, labs	40,850
8	BUR	Austin	Class rooms, lecture halls, offices, auditorium	9,610
9	NUR	Austin	Class rooms, lecture halls, lounges	8,810
10	WIN	Austin	Class rooms, offices, theatre	10,130
11	RAS	Austin	Class rooms, offices, labs	5,280
12	PAI	Austin	Class rooms, offices, labs	11,930
13	WCH	Austin	Class rooms, offices, workshops, auditorium	4,550
14	ZEC	College Station	Class rooms, labs, offices, computer facilities	30,150
15	BUS	Arlington	Class rooms, lecture halls	13,930
16	TDH	Austin	Offices, labs	12,730
17	SIM	Fort Worth	School	5,800
18	DMS	Fort Worth	School	8,630

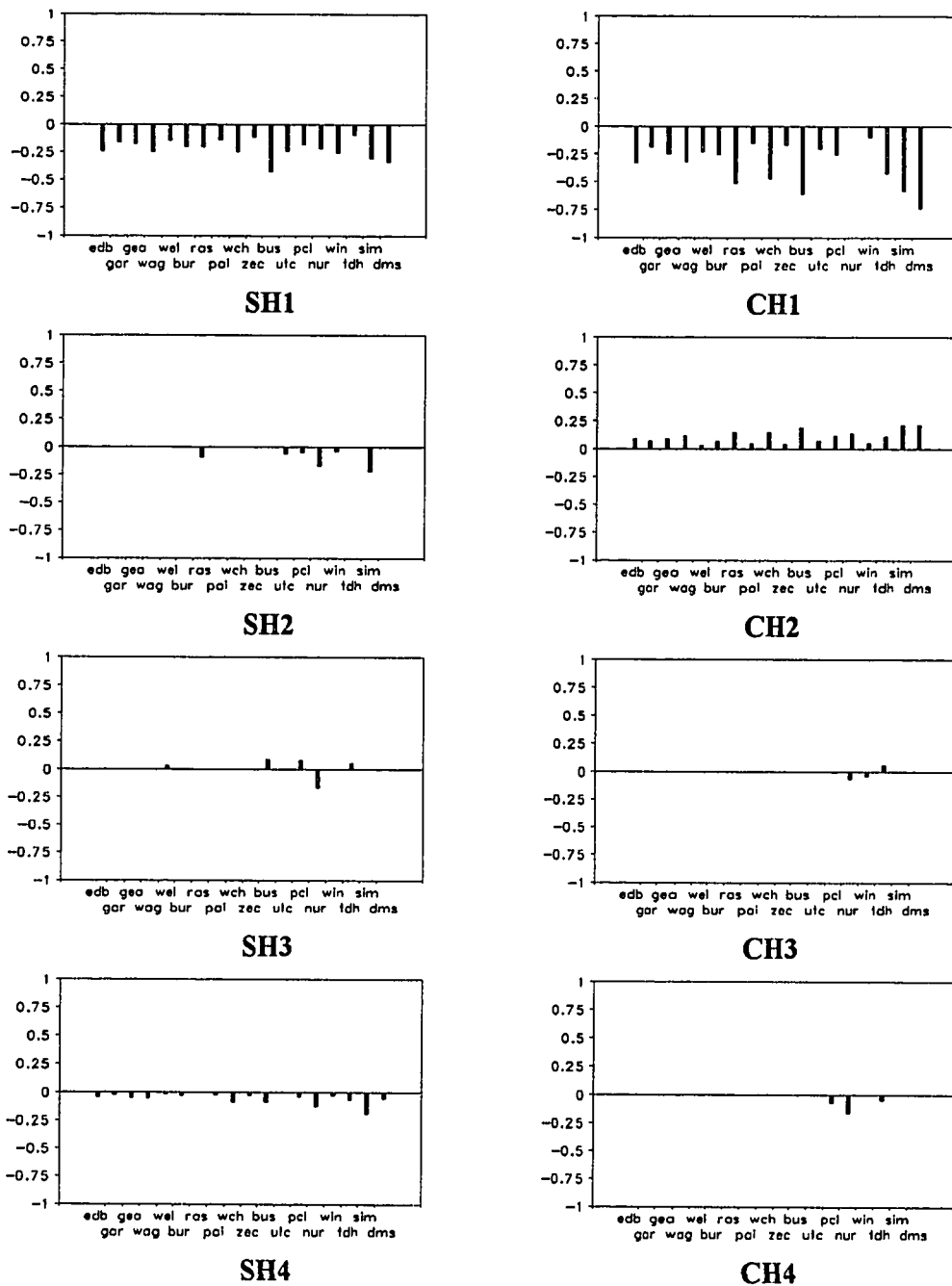


Figure 4.8 Plots of normalized (divided by model intercept, i.e., mean energy use) Fourier coefficients of weather independent energy use models at eighteen sites. Note that SH1, CH1, CH2 and SH4 are common to nearly all models.

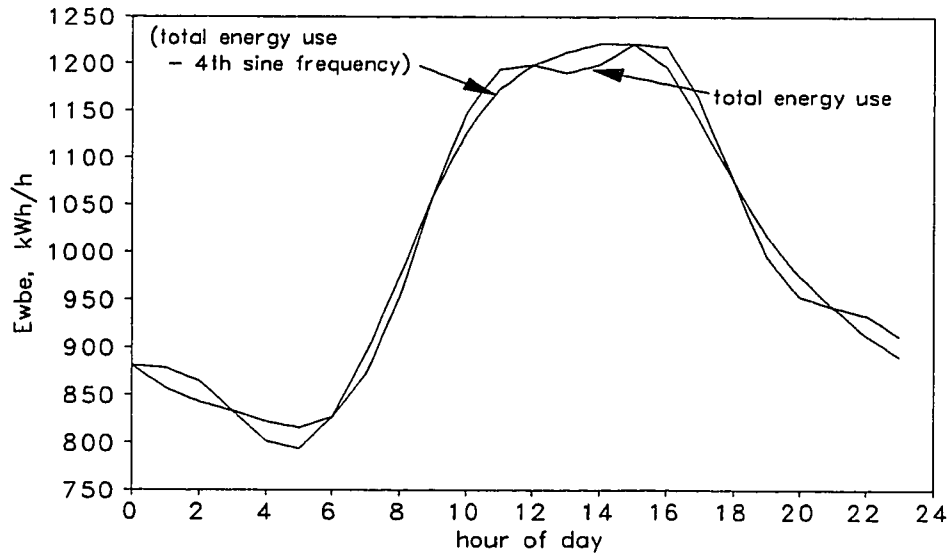


Figure 4.9 The plot shows how fourth sine frequency modifies the diurnal profile to model the dip in energy use around noon.

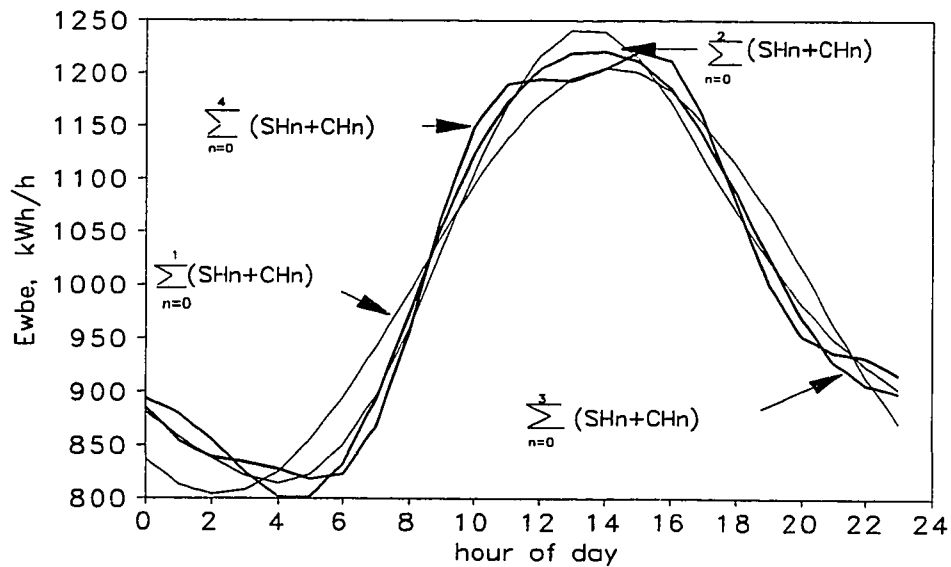


Figure 4.10 Cumulative frequency plot of the Fourier series model for E_{wbe} in ZEC during weekdays.

Summary

In this chapter, we have discussed in detail the Generalized Fourier Series (GFS) approach for modeling weather independent energy use in commercial buildings in detail. This modeling approach has been illustrated by examples from several commercial buildings. The results show that (i) the GFS approach gives high prediction accuracy consistently, (ii) the model development is easy and (iii) the frequency content can be interpreted to gain physical understanding of operating schedule of building systems.

In the next chapter, the GFS approach for modeling weather dependent energy use in commercial buildings will be presented.

CHAPTER V

GENERALIZED FOURIER SERIES (GFS) MODELING OF WEATHER DEPENDENT ENERGY USE

Introduction

Cooling and heating energy use in a commercial building are weather dependent and are affected by the systematic scheduling of building systems. A suitable model, therefore, needs to be developed that will incorporate the effect of the scheduling periodicity and of the weather variables. In this chapter, the Generalized Fourier Series (GFS) approach to model weather dependent energy use is presented. The methodology is illustrated by application to monitored data from several buildings.

Model Equation

A suitable model for weather dependent energy use, that incorporates the effects of both scheduling and periodicity in the weather variables can be developed by combining the weather variables with Fourier series. Both heating and cooling energy use may have significant dependence on outdoor temperature, outdoor humidity and solar radiation. Moreover, building cooling loads have two components: sensible and latent. The sensible heat gains are mainly due to the internal sensible heat load, the transmission and radiation gains through walls, roofs and windows. The latent heat gains are primarily affected by the moisture content of the fresh air intake, and also by the internal latent heat gains which are typically smaller. Instead of simply including, say the outdoor specific humidity (W) as a variable in the model, it is more appropriate to choose the humidity difference between W and the saturated specific humidity of air at the mean cooling coil surface temperature of the HVAC system (Katipamula et al., 1994). For the educational buildings, this temperature is typically close to 12.8 °C (55 °F). The saturated specific humidity corresponding to this temperature being 0.0092 kg. per kg. of dry air, the driver for the latent load is $W^+ = (W - 0.0092)^+$ where $^+$ signifies that W^+ should be set to zero if $W < 0.0092$ kg. per kg. of dry air.

Thus, a general linear equation for modeling thermal cooling energy use at each individual hour h (and for each day-type) is:

$$E_h = a_h + b_h T_h + c_h W_h + d_h I_h + \varepsilon_h \quad (5.1)$$

where T is the outdoor dry bulb temperature and I is the global solar radiation on a unit horizontal surface. Subscript h stands for a particular hour of day and can be arbitrarily assumed to be 0 at midnight, 1 at 1 a.m. and so on. When sensible heating energy use is being modeled, the coefficient c_h should be set to zero.

The coefficients of the above model may vary significantly from one hour to the next over the day due to the combined effect of several factors. Internal heat gain varies according to the diurnal operating schedule of the building. Variation of b_h over a day is due to the thermal lag behavior of a building. The coefficients c_h vary over a day due to the varying infiltration or ventilation rate. Also, solar gain of the building shows different linear relationships with horizontal solar flux due to the changing position of the sun during different hours of the day and days of the year. A model such as equation 5.1, if used for all hours of the day (without distinguishing between individual hours), forces the coefficients to assume "mean" values which are oblivious to the combined effect of factors mentioned above. As a result, poorer fits are obtained (Katipamula et al., 1994). More importantly, physical insight into the building operating schedule is lost. Analysis of monitored data from several Texas LoanSTAR buildings (Claridge et al., 1991) has suggested that the diurnal variation of each of these coefficients is also conveniently modeled by a Fourier series. To illustrate the fact, the results of application to cooling and heating energy use data from ZEC during September 01, 1989 to December 22, 1989 are presented here. The regressions have been performed for each hour of the day separately, using equation 5.1. Variation of the coefficients a , b , c and d of equation 5.1 from hour to hour for cooling and heating energy use are presented in Figures 5.1 and 5.2 while Figure 5.3 presents the R^2 values and the C.V. values for each hour of the day. Though the patterns shown in Figures 5.1 and 5.2 vary from building to building, it has been found

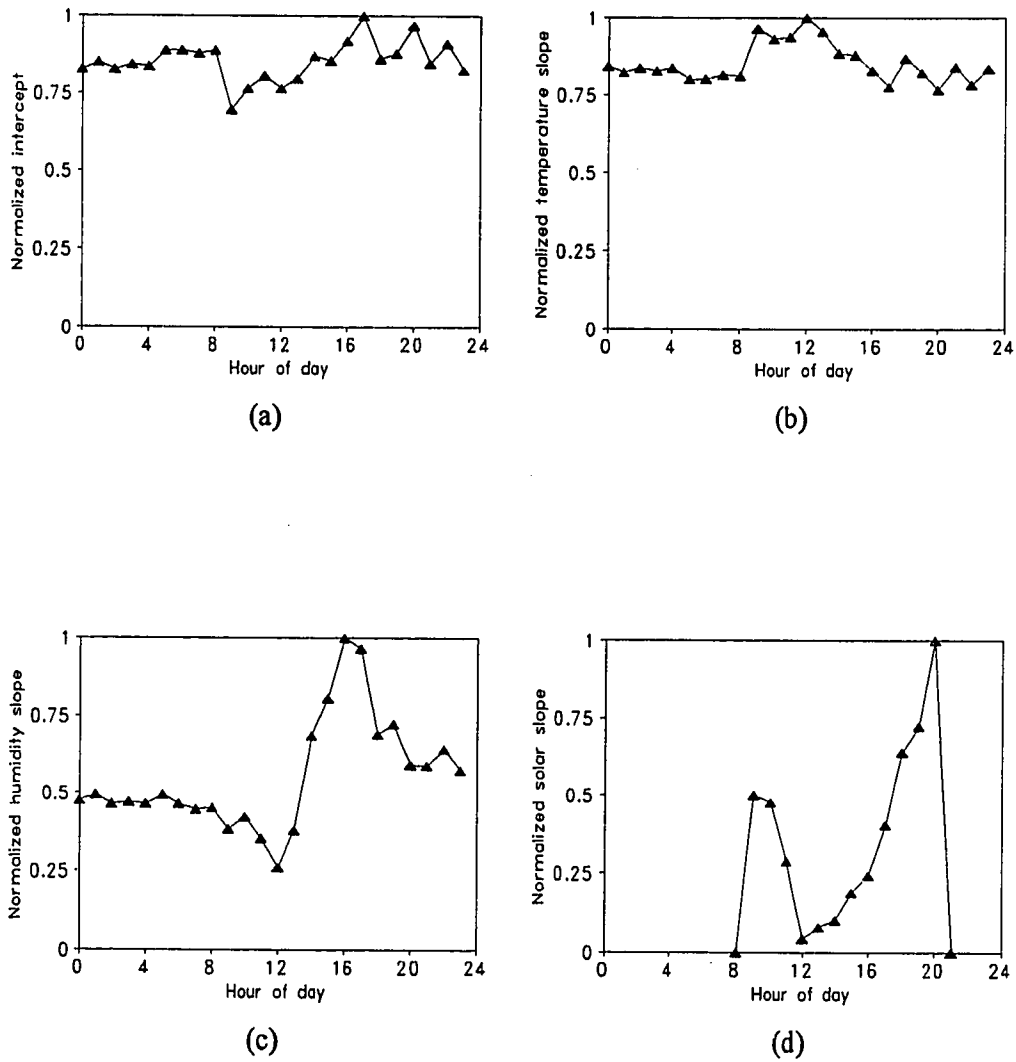


Figure 5.1 A plot illustrating how (i) the normalized coefficients (intercept (a), temperature slope (b), humidity slope (c) and solar slope (d)) in equation 5.1 vary from hour to hour of the day when regressions are performed for each hour of the day separately. Data chosen is the cooling energy use in ZEC from 1st September 1989 to 22nd December 1989 (working weekdays only).

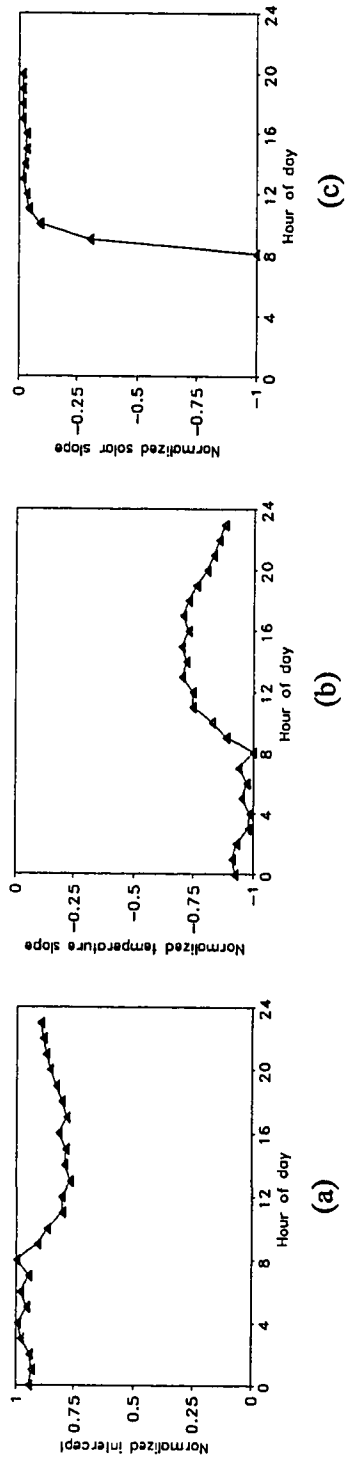


Figure 5.2 A plot illustrating how (i) the normalized coefficients (intercept (a), temperature slope (b), and solar slope (c)) in equation 5.1 vary from hour to hour of the day when regressions are performed for each hour of the day separately. Data chosen is the heating energy use in ZEC from 1st September 1989 to 22nd December 1989 (working weekdays only).

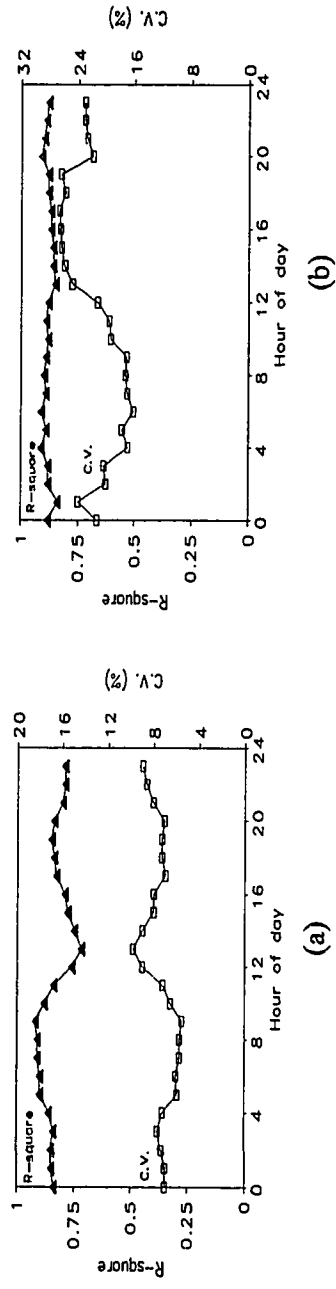


Figure 5.3 R-square and C.V. plots of individual hourly models of cooling energy use (a) and heating energy use (b) in ZEC during September 01, 1989 to December 22, 1989 (working weekdays only).

that these diurnal variations, if modeled by low order Fourier frequency models, yield overall model fits which sacrifice little in terms of accuracy when compared to individual hourly regression models. For example, the individual hourly model approach, when applied to the above chilled water data, yields C.V. values of 7.5% and 6.3% for weekdays and weekends respectively. Fourier modeling, on the other hand, results in C.V. values of 7.7% (with 5 terms in the model) and 6.3% (with 4 terms in the model) for weekdays and weekends respectively. The reduction in the number of model terms is substantial as the individual hour model requires four parameters for each individual hour of the day, i.e., 96 model parameters for the entire day.

The variation of each coefficient of equation 5.1 from hour to hour in a day, if represented by a Fourier series, results in a complete Generalized Fourier Series (GFS) model equation for weather dependent energy use which takes the following functional form:

$$E_{h,d} = \sum_k k \cdot (X_k + Y_k + Z_k) \quad (5.2)$$

where $k = I, T, W^+$ and I ,

$$X = \sum_{k=0}^{k_{\max}} \left[\gamma_k \sin \frac{2\pi k}{365} d + \delta_k \cos \frac{2\pi k}{365} d \right], \quad Y = \sum_{j=0}^{j_{\max}} \left[\alpha_j \sin \frac{2\pi j}{24} h + \beta_j \cos \frac{2\pi j}{24} h \right]$$

and

$$Z = \sum_{k=0}^{k_{\max}} \sum_{j=0}^{j_{\max}} \left[\phi_k \sin \frac{2\pi k}{365} d + \psi_k \cos \frac{2\pi k}{365} d \right] \cdot \left[\eta_j \sin \frac{2\pi j}{24} h + \zeta_j \cos \frac{2\pi j}{24} h \right]$$

The specific humidity terms should be omitted for purely sensible heating energy use models. It may be noted that the right hand side of equation 5.2 has a large number of terms. However, as will be illustrated later, the data for weather dependent energy use will only support a regression model with some of these terms. The choice of which terms to retain is made based on a combination of statistical tests and arbitrary but realistic cut-off criteria which will be described later.

Modeling Procedure

The modeling procedure for weather dependent energy use consists of two steps: (i) day-typing and (ii) model development. The proposed day-typing methodology for weather dependent energy use is less rigorous than the day-typing technique described for weather independent energy use in Chapter IV. The entire data set is regressed by using the following equation and Duncan's multiple range test is then performed on the residuals (ϵ_h):

$$E_h = a + bT_h + cW_h^+ + dI_h + \epsilon_h \quad (5.3)$$

The groups with insignificant difference in mean as suggested by the Duncan's test are aggregated together to arrive at the final day-types.

Although an elaborate day-typing of weather dependent energy use can be performed using the above equation, a mere separation of data into weekday and weekend groups is adequate in many cases (Dhar et al., 1994). This is possible because in most of the buildings, the effect of weather variables on heating or cooling energy use is more dominant than the effect of scheduling. The holidays and Christmas-days may be merged with the weekends, while other possible day-types may be merged with the weekdays. A detailed day-typing is recommended only when a mere separation to weekdays and weekends groups does not give adequate prediction accuracy.

Once day-typing is complete, the model equation for each day-type is developed using the procedure described for weather independent energy use, but the functional form used is as given in equation 5.2.

Application to Monitored Data

Several channels of pre-screened hourly energy data from different buildings in Texas have been modeled by using the GFS approach. In order to illustrate the methodology, modeling (i) hourly cooling energy use during the complete year of 1992 in the ZEC building and during June 1993 to August 1993 in the TCOM building and (ii)

heating energy use in the Burdine building during January 1992 to June 1992 will be elaborated. In addition, results of application to monitored data from several other buildings will be presented.

Cooling Energy Use. Hourly cooling energy use (E_{cw}) was regressed by using the model equation 5.3 and the residuals (ϵ_h) were grouped by using the calendar. The groups initially identified were (i) weekdays, (ii) weekends, (iii) holidays (spring break: 16th March to 20th March, 3rd July, Thanksgiving; 26th and 27th November) and (iv) Christmas (23rd December to 31st December). The Duncan's multiple range test was then performed the results of which are summarized in Table 5.1. The results indicated significant differences between the groups. The initial groups were, therefore, retained as the final day-types. Note that the results of the Duncan's test performed on the residuals supports the recommended weekday-weekend grouping without doing the day-typing, as mentioned earlier in this chapter.

The procedure for model development in this case is similar to that described for weather independent energy use. Again, stepwise regression is used to determine the significant terms from the set of variables suggested by equation 5.2. The model results of hourly cooling energy use in two sites (ZEC and TCOM, medical buildings 1 and 2 combined) are summarized in Table 5.2. The ZEC models exhibit a dramatic switch in the contributions of T and W^+ from weekdays to weekends. This is unphysical and is probably due to the multi-collinearity effect between both variables, a problem inherent in any multivariate regression model. The previous cut-off of partial R-square < 0.005 is also used for final selection of the set of independent variables. It is noted that standard errors of coefficients are all within an acceptable limit (probability value ≈ 0.05). R-square values of the models for ZEC are 0.91 for weekdays and weekends while C.V. RMSE values are 11.4% and 10.5% respectively.

From Table 5.2 we notice that, again, none of the Z terms (see equation 5.2) are significant. Also, in the weekday model for ZEC, the sine or cosine frequencies do not appear with as significant partial R-square as in the case of TCOM. This is probably due

Table 5.1 Results of Duncan's multiple range test performed on the cooling energy use residuals in ZEC in 1992.

Analysis of Variance Procedure performed on residual cooling energy use			
Duncan's Multiple Range Test for variable: CW			
Alpha= 0.1 df= 7917 MSE= 0.270353			
Harmonic Mean of cell sizes= 265.65			
Number of Means 2 3 4			
Critical Range .07494 .07922 .08222			
Means with the same letter are not significantly different.			
Duncan Grouping	Mean	N	DAYTYPE
A	0.16825	5385	1 weekdays
B	-0.35661	2251	2 weekends
B			
B	-0.35904	166	3 holidays
B			
B	-0.36748	119	4 Christmas

Table 5.2 Summary of Fourier series modeling for hourly cooling energy use in ZEC (calendar year 1992) and TCOM (June 1993 to August 1993).

Day-type	Site : ZEC			Site : TCOM, Medical bldg.#1 and #2		
	Variable	Parameter estimate	Partial R ²	Variable	Parameter estimate	Partial R ²
Week-days	INTERCEPT	-0.676646	---	INTERCEPT	741.178092	---
	T	0.060440	0.8042	T	15.544362	0.6902
	W ⁺	220.226594	0.0719	T*CH1	-3.587543	0.1146
	T*CH1	-0.008279	0.0179	SH2	-130.040015	0.0369
	I*SH1	-9.291279	0.0082	SH1	-10.938855	0.0183
	CH1	0.347601	0.0024	W ⁺	49790	0.0364
	---	---	---	CH2	82.483933	0.0094
	---	---	---	T*CH3	0.82728	0.0074
Week-ends	---	---	---	T*SH1	-2.460015	0.0028
	INTERCEPT	-0.336695	---	INTERCEPT	386.8111	---
	T	0.047930	0.1420	T	15.683302	0.7685
	W ⁺	227.931758	0.7780	W ⁺	28765	0.0357
	SH1	0.413418	0.0010	W ⁺ *CH3	64.547557	0.0053

to the considerable diurnal variation of the internal load in TCOM. R-square and C.V. RMSE values for TCOM are 0.91 and 7.31% during weekdays and 0.82 and 9.69% during weekends. The time series plots of measured cooling energy use and of the residuals in ZEC are shown in Figure 5.4.

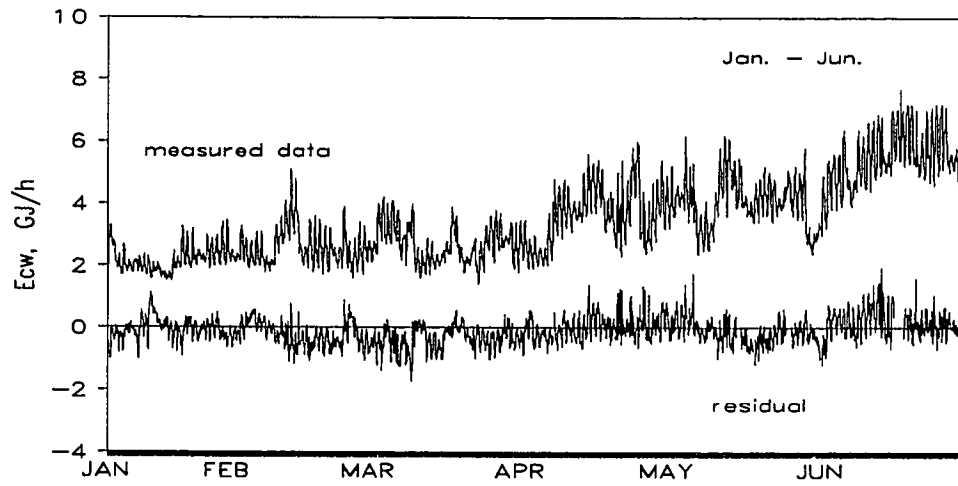
Heating Energy Use. The procedure used to develop the heating energy use model follows that for cooling energy use except that the humidity terms are dropped from equation 5.2 before it is used for model development. The heating energy use in the Burdine building in UT Austin campus from January 1992 to June 1992 was day-typed into weekday and weekend groups and models were developed for both groups. The model parameters and their partial R-squares are summarized in Table 5.3. It may be noted from Table 5.3 that the cosine frequency and the product of the sine frequency and outdoor temperature appeared with significant partial R-square in the final model, reconfirming the variation in slope from hour to hour as illustrated in Figure 5.2. R-square and C.V. values are 0.87 and 17.03% for weekdays and 0.87 and 16.59% for weekends respectively. The time series plots of measured energy use and of residuals are shown in Figure 5.5.

Results from Several Buildings

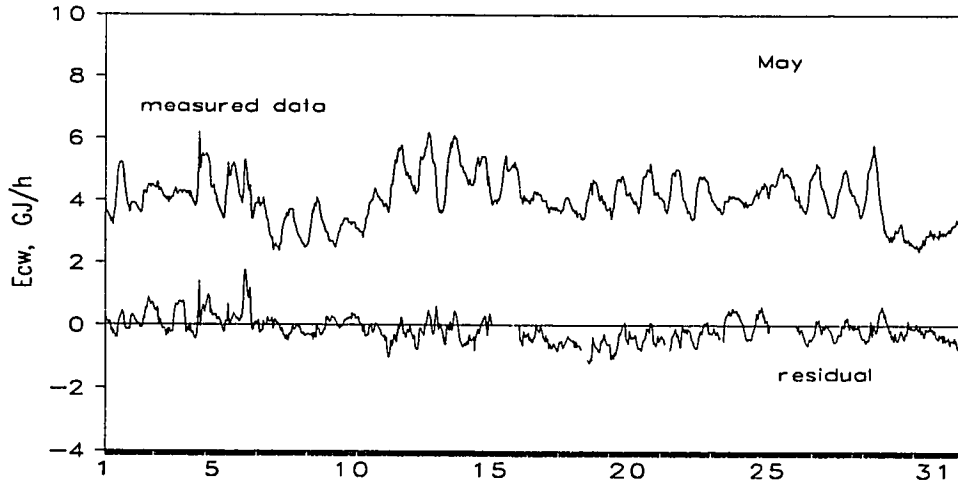
Results from use of the Fourier series modeling approach on weather dependent energy data from five buildings are summarized in Table 5.4. We note from the R-square and C.V. values that the present Fourier series approach gives consistently good fit with R-square values being generally higher than 0.8. The four highest C.V. values are all for the heating energy use models. This is consistent with results from other models of heating energy use (Kissock et al., 1992).

Effect of Short Data Sets

Very often, we do not have energy use data for a whole year. When data for one, two or three months are available, models developed from such short data sets do not

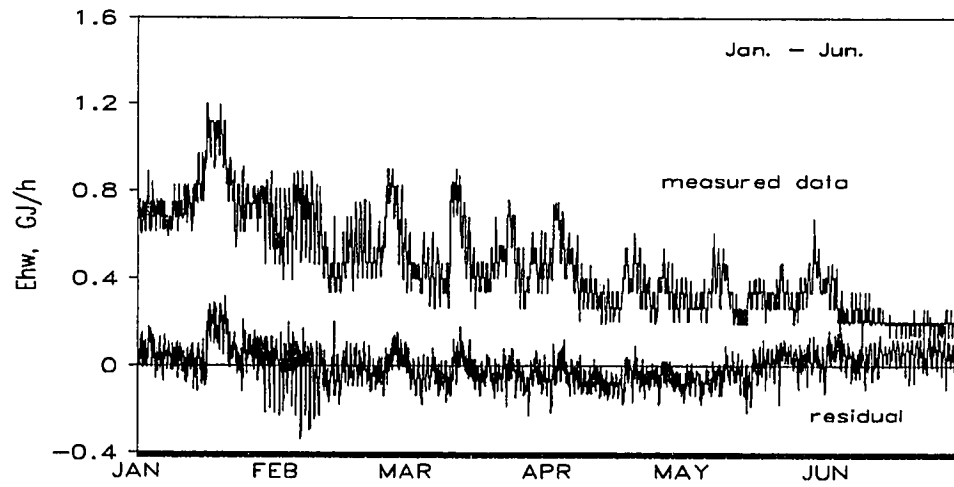


(a)

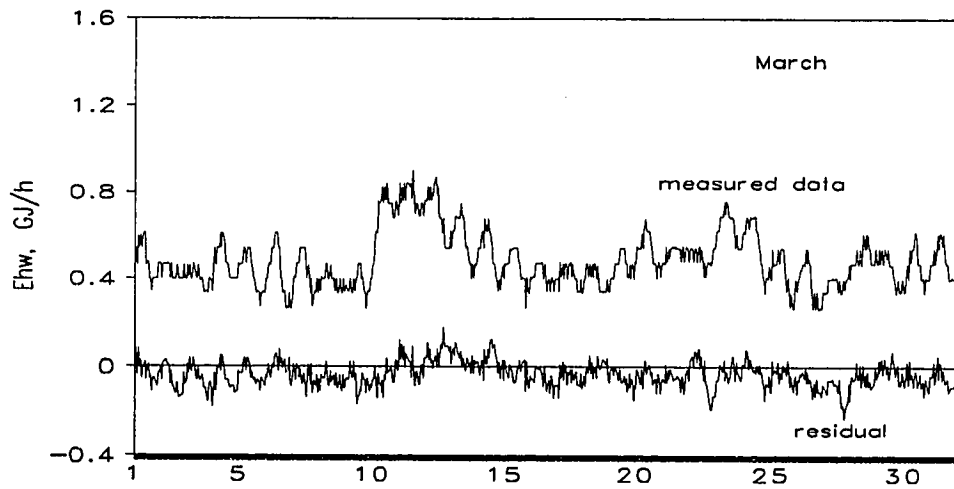


(b)

Figure 5.4 Time series plots of cooling energy use in ZEC during January 1992 to June 1992 (a) and May 1992 (b).



(a)



(b)

Figure 5.5 Time series plots of heating energy use in BUR during January 1992 to June 1992 (a) and March 1992 (b).

Table 5.3 Summary of Fourier series modeling for hourly heating energy use in the Burdine Building from January 1992 to June 1992.

Day-type	Variable	Parameter estimate	Partial R ²
Weekdays	INTERCEPT	1.471661	---
	T	-0.015095	0.8396
	T*SH1	-0.000701	0.0205
	CHI	-0.036113	0.0131
Weekends	INTERCEPT	1.511257	---
	T	-0.015492	0.8168
	T*SH1	-0.000819	0.0323
	CHI	-0.036811	0.0154

Table 5.4 Generalized Fourier Series (GFS) models of hourly energy use at various buildings in Texas.

Building name	Type of energy use	Period	Day type	R ²	C.V. %
TDH (Lab & Main bldg.)	E _{cw} (GJ/h)	02/16/91-08/12/92	Weekdays	0.85	17.07
			Weekends	0.82	17.85
TDH (All bldgs.)	E _{hw} (GJ/h)	02/16/91-08/12/92	Weekdays	0.81	20.96
			Weekends	0.73	24.55
MCC	E _{wbe} and chiller (kWh/hr)	04/07/92-05/15/92	Weekdays	0.89	13.88
			Weekends	0.80	11.96
TCOM (Med bldg. 1 & 2)	E _{wbe} and chiller (kWh/hr)	06/01/93-08/31/93	Weekdays	0.91	7.31
			Weekends	0.82	9.69
ZEC	E _{cw} (GJ/h)	01/01/92-12/22/92	Weekdays	0.91	11.4
			Weekends	0.91	10.5
BUR	E _{hw} (GJ/h)	01/01/92-06/30/92	Weekdays	0.87	17.03
			Weekends	0.86	16.59
ZEC	E _{cw} (GJ/h)	09/01/89-12/22/89	Weekdays	0.87	7.7
			Weekends	0.91	6.3
ZEC	E _{hw} (GJ/h)	09/01/89-12/22/89	Weekdays	0.90	20.8
			Weekends	0.87	21.1

predict energy use very well for other months of the year. The prediction error depends on the (i) type of the HVAC system, (ii) range of drybulb temperature of the data period from which the model is developed, (iii) range of drybulb temperature of the prediction period and (iv) on the average temperature of the data period and prediction period.

Cooling energy consumption data from two buildings (ZEC and BUS at Texas A&M and UT Arlington Campus respectively) have been analyzed to illustrate how GFS models developed from short data sets predict for different periods of the year 1992. The temperature data from these two sites were grouped according to the months of the year and Duncan's multiple range test was then performed to identify temperature based month-types. The results of Duncan's test for ZEC and BUS temperature data are summarized in Tables 5.5a and 5.5b respectively.

It may be noted that the results of Duncan's test for both the sites (Tables 5.5a and 5.5b) indicated a large number of groups with significant difference in mean and scatter of the data but the (i) June through September (6, 7, 8 and 9) and, likewise, (ii) April, May and October (4, 5 and 10), (iii) February, March and November (2, 3 and 11) and (iv) January and December (1 and 12) are close by the comparison of mean and may be grouped together to arrive at a fewer month-types. Thus, the final temperature based month-types were obtained as follows:

- (1) January 1992 and December 1992,
- (2) February 1992, March 1992 and November 1992,
- (3) April 1992, May 1992 and October 1992 and
- (4) June 1992 through September 1992.

Five models for cooling energy use developed from (a) January 1992, (b) February 1992 and March 1992, (c) April 1992 and May 1992, (d) June 1992 through September 1992 data and (e) 1992 yearlong data are then applied to predict energy use for all the months of the year. The C.V.s are calculated for all the groups and plotted in Figures 5.6 and 5.7 for ZEC and BUS respectively. It may be noted that C.V.s are different for different months and that model developed from a particular month's data predict with higher C.V.s when applied to predict energy use for the other months. Also, the model

Table 5.5a Results of Duncan's multiple range test used for grouping outdoor drybulb temperature data of Zachry Engineering Center at College Station, Texas in 1992.

Analysis of Variance Procedure		
Duncan's Multiple Range Test for variable: TEMP = outdoor drubulb temperature		
Alpha= 0.1 df= 8579 MSE= 68.29345		
Harmonic Mean of cell sizes= 712.5015		
Number of Means	2	3 4 5 6 7
Critical Range	.7273	.7688 .7979 .8137 .8291 .8423
Number of Means	8	9 10 11 12
Critical Range	.8533	.8625 .8702 .8766 .8820
Means with the same letter are not significantly different.		
Duncan Grouping	Mean	N MM
A	82.2431	744 7
B	80.4372	700 6
	B	
B	80.2027	742 8
C	78.4169	720 9
D	71.3893	744 5
D		
D	71.0839	576 10
E	67.0761	718 4
F	62.5273	744 3
G	57.7450	696 2
H	55.8202	719 11
I	54.4535	744 12
J	50.1795	744 1

Table 5.5b Results of Duncan's multiple range test used for grouping outdoor drybulb temperature data of Business Building at UT Arlington, Texas in 1992.

Analysis of Variance Procedure			
Duncan's Multiple Range Test for variable: TEMP = outdoor drybulb temperature			
Alpha= 0.1 df= 8685 MSE= 89.71238			
Harmonic Mean of cell sizes= 724.0673			
Number of Means	2	3	4
Critical Range	0.827	0.874	0.907
Number of Means	5	6	7
Critical Range	0.925	0.943	0.958
Number of Means	8	9	10
Critical Range	0.970	0.981	0.989
Number of Means	11	12	
Critical Range	0.997	1.003	
Means with the same letter are not significantly different.			
Duncan Grouping	Mean	N	MM = month
A	82.2822	744	7
B	78.7378	744	8
B	78.6742	720	6
C	76.1680	685	9
D	73.7907	744	5
E	69.0847	719	4
E	68.9073	722	10
F	62.8851	744	3
G	56.9841	694	2
H	52.1351	693	11
I	49.5540	744	1
J	48.7237	744	12

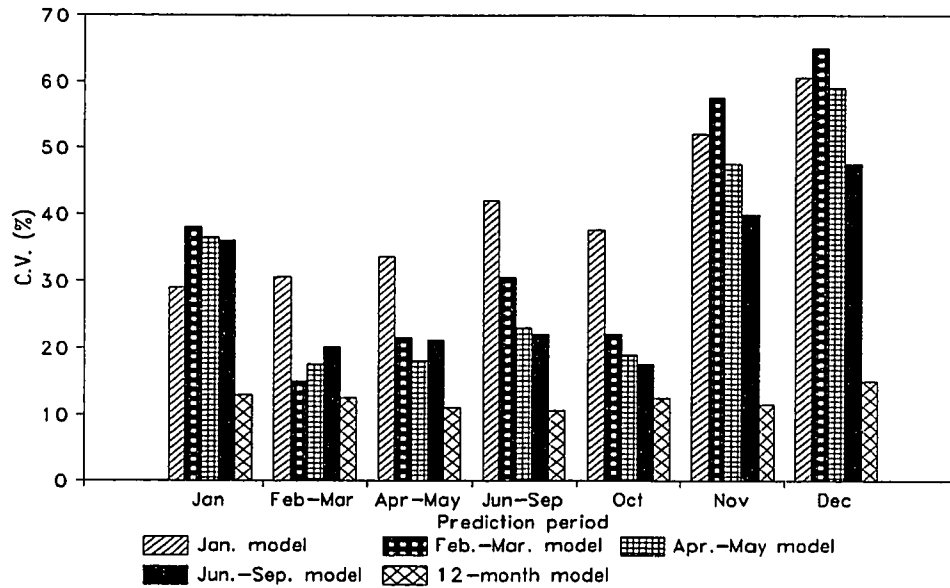


Figure 5.6 Bar chart of C.V.s for all the months of 1992 using prediction by five cooling energy models developed from data of January, February-March, April-May, June-September and twelve months' data. This site is ZEC.

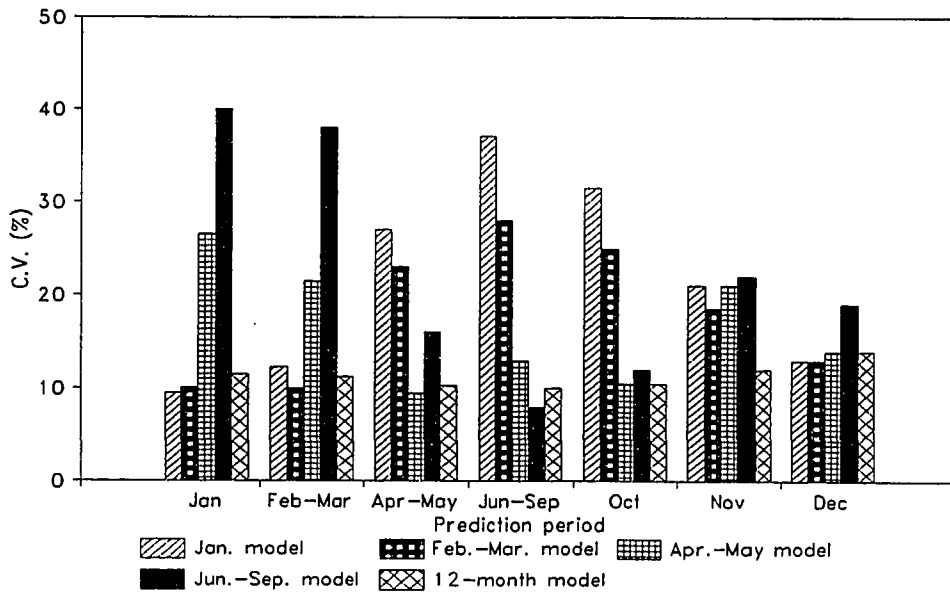


Figure 5.7 Bar chart of C.V.s for all the months of 1992 using prediction by five cooling energy models developed from data of January, February-March, April-May, June-September and twelve months' data. The site is BUS.

developed from January data has a very high C.V. while predicting energy use in December in ZEC, although both these months belong to the same month-types. However, the twelve-month model has fitted the data with a small range of C.V. RMSE (about 10% to 15%) throughout the year in both the examples.

The above observations may be explained by the behavior of the air handling system. Variable Air Volume (VAV) systems were installed in ZEC and BUS before 1992. For VAV systems, a model developed from a data set containing the entire range of outdoor temperature (about $-6.7\text{ }^{\circ}\text{C}$ to $33.8\text{ }^{\circ}\text{C}$ ($\approx 20\text{ }^{\circ}\text{F}$ to $100\text{ }^{\circ}\text{F}$) in the case of College Station and Arlington) will show a nonlinear behavior which can be approximated by a 4-P model equation (Reddy et al., 1994). Such behavior is exhibited by cooling energy use due to cold deck set point temperature, exterior zone balance point temperature (a building may be considered to have two zones: exterior and interior, and balance point temperature can be calculated separately for each zone) and scheduling effects. For university buildings, the change point of a 4-P model for cooling energy use is expected to appear approximately in the range of $13\text{ }^{\circ}\text{C}$ to $17\text{ }^{\circ}\text{C}$ outdoor temperature due to the combined effect of all the factors mentioned above. A model developed from a short data set covering only a part of the entire range of outdoor temperature may, therefore, be unphysical and also suffer from extrapolation error. This is reconfirmed by the results plotted in Figures 5.6 and 5.7. The poor prediction of the January model for December 1992 in ZEC, however, is due to Christmas. The fact that the twelve month model fitted the data consistently throughout the year is because the yearlong data set contains the entire range of outdoor temperature variation.

Summary

In this chapter, the Generalized Fourier Series (GFS) approach to model weather dependent energy use in commercial buildings is presented and illustrated by application to monitored data from several buildings. It is found that the GFS approach gives consistently good fit to cooling and heating energy use. However, C.V.s for heating energy use are higher than those of cooling energy use. This is consistent with results from other models of heating energy use (Kissock et al., 1992). Models developed from

short data sets are found to predicted less accurately when applied to periods other than those from which the model is developed, in two examples. Model developed from twelve months' data is found to fit the data reasonably throughout the year in both the examples.

In the next chapter, a Temperature based Fourier Series (TFS) approach to model heating and cooling energy use in commercial buildings will be presented.

CHAPTER VI

TEMPERATURE BASED FOURIER SERIES MODELING OF HEATING AND COOLING ENERGY USE

Introduction

In the previous chapter, the Generalized Fourier Series (GFS) approach to model heating and cooling energy use in commercial buildings was presented. A GFS model can be developed when hourly outdoor temperature, outdoor humidity and horizontal solar flux data are available. However, there are situations when only outdoor temperature data are available, data for other weather variables being either unavailable or spurious. A temperature based modeling equation is, therefore, needed for modeling hourly cooling and heating energy use.

Model Concept

Two parameter (2-P), three parameter (3-P) (Fels, 1986) and four parameter (4-P) (Ruch and Claridge, 1992) types of regression models with temperature as the only variable are conventionally used to model heating and cooling energy consumption at the daily level (Kissock 1993) in order to determine retrofit savings. These models, when developed for predicting hourly energy use, may give poor prediction accuracy as they are oblivious to the effect of systematic scheduling on hourly heating and cooling energy use. The individual hourly approach can be adopted for modeling weather dependent loads at the hourly level. In the individual hourly approach, energy consumption data are binned into twenty-four hourly groups and multiple linear regression models using temperature as the only variable are developed separately for each hour. The model equation is of the following form:

$$E_h = a_h + b_h T \quad (6.1)$$

where T is the ambient temperature. The subscript h stands for the hour of the day and can be arbitrarily assumed to be 0 at midnight, 1 at 1 a.m. and so on. A more sophisticated approach that will give almost the same prediction accuracy as equation 6.1 is the truncated form of GFS equation 5.2 with humidity and solar terms dropped:

$$E_h = \beta_0 + \sum_{n=1}^{11} \left[\alpha_n \sin \frac{2\pi}{P_j} h + \beta_n \cos \frac{2\pi}{P_j} h \right] + T_h \sum_{n=0}^{11} \left[\gamma_n \sin \frac{2\pi}{P_j} h + \delta_n \cos \frac{2\pi}{P_j} h \right] \quad (6.2)$$

However, a careful examination of equations 6.1 and 6.2 reveals that both are, in essence similar, representing a 2-P type of linear temperature dependence of energy use for a particular hour of day. On the contrary, previous studies (Ruch and Claridge, 1992) have shown that this assumption is invalid due to a combination of humidity effects and HVAC system behavior (Reddy et al., 1994). These combined effects can be indirectly captured by 3-P, 4-P or nonlinear functional forms. The twentyfour 2-P, 3-P, 4-P or nonlinear equations can be combined conveniently by using a temperature based Fourier series as explained in the following paragraphs.

A function $f(T)$ is represented by the following expressions for 2-P, 3-P, 4-P, etc. cases:

$$f(T) = a + bT \quad \text{for all } T; \quad \text{2P model} \quad (6.3a)$$

$$f(T) = \left. \begin{array}{l} a_1 \quad \text{for } T \leq T_{CP}, \\ a_2 + b_2 T \quad \text{for } T > T_{CP} \end{array} \right\} \quad \text{3P model} \quad (6.3b)$$

$$f(T) = \left. \begin{array}{l} a_1 + b_1 T \quad \text{for } T \leq T_{CP}, \\ a_2 + b_2 T \quad \text{for } T > T_{CP} \end{array} \right\} \quad \text{4P model} \quad (6.3c)$$

$$f(T) = \left. \begin{array}{l} a_1 \quad \text{for } T \leq T_{CP_1}, \\ a_2 + b_2 T \quad \text{for } T_{CP_1} < T \leq T_{CP_2}, \\ a_3 + b_3 T \quad \text{for } T > T_{CP_2} \end{array} \right\} \quad \text{5P model} \quad (6.3d)$$

$$f(T) = \left. \begin{array}{ll} a_1 + b_1 T & \text{for } T \leq T_{CP1}, \\ a_2 + b_2 T & \text{for } T_{CP1} < T \leq T_{CP2}, \\ a_3 + b_3 T & \text{for } T > T_{CP2}, \end{array} \right\} \quad \text{6P model} \quad (6.3e)$$

so on.....

A generalized n-P model representation is analogous to a Fourier series model such as:

$$f(x) = \alpha + \beta T + \sum_{m=1}^m \left[\alpha_m \sin \frac{2\pi}{P_m} T + \beta_m \cos \frac{2\pi}{P_m} T \right] \quad (6.4)$$

where α and β are the coefficients and subscript m stands for frequency. In order to generate a model within the temperature range of T_{\min} to T_{\max} , equation 6.4 will take the following form:

$$E_T = \alpha' + \beta' T + \sum_{m=1}^{m_{\max}} \left[\alpha_m \sin \frac{2\pi m}{\Delta T} (T - T_{\min}) + \beta_m \cos \frac{2\pi m}{\Delta T} (T - T_{\min}) \right] \quad (6.5)$$

$$\text{where } \Delta T = T_{\max} - T_{\min}, \quad x = \frac{T - T_{\min}}{\Delta T}, \quad \alpha' = \alpha - \frac{\beta T_{\min}}{\Delta T} \quad \text{and} \quad \beta' = \frac{\beta}{\Delta T}.$$

In order to illustrate how equation 6.5 can be fitted to a set of 3-P, 4-P and 6-P models, some reasonable values of parameters in equations (6.3a to 6.3e) can be assumed:

$$E_c = \left. \begin{array}{ll} 20 & \text{for } -6.67^\circ\text{C} \leq T \leq 15.55^\circ\text{C}, \\ 9.89 + 0.65T & \text{for } 15.55^\circ\text{C} < T \leq 33.77^\circ\text{C} \end{array} \right\} \quad \text{3P model} \quad (6.6a)$$

$$E_c = \begin{cases} 20 + 0.3T & \text{for } -6.67^\circ\text{C} \leq T \leq 15.55^\circ\text{C} \\ 14.56 + 0.65T & \text{for } 15.55^\circ\text{C} < T \leq 33.77^\circ\text{C} \end{cases} \quad \left. \vphantom{E_c} \right\} \begin{array}{l} \text{4P model with} \\ \text{low slope change} \end{array} \quad (6.6b)$$

$$E_c = \begin{cases} 20 + 0.3T & \text{for } -6.67^\circ\text{C} \leq T \leq 15.55^\circ\text{C} \\ 4.45 + 1.3T & \text{for } 15.55^\circ\text{C} < T \leq 33.77^\circ\text{C} \end{cases} \quad \left. \vphantom{E_c} \right\} \begin{array}{l} \text{4P model with} \\ \text{high slope change} \end{array} \quad (6.6c)$$

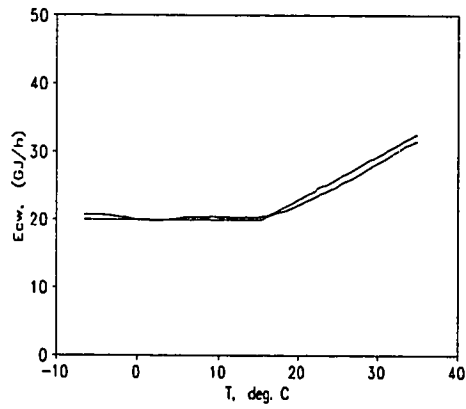
$$E_c = \begin{cases} 20 + 0.3T & \text{for } -6.67^\circ\text{C} \leq T \leq 15.55^\circ\text{C} \\ 14.56 + 0.65T & \text{for } 15.55^\circ\text{C} < T \leq 21.11^\circ\text{C} \\ 0.84 + 1.3T & \text{for } 21.11^\circ\text{C} < T \leq 33.77^\circ\text{C} \end{cases} \quad \left. \vphantom{E_c} \right\} \begin{array}{l} \text{6P model} \end{array} \quad (6.6d)$$

where equations 6.6a, 6.6b, 6.6c and 6.6d are representatives of 2-P, 4-P with low slope change, 4-P with high slope change and 6-P functional forms respectively (Figure 6.1). When equation 6.5 was used in conjunction with a temperature range of -6.7°C (20°F) to 33.8°C (100°F) to represent the equations 6.6a through 6.6d only a few frequencies were found adequate (Table 6.1). Figure 6.1 shows how well the n-P models (eq. 6.5) with a few important frequencies are able to fit eqs. 6.6a through 6.6d.

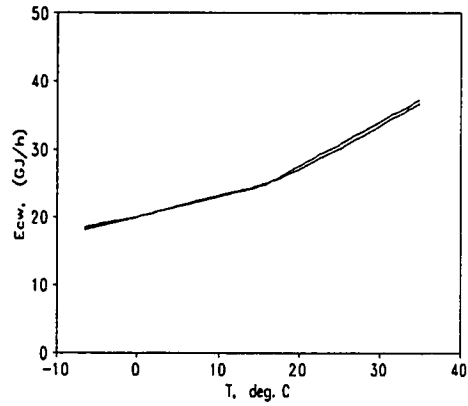
Eq. 6.5, therefore, is able to represent a functional form of weather dependent energy use for a particular hour of day with temperature as the only variable. However, the relationship between weather dependent energy use and ambient temperature may vary from hour to hour of a day depending on the operating pattern of the building HVAC system. A generalized equation of energy use for all hours of the day can be

Table 6.1 Results of equation (6.5) fitted to data generated by equation (6.6a) through equation (6.6d). ST_i and CT_i are the ith sine temperature frequencies and cosine temperature frequencies respectively.

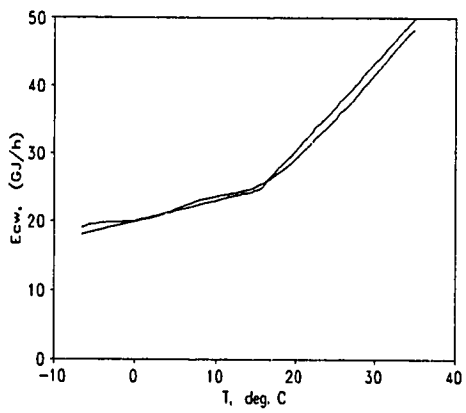
Model type	Partial R-squares						Model R ²	C.V. (%)
	T	ST1	CT1	ST2	CT2	CT3		
3-P	0.721	0.0005	0.2634	0.0026	0.0014	0.0021	0.9913	2.20
4-P, low slope change	0.961	0.0001	0.0368	0.0004	0.0002	0.0003	0.9987	1.06
4-P, high slope change	0.885	0.0002	0.1079	0.0011	0.0006	0.0009	0.9962	2.70
6-P	0.880	0.0067	0.1026	0.0013	0.0042	0.0003	0.9950	2.80



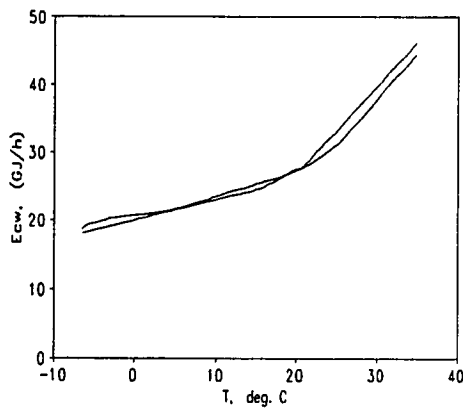
(a)



(b)



(c)



(d)

Figure 6.1 Plots of 2-P (a), 4-P with low slope change (b), 4-P with high slope change (c) and 6-P (d) equations and the corresponding n -P Fourier model fit.

obtained by multiplying the right hand side of Eq. 6.5 by a Fourier series using hour of day as the variable. The model equation then takes the following form:

$$E_{T,h} = [\alpha' + \beta'T + \sum_{m=1}^m \{ \alpha_m \sin \frac{2\pi m}{\Delta T} (T - T_{\min}) + \beta_m \cos \frac{2\pi m}{\Delta T} (T - T_{\min}) \}] \bullet \quad (6.7)$$

$$\sum_{n=0}^n \max [\gamma_n \sin \frac{2\pi n}{24} h + \delta_n \cos \frac{2\pi n}{24} h]$$

⇒

$$E_{T,h} = [\alpha' + \beta'T - \beta_0 + \sum_{m=0}^m \{ \alpha_m \sin \frac{2\pi m}{\Delta T} (T - T_{\min}) + \beta_m \cos \frac{2\pi m}{\Delta T} (T - T_{\min}) \}] \bullet$$

$$\sum_{n=0}^n \max [\gamma_n \sin \frac{2\pi n}{24} h + \delta_n \cos \frac{2\pi n}{24} h]$$

⇒

$$E_{T,h} = \beta'T \sum_{n=0}^n \max [\gamma_n \sin \frac{2\pi n}{24} h + \delta_n \cos \frac{2\pi n}{24} h] + [\alpha' - \beta_0 +$$

$$\sum_{m=0}^m \{ \alpha_m \sin \frac{2\pi m}{\Delta T} (T - T_{\min}) + \beta_m \cos \frac{2\pi m}{\Delta T} (T - T_{\min}) \}] \bullet$$

$$\sum_{n=0}^n \max [\gamma_n \sin \frac{2\pi n}{24} h + \delta_n \cos \frac{2\pi n}{24} h]$$

⇒

$$E_{T,h} = T \sum_{n=0}^n \max [\phi_n \sin \frac{2\pi n}{24} h + \psi_n \cos \frac{2\pi n}{24} h] + \quad (6.8)$$

$$\sum_{m=0}^m \max [\eta_m \sin \frac{2\pi m}{\Delta T} (T - T_{\min}) + \zeta_m \cos \frac{2\pi m}{\Delta T} (T - T_{\min})] \bullet$$

$$\sum_{n=0}^n \max [\gamma_n \sin \frac{2\pi n}{24} h + \delta_n \cos \frac{2\pi n}{24} h]$$

Note that ΔT in equation 6.8 represents the range within which ambient temperature varies in a particular location. In order to avoid high extrapolation error, the data set from which the model is to be developed, should have fairly uniform data density over the range of ΔT .

Equation 6.8 is the Temperature based Fourier Series (TFS) model that can be used to predict weather dependent loads in commercial buildings. Although equation 6.8 suggests a large number of parameters, application to monitored data from several buildings showed that only a few of them are significant. The significant frequencies are selected from the set of terms suggested by equation 6.8 by performing stepwise regression.

Application to Monitored Data

The first step in data processing prior to model identification is to day-type the data in order to remove major changes in operating schedule during weekdays, weekends, Christmas etc. Although a mere separation of data into weekdays and weekends may produce very good fits (Dhar et al. 1994a), one might adopt a rigorous day-typing technique, when necessary. Details of a day-typing procedure are described in Chapter IV. Once day-typing is performed, separate models are developed for each day-type. The usefulness of the TFS model is illustrated by examples of (i) cooling energy use in ZEC and (ii) heating energy use in BUR, during working weekdays and weekends of January 1992 to June 1992. In addition, the results of applying the TFS to several other channels at different sites are discussed.

Cooling Energy Use. Stepwise forward regression for cooling energy use in ZEC was performed using equation 6.8 to select the significant independent parameters. Values of maximum and minimum ambient temperatures in College Station range from $-6.7\text{ }^{\circ}\text{C}$ ($\approx 20\text{ }^{\circ}\text{F}$) to $33.8\text{ }^{\circ}\text{C}$ ($\approx 100\text{ }^{\circ}\text{F}$) for the data examined. A statistical criterion for selecting the significant parameters is to use Mallows's $C(p) \approx p$ criteria, where p is the number of parameters. However, this criterion often retains a large number of

parameters in the final model, many of them having insignificant partial R-square. An arbitrary but reasonable cut-off of 0.005 partial R-square may be adopted in such cases to simplify the model without sacrificing much in prediction accuracy (Dhar et al., 1994a).

The results of stepwise regression for weekdays and weekends are summarized in Table 6.2. The interaction terms between temperature and hour of day appear as significant for both weekdays and weekends, the interaction effect being higher during weekends. This is probably due to more variation in internal loads and occupancy during the weekdays than during weekends which makes the cooling energy use more temperature dependent during weekends. The first and second temperature frequencies contributed a partial R-square of 0.0697 during weekdays and 0.1502 during weekends which are about 7.7% and 17.9% of the model R-squares 0.8946 and 0.8438 respectively. This illustrates the relevance of considering temperature frequencies and their interaction terms in the TFS model equation. The C.V. RMSE of the models during weekdays and weekends are 12.45% and 14.18% respectively (Table 6.3). The fit of the model to the measured data can be seen in the time series plots of measured and residual energy use in Figure 6.2.

A three dimensional plot of predicted cooling energy use against ambient temperature and hour of the day for weekdays is shown in Figure 6.3. The plot shows how the model has captured the effect of the factors like humidity and HVAC system related effects beyond a temperature of about 16 °C.

Heating Energy Use. A similar approach was adopted to identify a model for heating energy use during weekdays and weekends in BUR. The period chosen is from January 01 to June 30, 1992. The result of stepwise regression as shown in Table 6.2 indicates that temperature frequencies have been useful for modeling heating energy use. Heating energy use not being dependent on humidity, the TFS model gives better fits to the measured data than the GFS approach (Table 6.3). The time series plots of

Table 6.2 Contribution of Fourier frequencies to the TFS model for heating and cooling energy use at two sites from January 01 to June 30, 1992. SHi and CHi are Fourier sine and cosine time frequencies, whereas STi and CTi are Fourier sine and cosine temperature frequencies respectively.

Day-type	Variable	Cooling energy use (GJ/h) in ZEC		Heating energy use (GJ/h) in BUR	
		Partial R ²	Cumulative R ²	Partial R ²	Cumulative R ²
Weekdays	T	0.8149	0.8149	0.8370	0.8370
	ST1	0.0537	0.8685	0.0352	0.8722
	SH1	---	---	0.0135	0.8857
	CH1	---	---	0.0137	0.8994
	ST1*SH1	0.0190	0.8876	---	---
	T1*CH1	0.0070	0.8946	---	---
Weekends	T	0.6936	0.6936	0.8168	0.8168
	CT1	0.0463	0.7400	0.0355	0.8523
	SH1	---	---	0.0282	0.8805
	CH1	---	---	0.0151	0.8956
	ST1*SH1	0.0681	0.8080	---	---
	T1*SH1	0.0173	0.8253	---	---
	T1*CH1	0.0107	0.8360	---	---
	CT2*SH1	0.0078	0.8438	---	---

measured heating energy use and residuals are shown in Figure 6.4. It is noted that the model fitted the data well throughout except the period shown from the last week of January to second week of February. It is obvious from the time series plot of measured energy use that something unusual happened during this period. The site representative confirmed that there was an unusual change in the valve operation of the heating system. The time series plot of the residuals generated by the TFS model of heating energy use captures this unusual pattern conveniently. This illustrates how the model can be useful for diagnostic purposes.

A three dimensional plot of heating energy use in BUR during weekdays plotted against hour of day and ambient temperature is shown in Figure 6.5. The plot shows that heating energy use drops faster with decreases in ambient temperature in the range of about 5 °C and 20 °C compared to its variation at lower and higher temperatures.

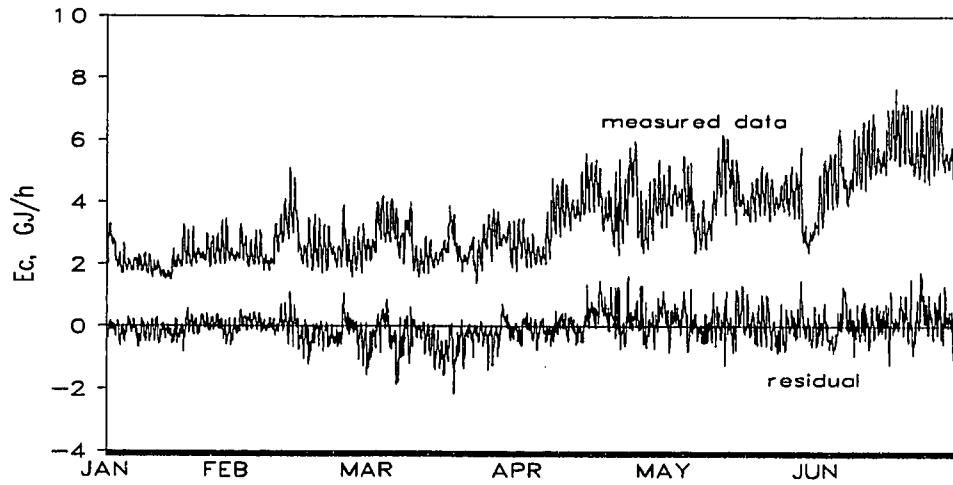


Figure 6.2 Time series plots of measured and residual cooling energy use in ZEC from January to June in 1992 when the TFS model is used.

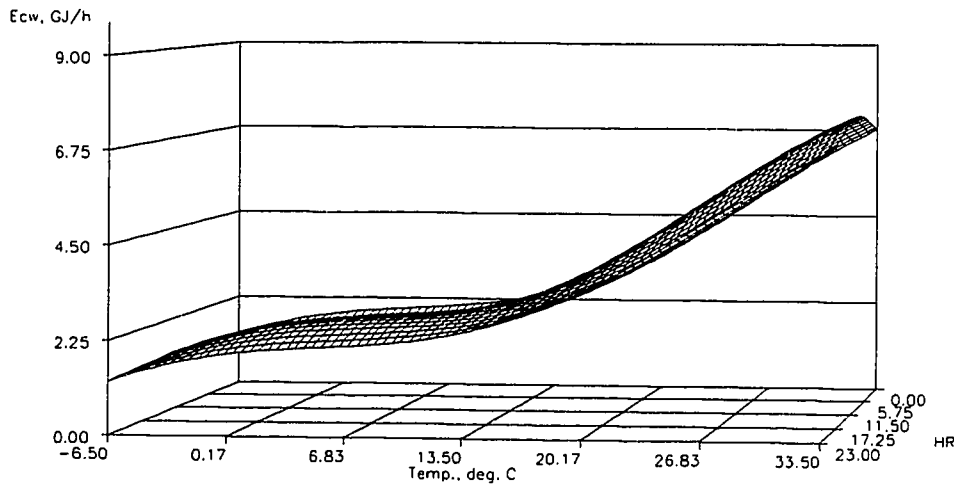


Figure 6.3 A three dimensional plot of cooling energy use versus hour of day and ambient temperature during working weekdays of January to June 1992 in ZEC.

The daily profile does not change with temperature which means that there is no interaction between hour of day and temperature (see Table 6.2).

Comparison with GFS Approach

TFS and GFS models were developed for weekdays and weekends for cooling energy use, heating energy use and weather dependent whole building electric energy use (includes chiller electricity consumption) at various sites in Texas. The R-square and C.V. values of these models are summarized in Table 6.3. GFS cooling energy use models may be noted to have a little higher R-squares and a little lower C.V.s. However, TFS though not able to model cooling energy use as accurately as GFS, nevertheless captures most of the variations due to humidity and solar effects. But the TFS provided better models of heating energy use than the GFS models, as indicated by

Table 6.3 Comparison of R-square and C.V. values of Generalized Fourier Series (GFS) and Temperature based Fourier Series (TFS) models of weather dependent energy use in several buildings.

Site	Energy use	Period	Day-type	R-square		C.V.(%)	
				GFS	TFS	GFS	TFS
ZEC	E_{cw} (GJ/h)	01/07/92- 06/30/92	Weekdays	0.89	0.89	12.45	12.05
			Weekends	0.89	0.84	12.02	14.18
ZEC	E_{cw} (GJ/h)	09/01/89- 12/20/89	Weekdays	0.87	0.83	7.7	8.42
			Weekends	0.91	0.89	6.3	7.07
TDH (Lab & Main)	E_{cw} (GJ/h)	02/16/91- 08/12/92	Weekdays	0.85	0.81	17.07	18.75
			Weekends	0.82	0.80	17.85	18.02
TDH	E_{hw} (GJ/h)	02/16/91- 08/12/92	Weekdays	0.81	0.82	20.96	20.60
			Weekends	0.73	0.80	24.55	21.32
ZEC	E_{hw} (GJ/h)	09/01/89- 12/20/89	Weekdays	0.90	0.91	20.8	19.37
			Weekends	0.87	0.89	21.1	20.1
BUR	E_{hw} (GJ/h)	01/01/92- 06/30/92	Weekdays	0.87	0.90	17.03	14.94
			Weekends	0.86	0.90	16.59	14.57
TCOM (Med. bldg. 1 & 2)	E_{wbe} including chiller (kWh/h)	06/01/93- 08/31/93	Weekdays	0.85	0.83	6.17	6.70
			Weekends	0.46	0.47	8.68	8.64
MCC	E_{wbe} including chiller (kWh/h)	04/07/92- 05/15/92	Weekdays	0.89	0.90	13.88	13.02
			Weekends	0.80	0.92	11.96	8.69

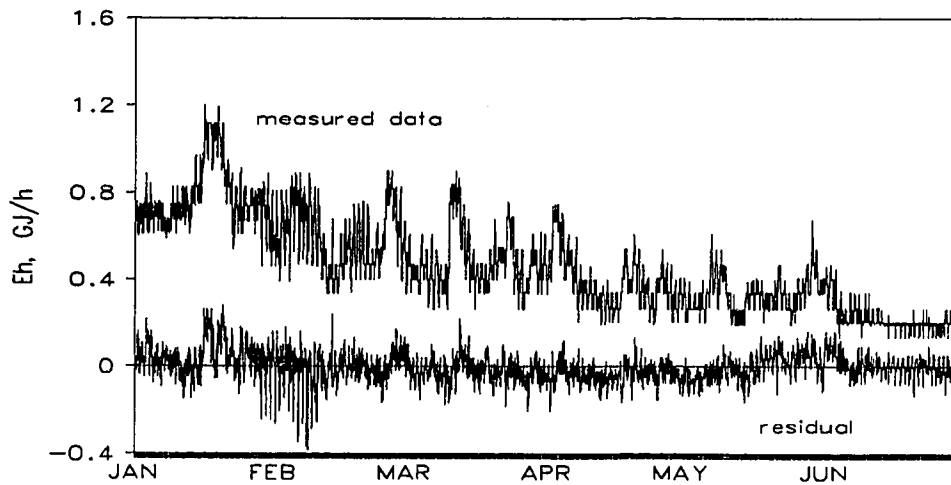


Figure 6.4 Time series plots of measured heating energy use from January to June, 1992 in BUR. The residual plot after modeling with equation 6.9 is also shown. Note the relatively higher negative residual values from the end of January to mid February which identified the unusual valve operation of the heating system during that period.

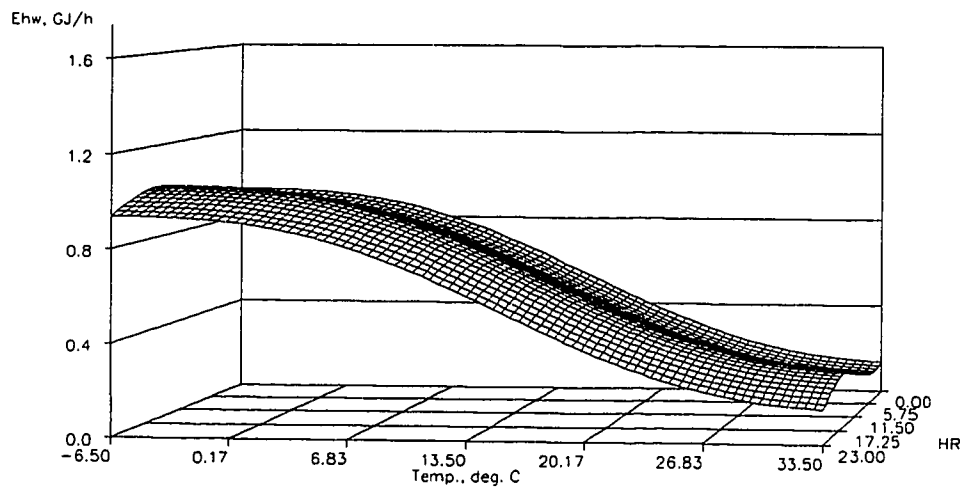


Figure 6.5 A three dimensional plot of heating energy use versus hour of day and ambient temperature during working weekdays of January to June 1992 in BUR.

higher R-squares and lower C.V.s in all the cases. TFS model performance was similar to that of GFS models for whole building electric energy use, the only exception being during weekends in MCC, where the TFS model is significantly better than the GFS model. This comparison indicates that TFS is a useful modeling approach.

Summary

In this chapter, a Temperature based Fourier Series (TFS) approach was presented and illustrated with application to monitored data from several buildings. This approach is useful for modeling cooling energy use when only temperature data is available, data of other weather variables being either unavailable or spurious. Results of application to monitored data from several buildings shows that the TFS model is able to (i) indirectly account for humidity and solar effects to a large extent while modeling cooling energy use and (ii) provide a better fit to heating energy consumption data than the GFS model.

In the next two chapters, fundamentals of wavelet analysis will be discussed and application of an Artificial Neural Network with wavelet basis functions will be presented.

CHAPTER VII

AN ARTIFICIAL NEURAL NETWORK WITH WAVELET BASIS FUNCTIONS TO PREDICT HOURLY HEATING AND COOLING ENERGY USE

Introduction

Artificial Neural Networks (ANN) have attracted the attention of many researchers because of their ability to model time series data with high prediction accuracy (Willis et al., 1991). ANNs with Back Propagation Network (BPN) algorithms have been applied to predict heating and cooling energy use in commercial buildings in recent years (Wang and Kreider, 1992; Dodier et al., 1993). A detailed review of the application of ANNs to model energy use in commercial buildings is presented in Chapter II (Literature Review). It was noted that although Back Propagation Network (BPN) algorithms offer high prediction accuracy, the challenge of reducing training time still remains. The neural networks with local basis functions have several advantages over the conventional BPNs, the most important being a significantly shorter training time requirement.

As mentioned in earlier chapters, hourly heating and cooling energy use in commercial buildings depends on the operating schedule of the building systems and weather variables such as outdoor temperature, specific humidity and solar radiation. However, a model with hour of day and outdoor temperature may be able to indirectly account for some part of the effects of humidity and solar radiation (Dhar et al., 1995), as discussed in Chapter VI. A family of two-dimensional wavelets can be generated with hour of day and outdoor temperature as the variables and can be used as the basis functions in a one-hidden-layer ANN. The number of hidden layer units can be determined by a well defined statistical criterion, thereby removing the apparent arbitrariness involved in determining the network architecture as in the case of BPNs.

This chapter describes a methodology for modeling hourly heating and cooling energy use in commercial buildings which combines a model equation with outdoor temperature and hour of day as the regressor variables and an ANN with two

dimensional wavelet basis functions (Wave-Net) derived from a cubic spline. The ANN is used to model the nonlinear component of energy use not accounted for by outdoor temperature and the hour of day. Wavelet basis functions have been chosen for the ANN because of their good localization characteristics. As will be discussed later in this chapter, application to monitored data from several sites showed that Wave-Net offers much faster training than BPN with insignificant sacrifice of prediction accuracy.

Wavelets

Wavelets can be viewed as an alternative to Fourier series for the purpose of modeling nonlinear behavior. Wavelets have a significant advantage over Fourier series for modeling some functions because of their good localization characteristics. To see why this is so, we first note that a family of wavelets is defined in terms of translations and dilations of a single function, a “parent” wavelet $\psi(x)$:

$$\psi_{m,k}(x) = \sqrt{2^{-m}} \psi(2^{-m}x - k) \quad \text{for } (m, k) \in Z^2 \quad (7.1)$$

where $(m, k) \in Z^2$ means that m and k , the frequency (or scale) and location of any wavelet respectively, belong to the integer set Z^2 . Powers of two are used to generate the family of wavelets in equation 7.1 for computational efficiency (Chui, 1992).

If the “parent” wavelet $\psi(x)$ decays quickly, then linear combinations of functions from the family defined in equation 7.1 will retain this property and have good localization characteristics. Various wavelet bases have been developed by many researchers and the right choice of wavelets for a particular application is important for achieving high prediction accuracy.

The cubic spline wavelets used here have good localization properties. They are also easy to calculate, being piecewise polynomials. Although cubic spline basis functions do not form an orthonormal set, some advantages of orthonormality are retained. For example, translations of cubic B-spline scaling functions and wavelets have

very little correlation among themselves so that the coefficients of the regressor variables do not change significantly when one or more terms are dropped from a model.

If wavelets are to be used as the basis functions in an ANN, we must be able to express well-behaved functions in terms of the wavelet components. The way in which this is accomplished is best described in the context of a multiresolution analysis.

Multiresolution Analysis

Approximation of a function in a multiresolution hierarchy is useful when training data is distributed non uniformly in the input space. Learning in a higher resolution may be necessary when data density is high. On the other hand, a coarse resolution may be good enough for lower data density. We will briefly describe the mathematical framework of multiresolution analysis in this section.

A multiresolution analysis is a sequence of approximation spaces V_j that satisfy certain properties, some of which are discussed below; however, one may refer to Daubechies (1992) or Chui (1992) for a detailed description. The spaces V_j are related to each other as follows:

$$\dots \subset V_2 \subset V_1 \subset V_0 \subset V_{-1} \subset V_{-2} \dots \quad (7.2)$$

which means that V_2 is a subset of V_1 , V_1 is a subset of V_0 and so on.

There is a special function $\phi(x)$, called a scaling function, which lies in V_0 . All functions in V_0 are linear combinations of translations of this scaling function $\phi(x)$ and V_0 is "translation invariant":

$$\phi(x) \in V_0 \Leftrightarrow \phi(x - k) \in V_0, \quad k \in Z \quad (7.3)$$

Equation 7.3 means that if $\phi(x)$ belongs to the space V_0 , then the translations of $\phi(x)$ which are $\phi(x - k)$, will also belong to the space V_0 where k is an integer denoting the

location of the function $\phi(x - k)$. In fact, the scaling function $\phi(x)$ generates the entire sequence of V_j spaces in a sense. To be precise, if we define $\phi(x)$ as

$$\phi_{m,k}(x) = \sqrt{2^{-m}} \phi(2^{-m}x - k) \quad \text{for } (m, k) \in \mathbb{Z}^2 \quad (7.4)$$

then $\{\phi_{m,k}(x): (m, k) \in \mathbb{Z}^2\}$ is a basis for the space V_m . It can be shown that the scaling function and the wavelets are linked by a refinement equation (Daubechies, 1992):

$$\psi(x) = \sum_{k=-\infty}^{\infty} c_k \phi_{-1,k}(x) \quad (7.5)$$

where c_k s are the coefficients. Note that this says that $\psi(x)$ is in the space V_{-1} , because $\phi_{-1,k}$ s are the bases for the space V_{-1} .

For a square integrable function $f(x)$, if $F_m(x) = A_m f(x)$ denotes the best approximation to $f(x)$ in the space V_m (A_m is a projection operator), then considering that $\{\phi_{m,k}(x): (m, k) \in \mathbb{Z}^2\}$ is a basis for the space V_m we can write:

$$F_m(x) \equiv A_m f(x) = \sum_{k=-\infty}^{+\infty} \alpha_{mk} \phi_{mk}(x) \quad (7.6)$$

We now describe how this refinement is carried out. First of all, the spaces V_j are simply scaled versions of each other:

$$F_m(x) = A_m f(x) \in V_m \quad \text{means} \quad F_{m-1}(2x) = A_{m-1} f(2x) \in V_{m-1} \quad \text{and vice versa.} \quad (7.7)$$

Observe that this scaling property corresponds to the scaling (or dilation) property of the wavelet family of functions described in equation 7.1. The difference between an

approximation $F_m(x) = A_m f(x)$ in V_m and a finer approximation $F_{m-1}(x) = A_{m-1} f(x)$ can be found explicitly in terms of wavelet basis functions $\psi_{mk}(x)$. To be more precise,

$$A_{m-1} f(x) - A_m f(x) = \sum_{k=-\infty}^{\infty} \delta_{mk}(x) \psi_{mk}(x) \quad (7.8)$$

We can put this together with equation 7.7 to get

$$F_{m-1}(x) = \sum_{k=-\infty}^{+\infty} \alpha_{mk} \phi_{mk}(x) + \sum_{k=-\infty}^{+\infty} \delta_{mk} \psi_{mk}(x) \quad (7.9)$$

This gives us a complete expression of the best approximation to $f(x)$ at resolution level $m - 1$ in terms of the scaling function and parent wavelet.

Two Dimensional Cubic Spline Wavelets

A p^{th} order cardinal B-spline ($N_p(x)$) is defined recursively by integral convolution as follows:

$$N_p(x) = (N_{p-1} * N_1)(x) = \int_0^1 N_{p-1}(x-t) dt, \quad p \geq 2 \quad (7.10)$$

$$\text{where } N_1(x) = \begin{cases} 1 & \text{for } 0 \leq x < 1 \\ 0 & \text{otherwise} \end{cases}$$

$N_1(x)$ is also known as the Haar function. A B-spline becomes a Gaussian function when the order of the spline tends to infinity. Gaussian approximations of a one dimensional cubic B-spline scaling function and corresponding wavelets are as given below (Unser and Aldroubi, 1992):

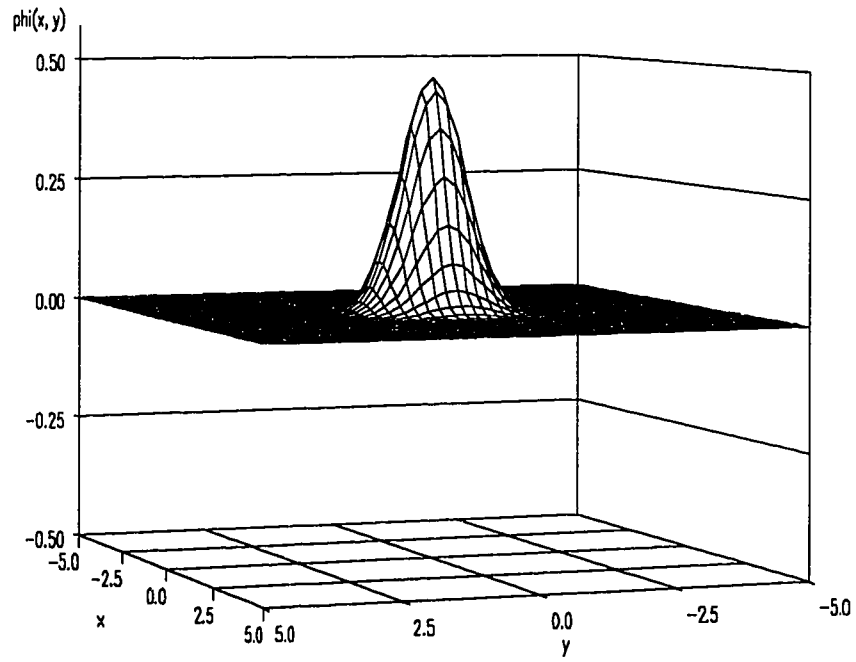
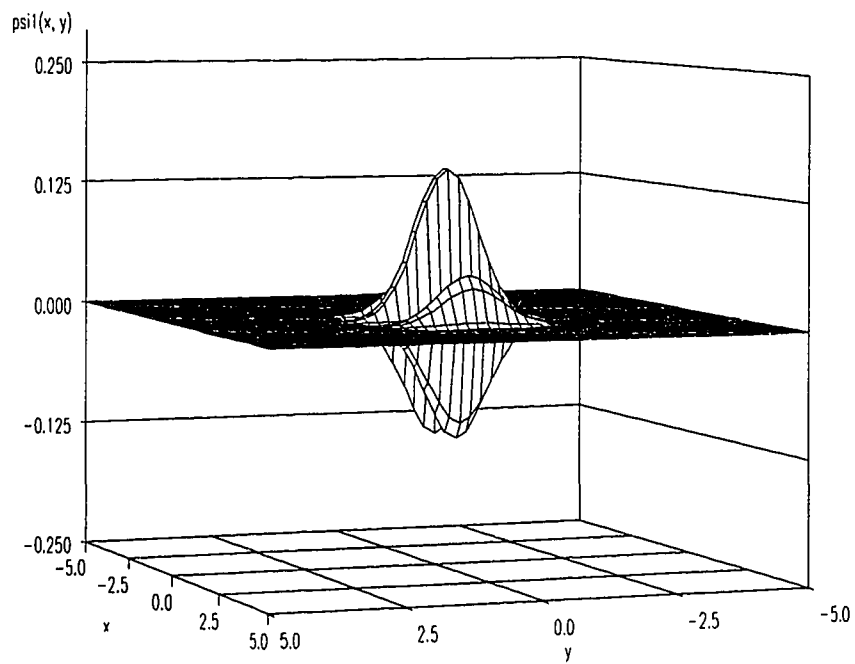
$$\phi(x) = 0.690988 \exp(-1.5x^2) \quad (7.11)$$

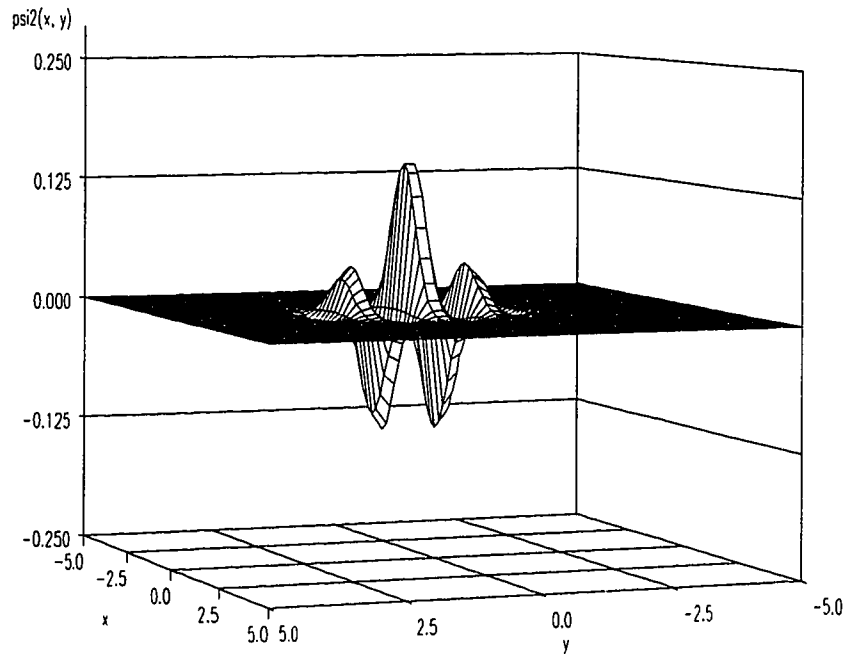
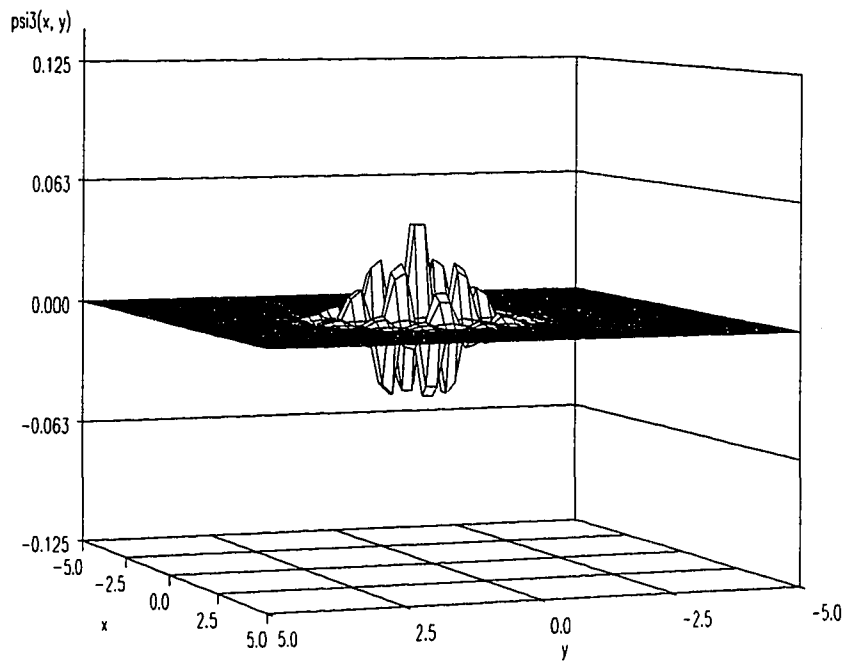
$$\psi(x) = 0.251477 \cos\{2.570935(2x - 1)\} \bullet \exp\{-0.222759(2x - 1)^2\} \quad (7.12)$$

A two dimensional family of wavelets can be generated by taking the product of one dimensional wavelets (Mallat, 1989a). If the hour of day (h) and outdoor temperature (T) are used as the two variables for modeling heating and cooling energy use, then the set of two dimensional scaling function and wavelets at any scale (m) and location (i, j) will be as follows:

$$\left. \begin{aligned} \phi_{mij}(h, T) &= \phi_{mi}(h) \phi_{mj}(T) \\ \psi_{mij}^1(h, T) &= \phi_{mi}(h) \psi_{mj}(T) \\ \psi_{mij}^2(h, T) &= \psi_{mi}(h) \phi_{mj}(T) \\ \psi_{mij}^3(h, T) &= \psi_{mi}(h) \psi_{mj}(T) \end{aligned} \right\} \quad (7.13)$$

The formulae for the scaling function and wavelet in equations 7.11 and 7.12 are for the actual scale (also called the finest resolution) of the data available with the location (centering of $\phi(x)$) defined by $k = 0$. For a particular m, the location of the scaling function or wavelet gets shifted by 2^m units. The one dimensional scaling functions and wavelets at any scale m and location k can be found using equations 7.4 and 7.1. The two dimensional scaling functions and wavelets are then found using equation 7.13. Note that for the two dimensional case, there is one scaling function and three wavelets for any location (i, j) at a particular scale (m). Two dimensional scaling function and wavelets with any two independent variables x and y at scale = 0 and location = (0, 0) have been illustrated in Figure 7.1a through 7.1d.

Figure 7.1a Scaling function $\phi_{000}(x, y)$ Figure 7.1b Wavelet $\psi^1_{000}(x, y)$

Figure 7.1c Wavelet $\psi^2_{000}(x, y)$ Figure 7.1d Wavelet $\psi^3_{000}(x, y)$

Wave-Net Modeling of Heating and Cooling Energy Use

As pointed out earlier, hourly heating and cooling energy use in commercial buildings depend on the operating schedule of the building and the weather variables like outdoor temperature, humidity and solar radiation. However, a model with outdoor temperature can indirectly account for the effects due to humidity and solar radiation to a large extent (Dhar et al., 1995). Moreover, there are situations when only outdoor temperature data is available for modeling because the humidity or solar radiation data was not measured or the sensor went bad. Physically, heating and cooling energy use may have both linear and nonlinear relationships with outdoor temperature and hour of day (Kissock, 1993). As a first step to model heating and cooling energy use, we propose to remove the linear dependence of energy use by performing a linear regression of energy consumption using the following equation:

$$E_{h,T} = a + bT + ch + \varepsilon_{h,T} \quad (7.14)$$

The residual $\varepsilon_{h,T}$ can then be modeled using Wave-Net in order to capture the nonlinearities. A Wave-Net has an input layer, a hidden layer and an output layer of nodes. All the weights between the input and hidden layers are fixed as unity whereas the weights between the hidden and output layers are determined through network optimization. Locating the basis functions (or the hidden nodes) is done by generating a two dimensional grid of hour of day and outdoor temperature (Figure 7.2). The sampling rate of energy data at the finest resolution ($m = 0$) is 1 hour along the time axis and $0.55\text{ }^{\circ}\text{C}$ ($1\text{ }^{\circ}\text{F}$) along the temperature axis. The basis functions need to be located within the outdoor temperature range supported by the data available. A range of $-6.67\text{ }^{\circ}\text{C}$ ($20\text{ }^{\circ}\text{F}$) to $37.8\text{ }^{\circ}\text{C}$ ($100\text{ }^{\circ}\text{F}$) has been considered to model energy use in various buildings in Texas. The sampling rate reduces by a factor of 2 when the scale increases (becomes coarser) by unity. The coarsest resolution will have at least two grid points. This means that the coarsest scale has $m = \inf\{\log_2 N\}$ (minimum integer value of $\log_2 N$; for example, if $\log_2 N = 4.7$ then $m = 4$) where N is the size of the grid at the finest

resolution. N is 24 along the time axis and 80 along the temperature axis, implying that there will be 5 ($0 \leq m \leq 4$) and 7 ($0 \leq m \leq 6$) scales along the time and temperature axes respectively. The coarsest scale from which learning can start is the minimum of these two quantities, which is the 4th scale ($m = 4$) in this case. The generation of grid points is illustrated in Figure 7.2 for $m = 4$ and $m = 3$.

Once the grid points are generated, training of the Wave-Net can be started. The scaling function nodes (also known as ϕ -nodes) and the wavelet nodes (also known as ψ -nodes) at the coarsest scale are added to the network first and addition of ψ -nodes at finer scales follows. Selection of which nodes are to be added to the network can be accomplished by performing stepwise regression with a reasonable cut-off criteria of partial R-square. Once the nodes are selected at a particular scale, the corresponding weights are determined by the method of least squares optimization. The residual is then used to select and train nodes at finer scales by the same method. As mentioned earlier, training the network essentially means determining the coefficients of the basis functions. The training process may continue until $m = 1$ is reached. The network architecture of a Wave-Net is shown in Figure 7.3.

Application to Monitored Data

Day-typing the data is important for removing the effects of major changes in operating schedule during weekdays, weekends, holidays and Christmas. Although a mere separation of data into weekdays and weekends may produce very good fits (Dhar et al. 1994a), one might perform a more detailed day-typing, as discussed in Chapter V, when necessary. Once day-typing is performed, modeling of energy use is done for each day-type separately. The usefulness of Wave-Net modeling is illustrated by two major examples: (i) cooling energy use during working weekdays and weekends from January 1992 to June 1992 in ZEC, a large institutional building that houses classrooms, labs, offices and computer facilities on the Texas A&M University campus; and (ii) heating energy use in BUR, another institutional building (classrooms, lecture halls, offices and

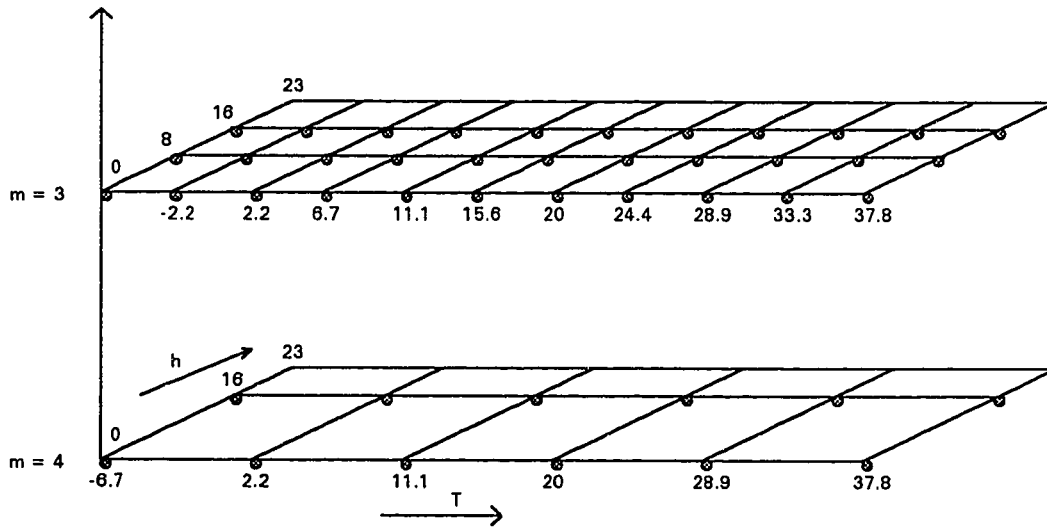


Figure 7.2 A two dimensional grid for locating the scaling functions and wavelets. One scaling function and three wavelets are located (centered) at each point marked with a filled circle for $m = 4$, while three wavelets are located at each grid point at finer scales ($1 \leq m \leq 3$).

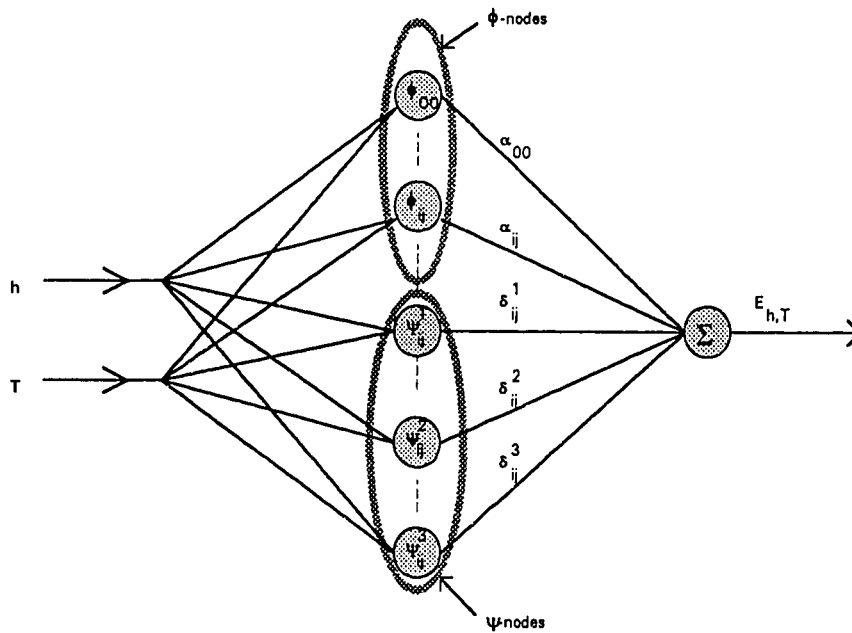


Figure 7.3 A schematic two dimensional Wave-Net to model heating and cooling energy use in commercial buildings.

Table 7.1 Location and basis function of various scaling function and wavelet nodes.

Site and type of energy use	Day-type	Scaling function nodes at scale = 4		Wavelet nodes at scale = 4		Wavelet nodes at scale = 3	
		Location (h, T)	Basis function	Location (h, T)	Basis function	Location (h, T)	Basis function
E _{cw} in ZEC, (GJ/h)	Weekdays	(16, 2.2)	ϕ_{11}	(0, 28.9)	ψ^2_{04}	(8, 20)	ψ^2_{16}
		(0, 37.8)	ϕ_{05}	(0, 37.8)	ψ^2_{05}	(8, 15.6)	ψ^3_{15}
		(0, 11.1)	ϕ_{02}	(16, 11.1)	ψ^2_{12}		
		(16, 20)	ϕ_{13}				
		(16, 28.9)	ϕ_{14}				
	Weekends	(0, 37.8)	ϕ_{05}	(16, 28.9)	ψ^2_{14}	(8, 20)	ψ^2_{16}
		(16, 2.2)	ϕ_{11}	(0, 28.9)	ψ^2_{04}		
		(0, 11.1)	ϕ_{02}	(0, 28.9)	ψ^3_{04}		
		(16, 37.8)	ϕ_{15}	(0, 20)	ψ^1_{03}		
		(16, 20)	ϕ_{13}	(16, 37.8)	ψ^2_{15}		
E _{hw} in ZEC, (GJ/h)	Weekdays	(16, 37.8)	ϕ_{15}	(16, 20)	ψ^2_{13}	(0, 6.7)	ψ^2_{03}
		(16, 20)	ϕ_{13}	(16, -6.7)	ψ^1_{10}	(16, -6.7)	ψ^3_{20}
		(16, 11.1)	ϕ_{12}	(16, 2.2)	ψ^2_{11}	(8, -2.2)	ψ^1_{11}
		(0, 37.8)	ϕ_{05}	(0, 20)	ψ^3_{03}	(16, -2.2)	ψ^1_{21}
		(16, -6.7)	ϕ_{10}	(0, -6.7)	ψ^3_{00}		
	Weekends	(16, -6.7)	ϕ_{10}	(16, 20)	ψ^2_{13}	(8, 2.2)	ψ^1_{12}
		(16, 20)	ϕ_{13}	(0, 37.8)	ψ^2_{05}	(0, 6.7)	ψ^2_{03}
		(16, 2.2)	ϕ_{11}	(16, 11.1)	ψ^2_{15}	(8, 2.2)	ψ^2_{12}
		(0, 37.8)	ϕ_{05}	(0, -6.7)	ψ^1_{00}	(16, 6.7)	ψ^3_{23}
		(0, 2.2)	ϕ_{01}	(16, 28.9)	ψ^2_{14}	(16, 6.7)	ψ^1_{23}
					(8, 20)	ψ^2_{16}	
					(16, 6.7)	ψ^1_{23}	
					(0, 6.7)	ψ^3_{03}	
				(8, -2.2)	ψ^3_{11}		

auditorium) on the UT Austin campus. In addition, the results of applying the Wave-Net to several other channels of data from different sites are discussed below.

Cooling Energy Use. Residuals of equation 7.14 are generated for cooling energy consumption and used to train the Wave-Net. As mentioned earlier, a temperature range of -6.7 °C (20 °F) to 37.8 °C (100 °F) has been used to locate the scaling function and wavelet nodes.

Addition of nodes starts at the coarsest scale ($m = 4$) that has a sampling interval of 16 hours along the time axis and $8.9\text{ }^{\circ}\text{C}$ ($16\text{ }^{\circ}\text{F}$) along the temperature axis. The nodes at any scale have been selected by performing stepwise regression on the residuals and using a cut-off criteria of partial R-square < 0.005 . As can be noted in Table 7.1, five scaling function nodes and three wavelet nodes have finally been added for the weekday group using this criterion. Once the nodes are added at $m = 4$, the residuals of the Wave-Net (the difference between measured energy use and Wave-Net output) are generated again and used to select and train the nodes at $m = 3$. The improvement in C.V. after training the nodes at $m = 4$ and $m = 3$ are shown in Table 7.2. As can be noted, improvement in C.V. by adding nodes at $m = 3$ is marginal for both weekdays (13.05% to 12.98%) and weekends (12.15% to 11.96%). Nodes at finer scales ($m \leq 2$) have thus been avoided without any significant sacrifice in prediction accuracy. The model fit to the data can be seen in the time series plots of measured and residual energy use in Figure 7.4.

Heating Energy Use. An approach similar to that for modeling cooling energy use was adopted for modeling heating energy use in BUR. As can be noted in Table 7.1, five scaling function and five wavelet nodes were added at scale = 4 to the network for both weekdays and weekends. Four and five wavelet nodes have been added at scale $m = 3$ for weekdays and weekends respectively. For both weekdays and weekends the improvement in C.V. was significant (18.14% to 14.04% for weekdays and 18.20% to 13.74% for weekends) when nodes were added at $m = 4$, however, not much of improvement in fit was achieved by adding the nodes at $m = 3$. Adding the nodes at finer scales was, therefore, avoided. The time series plots of measured energy use and residual energy use in Figure 7.5 show how well the model fits the data.

The Wave-Net methodology described in this chapter was applied to several other data channels from different sites and the C.V.s have been tabulated in Table 7.1. It may be noted that (i) Wave-Net has been consistently effective in improving the model

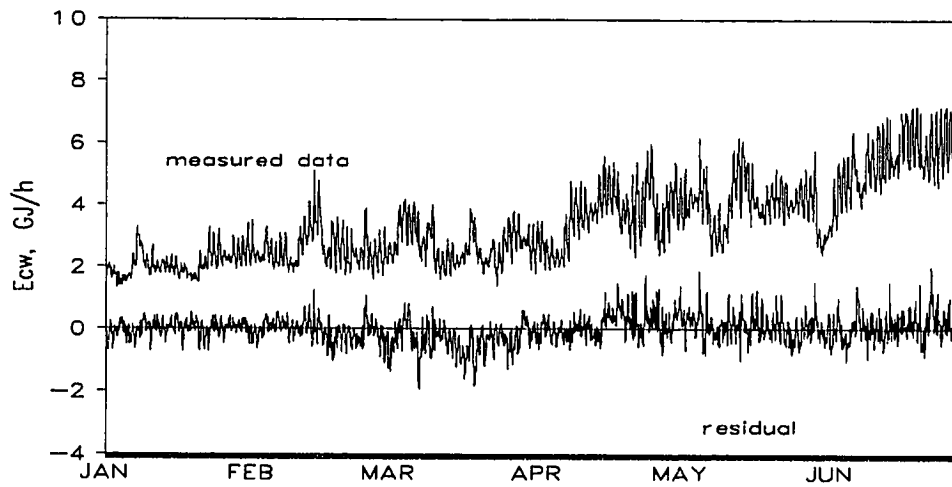


Figure 7.4 Time series plots of measured and residual cooling energy use in ZEC during January through June, 1992.

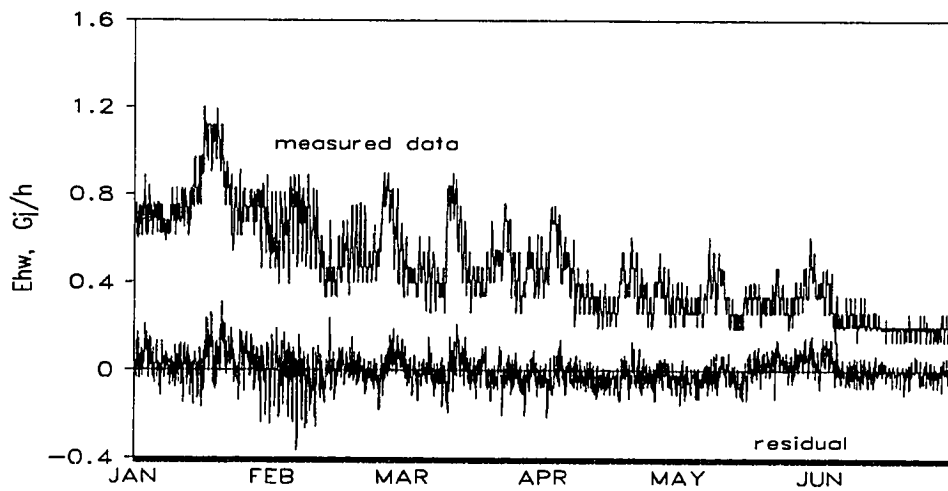


Figure 7.5 Time series plots of measured and residual heating energy use in BUR during January through June, 1992.

Table 7.2 Improvement of model C.V. (%) with addition of nodes at different scales in Wave-Net.

Site	Type of energy use	Period	Day-type	a+bT+ch C.V.(%)	At Scale = 4		At Scale = 3	
					Number of nodes added	Improved C.V.(%)	Number of nodes added	Improved C.V.(%)
ZEC	E_{cw} (GJ/h)	01/07/92- 06/30/92	Weekdays	15.71	8	13.05	2	12.98
			Weekends	16.59	12	12.15	1	11.96
ZEC	E_{cw} (GJ/h)	09/01/89- 12/20/89	Weekdays	9.15	8	8.25	3	8.15
			Weekends	8.90	11	6.88	7	6.64
TDH (L&M)	E_{cw} (GJ/h)	02/16/91- 08/12/92	Weekdays	28.24	19	18.92	1	18.81
			Weekends	31.00	13	19.58	3	18.70
BUR	E_{hw} (GJ/h)	01/01/92- 06/30/92	Weekdays	18.14	10	14.04	4	13.75
			Weekends	18.20	10	13.74	9	13.12
ZEC	E_{hw} (GJ/h)	09/01/89- 12/20/89	Weekdays	22.34	10	18.84	5	18.46
			Weekends	24.11	12	19.16	4	18.77
TDH	E_{hw} (GJ/h)	02/16/91- 08/12/92	Weekdays	31.03	18	23.65	7	22.58
			Weekends	34.46	21	22.05	1	21.93
TCOM (I & II)	E_{wbe} (kWh/h)	06/01/92- 08/31/92	Weekdays	12.25	9	8.26	5	6.96
			Weekends	9.23	3	9.07	4	8.61
MCC	E_{wbe} (kWh/h)	04/07/92- 05/15/92	Weekdays	30.20	8	15.46	14	13.49
			Weekends	18.62	11	12.49	4	9.70

fit, (ii) the number of nodes added at $m = 3$ are consistently less than the number of nodes added at $m = 4$ and (iii) improvement in fit decreases at finer scales. A plot of (i) measured heating energy use, (ii) model predicted heating energy use by using equation 7.14 (first approximation), (iii) model predicted energy use when scaling functions and wavelets at scale = 4 are added (second approximation) and (iv) the final model prediction with equation 7.14 plus the scaling functions and wavelets at scale = 4 and 3 are shown in Figure 7.6 to illustrate how model fit improves stage by stage.

Comparison with Conventional BPN

In order to compare the prediction accuracy of the Wave-Net methodology with a conventional Back Propagation Network, BPN models were also developed. The C.V.s of both Wave-Net and BPN for several channels have been tabulated in Table 7.3.

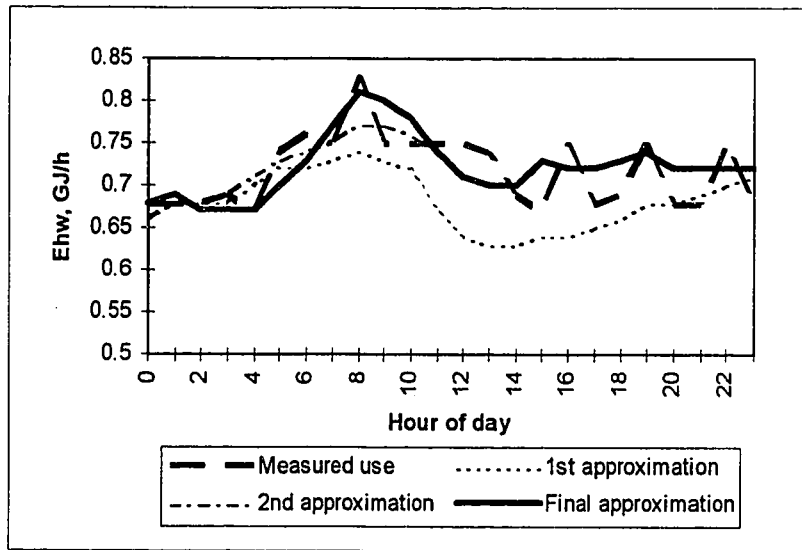


Figure 7.6 The plot shows how the approximation of measured heating energy use in BUR on January 09, 1992 improved at each stage of Wave-Net modeling. The first approximation is with the linear model only (eq. (7.14)) while the second and final approximations are made by subsequently adding scaling functions and wavelets at scale $m = 4$ and 3 respectively (also see Table 7.1).

A standard 4 layer BPN with the following parameters was adopted:

- (i) Three inputs: hour of day, outdoor temperature and day of week,
- (ii) Two hidden layers each having ten hidden nodes,
- (iii) one output,
- (iv) gain = 0.9, learning rate = 0.1, and bias = 0,
- (v) Sigmoid activation function, and
- (vi) A normalization range of 0 to 0.9 for all inputs and output.

However, for heating energy use in BUR, a learning rate of 0.05 had to be adopted in order to avoid the learning process getting stuck at local minima frequently. The results in Table 7.3 show that prediction accuracy of the Wave-Net algorithm has been better than the prediction accuracy of BPN in three out of eight cases. For the other cases, C.V. of Wave-Net is quite close to BPN except for heating energy use in TDH. This

shows that Wave-Net has the potential for offering high prediction accuracy. At the same time, the learning process of Wave-Net is faster by at least an order of magnitude (Bakshi and Stephanopolos, 1993) because a linear optimization technique was adopted to determine the weights.

The speed of a Wave-Net optimization is significantly better than a BPN optimization. In order to estimate how much faster the optimization of an Wave-Net algorithm is than a conventional BPN optimization, the number of operations (addition, subtraction, multiplication and division) involved in the computer program for both the algorithms was counted. If the time taken for each of these operations is assumed to be the same, the ratio of the total number of operations in the two cases will indicate how much faster the Wave-Net optimization is than the BPN optimization for a given training data set. Table 7.4 summarizes the results of this calculation.

The number of operations involved in the computer program written for Wave-Net optimization as well as for BPN optimization are:

$$N_{\text{Wave-Net}} = 20 \times (338550 + N_{\text{obs}})$$

$$N_{\text{BPN}} = N_{\text{epoch}} \times (554 + 1146 \times N_{\text{obs}})$$

where N_{epoch} and N_{obs} are the number of epochs needed in BPN optimization and number of observations in the training data set respectively. The ratio $N_{\text{Wave-Net}}/N_{\text{BPN}}$ indicates how faster the Wave-Net optimization is than the BPN optimization. The ratio $N_{\text{Wave-Net}}/N_{\text{BPN}}$ depends on both N_{obs} and N_{epoch} , however, it increases dramatically as N_{obs} increases. This can be noted from the results summarized in Table 7.4. Clearly, Wave-Net optimization, in general, is much faster than BPN optimization, as mentioned in the beginning of this chapter.

Predictive Ability of Wave-Net

The predictive ability of the Wave-Net algorithm was tested by applying the methodology to yearlong 1992 data obtained from four sites: (i) cooling energy use in ZEC, (ii) cooling energy use in RAS, (iii) heating energy use in BUR and (iv) heating energy use in PCL. The test was performed in two ways: (i) models developed from

Table 7.3 Comparison of C.V.s (%) of Back Propagation Network (BPN) and Wave-Net models for different sites in Texas.

Site	Type of energy use	Period	C.V. (%)	
			BPN model	Wave-Net model
ZEC	E_{cw} (GJ/h)	01/07/92-06/30/92	10.74	12.69
ZEC	E_{cw} (GJ/h)	09/01/89-12/20/89	6.32	7.72
TDH (L&M)	E_{cw} (GJ/h)	02/16/91-08/12/92	19.12	18.78
BUR	E_{hw} (GJ/h)	01/01/92-06/30/92	14.16	13.57
ZEC	E_{hw} (GJ/h)	09/01/89-12/20/89	16.96	18.34
TDH	E_{hw} (GJ/h)	02/16/91-08/12/92	16.60	22.39
TCOM (I & II)	E_{wbe} (kWh/h)	06/01/92-08/31/92	7.27	7.43
MCC	E_{wbe} (kWh/h)	04/07/92-05/15/92	14.79	12.40

Table 7.4 Comparison of optimization speed of Back Propagation Network (BPN) and Wave-Net for different sites in Texas.

Site	Type of energy use	Period	Number of observations	BPN epochs	Number of times Wave-Net faster than BPN
ZEC	E_{cw} (GJ/h)	01/07/92-06/30/92	4224	120	74.63
ZEC	E_{cw} (GJ/h)	09/01/89-12/20/89	2664	191	78.7
TDH (L&M)	E_{cw} (GJ/h)	02/16/91-08/12/92	13680	178	277.56
BUR	E_{hw} (GJ/h)	01/01/92-06/30/92	4368	119	76.19
ZEC	E_{hw} (GJ/h)	09/01/89-12/20/89	2664	139	57.28
TDH	E_{hw} (GJ/h)	02/16/91-08/12/92	13680	189	294.71
TCOM (I & II)	E_{wbe} (kWh/h)	06/01/92-08/31/92	2208	127	44.03
MCC	E_{wbe} (kWh/h)	04/07/92-05/15/92	936	936	25.01

January through June data were used to predict energy use from July through December (which we call continuous prediction) and (ii) models developed from January, March, May, July, September and November data were used to predict energy use in February, April, June, August, October and December (which we call alternate prediction). The mean energy use, Mean Bias Errors (MBEs) and Coefficient of Variance (C.V.) of Root Mean Square Errors (RMSEs) for the period for the data from which the models have

Table 7.5 Summary of results obtained from the prediction tests conducted on yearlong data of heating and cooling energy use in four sites in Texas.

	Site name	Energy use (GJ/h)	Continuous prediction			Alternate prediction		
			Mean (GJ/h)	MBE (%)	C.V. (%)	Mean (GJ/h)	MBE (%)	C.V. (%)
Model results	ZEC	E_{cw}	3.56	0	12.7	3.69	0	13.3
	RAS	E_{cw}	0.46	0	18.6	0.53	0	16.6
	BUR	E_{hw}	0.47	0	13.6	0.45	0	14.4
	PCL	E_{hw}	1.46	0	20.3	1.32	0	21.2
Prediction results	ZEC	E_{cw}	4.29	4.99	14.1	3.95	0.13	13.6
	RAS	E_{cw}	0.49	8.4	19.3	0.53	0.6	10.6
	BUR	E_{hw}	0.40	7.9	22	0.42	0.79	18.9
	PCL	E_{hw}	1.16	4.7	26.4	1.16	4.96	23.1

been developed (model results) as well as for the prediction period (prediction results) are summarized in Table 7.5.

Model Results. It may be noted in Table 7.5 that MBEs (the ratios of average residuals over corresponding mean energy use, expressed in percentage) of the models are zero. This is because the average of the residuals is zero when the method of least squares optimization is adopted. The C.V.s of continuous prediction models are lower than the C.V.s of alternate prediction models, except for cooling energy use in RAS. If the mode of operation of the building systems change from the first half of the year to the second half, the continuous prediction models will have lower C.V. than the corresponding alternate prediction models. The results suggest that cooling energy use in RAS did not have any significant systematic change in scheduling throughout 1992. The lower C.V. of an alternate prediction model for cooling energy use in RAS also suggests that the data of February, April and June have more scatter than the data of July, September and December.

Prediction Results. The choice of alternate months for prediction of energy use nullifies the effect of operational changes, if any, from the first half to the second half of

the year and, therefore, the MBEs of alternate prediction months are expected to be lower than the MBEs of continuous prediction months. This is confirmed by the results shown in Table 7.5.

The C.V.s of the prediction results are consistently less for alternate months than continuous months, the maximum change being from 19.3% to 10.6% for cooling energy use in RAS. This is obvious because the alternate month models are more stable than the continuous month models, the alternate month models having been able to cover a larger range of operations.

The time series plots of continuous and alternate prediction months for cooling energy use in ZEC and heating energy use in BUR and of the corresponding residuals are shown in Figures 7.7 through 7.10. The higher MBEs for continuous prediction periods may be observed in these plots. Also, higher local MBE during November and December in Figure 7.9 indicate significant operational changes.

Summary

A combined approach of linear and nonlinear modeling of heating and cooling energy use has been described in this chapter. While the linearities in energy use is captured by performing regression with hour of day and outdoor temperature as the variables, the nonlinearities in the energy use are conveniently modeled by a one-hidden-layer ANN with wavelet basis functions derived from cubic spline. The application of the combined approach has been illustrated by results of application to monitored data from several sites. The improvement of the prediction stage by stage has been explained.

Comparison between BPN and Wave-Net algorithm showed that (i) Wave-Net gave better results for three out of eight examples and (ii) Wave-Net optimization is much faster than BPN optimization. The results of prediction for both continuous and alternate prediction periods have been presented and discussed. In the next chapter, application of hourly energy use models to data screening will be presented.

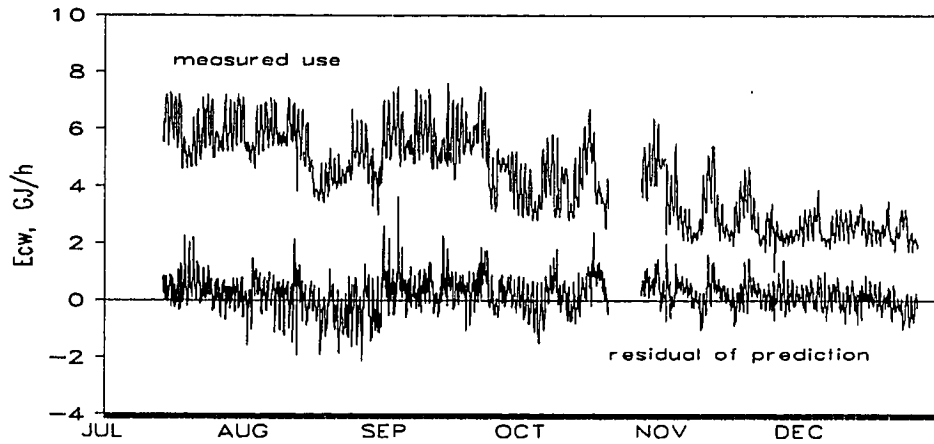


Figure 7.7 Cooling energy use and residuals of continuous prediction months in ZEC in 1992.

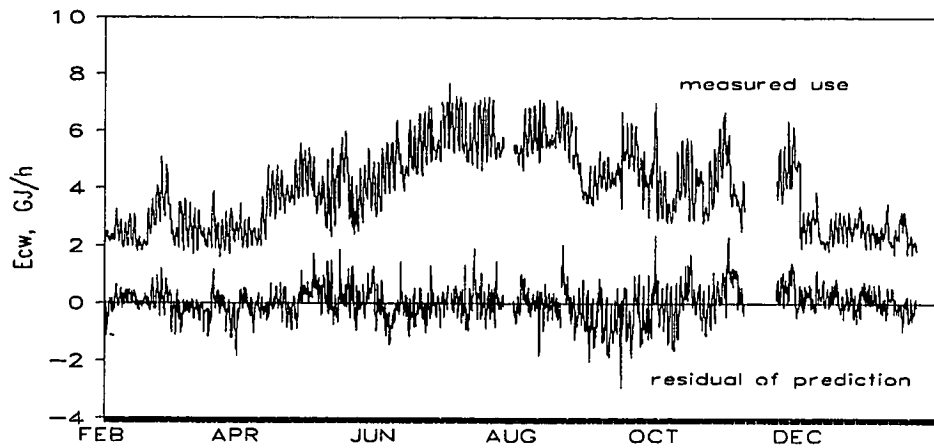


Figure 7.8 Cooling energy use and residuals of alternate prediction months in ZEC in 1992.

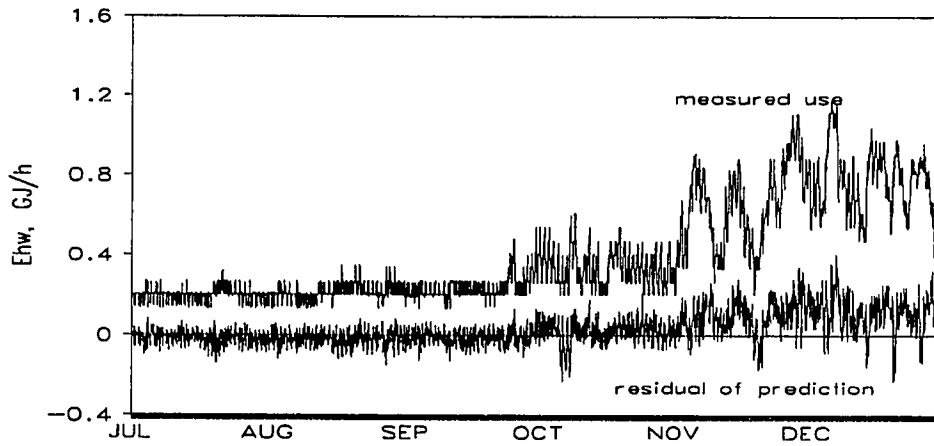


Figure 7.9 Heating energy use and residuals of continuous prediction months in BUR in 1992.

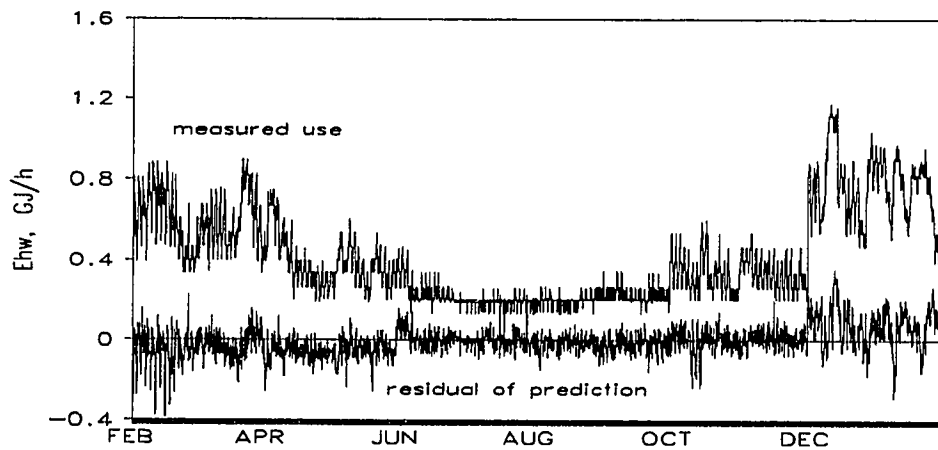


Figure 7.10 Heating energy use and residuals of alternate prediction months in BUR in 1992.

CHAPTER VIII

DATA-SCREENING

Introduction

Data-screening is an important step before data can be used for any purpose. Monitored building energy use data may be bad due to metering errors or failures. Energy consumption may also be affected by unusual operation of the building systems. While the major changes in mode of operation are taken care of by separating the whole data set into several groups (also known as day-typing) such as weekdays and weekends, bad or unusual data within a particular day-type are detected by performing data-screening. A model developed from a day-typed and screened data set will ensure physically consistent analysis for normal operating conditions of the building systems.

Although data-screening is very important for providing reliable data analysis and inferences, much less than required effort has been taken to document useful data quality control practices (Leipins and Uppuluri, 1990). However, some of the recent literature indicate that the methodology of developing a model and comparing the incoming data with the model to determine the quality is common (Little, 1990; Raghunathan and Rubin, 1990). The data quality control practice under Texas LoanSTAR MAP (Claridge et al., 1991) involves visual inspection and univariate modeling of incoming data (Abbas, 1993). In this chapter, a data-screening procedure for both weather independent and weather dependent energy use in commercial buildings, which involves several steps including the use of a multivariable regression model, is presented and illustrated with examples.

Data-screening Procedure

The data-screening procedure described in this chapter involves development of a suitable model and corresponding prediction interval from a reliable data set. An incoming observation is considered bad or unusual if it does not fall within the prediction band. Choosing data set of adequate length, an appropriate model equation and a

suitable confidence level to generate the prediction interval is crucial. The entire procedure for data-screening is shown in Figure 8.1 and the different aspects are discussed in the following sub-sections.

Unusual and Bad Data. Data is considered bad when the metering is wrong due to some error or failure of the metering instrument. It may also be bad if the metering instrument is installed or operated improperly. Such data may affect the conclusion of analysis adversely and, therefore, need to be removed. Unusual energy consumption data are due to unusual operation and maintenance of the building systems. The unusual data may not be used for model development but may be needed for some other purposes, for example, improving operation and maintenance, and, therefore, need to be retained. A suitable statistical or mathematical procedure can be adopted to identify bad and unusual data, as well as differentiating bad data from unusual data. Such a procedure combines information from the building operator on how the respective systems were operated during that period with analysis of the data. Using information from site on the operation and maintenance of the building systems on a regular basis is an integral part of a data-screening procedure.

Reliability and Length of Data Set. A highly reliable data set needs to be identified for using as the standard for performing data-screening. Visual inspection of various plots (Abbas, 1993) and using engineering and statistical judgement are necessary to accomplish this.

A data set of adequate length is required for developing an appropriate model. The effect of a short data set on modeling weather independent and weather dependent energy use has been discussed in Chapter IV and Chapter V respectively. Type of building is an important factor for deciding on the length of data set. For example, an institutional building may have a large number of day-types (see Chapter III, Figure 3.1) and consequently, a year long reliable data is necessary for developing model and

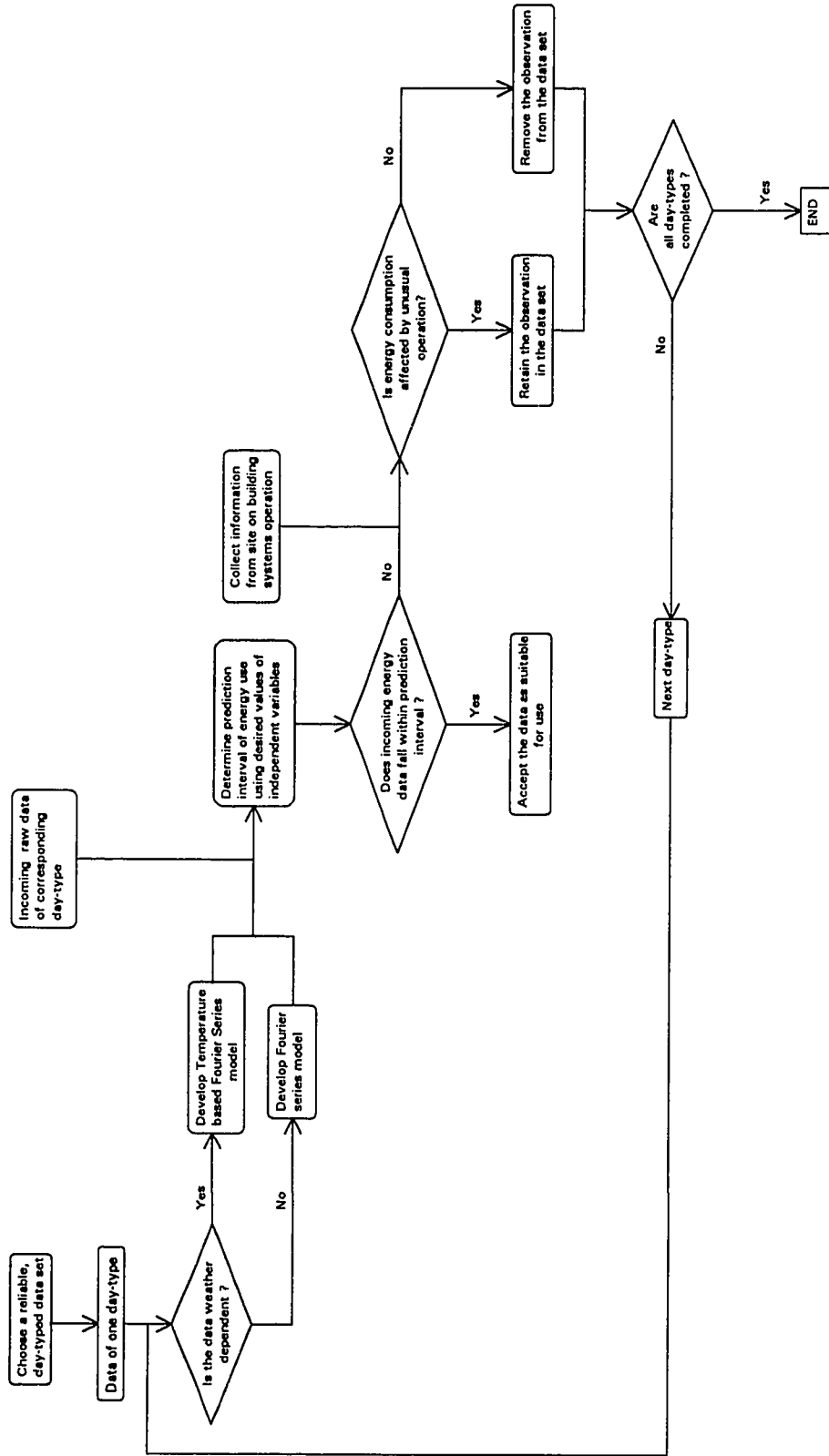


Figure 8.1 Data-screening procedure for weather independent and weather dependent energy use in commercial buildings.

prediction interval. On the other hand, an office building may eventually have only two day-types: weekdays and weekends (holidays are merged with the weekends). A data set of a few months may be adequate to start data-screening for these buildings. The decision is subjective to some extent because of unavailability of a firm statistical criteria to determine required data length.

For weather dependent energy use, the data set used for determining prediction interval needs to have data of the entire range of variation in order to avoid extrapolation error (See in Chapter V). In general, a data set covering the entire range of outdoor temperature variation may be considered adequate.

Until a data set of adequate length is available, the data quality may be checked by visual inspection and by using engineering judgement.

Choice of Modeling Approach. The first step of data-screening is to choose a modeling approach. The choice of modeling methodology for performing data-screening is dependent on the prediction accuracy and the speed of computation. An energy conservation program such as the Texas LoanSTAR MAP (Claridge et al., 1991) may have more than a thousand monitored data channels and one can not afford to have a slow computation for the purpose of performing data-screening on a regular basis.

For weather independent energy use, the Fourier series model described in Chapter IV may be used because it gives high prediction accuracy and can be developed within a short time. However, an addition criterion is involved while choosing model equation for performing data-screening of weather dependent energy use. Although the most appropriate model for weather dependent energy use will have all possible variables incorporated in its independent parameters, one is very often compelled to select a model that involves measurement of only one variable, for example, outdoor temperature. Using a model equation with outdoor temperature, outdoor humidity and solar flux (such as GFS approach described in Chapter V) involves measurement of three weather data channels. If any measuring instrument fails, resulting in lost humidity or solar data for a certain period, the model equation will no longer be able to predict energy use.

Moreover, measurement of outdoor temperature is easy and more reliable than the measurement of other variables. It is, therefore, recommended that a model with outdoor temperature as the only weather variable be used for data-screening.

Several techniques such as Fourier series approach (GFS and TFS)(Dhar et al., 1994 and 1995), ANN with Backpropagation algorithm (BPN) (Anstett et al., 1992), Wave-Net (Dhar et al., 1995) are available for modeling hourly weather dependent energy use in commercial buildings. These methodologies have been applied to monitored data from several buildings the results of which have been presented in Chapters IV, V and VI. When the Coefficient of Variance (C.V.) of these models are compared (Table 8.1), the temperature based models (TFS, BPN and Wave-Net) seem

Table 8.1 Comparison of C.V. (%) of four different modeling approaches applied to eight data channels from five sites in Texas. The shaded boxes indicate the lowest C.V. values among the temperature based modeling approaches (TFS, BPN and Wave-Net).

Site	Type of Energy use	Period	C.V. RMSE(%)			
			GFS	TFS	BPN	Wave-Net
ZEC	E_{CW} (GJ/h)	01/07/92 - 06/30/92	12.32	12.66	10.74	12.69
ZEC	E_{CW} (GJ/h)	09/01/89 - 12/20/89	7.30	8.03	6.32	7.72
TDH (Lab & Main)	E_{CW} (GJ/h)	02/16/91 - 08/12/92	17.29	18.54	19.12	18.78
TDH	E_{HW} (GJ/h)	02/16/91 - 08/12/92	21.98	20.80	14.16	13.57
ZEC	E_{HW} (GJ/h)	09/01/89 - 12/20/89	20.88	19.58	16.96	18.34
BUR	E_{HW} (GJ/h)	01/01/92 - 06/30/92	16.90	14.83	16.60	22.39
TCOM (Med. bldg. I & II)	E_{wbe} plus chiller (kWh/h)	06/01/93 - 08/31/93	6.88	7.25	7.27	7.43
MCC	E_{wbe} plus chiller (kWh/h)	04/07/92 - 05/15/92	13.33	11.78	14.79	12.40

to have predicted quite closely to GFS model that uses three weather variables (outdoor temperature, outdoor humidity and horizontal solar flux). At the same time, the TFS model is the fastest to develop among all the available temperature based modeling approaches. TFS approach is, therefore, adopted for performing data-screening of weather dependent energy use in commercial buildings.

Screening Outdoor Temperature Data. Although outdoor temperature data may be available from National Weather Services (NWS), using monitored data from site is preferred. This is because the weather conditions at site may differ from the weather conditions even at the nearest NWS station. However, sometimes the instrument measuring the outdoor temperature at site may fail resulting in missing or bad data. Such missing or bad data need to be replaced before TFS model equation can be used to predict and screen the weather dependent energy use data.

Outdoor temperature data from several sites show distinct linear correlation against temperature data from corresponding nearest NWS stations (Crowley and Haberl, 1994). This has been illustrated in Figures 8.2 through 8.5. The relationship may be expressed by the following functional form:

$$T_{\text{site}} = a + bT_{\text{NWS}} \quad (8.1)$$

A reliable set of outdoor temperature data is used to develop a model using equation 8.1 and corresponding prediction interval. The prediction interval so generated is then used to test whether the incoming temperature data is bad or not. The bad and missing observations are replaced by the model predicted values.

The methodology to screen outdoor temperature data as described above, however, assumes NWS data as correct. A suggested future improvement would be to

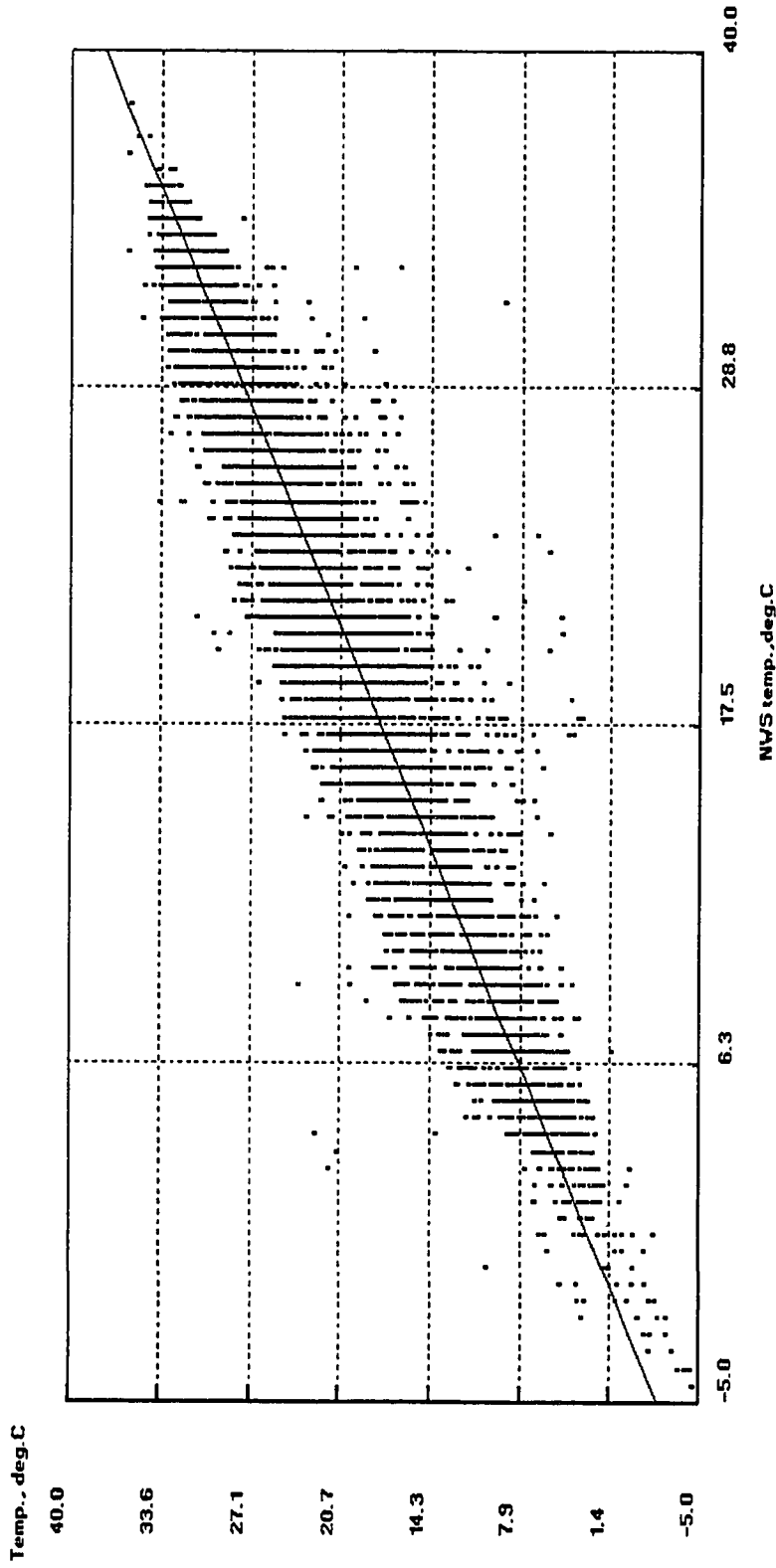


Figure 8.2 Drybulb temperature at Zachry Engineering Center versus drybulb temperature measured by the National Weather Service (NWS) at Easterwood Airport in College Station for 1992. The straight line shows a single variable linear regression fit ($R^2 = 0.88$, C.V. = 13.3%) to the data.

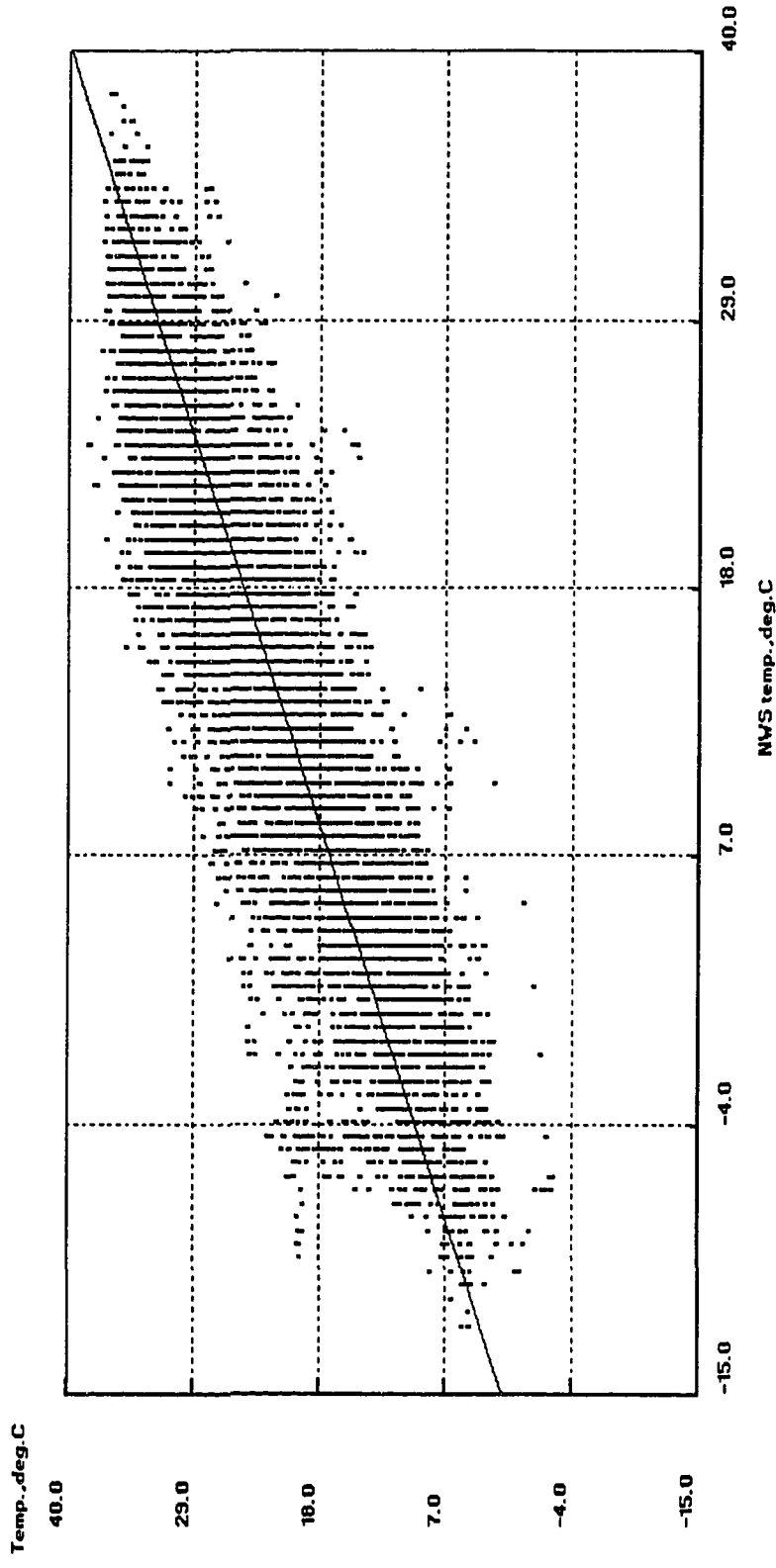


Figure 8.3 The drybulb temperature at S. F. Austin Building versus drybulb temperature measured by National Weather Service (NWS) at Austin in 1992. The straight line shows a single variable linear regression fit ($R^2 = 0.74$, C. V. = 19 %) to the data.

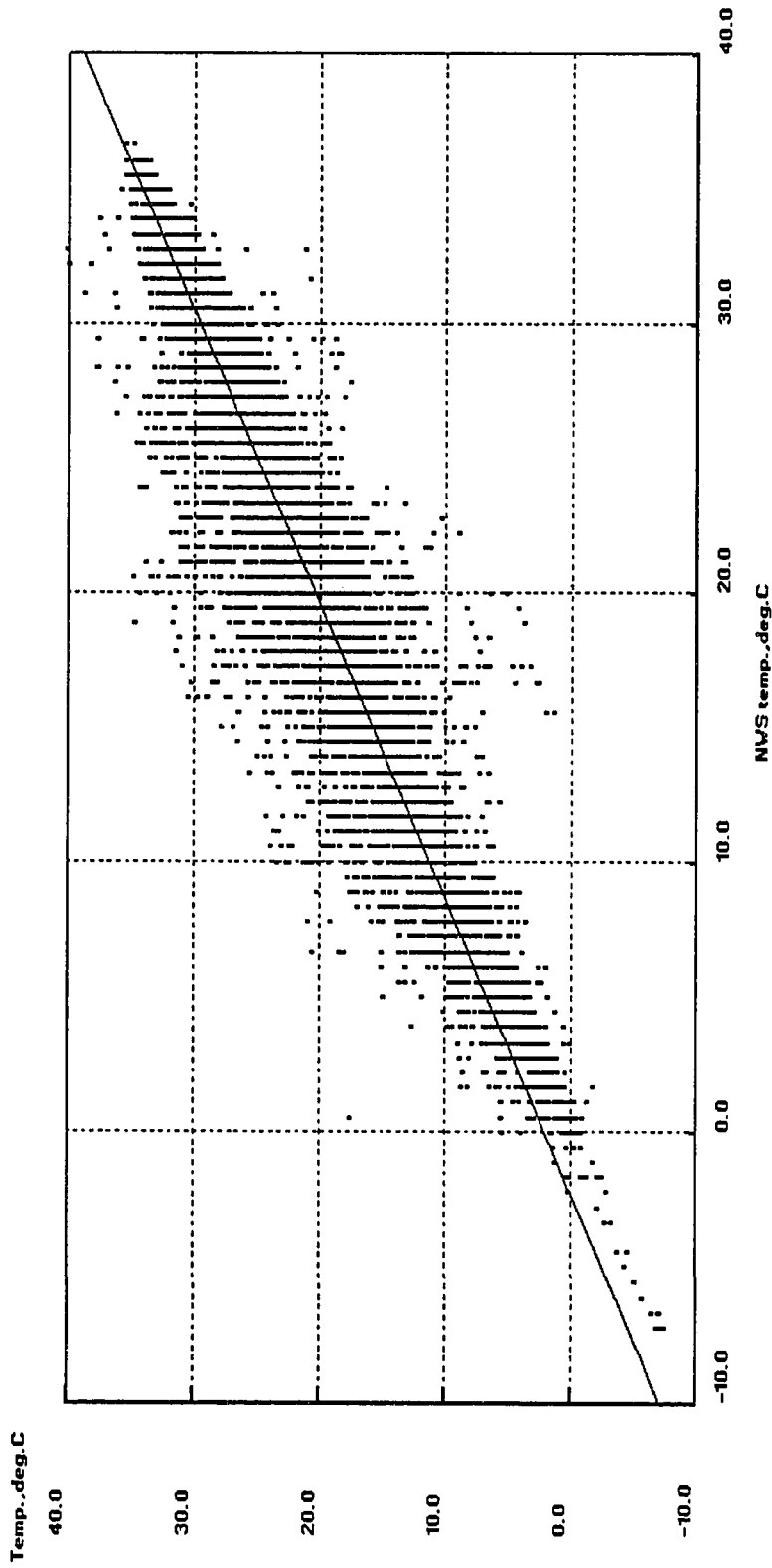


Figure 8.4 Drybulb temperature at the University Hall Building at UT Arlington versus drybulb temperature measured by the National Weather Service (NWS) at Dallas - Fort Worth Airport in 1992. The straight line shows a single variable linear regression fit ($R^2 = 0.87$, C.V. = 15.3 %) to the data.

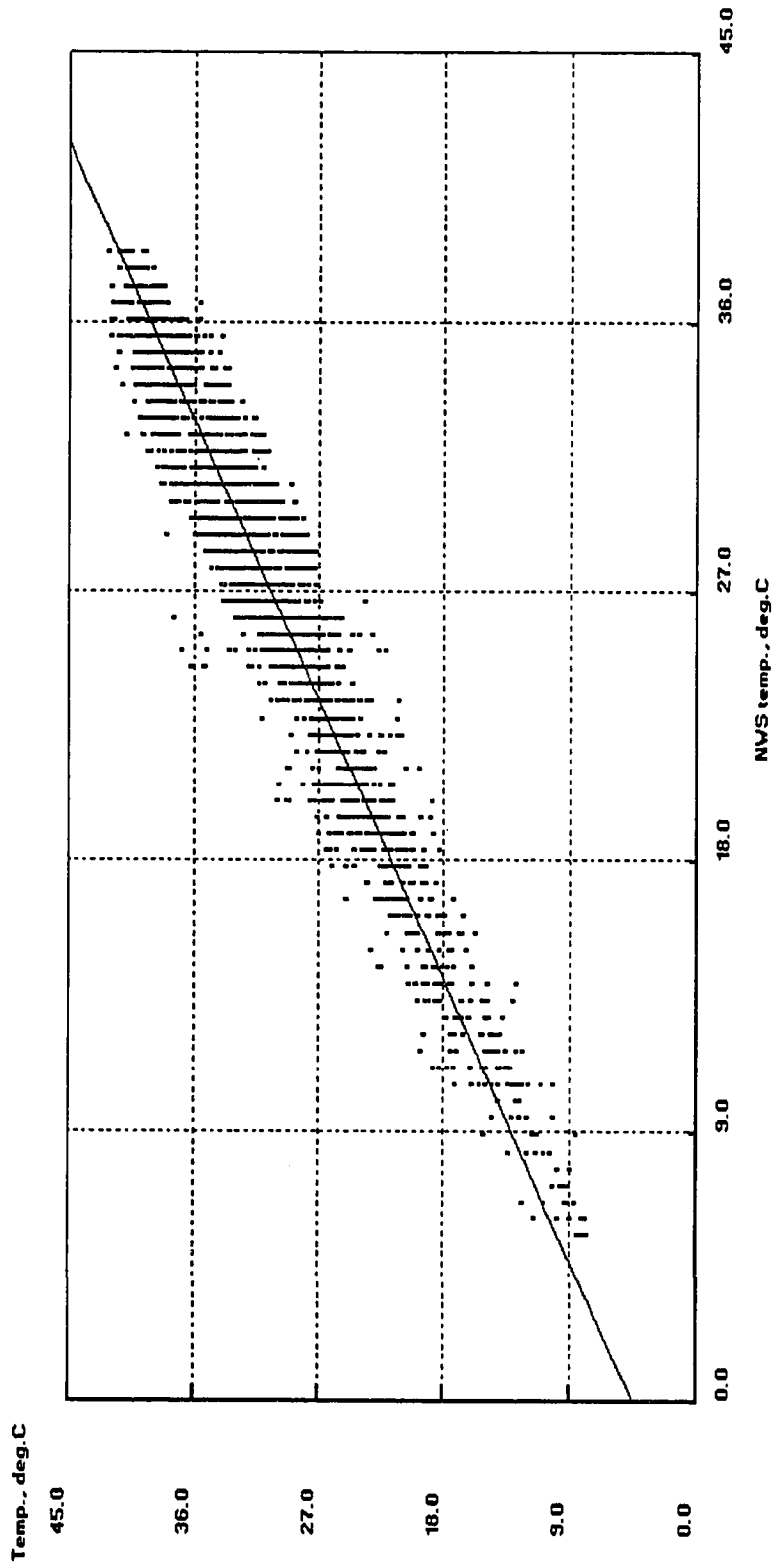


Figure 8.5 Drybulb temperature at TSTC, Harlingen versus drybulb temperature measured by National Weather Service (NWS) at Harlingen in 1992. The straight line shows a single variable linear regression fit ($R^2 = 0.92$, C.V. = 6.3 %) to the data.

consider the the trend of the NWS data as well as temperature data at site in order to decide on the data quality.

Prediction Interval of a Multivariate Model. The prediction interval of a model provides a range of value in which the future data is likely to be. Prediction interval can, therefore, be used for data-screening.

A multivariate regression model of a dependent variable y may be expressed as follows(Ott, 1988):

$$y = \beta_0 + \sum_{j=1}^k \beta_j x_j + \varepsilon \quad (8.2)$$

where x_j s are the independent variables, β_j s are the regression coefficients and ε is the random error. The β_j s in equation 8.2 can be estimated by the method of least squares. If n observations are available for model development then the dependent variable matrix Y , independent variable matrix X and coefficient matrix β of dimensions $1 \times n$, $(k+1) \times n$ and $1 \times (k+1)$ respectively are related as follows:

$$Y = X\beta + \varepsilon \quad (8.3)$$

The estimate of the coefficient matrix β can be calculated as

$$\hat{\beta} = (X^T X)^{-1} X^T Y \quad (8.4)$$

where the superscript T stands for the transposition of matrix and the superscript -1 stands for inversion of matrix. If the desired set of independent variables is contained in a matrix L of dimension $1 \times (k+1)$ then the prediction interval of dependent variable y is calculated as follows:

$$\hat{y} \pm t_{\alpha/2} s_e \sqrt{1 + L^T (X^T X)^{-1} L} \quad (8.5)$$

where (i) $t_{\alpha/2}$ is a transformed Gaussian normal distribution function and is used to determine if $(1 - \alpha)\%$ of data falls within a certain interval. The predicted y value (\hat{y}) and the Root Mean Square Error (s_e) are calculated as follows:

$$\hat{y} = L\hat{\beta} \quad \text{and} \quad s_e = \sqrt{\frac{(Y^T Y - \hat{\beta}^T X^T Y)}{n - (k + 1)}}$$

An inherent assumption in the calculation of prediction interval as shown in eq. 8.5 is the absence of autocorrelation in the residuals. However, the residuals of a multivariate model for predicting energy use in commercial buildings may be autocorrelated as a result of not incorporating all the driving forces such as weather variables, operating conditions of the building HVAC systems and the parameters that characterize the building envelope. In that case, the actual prediction interval may be higher than that calculated using equation 8.5. Although equation 8.5 has been used to determine prediction interval in this dissertation, one may want to consider the autocorrelation and develop the necessary equation to arrive at a better estimation of prediction interval (Kissock, 1993). Such a formula can be used once the presence of autocorrelation is detected by performing a Durbin-Watson test (Ott, 1988).

Application to Monitored Data

The method of data-screening described in this chapter is illustrated with the example of cooling energy use in ZEC building. Both outdoor temperature and cooling energy use models were developed from the data of January through June, 1992 and these models were used to screen the data from July through December in 1992. Figure 8.6 shows a scatter plot of measured outdoor temperature data versus outdoor

temperature recorded by National Weather Services. The model and the prediction interval are also shown. When this model was used to screen the outdoor temperature data from July through December in 1992, a few points fell outside the prediction interval (Figure 8.7). The points that had fallen outside the prediction interval were replaced by the model predicted values. The screened outdoor temperature data was then used to check the cooling energy use data during July through December in 1992.

Figures 8.8 and 8.9 show a scatter plot and a time series plot of cooling energy use during the weekdays of the second half of 1992 in ZEC. In Figure 8.9, an indicator variable is used to indicate unusual or bad data points. The indicator variable assumes zero value if the data is acceptable for model development, while it assumes a unity value otherwise. Figures 8.10 and 8.11 are similar to Figures 8.8 and 8.9 except that these plots are for weekends only. These plots show that the data-screening methodology adopted here indicated only a few points to be bad or unusual and, therefore, unsuitable for the purpose of analysis.

Summary

In this chapter a data-screening methodology based on model prediction has been described. While the energy use model can be used directly for screening weather independent energy data, screening weather dependent energy data requires screening the outdoor temperature data first and then using the screened temperature data to predict energy use and corresponding prediction interval. In the next chapter, conclusions on the work described in this dissertation and the future directions are presented.

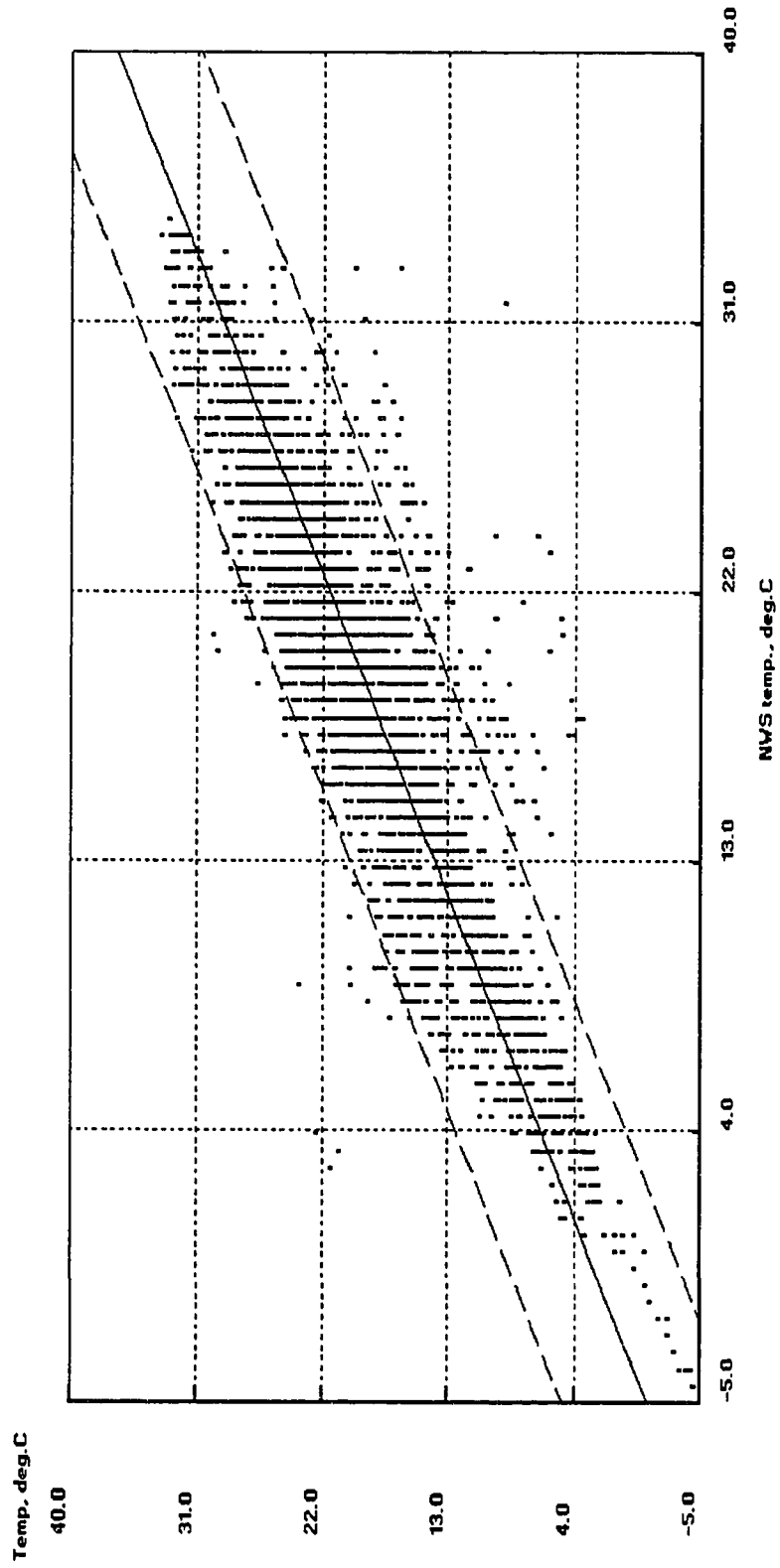


Figure 8.6 Measured temperature data from the Zachry Engineering Center versus NWS temperature with the model and prediction interval is shown for the data from January 1, 1992 through June 30, 1992.

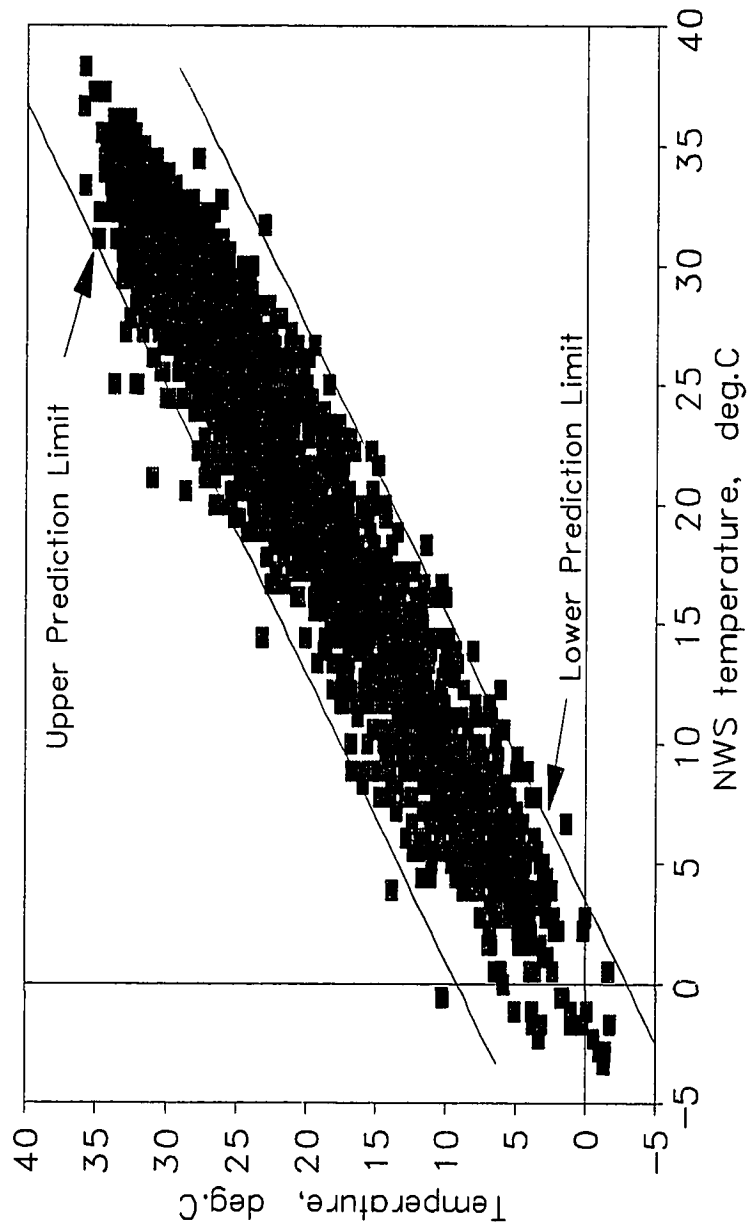


Figure 8.7 Measured temperature data and the prediction interval for the period from July 1, 1992 through December 31, 1992 shows that a few points fall outside the prediction limit. Such observations are replaced by model predicted values.

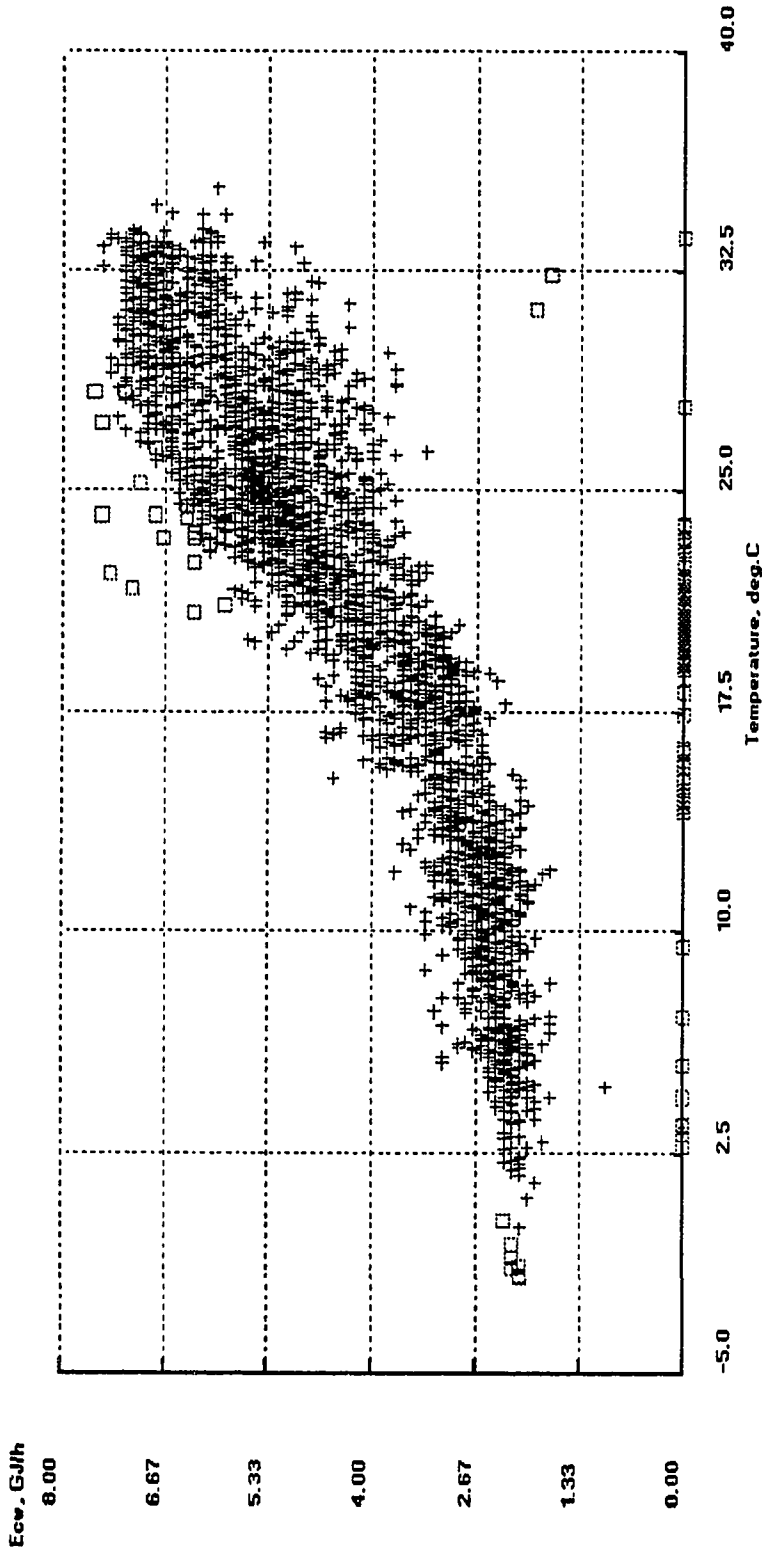


Figure 8.8 Scatter plot of measured cooling energy use versus screened outdoor temperature data during July 1, 1992 thru December 31, 1992 (weekdays only) in ZEC. The "plus" symbols denote normal energy use while the "square box" symbols denote the unusual data points.

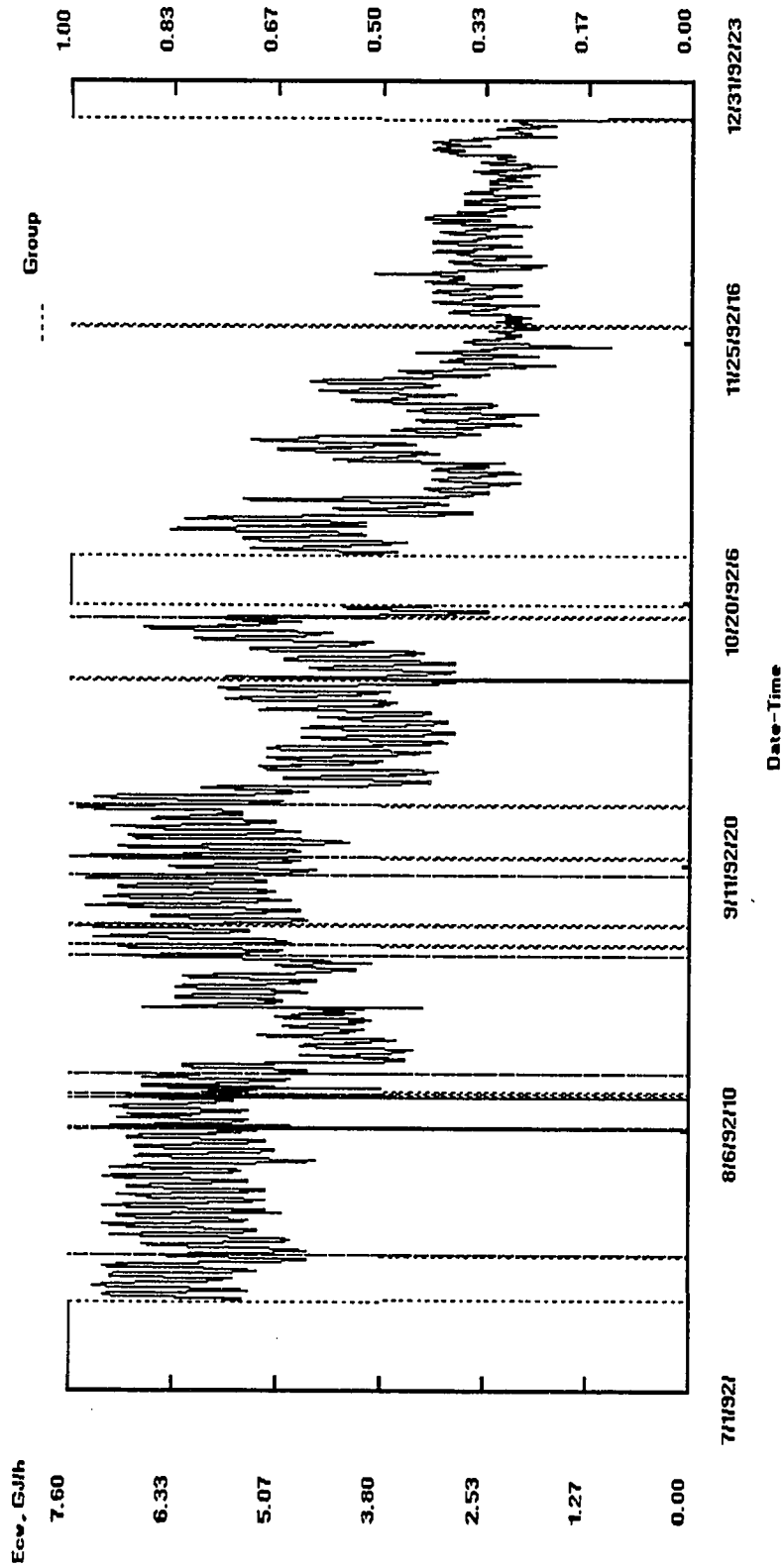


Figure 8.9 Time series plot of measured cooling energy use data from July 1, 1992 thru December 31, 1992 (weekdays only) in ZEC. The variable "group" is the indicator variable plotted on the secondary y - axis and is used to indicate the unusual or bad data. A "0" value indicates that the data is normal while a "1" value indicates unusual energy consumption or bad data.

Ecw, G/J/h

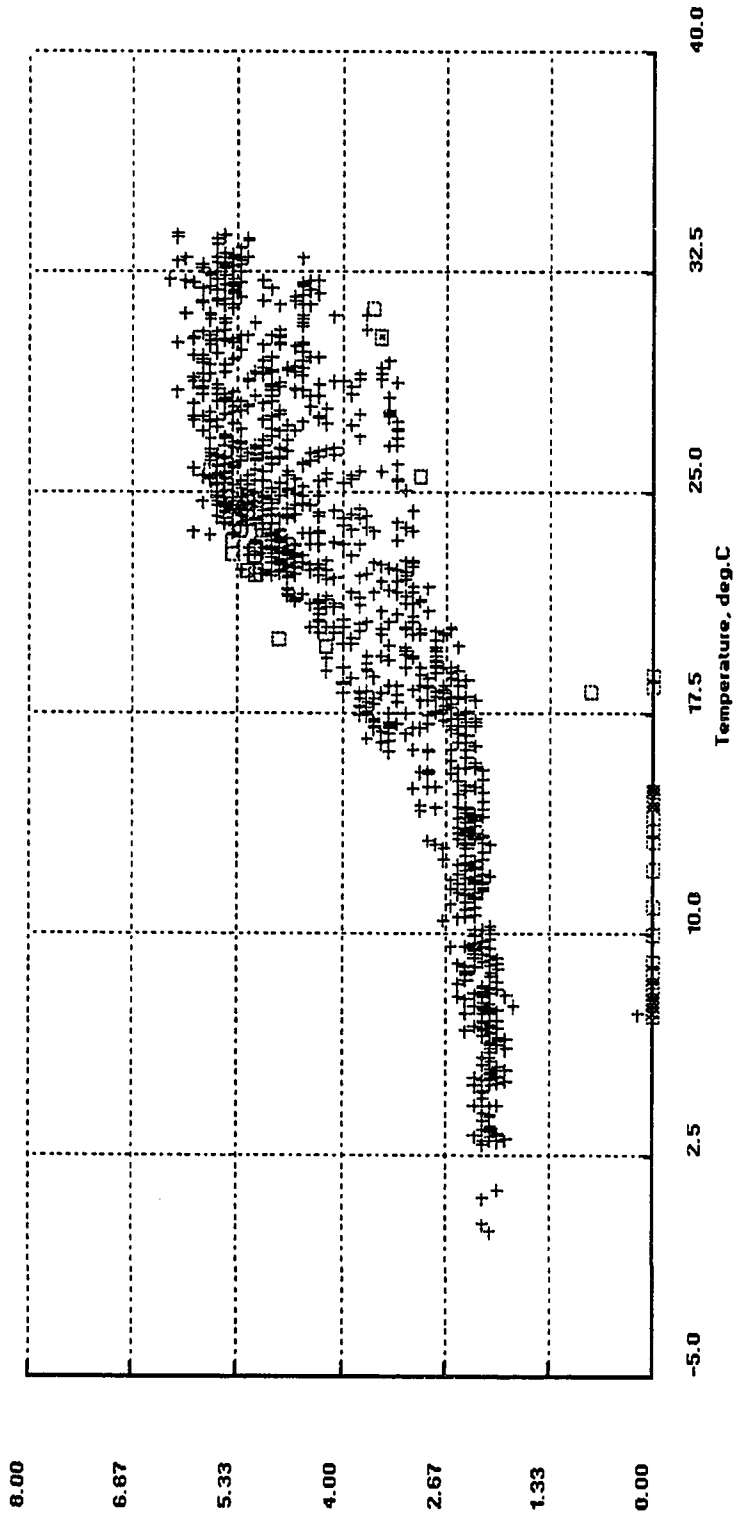


Figure 8.10 Scatter plot of measured cooling energy use versus screened outdoor temperature data from July 1, 1992 thru December 31, 1992 (weekends only) in ZEC. The "plus" symbols denote normal energy use while the "square box" symbols denote the unusual data points.

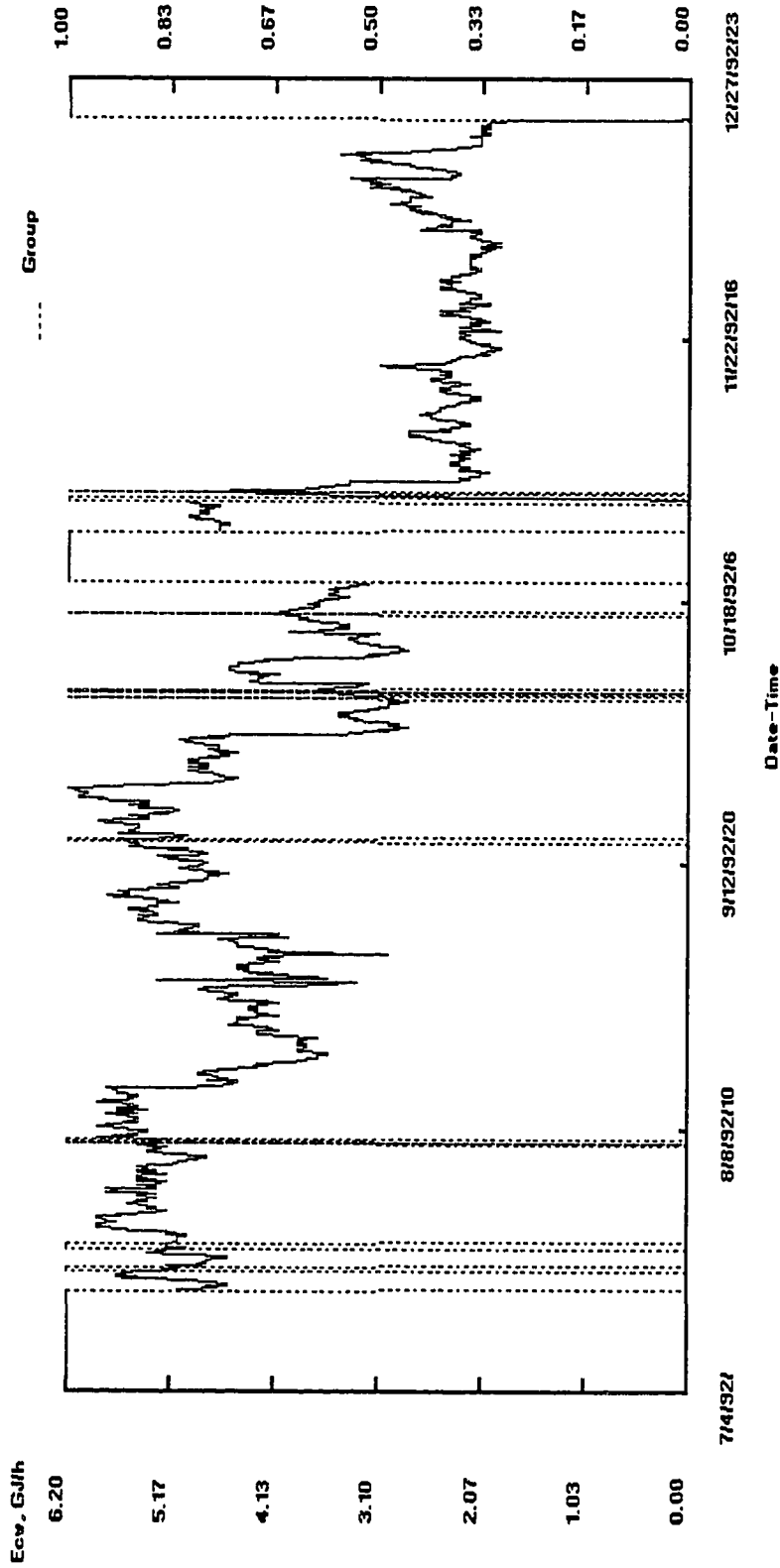


Figure 8.11 Time series plot of measured cooling energy use data from July 1, 1992 thru December 31, 1992 (weekends only) in ZEC. The variable "group" is the indicator variable plotted on the secondary y - axis and is used to indicate the unusual or bad data. A "0" value indicates that the data is normal while a "1" value indicates unusual energy consumption or bad data.

CHAPTER IX

CONCLUSIONS AND FUTURE DIRECTIONS

Introduction

A methodology to model weather independent energy use in commercial buildings using Fourier series functional form has been developed and its modeling ability verified by applying to monitored data from several buildings in Texas. For modeling weather dependent energy use, the following methodologies have been developed and applied to monitored data from buildings in Texas:

- (i) Generalized Fourier Series (GFS) approach which uses outdoor temperature, outdoor humidity and horizontal solar radiation as the weather variables in the model equation,
- (ii) A Temperature based Fourier Series (TFS) approach which considers the hour of day and outdoor temperature as the variables in the model equation and
- (iii) A combined linear and nonlinear approach using hour of day and outdoor temperature as the variables; the nonlinear modeling is performed with a one-hidden-layer Artificial Neural Network with two dimensional wavelet basis functions (Wave-Net) derived from a cubic spline.

A preliminary approach to data-screening using TFS model equation has been proposed and illustrated by monitored data from buildings in Texas.

GFS Approach

The GFS approach has been shown to be very appropriate for modeling hourly energy use in commercial buildings. Choice of a physically meaningful day-typing technique and the rational functional form of the regression model have been the two key factors that were instrumental in achieving consistently high prediction accuracy. Generalization of the approach has been provided by including interaction terms in the model equations that will be able to capture variation of both mean and amplitude of

energy use, if present in the data. This ensures wider range of applicability of Fourier series models in analyzing hourly building energy use. The validity of the approach can be verified further by applying to the data obtained from different parts of the world.

TFS Approach

Fourier series approach with outdoor temperature as the only weather variable has been found to model heating and cooling energy use in commercial buildings accurately. In fact, comparison of prediction accuracy of GFS, TFS, BPN and Wave-Net approaches showed that TFS provides modeling with the best prediction accuracy with only the hour of day and outdoor temperature as the variables. Also TFS modeling is easy to implement using standard software such as SAS (Statistical Analysis System). The power of the TFS approach lies in its ability to treat non-linear temperature dependence by using temperature frequency terms and the terms that account for interactions between hour of day and outdoor temperature. The key difference between the GFS and the TFS approach is that the TFS approach, although provides a little less accurate modeling than the GFS approach for cooling energy use, is practically more useful than the GFS approach because of its using the outdoor temperature as the only weather variable. Measurement of outdoor temperature is easy and more reliable than the measurement of humidity and solar radiation and, very often, either humidity and solar flux (which are used as variables in the GFS approach) are not measured or the metering instruments for humidity and solar radiation fails resulting in lost data.

The TFS approach needs to be applied to more buildings to verify its consistency in providing superior fit to measured data. The algorithm can be used to develop software for modeling hourly energy use in commercial buildings. Research on its application to short term forecasting may be interesting.

ANN with Wavelet Basis Functions - Wave-Net

Application to monitored data from several sites showed that a one-hidden-layer ANN with wavelet basis functions (Wave-Net) derived from a cubic spline is a powerful

tool for predicting heating and cooling energy use in commercial buildings. Moreover, learning of Wave-Net algorithm is faster at least by an order of magnitude than a BPN and convergence of the optimization process is guaranteed. However, the choice of appropriate scaling functions and wavelets is crucial for the success of a Wave-Net. There are different types of wavelets available, for example, Daubechies wavelets, Battle-Lemarie wavelets, Haar wavelets, etc. (Bakshi and Stephanopolos, 1993). An orthonormal set of scaling functions that are orthogonal to outdoor temperature and hour of day may be developed and applied to measured data to investigate the possibility of improving prediction accuracy.

It may be noted that for two dimensional application, three wavelets need to be placed at each grid point. This number increases rapidly in higher dimensions (2^{n-1} for n dimensions) which will result in a very large network when variables like humidity and horizontal solar flux are also considered in modeling. Multidimensional non-separable wavelets (Kokacevic and Vaterli, 1992) can be used in such cases to arrive at a compact network. Developing a multidimensional Wave-Net model using nonseparable wavelets to predict energy use in commercial buildings may be an interesting future direction.

Data-screening

Data-screening is an important step before it can be used for any purpose and, therefore, needs more attention. A preliminary data-screening algorithm has been described and the procedure illustrated by a few examples, however, the methodology needs several refinement. Application to more examples is needed to test its effectiveness. There is ample scope for research in this direction.

REFERENCES

Abbas, M. 1993, "Development of Graphical Indices for Building Energy Data", M.S. Thesis, Mechanical Engineering Department, Texas A&M University, College Station, Texas, December.

Anstett, M. and Kreider, J.F., 1993, "Application of Neural Networking Models to Predict Energy Use", *ASHRAE Transactions*, Vol. 99, Part 1, pp. 505 - 517.

Bakshi, B.R. and Stephanopolos, G., 1993, "Wave-Net: A Multiresolution Hierarchical Neural Network with Localized Learning", *AIChE Journal*, Vol. 39, Part 1, pp. 57 - 81.

Balcomb, J.D., Burch, J.D. and Subbarao, K., 1993, "Short-term Energy Monitoring of Residences", *ASHRAE Transactions*, Vol. 99, Part 2, pp. 935 - 944.

Balcomb, J.D., Burch, J.D., Westby, R.D., Subbarao, K. and Hancock C.E., 1994, "Short-term Energy Monitoring for Commercial Buildings", *Proceedings of the ACEEE 1994 Summer Study on Energy Efficiency in Buildings*, Vol. 5, pp. 5.1 - 5.11, Pacific Grove, California.

Battle, G., 1987, "A Block Spin Construction of Ondelettes. Part I: Lemarie Functions", *Communications on Mathematical Physics*, Vol. 110, pp. 601 - 625.

Beale, R. and Jackson, T., 1990, *Neural Computing*, IOP Publishing Ltd., Bristol, England.

Blum, A. 1992, *Neural Networks in C++*, John Wiley and Sons, Inc., New York.

Boubez, T.I and Peskin, R.L., 1993, "Wavelet Neural Networks and Receptive Field Partitioning", *Proceedings of the IEEE Conference on Neural Networks*, San Francisco, March, Vol. 3, pp. 1544 - 1549.

Bou-Saada, T., 1994, "An Improved Procedure for Developing a Calibrated Hourly Simulation Model of an Electrically Heated and Cooled Commercial Building", Master's Thesis, Mechanical Engineering Department, Texas A&M University, College Station, Texas, December.

Braun, J.E., Mitchell, J.W. Klein, S.A. and Beckman, W., 1987, "Performance and Control of a Large Cooling System", *ASHRAE Transactions* Vol. 93, Part 1, pp. 1830 - 1852.

- Bronson, J.D., 1992, "Calibrating DOE-2 to Weather and Non-weather Dependent Loads for a Commercial Building", Master's Thesis, Mechanical Engineering Department, Texas A&M University, College Station, Texas, May.
- Carpenter, G.A. and Grossberg, S., 1988, "The ART of Adaptive Pattern Recognition", *IEEE Transactions on Computer*, Vol. 21, pp. 107 - 121, March.
- Chakraborty, G., Shiratori, N. and Noguchi, S., 1993, "A Quickly Trained ANN with Single Hidden Layer Gaussian Units", *Proceedings of the IEEE International Conference on Neural Networks*, San Francisco, March, Vol. 1, pp. 466 - 471.
- Chang, C.H., Lin, J.L. and Cheung, J.Y., 1993, "Polynomial and Standard Higher Order Neural Neural Networks", *Proceedings of the IEEE International Conference on Neural Networks*, San Francisco, March, Vol. 2, pp. 989 - 994.
- Chen, D., Giles, C.L., Sun, G.Z., Chen, H.H., Lee, Y.C. and Goudreau, M.W., 1993, "Constructive Learning of Recurrent Neural Networks", *Proceedings of the IEEE International Conference on Neural Networks*, San Francisco, March, Vol. 2, pp. 1196 - 1201.
- Chen, F.C. and Lin, M.H., 1993, "On The Learning and Convergence of Radial Basis Networks", *Proceedings of the IEEE International Conference on Neural Networks*, San Francisco, March, Vol. 2, pp. 983 - 988.
- Chui, C.K. and Wang, J.Z., 1990, "A General Framework of Compactly Supported Splines and Wavelets", *CAT Report No.219*, Texas A&M University.
- Chui, C.K., 1992a, *An Introduction to Wavelets*, Academic Press Inc., San Diego, California.
- Chui, C.K., 1992b, *Wavelets: A Tutorial in Theory and Applications*, Academic Press Inc., San Diego, California.
- Claridge, D., Haberl, J., Turner, W., O'Neal, D., Heffington, W., Tombari, C. and Jeager, S., 1991, "Improving Energy Conservation Retrofits with Measured Savings", *ASHRAE Journal*, October, pp. 14 - 22.
- Clarke, J.A., Strachan, P.A. and Pernot, C., 1993, "An Approach to the Calibration of Building Energy Simulation Models", *ASHRAE Transactions*, Vol. 99, Part 2, pp. 917 - 927.
- Curtiss, P.S., Kreider, J.F. and Brandemuehl, M.J., 1993, "Adaptive Control of HVAC Processes Using Predictive Neural Networks", *ASHRAE Transactions*, Vol. 99, Part 1, pp. 496 - 504.

Daubechies, I., 1988, "Orthonormal Bases of Compactly Supported Wavelets", *Communications on Pure Applied Mathematics*, Vol. 41, pp. 909 -996.

Daubechies, I., 1990, "The Wavelet Transform, Time Frequency Localization and Signal Analysis", *IEEE Transactions on Information Theory*, Vol. 36, pp. 961-1005.

Daubechies, I., 1992, *Ten Lectures on Wavelets*, Society for Industrial and Applied Mathematics, Philadelphia, Pennsylvania.

Dhar, A., Reddy, T.A. and Claridge, D.E., 1994a, "Improved Fourier Series Approach to Modeling Hourly Energy Use in Commercial Buildings", *Proceedings of the ASME/JSME/JSES Solar Energy Conference*, pp. 455 - 468, San Francisco, March.

Dhar, A., Reddy, T.A. and Claridge, D.E., 1994b, "Generalization of the Fourier Series Approach to Model Hourly Energy Use in Commercial Buildings", Submitted to *ASME Journal of Solar Energy Engineering*.

Dhar, A., Reddy, T.A. and Claridge, D.E., 1995, "A Fourier Series Model to Predict Cooling and Heating Energy Use in Commercial Buildings with Outdoor Temperature as the Only Weather Variable", Accepted for presentation in *ASME/JSME/JSES Solar Energy Conference*, Hawaii, March.

Dhar, A., Claridge, D.E. and Ruch, D., 1995, "An Artificial Neural Network with Wavelet Basis Functions to Predict Hourly Heating and Cooling Energy Use in Commercial Buildings with Temperature as the Only Weather Variable", Accepted for presentation in *ASME/JSME/JSES Solar Energy Conference*, Hawaii, March.

Dingle, A.A., Andreae, J.H. and Jones, R.D., 1993, "A Chaotic Neural Unit", *Proceedings of the IEEE International Conference on Neural Networks*, Vol. 1, pp. 335 - 340, San Francisco, March.

Dodier, R., Krarti, M. and Kreider, J.F., 1993, "Artificial Neural Networks Applied to LoanSTAR Data", *JCEM TR/93/22*, University of Colorado, Boulder, Colorado.

Fels., M., 1986, Special Issue Devoted to "Measured Energy Savings, The Princeton Score Keeping Method (PRISM)", *Energy and Buildings*, Vol. 9, Nos. 1 and 2.

Feuston, B. and Thurtell, J., 1994, "Generalized Non-linear Regression with Ensemble of Neural Nets: The Great Energy Predictor Shootout", Submitted to *ASHRAE Transactions*.

Forrester, J. and Wepfer, W., 1984, "Formulation of a Load Prediction Algorithm for a Large Commercial Building", *ASHRAE Transactions*, Vol. 90, Part 1, pp. 536 -551.

Fourier, J., 1878, *The Analytical Theory of Heat*, Translated by A. Freeman, Cambridge, Great Britain.

Graybill, F. A., 1976, *Theory and Application of Linear Models*, Wadsworth & Brooks/Cole Advanced Books & Software, A Division of Wadsworth, Inc., Pacific Grove, California.

Greely K.M., Harris J.P., Hatcher A.M., 1990, "Measures Savings And Cost-Effectiveness of Conservation Retrofits in Commercial Buildings", *Lawrence Berkeley Laboratory Report - 275768*, Berkeley, California.

Griffith, D.M. and Anderson, K.J., 1994, "Commercial Building/System Characteristics Sensitivity Analysis", *Proceedings of the ACEEE 1994 Summer Study on Energy Efficiency in Buildings*, Vol. 5, pp. 5.105 - 5.112, Pacific Grove, California.

Grossberg, S., 1969, "Some Networks That Can Learn, Remember and Reproduce Any Number of Complicated Space-time Patterns", *Journal of Mathematics and Mechanics*, Vol. 19, pp. 53 - 91.

Haberl, J.S. and Komor, P.S., 1990, "Investigating an Analytical Framework for Improving Commercial Energy Audits: Results from a New Jersey Mall", *PU/CEES Report No. 234*, Princeton University, Princeton, New Jersey.

Hecht-Nielsen, R., 1987, "Counterpropagation Networks", *Proceedings of the IEEE First International Conference on Neural Networks*, Vol. 1, pp. 201 - 206, San Diego, California.

Hirst, E. and Reed, J., 1991, "Handbook of Evaluation of Utility DSM Programs", *Oak Ridge National Laboratory Report ORNL/CON-336*.

Hittle D.C. and Pedersen C.O., 1981, "Periodic and Stochastic Behavior of Weather Data", *ASHRAE Transactions* Vol. 87, Part 2, pp. 173 - 194.

Holcomb, T. and Morari, M. 1991. "Local Training for Radial Basis Function Networks: Towards Solving the Hidden Unit Problem", *American Control Conference*, Vol. 3, pp. 2331 - 2336, Boston.

Hopfield, J.J., 1984, "Neural Networks and Physical Systems with Emergent Collective Computational Abilities", *Proceedings of National Academy of Science*, United States of America, Vol. 81, pp. 3088 - 3093.

Hsieh, E.S., 1988, "Calibrated Computer Models of Commercial Buildings and Their Role in Building Design and Operation", Master's Thesis, *PU/CEES Report No. 230*, Princeton University, Princeton, New Jersey.

Hsieh, E.S., Norford, L.K., Socolow, R.H. and Spadaro, G.V. 1989, "Calibrated Computer models to Track Building Energy Use: The Role of Tenant and Operator Decisions", *Report forth-coming in Future Publications*.

Hsu, W., Hsu, L.S. and Tenorio, M.F., 1993, "A ClusNet Architecture for Prediction", *Proceedings of the IEEE International Conference on Neural Networks*, Vol. 1, pp. 329 - 334, San Francisco, March.

Iijima, M., et. al, 1994, "A Piecewise-linear Regression on the ASHRAE Time Series Data", Submitted to *ASHRAE Transactions*.

Kaplan, M.B., Jones, B. and Jansen, J. 1990, "DOE-2.1C Model Calibration with Monitored End-Use Data", *Proceedings of the ACEEE 1990 Summer Study on Energy Efficiency in Buildings*, Vol. 10, pp. 10.115 - 10.125.

Katipamula S. and Claridge, D.E., 1993, "Use of Simplified Systems Models to Measure Retrofit Savings", *ASME Journal of Solar Energy Engineering*, Vol. 115, pp. 57 - 63.

Katipamula, S., Reddy, T.A. and Claridge, D.E., 1994, "Development and Application of Regression Models to Predict Cooling Energy Consumption in Large Commercial Buildings", *Proceedings of the ASME/JSME/JSES Solar Energy Conference*, pp. 307 - 322, San Francisco, March.

Kawasima, M., 1994, "Artificial Neural Network Backpropagation Model with Three-phase Annealing Developed for the Building Energy Predictor Shootout", Submitted to *ASHRAE Transactions*.

Kissock, J.K., Reddy, T.A., Claridge, D.E., 1992, "A Methodology for Identifying Retrofit Energy Savings in Commercial Buildings", *Proceedings of the Eighth Annual Symposium on Improving Building Systems in Hot and Humid Climates*, pp. 234 - 246, Texas A&M University, College Station, Texas, October.

Kissock, J.K., 1993, "A Methodology to Measure Retrofit Energy Savings in Commercial Buildings", Ph.D. dissertation, Mechanical Engineering Department, Texas A&M University, College Station, Texas, December.

Koffman, S.J. and Meckl, P.H., 1993, "Gaussian Network Variants: A Preliminary Study", *Proceedings of the IEEE International Conference on Neural Networks*, Vol. 1, pp. 523 - 528, San Francisco, March.

Kohonen, T., 1990, *Self Organization and Associative Memory*, Third Edition, Springer-Verlag, New York.

Kosko, B., 1987a, "Bi-directional Associative Memories", *IEEE Transactions on Systems, Man and Cybernetics*, Vol. 18, Part 1, pp. 49 - 60.

Kosko, B., 1987b, "Competitive Adaptive Bi-directional Associative Memories", *Proceedings of the IEEE First International Conference*, Vol. 2, pp. 759-766, San Diego.

Kovacevic, J. and Vatterli, M., 1992, "Non-Separable Multi-dimensional Perfect Reconstruction Filter Banks and Wavelet Bases for R^m ", *IEEE Transactions on Information Theory*, Vol. 38, Part 2, pp. 533 - 541.

Kreider, J. and Wang, X., 1991, "Artificial Neural Networks Demonstrated for Automated Generation of Energy Use Predictors for Commercial Buildings", *ASHRAE Transactions*, Vol. 97, Part 1, pp. 775 - 779.

Lee, S. and Kil, R.M., 1991, "A Gaussian Potential Function Network With Hierarchically Self-Organizing Learning", *Neural Networks*, Vol. 4, pp. 207 - 212.

Leonard, J.A. and Kramer, M.A., 1991, "Radial Basis Function Networks for Classifying Process Faults", *IEEE Control Systems*, Vol. 31, pp. 509 - 517, April.

Liepins, G.E. and Uppuluri, V.R.R., 1990, *Data Quality Control*, Marcel Dekker, Inc., New York.

Little, R.J., 1990, "Editing and Imputation of Multivariate Data", *Data Quality Control (Eds. G.E. Liepins and V.R.R. Uppuluri)*, pp. 145 - 166, Marcel Dekker, Inc., New York.

Loh, A.P. and Fong, K.F., 1993, "Backpropagation Using Generalized Least Squares", *Proceedings of the IEEE International Conference on Neural Networks*, Vol. 1, pp. 592 - 597, San Francisco, March.

Mallat, S.G., 1989a, "Multiresolution Approximation and Wavelet Orthonormal Bases of L^2 ", *Transactions of American Mathematical Society*, pp. 504 - 511, June.

Mallat, S.G., 1989b, "A Theory of Multiresolution Signal Decomposition: The Wavelet Representation", *IEEE Transactions on Pattern Analysis and Machine Intelligence*, Vol. 11, Part 7, pp. 674 - 693.

Meyer, Y., 1985, "Principe d'Incertitude, Bases Hilbertiennes et Algebres d'Operateurs", *Bourbaki Seminar*, Report No. 662, Bourbaki, Spain.

Miller, R.C. and Seem, J.E., 1991, "Comparison of Artificial Neural Networks with Traditional Methods of Predicting Return Time from Night or Weekend Setback", *ASHRAE Transactions*, Vol. 97, Part 2 pp. 500 - 510.

Moody, J. and Darken, C., 1989, "Fast Learning in Networks of Locally-tuned Processing Units", *Neural Computation*, Vol. 1, pp. 281-294.

Narendra K.S. and Parthasarathy, K., 1990, "Identification and Control of Dynamical Systems Using Neural Networks", *IEEE Transactions on Neural Networks*, Vol. 1, Part 1, pp. 718 - 728.

Ohlsson, M., et. al, 1994, "Predicting Utility Loads with Artificial Neural Networks - Methods and Results from Great Energy Predictor Shootout", Submitted to *ASHRAE Transactions*.

Ott, L., 1988, *An Introduction to Statistical Methods and Data Analysis*, PWS-KENT Publishing Company, Boston.

Pandit, S.M., and Wu S.M., 1983, *Time Series and System Analysis with Applications*, John Wiley & Sons, New York.

Parthasarathi, S., Parlos, A.G. and Atiya, A.F., 1992, "Model Predictive Adaptive Control Using Recurrent Neural Networks", *Proceedings of the Power Plant Dynamics, Control and Testing Conference*, pp. 299 - 319, Knoxville, Tennessee.

Philips, W.F. 1984, "Harmonic Analysis of Climatic Data", *Solar Energy*, Vol. 32(3), pp. 319 - 328.

Poggio, T. and Girosi, F., 1989., "A Theory of Networks for Approximation and Learning", *Technical Report A.I. Memo No. 1140*, Massachusetts Institute of Technology, Cambridge, Massachusetts.

Puskorius, G.V. and Feldkamp, L.A., 1992a, "Recurrent Network Training with the Decoupled Extended Kalman Filter Algorithm", *SPIE*, Vol. 1710, Science of Artificial Neural Networks, Orlando, Florida, pp. 461 - 473.

Puskorius, G.V. and Feldkamp, L.A., 1992b, "Model Reference Adaptive Control with Recurrent Networks Trained by the Dynamic DEKF Algorithm", *Proceedings of the International Joint Conference on Neural Networks*, Baltimore, Vol. 2, pp. 106 - 113.

Puskorius, G.V. and Feldkamp, L.A., 1993, "Practical Considerations for Kalman Filter Training of Recurrent Neural Networks", *Proceedings of the IEEE International Conference on Neural Networks*, San Francisco, March, Vol. 2, pp. 1189 - 1194.

Rabl, A., 1988, "Parameter Estimation in Buildings: Methods for Dynamic Analysis of Measured Energy Use", *ASME Journal of Solar Energy Engineering*, Vol. 110, pp. 52 - 66.

Raghunathan, T.E. and Rubin, D.B., 1990, "An Application of Bayesian Statistics Using Sampling/Importance Resampling a Deceptively Simple Problem in Quality Control", *Data Quality Control (Eds. G.E. Liepins and V.R.R. Uppuluri)*, pp. 229 - 244, Marcel Dekker, Inc., New York.

Rao, S.S. and Ramamurthy, V., 1993, "A Hybrid Technique to Enhance The Performance of Recurrent Neural Networks for Time Series Prediction", *Proceedings of the IEEE International Conference on Neural Networks*, San Francisco, March, Vol. 1, pp. 52 - 57.

Reddy, T.A., Katipamula, S. and Claridge, D.E., 1994, "The Functional Basis of Thermal Energy Use in Air-side HVAC Equipment", accepted for publication by the *ASME Journal of Solar Energy Engineering*.

Refenes, A.N., Azema-Barac, M. and Zaprakis, A.D., 1993, "Stock Ranking: Neural Networks Vs. Multiple Linear Regression", *Proceedings of the IEEE International Conference on Neural Networks*, San Francisco, March, Vol.3, pp. 1419 - 1424.

Ruch, D. and Claridge, D.E., 1992, "A Four-Parameter Change Point Model for Predicting Energy Consumption in Commercial Buildings", *ASME Journal of Solar Energy Engineering*, Vol. 114, pp. 77 - 83.

Rumelhart, D.E. and McClelland, J.L. et al., 1989, *Parallel Distributed Processing*, Vol.1, The M.I.T. Press, Cambridge, Massachusetts.

Seem, J.E. and Braun, J.E., 1991, "Adaptive Methods for Real-Time Forecasting of Building Electrical Demand", *ASHRAE Transactions*, Vol.97, Part 1, pp. 710 -721.

Sejnowski, T.J. and Rosenberg, C.R., 1987. "Parallel Networks That Learn to Pronounce English", *Complex Systems*, Vol. 1, pp. 145 - 168.

Sterzing, V. and Schurmann, B., 1993, "Recurrent Neural Networks for Temporal Learning of Time Series", *Proceedings of the IEEE International Conference on Neural Networks*, Vol. 2, pp. 843 - 851, San Francisco, March.

Stokbro, K., Umberger, D.K. and Hertz, J.A. 1990. "Exploiting Neurons with Localized Receptive Fields to Learn Chaos", *Complex Systems*, Vol. 4, pp. 603 - 609.

Stornetta, W.S. and Huberman, B.A., 1987, "An Improved Three-layer, Back Propagation Algorithm", *Proceedings of the IEEE First International Conference on Neural Networks*, Vol. 1, pp. 711 - 718, San Diego.

Subbarao, K., Burch, J., Hancock, C.E., Lekov, A. and Balcomb, J.D., 1990, "Measuring the Energy Performance of Buildings Through Short-term Tests", *Proceedings of the ACEEE 1990 Summer Study on Energy Efficiency in Buildings*, Vol. 10, pp. 10.245 - 10.252.

Unser, M. and Aldroubi, A., 1992, "Polynomial Splines and Wavelets - A Signal Processing Perspective", *Wavelets - A Tutorial in Theory and Applications (Ed. C.K.Chui)*, pp. 91 - 122, Academic Press Inc., San Francisco.

Venkatasubramaniam, V. and Kavuri, S.N., 1991, "Improving Fault Classification by Neural Networks Using Ellipsoidal Activation Function", *AIChE Annual Meeting*, Los Angeles.

Wang, X.A. and Krieder, 1992, "Improved Artificial Neural Networks for Commercial Building energy Use Prediction", *Proceedings of the ASME/JSME/JSES International Solar Energy Conference*, pp. 305 - 312, New York, March.

Wasserman, D. 1989, *Neural Computing Theory and Practice*, Van Nostrand Reinhold, New York.

Willis, M.J., Montague, G.A., Morris, A.J. and Tham, M.T., 1991, "Artificial Neural Networks: A Panacea to Modelling Problems?", *American Control Conference*, Vol. 3, pp. 2337 - 2342, Boston.

Zhou, S., Popovic, D. and Schulz-Ekloff, G., 1993, "An Improved Learning Law for Backpropagation Networks", *Proceedings of the IEEE International Conference on Neural Networks*, Vol.1, pp. 573 - 582, San Francisco, March.

APPENDIX A
FOURIER SERIES APPROXIMATION AND
WAVELETS - AN INTRODUCTION

In this appendix, some basic information on Fourier series approximation of functions is discussed. The material has been taken from Churchill (1963). A few terms that have been used to explain the idea of approximation have been defined first, followed by the theory of Fourier approximation of functions. The appendix ends with an introduction to the idea of wavelet representation of functions.

Norm

If $g(1)$, $g(2)$ and $g(3)$ are three rectangular components of a three dimensional vector $g(r)$, then the length of $g(r)$ is the norm (denoted as $\|g\|$) and is determined as follows:

$$\|g\|^2 = [g(1)]^2 + [g(2)]^2 + [g(3)]^2 = \sum_{r=1}^3 [g(r)]^2 \quad (\text{A.1})$$

For an n - dimensional vector $g(n)$, the norm, therefore, would be

$$\|g\|^2 = \sum_{r=1}^n [g(r)]^2 \quad (\text{A.2})$$

Distance Between Two Vectors

The distance between two vectors g_1 and g_2 is determined as follows:

$$\|g_1 - g_2\| = \left\{ \sum_{r=1}^n [g_1(r) - g_2(r)]^2 \right\}^{\frac{1}{2}} \quad (\text{A.3})$$

Inner Product

The inner product of two vectors g_1 and g_2 is denoted as (g_1, g_2) and is determined as follows:

$$(g_1, g_2) = \|g_1\| \|g_2\| \cos \theta \quad (\text{A.4})$$

The norm of a vector, therefore, can be written as

$$\|g\| = (g, g)^{\frac{1}{2}} \quad (\text{A.5})$$

Orthonormal Set of Vectors

A vector of unit norm is called a unit vector and a set of mutually perpendicular unit vectors is called an orthonormal set of vectors (ϕ_n) . This condition can also be presented as follows:

$$\delta_{mn} = (\phi_m, \phi_n) = \begin{cases} 0 & \text{if } m \neq n \\ 1 & \text{if } m = n \end{cases} \quad (\text{A.6})$$

A simple example of orthonormal set of vectors is the set of unit vectors along the three coordinate axes.

Every vector f in the space can be expressed as a linear combination of orthonormal set of vectors.

$$f = c_1\phi_1 + c_2\phi_2 + c_3\phi_3 \quad (\text{A.7})$$

The coefficients c_n s can be found by taking the inner product of both sides of equation A.7.

$$(f, \phi_1) = c_1(\phi_1, \phi_1) + c_2(\phi_2, \phi_1) + c_3(\phi_3, \phi_1) = c_1 \quad (\text{A.8})$$

The coefficients are, therefore,

$$c_n = (f, \phi_n) \quad (\text{A.9})$$

Equation A.7 can now be rewritten as follows:

$$f = \sum_{n=1}^3 (f, \phi_n) \phi_n \quad (\text{A.10})$$

Equation A.10 is an orthonormal expansion of the arbitrary vector f .

Functions as Vectors

Any function $g(r)$ can be viewed as a vector if it has real values at $r = 1, 2, 3, \dots$, etc., and these values can be considered as components of the vector. The norm of the function $g(r)$ represents the length of the generalized vector $g(r)$. Within an interval of $a \leq r \leq b$, the norm of the function is

$$\|g\| = \left\{ \int_a^b [g]^2 dr \right\}^{\frac{1}{2}} = (g, g)^{\frac{1}{2}} \quad (\text{A.11})$$

The generalized distance between any two functions g_1 and g_2 is computed as

$$\|g_1 - g_2\| = \left\{ \int_a^b [g_1 - g_2]^2 dr \right\}^{\frac{1}{2}} \quad (\text{A.12})$$

which is a measure of mean distance between their graphs within the specified interval.

Generalized Fourier Series

Any function in an interval (a, b) can be represented by a linear combination of an orthonormal set of functions $\{\phi_n(x)\}$ ($n = 1, 2, \dots$) within that interval. This can be generalized to an infinite series:

$$f(x) = c_1\phi_1(x) + c_2\phi_2(x) + \dots + c_n\phi_n(x) + \dots, \quad (a < x < b)$$

where the coefficients c_n s are given by the following expression:

$$c_n = \int_a^b f(x)\phi_n(x)dx \quad (n = 1, 2, \dots)$$

The function $f(x)$ can, therefore, be written as follows:

$$f(x) = \sum_{n=1}^{\infty} \phi_n(x) \int_a^b f(\xi)\phi_n(\xi)d\xi$$

An orthonormal set $\{\phi_n(x)\}$ is said to be complete if in the function space under consideration there is no other function with positive norm which is orthogonal to the set $\{\phi_n(x)\}$. It can be shown that the best approximation of any function in a function space

may be possible by representing the function with a complete set of orthonormal functions $\{\phi_n(x)\}$. For example, let us consider a three dimensional vector (as shown in Figure A.1) which has to be approximated in two dimensions. The best approximation of such a function $f(x)$ is $k(x)$ if the distance d between $f(x)$ and $k(x)$ is minimum:

$$d = \|f - k\| \text{ is minimum.}$$

The above condition is satisfied only when a projection of a three dimensional vector $f(x)$ on a two dimensional plane is the function $k(x)$. The best approximation of $k(x)$ in one dimension is, as before, projections on ϕ_1 and ϕ_2 axes.

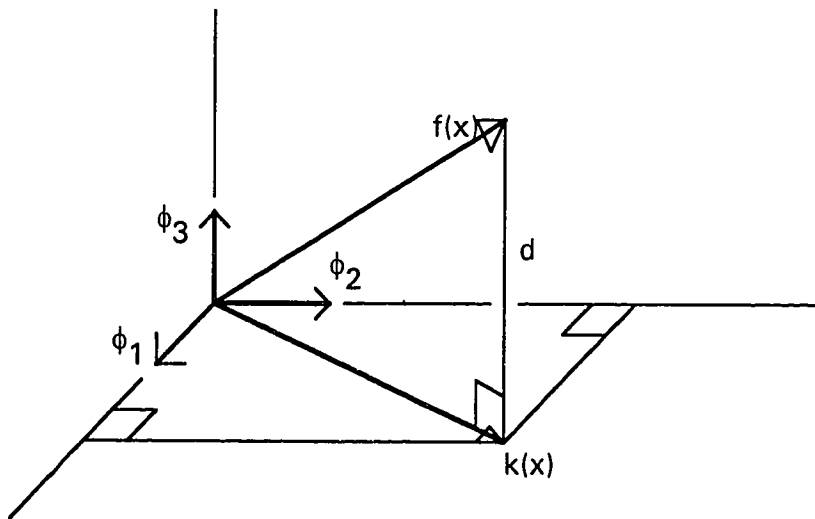


Figure A.1 Approximation of a three dimensional function $f(x)$ in two dimensional plane.

It can be proved that Fourier constant of a function $f(x)$ with respect to the functions $\phi_1, \phi_2, \phi_3, \dots, \phi_m$ of an orthonormal set are those coefficients for which a linear combination

of those m functions is the best approximation in the mean to $f(x)$, on the fundamental interval (Churchill, 1963):

$$c_1^2 + c_2^2 + \dots + c_m^2 \leq \int_a^b [f(x)]^2 dx = \|f\|^2 \quad (\text{A.13})$$

This is known as Bessel inequality.

More on Fourier series approximation of functions can be found in Churchill (1963) or any other classical literature.

Fourier Series and Wavelet Approximation

Fourier series representation of a function is, essentially, a representation with orthogonal set of basis functions such as sinusoidal and cosinusoidal functions, as shown in Chapter III. A time dependent function, for example, hourly energy use in commercial buildings can be represented in time domain as follows:

$$E_h = f(t) \quad (\text{A.14})$$

where t is the hour of day. The function $f(t)$ mentioned in eq. A.14 could also be represented with orthogonal bases such as sines and cosines of t . The advantage of representing a function with sines and cosines is that only a few important terms are adequate to recover the functional form in time domain with a high accuracy. This justifies the use of Fourier series representation of a function for approximation purposes.

We, therefore, can say that a function can be represented either in time domain or in frequency domain but frequency domain representation is more compact with insignificant loss of accuracy. One way to represent a function in frequency domain is to use the familiar sines and cosines (Fourier domain). However, there is another frequency domain, which may also be called as wavelet domain, in which a function can be

represented by using somewhat more complicated bases than the sines and cosines. These bases are called mother functions (or, scaling functions) and wavelets.

Wavelet bases are more interesting than the sines and cosines because of being quite localized in frequency (or characteristic scale). While sines and cosines oscillate between -1 and +1 from $-\alpha$ to $+\alpha$, the wavelet bases have local support and does not exist (or becomes zero) beyond a certain input range. The set of wavelet bases is generated by translating and dilating one function, called mother function. A large number of functions can, therefore, be represented in a much more compact way in wavelet domain than in Fourier domain.

There are infinitely many possible sets of wavelets and which set of wavelets is the most suitable for approximation of a function, depends on the type of the function itself. More details on wavelets and wavelet transforms are available in classical literature (Daubechies, 1992; Chui, 1992a and b).

An Example of One Dimensional Wavelet Approximation

A B-spline scaling function and corresponding wavelets can be approximated by the equations 7.11 and 7.12 which are reproduced below:

$$\phi(x) = 0.690988 \exp(-1.5x^2) \quad (7.11)$$

$$\psi(x) = 0.251477 \cos\{2.570935(2x - 1)\} \bullet \exp\{-0.222759(2x - 1)^2\} \quad (7.12)$$

The family of scaling functions ϕ_{mk} and wavelets ψ_{mk} at any scale m is represented as below, along with the equations 7.4 and 7.1:

$$\phi_{m,k}(x) = \sqrt{2^{-m}} \phi(2^{-m}x - k) \quad \text{for } (m, k) \in Z^2 \quad (7.4)$$

and

$$\psi_{m,k}(x) = \sqrt{2^{-m}} \psi(2^{-m}x - k) \quad \text{for } (m, k) \in Z^2 \quad (7.1)$$

To see how the above scaling functions and wavelets can be used to approximate weather independent energy use as a function of hour of day (i.e., time variable) only, the approximation of whole building electric energy use (E_{wbe}) for February 6, 1992 (a typical weekday) at the Zachry Engineering Center on the Texas A&M University campus is illustrated here. First, the locations of the scaling functions and the wavelets are fixed by generating a grid as shown in Figure A.2. The sampling spaces are denoted as V_m at any scale m . The sampling interval is one hour at the actual scale for which $m = 0$. The sampling interval increases by a factor of two when the value of m increases by unity. The coarsest scale must have at least two data points. The value of m is 4 for the coarsest scale in this case, as shown in Figure A.2. One may note that the approximation starts at the coarsest scale and proceeds towards the finer scales and the standard least squares regression is adopted to determine the coefficients at each scale. An overall shape of the function described by the measured data points is approximated at the coarser scales while the finer details of the function are captured by the wavelets at the finer scales. The number of parameters of the model is thereby optimized. The above description gives an intuitive explanation of how multiresolution analysis works in wavelet approximation algorithm.

Once the locations are determined by the grid shown in Figure A.2, The scaling functions and wavelets for any location (k) are calculated using equations 7.4 and 7.1. The orthogonal decomposition of the actual sampling space V_0 (which has twenty-four data points, as explained before) in this case can be performed as mentioned below:

$$V_0 = V_1 \oplus W_1 = (V_2 \oplus W_2) \oplus W_1 \quad (\text{A.15})$$

where the W_m spaces are the orthogonal complements of the respective V_m spaces. This means that each element of space W_m is orthogonal to the corresponding element of space V_m . One may note that the scaling functions are the bases for the V_m spaces, while the corresponding wavelets are the bases for W_m spaces. The decomposition algorithm

described here is the essence of wavelet approximation in a multiresolution hierarchy.

The final expression of the decomposition takes the following form:

$$V_0 = V_4 \oplus W_4 \oplus W_3 \oplus W_2 \oplus W_1 \quad (\text{A.16})$$

and, therefore, the final functional form will be as follows:

$$E_h \cong \sum_{k=0}^1 \alpha_{4k} \phi_{4k}(h) + \sum_{k=0}^1 \delta_{4k} \psi_{4k}(h) + \sum_{k=0}^2 \delta_{3k} \psi_{3k}(h) + \sum_{k=0}^5 \delta_{2k} \psi_{2k}(h) + \sum_{k=0}^{11} \delta_{1k} \psi_{1k}(h) \quad (\text{A.17})$$

where α and δ are the scaling function and wavelet coefficients in the above equation.

The indices k denote the locations in the equation which are shown in Figure A.2 for different scales. In Figure A.2, we note that two scaling functions at scale = 4 (for V_4) can be used to start the approximation. This approximation is shown in Figure A.3. The sampling interval at this scale is $2^4 = 16$ hours and two scaling functions are located (or centered) at 0 and 16 hours. The regression equation is as given below:

$$E_h = \sum_{k=0}^1 \alpha_{4k} \phi_{4k}(h) + \varepsilon_{4s,h} \quad (\text{A.18})$$

where

$$\phi_{40}(h) = 0.690988 \times \exp\left[-1.5 \times \left(\frac{h}{16}\right)^2\right] \text{ and}$$

$$\phi_{41}(h) = 0.690988 \times \exp\left[-1.5 \times \left(\frac{h}{16} - 1\right)^2\right].$$

The coefficients α_{40} and α_{41} are determined by the method of least squares optimization as 450.74 and 1090.17. Figure A.3 shows these scaling functions multiplied by the respective coefficients, the sum of which is the scaling function approximation. The difference between the measured energy use and the scaling function approximation is the residual which is also shown. Note that the B-spline scaling functions are well-

localized, as evident from the decay of both the scaling functions centered at hour 0 and hour 16.

Once the scaling function approximation is accomplished, the residual of the scaling function approximation is regressed with the wavelets at scale = 4 and location = 0 and 16 hours. The sampling interval is still 16 hours. Using the residual for this approximation is possible because the space W_4 is orthogonal to the space V_4 . The wavelet regression equation at scale = 4 is as follows:

$$\varepsilon_{4s,h} = \sum_{k=0}^1 \delta_{4k} \psi_{4k}(h) + \varepsilon_{4,h} \quad (\text{A.19})$$

where

$$\psi_{40}(h) = 0.251477 \times \cos[2.570935 \times \{2 \times (h / 16) - 1\}] \times \exp[-0.222759 \times \{2 \times (h / 16) - 1\}^2]$$

and

$$\psi_{41}(h) = 0.251477 \times \cos[2.570935 \times \{2 \times (h / 16 - 1) - 1\}] \times \exp[-0.222759 \times \{2 \times (h / 16 - 1) - 1\}^2]$$

The coefficients δ_{40} and δ_{41} are determined by the method of least squares regression as -74.57 and -0.46. The residuals of equation A.19 are then regressed with the wavelets at scale = 3. The sampling interval at this scale is $2^3 = 8$ hours and the wavelets are located at 0, 8 and 16 hours. The regression equation is:

$$\varepsilon_{4,h} = \sum_{k=0}^2 \delta_{3k} \psi_{3k}(h) + \varepsilon_{3,h} \quad (\text{A.20})$$

where

$$\psi_{30}(h) = 0.251477 \times \cos[2.570935 \times \{2 \times (h / 8) - 1\}] \times \exp[-0.222759 \times \{2 \times (h / 8) - 1\}^2],$$

$$\psi_{31}(h) = 0.251477 \times \cos[2.570935 \times \{2 \times (h / 8 - 1) - 1\}] \times \exp[-0.222759 \times \{2 \times (h / 8 - 1) - 1\}^2]$$

and

$$\psi_{31}(h) = 0.251477 \times \cos[2.570935 \times \{2 \times (h / 8 - 2) - 1\}] \times \exp[-0.222759 \times \{2 \times (h / 8 - 2) - 1\}^2]$$

The coefficients δ_{30} , δ_{31} and δ_{32} are determined by the method of least squares regression as -98.56, 113.57 and -100.89. The process can be continued until scale = 1, as suggested by equation A.17:

$$\epsilon_{3,h} = \sum_{k=0}^5 \delta_{2k} \psi_{2k}(h) + \epsilon_{2,h} \quad (\text{A.21})$$

$$\epsilon_{2,h} = \sum_{k=0}^{11} \delta_{1k} \psi_{1k}(h) + \epsilon_{1,h} \quad (\text{A.22})$$

The statistically insignificant scaling function and wavelet coefficients are dropped from the model. The approximations at scale = 4 and 3 are shown in Figures A.4 and A.5 respectively. The C.V. RMSE of fit achieved was 8.32% at the end of the scaling function approximation, while the C.V. RMSE fit of the wavelet approximations at $m = 4$ and 3 were 6.97% and 3.79% respectively. The details of the approximations at scale = 2 and 1 which are not shown here, improve the model fit to 2.95% and 1.58% C.V. RMSE respectively. The complete wavelet approximation scheme for the example discussed here is described also in the flow chart in Figure A.6.

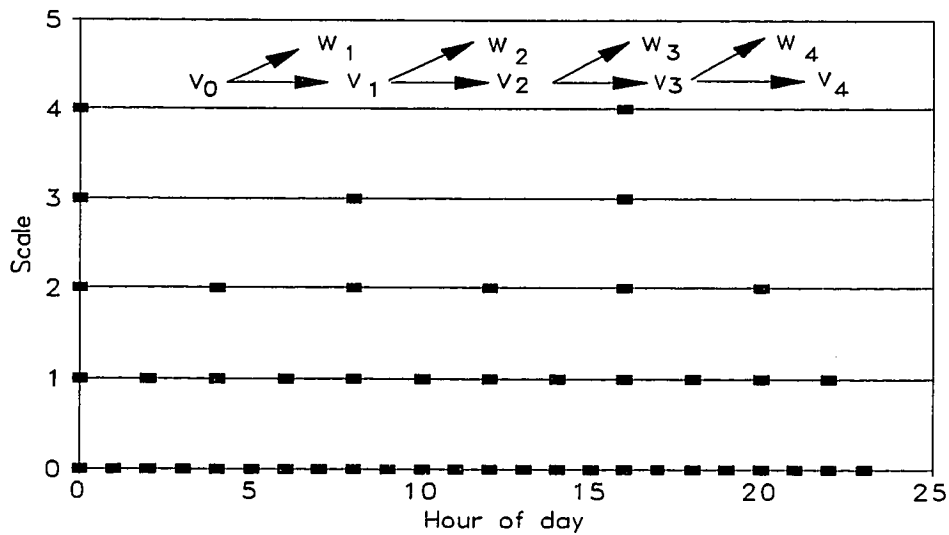


Figure A.2 Sampling spaces are shown at different scales for twenty-four hourly data points in a day. The sampling interval decreases by a factor of 2 as the scale increases (or becomes coarser). The sampling spaces are denoted as V_m while their orthogonal complements are denoted as W_m .

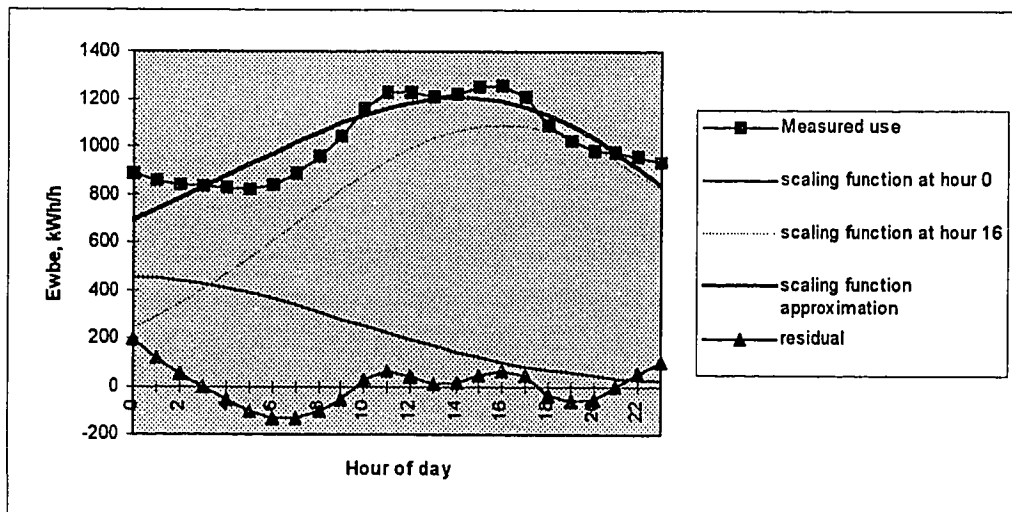


Figure A.3 Scaling function approximation of whole building electric energy use for February 6, 1992 (a typical weekday) at the Zachry Engineering Center on the Texas A&M University campus.

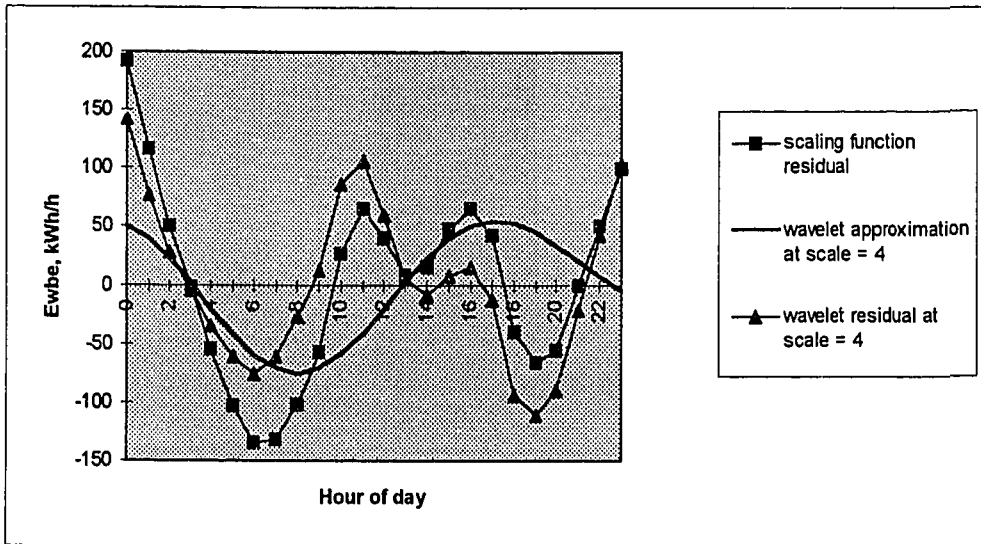


Figure A.4 Wavelet approximation (at scale = 4) of whole building electric energy use for February 6, 1992 (a typical weekday) at the Zachry Engineering Center on the Texas A&M University campus.

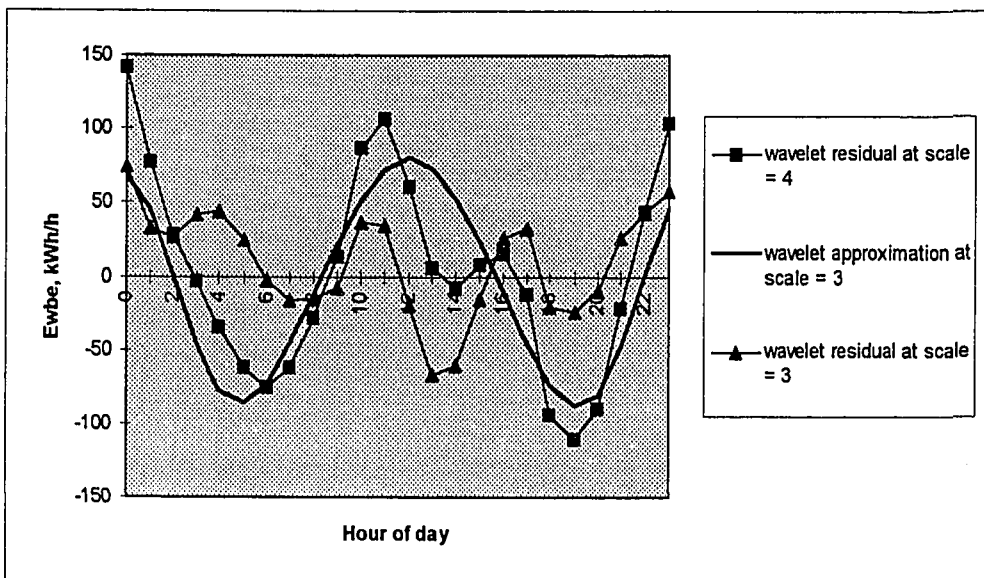


Figure A.5 Wavelet approximation (at scale = 3) of whole building electric energy use for February 6, 1992 (a typical weekday) at the Zachry Engineering Center on the Texas A&M University campus.

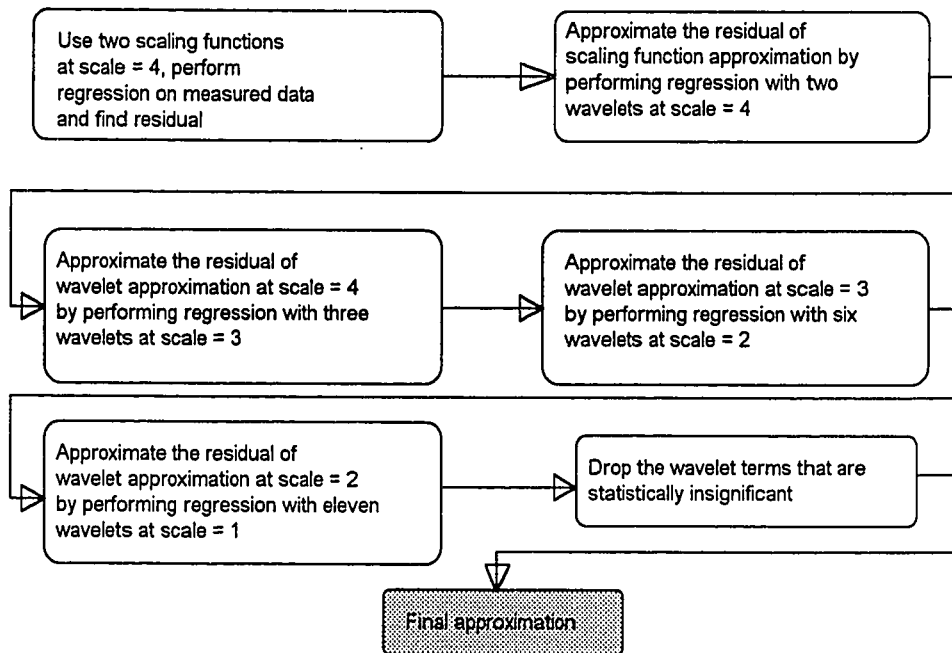


Figure A.6 A flow chart showing the complete scheme for wavelet approximation of hourly energy use on a day.

APPENDIX B

A SAMPLE SAS PROGRAM FOR FOURIER SERIES MODELING

```

TITLE1 'ATRAIN PRE-RETROFIT MODEL';
TITLE2 'PERIOD USED : 01SEP89 TO 31DEC89';

data indata;
  infile 'atrain.dat' LRECL=350 ;
  input mm dd yy hrm oatemp sphum solar wndspd wbelec cw hw ;
  if oatemp <= 0 then oatemp =.;
  if sphum <= 0 then sphum =.;
  if solar <= 10 then solar = 0;
  if wndspd <= 0 then wndspd =.;
  if wbelec <= 0 then wbelec =.;
  if cw <= 0 then cw =.;
  if hw <= 0 then hw = .;
  hr = hrm/100;
  date = mdy(mm,dd,yy);
  dow = weekday(date);
  shdiff = sphum - 0.0092 ;
  if shdiff < 0 then shdiff = 0 ;

  sh1 = sin((2*3.14/24)*(hr)) ; ch1 = cos((2*3.14/24)*(hr)) ;
  sh2 = sin((2*2*3.14/24)*(hr)) ; ch2 = cos((2*2*3.14/24)*(hr)) ;
  sh3 = sin((3*2*3.14/24)*(hr)) ; ch3 = cos((3*2*3.14/24)*(hr)) ;
  sh4 = sin((4*2*3.14/24)*(hr)) ; ch4 = cos((4*2*3.14/24)*(hr)) ;
  sh5 = sin((5*2*3.14/24)*(hr)) ; ch5 = cos((5*2*3.14/24)*(hr)) ;
  sh6 = sin((6*2*3.14/24)*(hr)) ; ch6 = cos((6*2*3.14/24)*(hr)) ;
  sh7 = sin((7*2*3.14/24)*(hr)) ; ch7 = cos((7*2*3.14/24)*(hr)) ;
  sh8 = sin((8*2*3.14/24)*(hr)) ; ch8 = cos((8*2*3.14/24)*(hr)) ;
  sh9 = sin((9*2*3.14/24)*(hr)) ; ch9 = cos((9*2*3.14/24)*(hr)) ;
  sh10 = sin((10*2*3.14/24)*(hr)) ; ch10 = cos((10*2*3.14/24)*(hr)) ;
  sh11 = sin((11*2*3.14/24)*(hr)) ; ch11 = cos((11*2*3.14/24)*(hr)) ;

  t1sh1=oatemp*sh1; t1ch1=oatemp*ch1; t1sh2=oatemp*sh2; t1ch2=oatemp*ch2;
  t1sh3=oatemp*sh3; t1ch3=oatemp*ch3; t1sh4=oatemp*sh4; t1ch4=oatemp*ch4;
  t1sh5=oatemp*sh5; t1ch5=oatemp*ch5; t1sh6=oatemp*sh6; t1ch6=oatemp*ch6;
  t1sh7=oatemp*sh7; t1ch7=oatemp*ch7; t1sh8=oatemp*sh8; t1ch8=oatemp*ch8;
  t1sh9=oatemp*sh9; t1ch9=oatemp*ch9; t1sh10=oatemp*sh10; t1ch10=oatemp*ch10;
  t1sh11=oatemp*sh11; t1ch11=oatemp*ch11;

```



```

s1sh1=shdiff*sh1; s1ch1=shdiff*ch1; s1sh2=shdiff*sh2; s1ch2=shdiff*ch2;
s1sh3=shdiff*sh3; s1ch3=shdiff*ch3; s1sh4=shdiff*sh4; s1ch4=shdiff*ch4;
s1sh5=shdiff*sh5; s1ch5=shdiff*ch5; s1sh6=shdiff*sh6; s1ch6=shdiff*ch6;
s1sh7=shdiff*sh7; s1ch7=shdiff*ch7; s1sh8=shdiff*sh8; s1ch8=shdiff*ch8;
s1sh9=shdiff*sh9; s1ch9=shdiff*ch9; s1sh10=shdiff*sh10; s1ch10=shdiff*ch10;
s1sh11=shdiff*sh11; s1ch11=shdiff*ch11;

s1sh1=solar*sh1; s1ch1=solar*ch1; s1sh2=solar*sh2; s1ch2=solar*ch2;
s1sh3=solar*sh3; s1ch3=solar*ch3; s1sh4=solar*sh4; s1ch4=solar*ch4;
s1sh5=solar*sh5; s1ch5=solar*ch5; s1sh6=solar*sh6; s1ch6=solar*ch6;
s1sh7=solar*sh7; s1ch7=solar*ch7; s1sh8=solar*sh8; s1ch8=solar*ch8;
s1sh9=solar*sh9; s1ch9=solar*ch9; s1sh10=solar*sh10; s1ch10=solar*ch10;
s1sh11=solar*sh11; s1ch11=solar*ch11;

run;

data prewd;
set indata;
format date date7.;
if date >= '21dec89'd then delete;
if dow = 1 or dow = 7 then delete ;
proc stepwise ;
model cw = oatemp shdiff solar sh1 sh2 sh3 sh4 sh5 sh6 sh7 sh8 sh9 sh10 sh11
ch1 ch2 ch3 ch4 ch5 ch6 ch7 ch8 ch9 ch10 ch11
t1sh1 t1sh2 t1sh3 t1sh4 t1sh5 t1sh6 t1sh7 t1sh8 t1sh9 t1sh10 t1sh11
t1ch1 t1ch2 t1ch3 t1ch4 t1ch5 t1ch6 t1ch7 t1ch8 t1ch9 t1ch10 t1ch11
s1sh1 s1sh2 s1sh3 s1sh4 s1sh5 s1sh6 s1sh7 s1sh8 s1sh9 s1sh10 s1sh11
s1ch1 s1ch2 s1ch3 s1ch4 s1ch5 s1ch6 s1ch7 s1ch8 s1ch9 s1ch10 s1ch11
s1sh1 s1sh2 s1sh3 s1sh4 s1sh5 s1sh6 s1sh7 s1sh8 s1sh9 s1sh10 s1sh11
s1ch1 s1ch2 s1ch3 s1ch4 s1ch5 s1ch6 s1ch7 s1ch8 s1ch9 s1ch10 s1ch11
/f;

run;

/*

data prewe;
set indata;
format date date7.;
if date >= '21dec89'd then delete;

```

```
if dow = 1 or dow = 7 ;  
proc sort; by hr;
```

```
run;
```

```
TITLE3 'ENERGY USE: CW';  
TITLE4 'WEEKDAYS ONLY';  
proc reg data = prewd;  
model cw = oatemp solar shdiff ;  
by hr ;  
run;
```

```
TITLE3 'ENERGY USE: CW';  
TITLE4 'WEEKENDS ONLY';  
proc reg data = prewe ;  
model cw = oatemp solar shdiff ;  
by hr ;  
run;  
*/
```

APPENDIX C

ANSI C PROGRAM FOR ARTIFICIAL NEURAL NETWORK WITH BACK PROPAGATION ALGORITHM

```

/* LAST UPDATE : 28 Oct '93.
   ANN program for variable layer, variable input, variable middle node architecture
   for modeling weather independent energy use in university buildings */

#include <stdio.h>
#include <stdlib.h>
#include <math.h>
#include <float.h>
#include <time.h>

#define maxerror 0.1
#define tolerance 0.0001
#define maxline 10001
#define cols 30

double d[maxline][cols] ;
void min_max() ;
void sigmoid() ;
void tan_hyp() ;

main(int argc, char *argv[])

{

int i, j, k, n, epoch, column, lines, in_node, h1_node, h2_node, h3_node ;
int maxepoch, function, layers ;
double gain, xbias, ybias, lrate ;
double min[cols], max[cols] ;
double w12[21][21], w23[21][21], w34[21][21], w45[21][2], x[6][21], y[6][21],
delta[6][21] ;
char s[250] ;
double a, b, r, avgerror, lasterr, toterror, abserror, wbetot, wbemean ;

```

```

double wbe, wbepred, resid, sse, mse, rmse, cv_rmse, diff;
FILE *ifp, *ofp1, *ofp2;

if (argc != 4) {
    printf("\n\n Improper command, please try again ! \n\n");
    printf("Proper Usage: compfile ");
    printf("infile outfile1 outfile2 \n\n");
    printf("The program reads data from an input data file( *.dat file), \n");
    printf("writes ANN model results in output file1( *.log file) \n");
    printf("and writes target and predicted value ");
    printf("in output file2( *p.dat file). \n");
    exit(1);
}

ifp = fopen(argv[1], "r");
ofp1 = fopen(argv[2], "w");
ofp2 = fopen(argv[3], "w");

/* Reads number of layers of the network */

layers = 0;
while (layers < 3 || layers > 5) {
    printf("\n Input number of layers of the network (3 to 5) : ");
    scanf("%d", &layers); }

/* Reads number of input layer units and hidden layer units */

in_node = 0;
while (in_node < 1 || in_node > 20) {
    printf("\n Input number of input layer nodes (between 1 and 20) : ");
    scanf("%d", &in_node); }

h1_node = 0;
while (h1_node < 1 || h1_node > 20) {
    printf("\n Input number of first hidden layer nodes (between 1 and 20) : ");
    scanf("%d", &h1_node); }

if (layers > 3) {

h2_node = 0;
while (h2_node < 1 || h2_node > 20) {

```

```

printf("\n Input number of second hidden layer nodes (between 1 and 20) : ");
scanf("%d", &h2_node); }

if (layers > 4) {

h3_node = 0;
while (h3_node < 1 || h3_node > 20) {
    printf("\n Input number of third hidden layer nodes (between 1 and 20) : ");
    scanf("%d", &h3_node); }
}
}
/* Reads gain, xbias, ybias, learning rate and maximum epoch */

gain = 0.0;
xbias = -2.0;
ybias = -2.0;
lrate = 0.0;
maxepoch = 0;

while (gain <= 0.0 || gain > 1.0) {
    printf("\n Input gain of squashing function (0 < gain <= 1) : ");
    scanf("%lf", &gain); }

while (xbias < -1.0 || xbias > 1.0) {
    printf("\n Input xbias of squashing function (-1.0 <= xbias <= 1.0) : ");
    scanf("%lf", &xbias); }

while (ybias < -0.5 || ybias > 0.5) {
    printf("\n Input ybias of squashing function (-0.5 <= ybias <= 0.5) : ");
    scanf("%lf", &ybias); }

while (lrate <= 0 || lrate > 3) {
    printf("\n Input learning rate (0 < learning rate <= 3) : ");
    scanf("%lf", &lrate); }

while ((maxepoch < 1) || (maxepoch > 10000)) {
    printf("\n Input number of iterations (1 <= iteration <= 10000) : ");
    scanf("%d", &maxepoch); }

/* Reads the squashing function you want to use */

function = 0;
while ((function != 1) && (function != 2)) {
printf("\n Which squashing function do you want to use ? ");

```



```

if (in_node == 3) sscanf(s, "%lf%lf%lf%lf%lf%lf%lf",
    &d[n][1], &d[n][2], &d[n][3], &d[n][4], &d[n][5], &d[n][6], &d[n][7],
    &d[n][8]);

if (in_node == 2) sscanf(s, "%lf%lf%lf%lf%lf%lf",
    &d[n][1], &d[n][2], &d[n][3], &d[n][4], &d[n][5], &d[n][6], &d[n][7]);

if (in_node == 1) sscanf(s, "%lf%lf%lf%lf%lf",
    &d[n][1], &d[n][2], &d[n][3], &d[n][4], &d[n][5], &d[n][6]);

    wbetot += d[n][column];
    n++;
}

    lines = n - 1;
    wbemean = wbetot / lines;

/* Normalizing input and target of ANN */

    for (j = 5; j <= column; j++) {
        min_max(j, lines, &min[j], &max[j]);

        for (i = 1; i <= lines; i++) {
            d[i][j] = (d[i][j] - min[j]) * (b - a) / (max[j] - min[j]) + a;
        }
    }

    printf("\n\n All the inputs and target have been normalized \n");

/* Initializing weights with random values between -0.25 and 0.25 */

    for(i = 1; i <= in_node; i++) {
        for(j = 1; j <= h1_node; j++) {
            r = 0.5*rand() / RAND_MAX;
            w12[i][j] = r - 0.25;
        }
    }

```

```

if(layers > 3) {

    for(i = 1; i <= h1_node; i++) {
        for(j = 1; j <= h2_node; j++) {
            r = 0.5*rand() / RAND_MAX ;
            w23[i][j] = r - 0.25 ;

        }
    }

if(layers > 4) {

    for(i = 1; i <= h2_node; i++) {
        for(j = 1; j <= h3_node; j++) {
            r = 0.5*rand() / RAND_MAX ;
            w34[i][j] = r - 0.25 ;

        }
    }

}

}

if(layers == 3) h3_node = h1_node ;
if(layers == 4) h3_node = h2_node ;

for(j = 1; j <= h3_node; j++) {
    r = 0.5*rand() / RAND_MAX ;

if(layers == 5) w45[j][1] = r - 0.25 ;
if(layers == 4) w34[j][1] = r - 0.25 ;
if(layers == 3) w23[j][1] = r - 0.25 ;
}

epoch = 0 ;
diff = 1.0 ;
avgerror = 1.0 ;

```

```

i = 0 ;
while ((epoch < maxepoch) && (avgerror > maxerror) && (diff > tolerance)) {

    i += 1 ;

    if (i == lines + 1) {
        lasterr = avgerror ;
        epoch += 1 ;
        avgerror = toterror / lines ;
        diff = lasterr - avgerror ;
        if (diff < 0) diff = - diff ;

        printf("ANNMODEL.C VERSION 1.0 BY AMITAVA DHAR \n") ;
        printf("Please do not turn off this computer until it reaches %d epochs.\n", maxepoch)
;
        printf("Epochs completed = %d\n ", epoch) ;
        printf("Average error = %f\n", avgerror) ;

        toterror = 0.0 ;

        if ((epoch < maxepoch) && (avgerror > maxerror) && (diff > tolerance))
            sse = 0.0 ;
        i = 1 ;
    }

    /* Sets output of first layer equal to input */

    for (j = 1; j <= in_node; j++) {
        k = j + 4 ;
        y[1][j] = d[i][k] ;
    }

    /* Calculates activation(x) and output(y) of first hidden layer */

    for (j = 1; j <= h1_node; j++) {
        x[2][j] = 0 ;
        for (k=1; k <= in_node; k++)
            x[2][j] += y[1][k] * w12[k][j] ;

        if (function == 1) sigmoid(x[2][j], gain, xbias, ybias, &y[2][j]) ;
        if (function == 2) tan_hyp(x[2][j], gain, xbias, ybias, &y[2][j]) ;
    }
}

```

```

    }

/* Calculates activation(x) and output(y) of second hidden layer */

if (layers > 3) {
    for (j = 1; j <= h2_node; j++) {
        x[3][j] = 0;
        for (k = 1; k <= h1_node; k++)
            x[3][j] += y[2][k] * w23[k][j];

        if (function == 1) sigmoid(x[3][j], gain, xbias, ybias, &y[3][j]);
        if (function == 2) tan_hyp(x[3][j], gain, xbias, ybias, &y[3][j]);
    }

/* Calculates activation(x) and output(y) of third hidden layer */

if (layers > 4) {
    for (j = 1; j <= h3_node; j++) {
        x[4][j] = 0;
        for (k = 1; k <= h2_node; k++)
            x[4][j] += y[3][k] * w34[k][j];

        if (function == 1) sigmoid(x[4][j], gain, xbias, ybias, &y[4][j]);
        if (function == 2) tan_hyp(x[4][j], gain, xbias, ybias, &y[4][j]);
    }
}

/* Calculates activation(x) and output(y) of output layer */

x[5][1] = 0;
for (j = 1; j <= h3_node; j++) {
    if (layers == 3) x[5][1] += y[2][j] * w23[j][1];
    if (layers == 4) x[5][1] += y[3][j] * w34[j][1];
    if (layers == 5) x[5][1] += y[4][j] * w45[j][1];
}

if (function == 1) sigmoid(x[5][1], gain, xbias, ybias, &y[5][1]);
if (function == 2) tan_hyp(x[5][1], gain, xbias, ybias, &y[5][1]);

```

```

wbepred = (y[5][1] - a) * (max[column] - min[column]) / (b - a) + min[column];
wbe = (d[i][column] - a) * (max[column] - min[column]) / (b - a) + min[column];
abserror = wbe - wbepred;
if (abserror < 0) abserror = -abserror;
toterror += abserror;
if ((epoch < maxepoch) && (avgerror > maxerror) && (diff > tolerance)) {

    sse += pow(abserror, 2.0);

/* Begin adjusting output layer weights */

if (function == 1) delta[5][1] = y[5][1] * (1 - y[5][1]) * (d[i][column] - y[5][1]);
if (function == 2) delta[5][1] = (1 - pow(y[5][1], 2.0)) * (d[i][column] - y[5][1]);

    for (j = 1; j <= h3_node; j++) {
        if (layers == 5) w45[j][1] += lrate * y[4][j] * delta[5][1];
        if (layers == 4) w34[j][1] += lrate * y[3][j] * delta[5][1];
        if (layers == 3) w23[j][1] += lrate * y[2][j] * delta[5][1];
    }

/* Begin adjusting w34 weights */
if (layers > 3) {
    if (layers > 4) {

        for (j = 1; j <= h3_node; j++) {
            delta[4][j] = 0;
if (function == 1) delta[4][j] += y[4][j] * (1 - y[4][j]) * delta[5][1] * w45[j][1];
if (function == 2) delta[4][j] += (1 - pow(y[4][j], 2.0)) * delta[5][1] * w45[j][1];

            }

        for (j = 1; j <= h2_node; j++) {
            for (k = 1; k <= h3_node; k++)
                w34[j][k] += lrate * y[3][j] * delta[4][k];
        }
    }
}

/* Begin adjusting w23 weights */

```

```

for (j = 1; j <= h2_node; j++) {
    delta[3][j] = 0 ;

    for (k = 1; k <= h3_node; k++) {

if (layers == 4) {
    h3_node = 1 ;
    delta[4][1] = delta[5][1] ;
    }

if (function == 1) delta[3][j] += y[3][j] * (1 - y[3][j]) * delta[4][k] * w34[j][k] ;
if (function == 2) delta[3][j] += (1 - pow(y[3][j], 2.0)) * delta[4][k] * w34[j][k] ;
    }

if (layers == 4) h3_node = h2_node ;
    }

    for (j = 1; j <= h1_node; j++) {
        for (k = 1; k <= h2_node; k++)
            w23[j][k] += lrate * y[2][j] * delta[3][k] ;
    }
}

/* Begin adjusting w12 weights */

for (j = 1; j <= h1_node; j++) {
    delta[2][j] = 0 ;

    for (k = 1; k <= h2_node; k++) {

if (layers == 3) {
    h2_node = 1 ;
    delta[3][1] = delta[5][1] ;
    }

if (function == 1) delta[2][j] += y[2][j] * (1 - y[2][j]) * delta[3][k] * w23[j][k] ;
if (function == 2) delta[2][j] += (1 - pow(y[2][j], 2.0)) * delta[3][k] * w23[j][k] ;
    }
}

for (j = 1; j <= in_node; j++) {
    for (k = 1; k <= h1_node; k++)
        w12[j][k] += lrate * y[1][j] * delta[2][k] ;
}

```

```

        }
    }
}

if (avgerror < maxerror) printf("avgerror < %f\n\n", maxerror);
if (diff < tolerance) printf("Error diff. < tolerance = %lf\n\n", tolerance);
if (epoch > maxepoch) printf("Optimization complete for %d epochs\n\n", epoch);

/* printf("\n DONE !\n"); */

mse = sse / (lines - 1);

rmse = pow(mse, 0.5);

cv_rmse = 100 * rmse / wbemean;

printf("\n SSE = %f\n", sse);

printf("\n MSE = %f\n", mse);

printf("\n RMSE = %f\n", rmse);

printf("\n CV_RMSE = %f\n", cv_rmse);

/* Prints model results to log file */

fprintf(ofp1, "OUTPUT TO ANNMODEL.C VERSION 1.0 BY AMITAVA DHAR
\n");

fprintf(ofp1, "It is a %d layers ann model.\n\n", layers);

fprintf(ofp1, "Number of input layer nodes = %d\n", in_node);

fprintf(ofp1, "Number of first hidden layer nodes = %d\n", h1_node);

if (layers > 3) {
    fprintf(ofp1, "Number of second hidden layer nodes = %d\n", h2_node);

if (layers > 4)
    fprintf(ofp1, "Number of third hidden layer nodes = %d\n\n", h3_node);
}
}

```

```

fprintf(ofp1, "Gain = %f\n", gain);
fprintf(ofp1, "Xbias = %f\n", xbias);
fprintf(ofp1, "Ybias = %f\n", ybias);
fprintf(ofp1, "Learning rate = %f\n\n", lrate);
fprintf(ofp1, "Normalization range : %f to %f.\n", a, b);
if (function == 1) fprintf(ofp1, "Squashing Function is sigmoid.\n\n");
if (function == 2) fprintf(ofp1, "Squashing Function is tan hyperbolic.\n\n");
fprintf(ofp1, "Epoch = %d\n", epoch);
fprintf(ofp1, "Average error = %f\n", avgerror);
fprintf(ofp1, "Maximum allowable error = %f\n", maxerror);
fprintf(ofp1, "Number of observations = %d.\n", lines);
fprintf(ofp1, "Mean wbe = %f\n", wbemean);
fprintf(ofp1, "RMSE = %f\n", rmse);
fprintf(ofp1, "CV_RMSE = %f\n\n", cv_rmse);
/* Prints values of w12 weights to log file */
for (j = 1; j <= in_node; j++) {
    for (k = 1; k <= h1_node; k++)
        fprintf(ofp1, "w12[%d][%d] = %f\n", j, k, w12[j][k]);
}
/* Prints values of w23 weights to log file */
if (layers > 3) {
    for (j = 1; j <= h1_node; j++) {
        for (k = 1; k <= h2_node; k++)
            fprintf(ofp1, "w23[%d][%d] = %f\n", j, k, w23[j][k]);
    }
}

```



```

/* Prints values of w34 weights to log file */

if (layers > 4) {

    for (j = 1; j <= h2_node; j++) {
        for (k = 1; k <= h3_node; k++)
            fprintf(ofp1, "w34[%d][%d] = %f\n", j, k, w34[j][k]);
    }

}

/* Prints values of w45 weights to log file */

for (k = 1; k <= h3_node; k++) {
    if (layers == 5) fprintf(ofp1, "w45[%d][1] = %f\n", k, w45[k][1]);
    if (layers == 4) fprintf(ofp1, "w34[%d][1] = %f\n", k, w34[k][1]);
    if (layers == 3) fprintf(ofp1, "w23[%d][1] = %f\n", k, w23[k][1]);
}

/* Calculates and prints predicted values to *pred.dat file */

for (i = 1; i <= lines; i++) {
    for (j = 1; j <= in_node; j++) {
        k = j + 4;
        y[1][j] = d[i][k];
    }

    for (j = 1; j <= h1_node; j++) {
        x[2][j] = 0;
        for (k = 1; k <= in_node; k++) x[2][j] += y[1][k] * w12[k][j];

        if (function == 1) sigmoid(x[2][j], gain, xbias, ybias, &y[2][j]);
        if (function == 2) tan_hyp(x[2][j], gain, xbias, ybias, &y[2][j]);
    }

}

if (layers > 3) {

    for (j = 1; j <= h2_node; j++) {
        x[3][j] = 0;
        for (k = 1; k <= h1_node; k++) x[3][j] += y[2][k] * w23[k][j];

        if (function == 1) sigmoid(x[3][j], gain, xbias, ybias, &y[3][j]);
    }
}

```

```

        if (function == 2) tan_hyp(x[3][j], gain, xbias, ybias, &y[3][j]);
    }

if (layers > 4) {
    for (j = 1; j <= h3_node; j++) {
        x[4][j] = 0;
        for (k = 1; k <= h2_node; k++) x[4][j] += y[3][k] * w34[k][j];

        if (function == 1) sigmoid(x[4][j], gain, xbias, ybias, &y[4][j]);
        if (function == 2) tan_hyp(x[4][j], gain, xbias, ybias, &y[4][j]);
    }
}

}
}

x[5][1] = 0;
for (j = 1; j <= h3_node; j++) {
    if (layers == 5) x[5][1] += y[4][j] * w45[j][1];
    if (layers == 4) x[5][1] += y[3][j] * w34[j][1];
    if (layers == 3) x[5][1] += y[2][j] * w23[j][1];
}

if (function == 1) sigmoid(x[5][1], gain, xbias, ybias, &y[5][1]);
if (function == 2) tan_hyp(x[5][1], gain, xbias, ybias, &y[5][1]);

wbe = (d[i][column] - a) * (max[column] - min[column]) / (b - a) + min[column]
;
wbepred = (y[5][1] - a) * (max[column] - min[column]) / (b - a) + min[column]
;
resid = wbe - wbepred;

fprintf(ofp2, "%f%f%f%f%f %f %f\n", d[i][1], d[i][2], d[i][3], d[i][4], wbe,
wbepred, resid);
}

fclose(ifp);
fclose(ofp1);
fclose(ofp2);
}

```

```
/* This function calculates minimum and maximum of each column in the input
data file which are later used to normalize input and target to the ANN */
```

```
void min_max(int col, int lines, double *min, double *max)
```

```
{
int i;

    *min = d[1][col];
    *max = d[1][col];

for ( i = 2; i <= lines; i++) {
    if (d[i][col] < *min) *min = d[i][col];
    if (d[i][col] > *max) *max = d[i][col];
    }

}
```

```
/* Calculates the value of squashing function */
```

```
void sigmoid(double net, double gain, double xbias, double ybias, double *out)
```

```
{
    *out = ybias + 1 / (1 + exp(-gain * (net + xbias)));
}
```

```
void tan_hyp(double net, double gain, double xbias, double ybias, double *out)
```

```
{
double numer, denom;

    numer = exp(gain * (net + xbias)) - exp(-gain * (net + xbias));
    denom = exp(gain * (net + xbias)) + exp(-gain * (net + xbias));

    *out = ybias + (numer / denom);

}
```

APPENDIX D

**SAS PROGRAM FOR ARTIFICIAL NEURAL NETWORK WITH WAVELET
BASIS FUNCTIONS**

/*

Program listing for Wave-Net modeling upto scale = 4 and generating residuals for modeling at scale = 3 for weekdays only. For weekends, "if dow >=2 and dow <= 6;" needs to be replaced by "if dow = 1 or dow = 7;". The stepwise regression is performed first to identify the important frequencies. Once this is done, PROC REG procedure is used to determine the amplitudes (regression co-efficients)

*/

```
filename out1 'C:\temp\hwwd1.dat' ;
data indata ;
infile 'c:\temp\ras.dat' ;
input mm dd yy hr hw temp ;
date = mdy(mm,dd,yy) ;
dow = weekday(date) ;
if dow >= 2 and dow <= 6 ;
if temp <= 0 then temp = . ;
if hw <= 0 then hw = . ;
run ;

proc reg data = indata ;
model hw = hr temp ;
output out = wkdy1
       r = reshwh ;
run ;

data wkdy2 ;
set wkdy1 ;

m = 4 ;

file out1 ;
put (mm dd yy hr temp hw reshwh) (4*5.0 3*7.2) ;

temp = temp - 20 ;
h = (2**(-m))*hr ;
t = (2**(-m))*temp ;
```

```

ph0 = sqrt(6/(3.14*(3+1)))*exp(-6*((h - 0)**2)/(3+1)) ;
ph1 = sqrt(6/(3.14*(3+1)))*exp(-6*((h - 1)**2)/(3+1)) ;

pt0 = sqrt(6/(3.14*(3+1)))*exp(-6*((t - 0)**2)/(3+1)) ;
pt1 = sqrt(6/(3.14*(3+1)))*exp(-6*((t - 1)**2)/(3+1)) ;
pt2 = sqrt(6/(3.14*(3+1)))*exp(-6*((t - 2)**2)/(3+1)) ;
pt3 = sqrt(6/(3.14*(3+1)))*exp(-6*((t - 3)**2)/(3+1)) ;
pt4 = sqrt(6/(3.14*(3+1)))*exp(-6*((t - 4)**2)/(3+1)) ;
pt5 = sqrt(6/(3.14*(3+1)))*exp(-6*((t - 5)**2)/(3+1)) ;

wh0 = cos(2.570935*(2*(h - 0) - 1))*exp(-0.222759*((2*(h - 0) - 1)**2)) ;
wh1 = cos(2.570935*(2*(h - 1) - 1))*exp(-0.222759*((2*(h - 1) - 1)**2)) ;

wt0 = cos(2.570935*(2*(t - 0) - 1))*exp(-0.222759*((2*(t - 0) - 1)**2)) ;
wt1 = cos(2.570935*(2*(t - 1) - 1))*exp(-0.222759*((2*(t - 1) - 1)**2)) ;
wt2 = cos(2.570935*(2*(t - 2) - 1))*exp(-0.222759*((2*(t - 2) - 1)**2)) ;
wt3 = cos(2.570935*(2*(t - 3) - 1))*exp(-0.222759*((2*(t - 3) - 1)**2)) ;
wt4 = cos(2.570935*(2*(t - 4) - 1))*exp(-0.222759*((2*(t - 4) - 1)**2)) ;
wt5 = cos(2.570935*(2*(t - 5) - 1))*exp(-0.222759*((2*(t - 5) - 1)**2)) ;

sc00 = ph0*pt0 ; wv100 = ph0*wt0 ; wv200 = wh0*pt0 ; wv300 = wh0*wt0 ;
sc01 = ph0*pt1 ; wv101 = ph0*wt1 ; wv201 = wh0*pt1 ; wv301 = wh0*wt1 ;
sc02 = ph0*pt2 ; wv102 = ph0*wt2 ; wv202 = wh0*pt2 ; wv302 = wh0*wt2 ;
sc03 = ph0*pt3 ; wv103 = ph0*wt3 ; wv203 = wh0*pt3 ; wv303 = wh0*wt3 ;
sc04 = ph0*pt4 ; wv104 = ph0*wt4 ; wv204 = wh0*pt4 ; wv304 = wh0*wt4 ;
sc05 = ph0*pt5 ; wv105 = ph0*wt5 ; wv205 = wh0*pt5 ; wv305 = wh0*wt5 ;

sc10 = ph1*pt0 ; wv110 = ph1*wt0 ; wv210 = wh1*pt0 ; wv310 = wh1*wt0 ;
sc11 = ph1*pt1 ; wv111 = ph1*wt1 ; wv211 = wh1*pt1 ; wv311 = wh1*wt1 ;
sc12 = ph1*pt2 ; wv112 = ph1*wt2 ; wv212 = wh1*pt2 ; wv312 = wh1*wt2 ;
sc13 = ph1*pt3 ; wv113 = ph1*wt3 ; wv213 = wh1*pt3 ; wv313 = wh1*wt3 ;
sc14 = ph1*pt4 ; wv114 = ph1*wt4 ; wv214 = wh1*pt4 ; wv314 = wh1*wt4 ;
sc15 = ph1*pt5 ; wv115 = ph1*wt5 ; wv215 = wh1*pt5 ; wv315 = wh1*wt5 ;

run ;

proc stepwise data = wkdy2 ;
model reshw = sc00 wv100 wv200 wv300 sc01 wv101 wv201 wv301
          sc02 wv102 wv202 wv302 sc03 wv103 wv203 wv303
          sc04 wv104 wv204 wv304 sc05 wv105 wv205 wv305
          sc10 wv110 wv210 wv310 sc11 wv111 wv211 wv311
          sc12 wv112 wv212 wv312 sc13 wv113 wv213 wv313
          sc14 wv114 wv214 wv314 sc15 wv115 wv215 wv315 / noint f ;

```

```
run ;
```

```
/*
```

```
proc reg data = wkdy2 ;
model resh = wv214 wv204 sc01 sc03 wv303 wv212 wv203 sc14 sc04
      wv101 wv211 sc13 sc11 wv305 wv213 wv105 / noint ;
output out = wkdy3
      r = hwresid ;
run ;
```

```
filename out2 'c:\temp\hwwd2.dat' ;
```

```
data wkdy4 ;
set wkdy3 ;
file out2 ;
temp = temp + 20 ;
put (mm dd yy hr temp hw hwresid) (4*5.0 3*10.2) ;
run ;
*/
```

```
/*
```

Program listing for Wave-Net modeling at scale = 3 by using the residuals data from the program listed above. The stepwise regression is performed first to identify the important frequencies. Once this is done, PROC REG procedure is used to determine the amplitudes (regression co-efficients)

```
*/
```

```
data indata ;
infile 'c:\temp\hwwd2.dat' ;
input mm dd yy hr temp hw resh ;
if temp <= 0 then temp = . ;
if hw <= 0 then hw = . ;
run ;
```

```
/*
```

```
proc means data = indata ;
var resh ;
run ;
*/
```

```
data wkdy1 ;
```

```
set indata ;
```

```
m = 3 ;
```

```
temp = temp - 20 ;
h = (2**(-m))*hr ;
t = (2**(-m))*temp ;
```

```
ph0 = sqrt(6/(3.14*(3+1)))*exp(-6*((h - 0)**2)/(3+1)) ;
ph1 = sqrt(6/(3.14*(3+1)))*exp(-6*((h - 1)**2)/(3+1)) ;
ph2 = sqrt(6/(3.14*(3+1)))*exp(-6*((h - 2)**2)/(3+1)) ;
```

```
pt0 = sqrt(6/(3.14*(3+1)))*exp(-6*((t - 0)**2)/(3+1)) ;
pt1 = sqrt(6/(3.14*(3+1)))*exp(-6*((t - 1)**2)/(3+1)) ;
pt2 = sqrt(6/(3.14*(3+1)))*exp(-6*((t - 2)**2)/(3+1)) ;
pt3 = sqrt(6/(3.14*(3+1)))*exp(-6*((t - 3)**2)/(3+1)) ;
pt4 = sqrt(6/(3.14*(3+1)))*exp(-6*((t - 4)**2)/(3+1)) ;
pt5 = sqrt(6/(3.14*(3+1)))*exp(-6*((t - 5)**2)/(3+1)) ;
pt6 = sqrt(6/(3.14*(3+1)))*exp(-6*((t - 6)**2)/(3+1)) ;
pt7 = sqrt(6/(3.14*(3+1)))*exp(-6*((t - 7)**2)/(3+1)) ;
pt8 = sqrt(6/(3.14*(3+1)))*exp(-6*((t - 8)**2)/(3+1)) ;
pt9 = sqrt(6/(3.14*(3+1)))*exp(-6*((t - 9)**2)/(3+1)) ;
pt10 = sqrt(6/(3.14*(3+1)))*exp(-6*((t - 10)**2)/(3+1)) ;
```

```
wh0 = cos(2.570935*(2*(h - 0) - 1))*exp(-0.222759*((2*(h - 0) - 1)**2)) ;
wh1 = cos(2.570935*(2*(h - 1) - 1))*exp(-0.222759*((2*(h - 1) - 1)**2)) ;
wh2 = cos(2.570935*(2*(h - 2) - 1))*exp(-0.222759*((2*(h - 2) - 1)**2)) ;
```

```
wt0 = cos(2.570935*(2*(t - 0) - 1))*exp(-0.222759*((2*(t - 0) - 1)**2)) ;
wt1 = cos(2.570935*(2*(t - 1) - 1))*exp(-0.222759*((2*(t - 1) - 1)**2)) ;
wt2 = cos(2.570935*(2*(t - 2) - 1))*exp(-0.222759*((2*(t - 2) - 1)**2)) ;
wt3 = cos(2.570935*(2*(t - 3) - 1))*exp(-0.222759*((2*(t - 3) - 1)**2)) ;
wt4 = cos(2.570935*(2*(t - 4) - 1))*exp(-0.222759*((2*(t - 4) - 1)**2)) ;
wt5 = cos(2.570935*(2*(t - 5) - 1))*exp(-0.222759*((2*(t - 5) - 1)**2)) ;
wt6 = cos(2.570935*(2*(t - 6) - 1))*exp(-0.222759*((2*(t - 6) - 1)**2)) ;
wt7 = cos(2.570935*(2*(t - 7) - 1))*exp(-0.222759*((2*(t - 7) - 1)**2)) ;
wt8 = cos(2.570935*(2*(t - 8) - 1))*exp(-0.222759*((2*(t - 8) - 1)**2)) ;
wt9 = cos(2.570935*(2*(t - 9) - 1))*exp(-0.222759*((2*(t - 9) - 1)**2)) ;
wt10 = cos(2.570935*(2*(t - 10) - 1))*exp(-0.222759*((2*(t - 10) - 1)**2)) ;
```

```
/*
```

```
wv100 = ph0*wt0 ; wv200 = wh0*pt0 ; wv300 = wh0*wt0 ;
wv101 = ph0*wt1 ; wv201 = wh0*pt1 ; wv301 = wh0*wt1 ;
wv102 = ph0*wt2 ; wv202 = wh0*pt2 ; wv302 = wh0*wt2 ;
wv103 = ph0*wt3 ; wv203 = wh0*pt3 ; wv303 = wh0*wt3 ;
wv104 = ph0*wt4 ; wv204 = wh0*pt4 ; wv304 = wh0*wt4 ;
wv105 = ph0*wt5 ; wv205 = wh0*pt5 ; wv305 = wh0*wt5 ;
wv106 = ph0*wt6 ; wv206 = wh0*pt6 ; wv306 = wh0*wt6 ;
wv107 = ph0*wt7 ; wv207 = wh0*pt7 ; wv307 = wh0*wt7 ;
wv108 = ph0*wt8 ; wv208 = wh0*pt8 ; wv308 = wh0*wt8 ;
wv109 = ph0*wt9 ; wv209 = wh0*pt9 ; wv309 = wh0*wt9 ;
wv1010 = ph0*wt10 ; wv2010 = wh0*pt10 ; wv3010 = wh0*wt10 ;
```

```
wv110 = ph1*wt0 ; wv210 = wh1*pt0 ; wv310 = wh1*wt0 ;
wv111 = ph1*wt1 ; wv211 = wh1*pt1 ; wv311 = wh1*wt1 ;
wv112 = ph1*wt2 ; wv212 = wh1*pt2 ; wv312 = wh1*wt2 ;
wv113 = ph1*wt3 ; wv213 = wh1*pt3 ; wv313 = wh1*wt3 ;
wv114 = ph1*wt4 ; wv214 = wh1*pt4 ; wv314 = wh1*wt4 ;
wv115 = ph1*wt5 ; wv215 = wh1*pt5 ; wv315 = wh1*wt5 ; */
wv116 = ph1*wt6 ; wv216 = wh1*pt6 ; wv316 = wh1*wt6 ;
wv117 = ph1*wt7 ; wv217 = wh1*pt7 ; wv317 = wh1*wt7 ;
/* wv118 = ph1*wt8 ; wv218 = wh1*pt8 ; wv318 = wh1*wt8 ;
wv119 = ph1*wt9 ; wv219 = wh1*pt9 ; wv319 = wh1*wt9 ;
wv1110 = ph1*wt10 ; wv2110 = wh1*pt10 ; wv3110 = wh1*wt10 ;
```

```
wv120 = ph2*wt0 ; wv220 = wh2*pt0 ; wv320 = wh2*wt0 ;
wv121 = ph2*wt1 ; wv221 = wh2*pt1 ; wv321 = wh2*wt1 ;
wv122 = ph2*wt2 ; wv222 = wh2*pt2 ; wv322 = wh2*wt2 ;
wv123 = ph2*wt3 ; wv223 = wh2*pt3 ; wv323 = wh2*wt3 ;
wv124 = ph2*wt4 ; wv224 = wh2*pt4 ; wv324 = wh2*wt4 ;
wv125 = ph2*wt5 ; wv225 = wh2*pt5 ; wv325 = wh2*wt5 ;
wv126 = ph2*wt6 ; wv226 = wh2*pt6 ; wv326 = wh2*wt6 ;
wv127 = ph2*wt7 ; wv227 = wh2*pt7 ; wv327 = wh2*wt7 ;
wv128 = ph2*wt8 ; wv228 = wh2*pt8 ; wv328 = wh2*wt8 ; */
wv129 = ph2*wt9 ; wv229 = wh2*pt9 ; wv329 = wh2*wt9 ;
wv1210 = ph2*wt10 ; wv2210 = wh2*pt10 ; wv3210 = wh2*wt10 ;
```

```
run ;
```

```
/*
```

```
proc stepwise data = wkdy1 ;
```



```

model reshw = wv100 wv200 wv300 wv101 wv201 wv301 wv102 wv202 wv302
    wv103 wv203 wv303 wv104 wv204 wv304 wv105 wv205 wv305
    wv106 wv206 wv306 wv107 wv207 wv307 wv108 wv208 wv308
    wv109 wv209 wv309 wv1010 wv2010 wv3010
    wv110 wv210 wv310 wv111 wv211 wv311 wv112 wv212 wv312
    wv113 wv213 wv313 wv114 wv214 wv314 wv115 wv215 wv315
    wv116 wv216 wv316 wv117 wv217 wv317 wv118 wv218 wv318
    wv119 wv219 wv319 wv1110 wv2110 wv3110
    wv120 wv220 wv320 wv121 wv221 wv321 wv122 wv222 wv322
    wv123 wv223 wv323 wv124 wv224 wv324 wv125 wv225 wv325
    wv126 wv226 wv326 wv127 wv227 wv327 wv128 wv228 wv328
    wv129 wv229 wv329 wv1210 wv2210 wv3210 / noint f;

```

```

run ;
*/

```

```

proc reg data = wkdy1 ;
model reshw = wv229 wv316 wv317 / noint ;
output out = wkdy2
    r = hwresid ;
run ;

```

```

filename out 'c:\temp\hwwd3.dat' ;

```

```

data wkdy3 ;
set wkdy2 ;

```

```

file out ;
temp = temp + 20 ;
put (mm dd yy hr temp hw hwresid) (4*5.0 3*7.2) ;
run ;

```

```

/*

```

Program listing for determining Wave-net prediction at scale = 4 (second approximation.

```

*/

```

```

data indata ;
infile 'c:\temp\raspred.dat' ;
input mm dd yy hr hw temp ;

```

```

date = mdy(mm,dd,yy) ;
dow = weekday(date) ;
if temp <= 0 then temp = . ;
if hw <= 0 then hw = . ;

```

```

m = 4 ;

```

```

temp1 = temp - 20 ;
h = (2**(-m))*hr ;
t = (2**(-m))*temp1 ;

```

```

ph0 = sqrt(6/(3.14*(3+1)))*exp(-6*((h - 0)**2)/(3+1)) ;
ph1 = sqrt(6/(3.14*(3+1)))*exp(-6*((h - 1)**2)/(3+1)) ;

```

```

pt0 = sqrt(6/(3.14*(3+1)))*exp(-6*((t - 0)**2)/(3+1)) ;
pt1 = sqrt(6/(3.14*(3+1)))*exp(-6*((t - 1)**2)/(3+1)) ;
pt2 = sqrt(6/(3.14*(3+1)))*exp(-6*((t - 2)**2)/(3+1)) ;
pt3 = sqrt(6/(3.14*(3+1)))*exp(-6*((t - 3)**2)/(3+1)) ;
pt4 = sqrt(6/(3.14*(3+1)))*exp(-6*((t - 4)**2)/(3+1)) ;
pt5 = sqrt(6/(3.14*(3+1)))*exp(-6*((t - 5)**2)/(3+1)) ;

```

```

wh0 = cos(2.570935*(2*(h - 0) - 1))*exp(-0.222759*((2*(h - 0) - 1)**2)) ;
wh1 = cos(2.570935*(2*(h - 1) - 1))*exp(-0.222759*((2*(h - 1) - 1)**2)) ;

```

```

wt0 = cos(2.570935*(2*(t - 0) - 1))*exp(-0.222759*((2*(t - 0) - 1)**2)) ;
wt1 = cos(2.570935*(2*(t - 1) - 1))*exp(-0.222759*((2*(t - 1) - 1)**2)) ;
wt2 = cos(2.570935*(2*(t - 2) - 1))*exp(-0.222759*((2*(t - 2) - 1)**2)) ;
wt3 = cos(2.570935*(2*(t - 3) - 1))*exp(-0.222759*((2*(t - 3) - 1)**2)) ;
wt4 = cos(2.570935*(2*(t - 4) - 1))*exp(-0.222759*((2*(t - 4) - 1)**2)) ;
wt5 = cos(2.570935*(2*(t - 5) - 1))*exp(-0.222759*((2*(t - 5) - 1)**2)) ;

```

```

sc00 = ph0*pt0 ; wv100 = ph0*wt0 ; wv200 = wh0*pt0 ; wv300 = wh0*wt0 ;
sc01 = ph0*pt1 ; wv101 = ph0*wt1 ; wv201 = wh0*pt1 ; wv301 = wh0*wt1 ;
sc02 = ph0*pt2 ; wv102 = ph0*wt2 ; wv202 = wh0*pt2 ; wv302 = wh0*wt2 ;
sc03 = ph0*pt3 ; wv103 = ph0*wt3 ; wv203 = wh0*pt3 ; wv303 = wh0*wt3 ;
sc04 = ph0*pt4 ; wv104 = ph0*wt4 ; wv204 = wh0*pt4 ; wv304 = wh0*wt4 ;
sc05 = ph0*pt5 ; wv105 = ph0*wt5 ; wv205 = wh0*pt5 ; wv305 = wh0*wt5 ;

```

```

sc10 = ph1*pt0 ; wv110 = ph1*wt0 ; wv210 = wh1*pt0 ; wv310 = wh1*wt0 ;
sc11 = ph1*pt1 ; wv111 = ph1*wt1 ; wv211 = wh1*pt1 ; wv311 = wh1*wt1 ;

```

```

sc12 = ph1*pt2 ; wv112 = ph1*wt2 ; wv212 = wh1*pt2 ; wv312 = wh1*wt2 ;
sc13 = ph1*pt3 ; wv113 = ph1*wt3 ; wv213 = wh1*pt3 ; wv313 = wh1*wt3 ;
sc14 = ph1*pt4 ; wv114 = ph1*wt4 ; wv214 = wh1*pt4 ; wv314 = wh1*wt4 ;
sc15 = ph1*pt5 ; wv115 = ph1*wt5 ; wv215 = wh1*pt5 ; wv315 = wh1*wt5 ;

if dow >= 2 and dow <= 6 then
approx2 = -938.6+2.65*hr+19.8*temp-191.04*wv214+156.8*wv204+414.4*sc01
          -33.9*sc03-46.8*wv303-134*wv212+68.4*wv203+169.7*sc14-189.9*sc04
          -100.9*wv101+252.7*wv211-68.9*sc13+327.4*sc11+251.9*wv305
          -72.9*wv213+487.7*wv105 ;

if dow = 1 or dow = 7 then
approx2 = -701.5-1.76*hr+15.4*temp+176.6*sc11-168.7*sc13+138.5*sc15
          +123.1*wv204+251.6*sc12-50.1*wv214+102.3*sc14-60.7*sc03-37*wv103
          -34.1*wv213 ;

run ;

filename out2 'c:\temp\rascwpr1.dat' ;

data indata1 ;
set indata ;
file out2 ;

if temp = . then temp = -99 ;
if hw = . then hw = -99 ;
if approx2 = . then approx2 = -99 ;

put (mm dd yy hr temp hw approx2) (4*5.0 3*11.2) ;
run ;

/*
Program listing for determining Wave-net prediction at scale = 3 (final approximation.
*/

data indata ;
infile 'c:\temp\rascwpr1.dat' ;
input mm dd yy hr temp hw approx2 ;
date = mdy(mm,dd,yy) ;
dow = weekday(date) ;

```

```

if temp = -99 then temp = . ;
if hw = -99 then hw = . ;
if approx2 = -99 then approx2 = . ;

```

```
m = 3 ;
```

```

temp1 = temp - 20 ;
h = (2**(-m))*hr ;
t = (2**(-m))*temp1 ;

```

```

ph0 = sqrt(6/(3.14*(3+1)))*exp(-6*((h - 0)**2)/(3+1)) ;
ph1 = sqrt(6/(3.14*(3+1)))*exp(-6*((h - 1)**2)/(3+1)) ;
ph2 = sqrt(6/(3.14*(3+1)))*exp(-6*((h - 2)**2)/(3+1)) ;

```

```

pt0 = sqrt(6/(3.14*(3+1)))*exp(-6*((t - 0)**2)/(3+1)) ;
pt1 = sqrt(6/(3.14*(3+1)))*exp(-6*((t - 1)**2)/(3+1)) ;
pt2 = sqrt(6/(3.14*(3+1)))*exp(-6*((t - 2)**2)/(3+1)) ;
pt3 = sqrt(6/(3.14*(3+1)))*exp(-6*((t - 3)**2)/(3+1)) ;
pt4 = sqrt(6/(3.14*(3+1)))*exp(-6*((t - 4)**2)/(3+1)) ;
pt5 = sqrt(6/(3.14*(3+1)))*exp(-6*((t - 5)**2)/(3+1)) ;
pt6 = sqrt(6/(3.14*(3+1)))*exp(-6*((t - 6)**2)/(3+1)) ;
pt7 = sqrt(6/(3.14*(3+1)))*exp(-6*((t - 7)**2)/(3+1)) ;
pt8 = sqrt(6/(3.14*(3+1)))*exp(-6*((t - 8)**2)/(3+1)) ;
pt9 = sqrt(6/(3.14*(3+1)))*exp(-6*((t - 9)**2)/(3+1)) ;
pt10 = sqrt(6/(3.14*(3+1)))*exp(-6*((t - 10)**2)/(3+1)) ;

```

```

wh0 = cos(2.570935*(2*(h - 0) - 1))*exp(-0.222759*((2*(h - 0) - 1)**2)) ;
wh1 = cos(2.570935*(2*(h - 1) - 1))*exp(-0.222759*((2*(h - 1) - 1)**2)) ;
wh2 = cos(2.570935*(2*(h - 2) - 1))*exp(-0.222759*((2*(h - 2) - 1)**2)) ;

```

```

wt0 = cos(2.570935*(2*(t - 0) - 1))*exp(-0.222759*((2*(t - 0) - 1)**2)) ;
wt1 = cos(2.570935*(2*(t - 1) - 1))*exp(-0.222759*((2*(t - 1) - 1)**2)) ;
wt2 = cos(2.570935*(2*(t - 2) - 1))*exp(-0.222759*((2*(t - 2) - 1)**2)) ;
wt3 = cos(2.570935*(2*(t - 3) - 1))*exp(-0.222759*((2*(t - 3) - 1)**2)) ;
wt4 = cos(2.570935*(2*(t - 4) - 1))*exp(-0.222759*((2*(t - 4) - 1)**2)) ;
wt5 = cos(2.570935*(2*(t - 5) - 1))*exp(-0.222759*((2*(t - 5) - 1)**2)) ;
wt6 = cos(2.570935*(2*(t - 6) - 1))*exp(-0.222759*((2*(t - 6) - 1)**2)) ;
wt7 = cos(2.570935*(2*(t - 7) - 1))*exp(-0.222759*((2*(t - 7) - 1)**2)) ;
wt8 = cos(2.570935*(2*(t - 8) - 1))*exp(-0.222759*((2*(t - 8) - 1)**2)) ;
wt9 = cos(2.570935*(2*(t - 9) - 1))*exp(-0.222759*((2*(t - 9) - 1)**2)) ;
wt10 = cos(2.570935*(2*(t - 10) - 1))*exp(-0.222759*((2*(t - 10) - 1)**2)) ;

```

```

wv100 = ph0*wt0 ; wv200 = wh0*pt0 ; wv300 = wh0*wt0 ;
wv101 = ph0*wt1 ; wv201 = wh0*pt1 ; wv301 = wh0*wt1 ;
wv102 = ph0*wt2 ; wv202 = wh0*pt2 ; wv302 = wh0*wt2 ;
wv103 = ph0*wt3 ; wv203 = wh0*pt3 ; wv303 = wh0*wt3 ;
wv104 = ph0*wt4 ; wv204 = wh0*pt4 ; wv304 = wh0*wt4 ;
wv105 = ph0*wt5 ; wv205 = wh0*pt5 ; wv305 = wh0*wt5 ;
wv106 = ph0*wt6 ; wv206 = wh0*pt6 ; wv306 = wh0*wt6 ;
wv107 = ph0*wt7 ; wv207 = wh0*pt7 ; wv307 = wh0*wt7 ;
wv108 = ph0*wt8 ; wv208 = wh0*pt8 ; wv308 = wh0*wt8 ;
wv109 = ph0*wt9 ; wv209 = wh0*pt9 ; wv309 = wh0*wt9 ;
wv1010 = ph0*wt10 ; wv2010 = wh0*pt10 ; wv3010 = wh0*wt10 ;

```

```

wv110 = ph1*wt0 ; wv210 = wh1*pt0 ; wv310 = wh1*wt0 ;
wv111 = ph1*wt1 ; wv211 = wh1*pt1 ; wv311 = wh1*wt1 ;
wv112 = ph1*wt2 ; wv212 = wh1*pt2 ; wv312 = wh1*wt2 ;
wv113 = ph1*wt3 ; wv213 = wh1*pt3 ; wv313 = wh1*wt3 ;
wv114 = ph1*wt4 ; wv214 = wh1*pt4 ; wv314 = wh1*wt4 ;
wv115 = ph1*wt5 ; wv215 = wh1*pt5 ; wv315 = wh1*wt5 ;
wv116 = ph1*wt6 ; wv216 = wh1*pt6 ; wv316 = wh1*wt6 ;
wv117 = ph1*wt7 ; wv217 = wh1*pt7 ; wv317 = wh1*wt7 ;
wv118 = ph1*wt8 ; wv218 = wh1*pt8 ; wv318 = wh1*wt8 ;
wv119 = ph1*wt9 ; wv219 = wh1*pt9 ; wv319 = wh1*wt9 ;
wv1110 = ph1*wt10 ; wv2110 = wh1*pt10 ; wv3110 = wh1*wt10 ;

```

```

wv120 = ph2*wt0 ; wv220 = wh2*pt0 ; wv320 = wh2*wt0 ;
wv121 = ph2*wt1 ; wv221 = wh2*pt1 ; wv321 = wh2*wt1 ;
wv122 = ph2*wt2 ; wv222 = wh2*pt2 ; wv322 = wh2*wt2 ;
wv123 = ph2*wt3 ; wv223 = wh2*pt3 ; wv323 = wh2*wt3 ;
wv124 = ph2*wt4 ; wv224 = wh2*pt4 ; wv324 = wh2*wt4 ;
wv125 = ph2*wt5 ; wv225 = wh2*pt5 ; wv325 = wh2*wt5 ;
wv126 = ph2*wt6 ; wv226 = wh2*pt6 ; wv326 = wh2*wt6 ;
wv127 = ph2*wt7 ; wv227 = wh2*pt7 ; wv327 = wh2*wt7 ;
wv128 = ph2*wt8 ; wv228 = wh2*pt8 ; wv328 = wh2*wt8 ;
wv129 = ph2*wt9 ; wv229 = wh2*pt9 ; wv329 = wh2*wt9 ;
wv1210 = ph2*wt10 ; wv2210 = wh2*pt10 ; wv3210 = wh2*wt10 ;

```

```

if dow >= 2 and dow <= 6 then

```

```

  approx3 = approx2 +73.1*wv229+50.4*wv316-50.5*wv317 ;

```

```
if dow = 1 or dow = 7 then  
approx3 = approx2 +58.9*ww127-41.9*ww324-52.8*ww128-707.4*ww2010 ;
```

```
hwresid = hw - approx3 ;
```

```
run ;
```

```
filename out2 'c:\temp\rascwpr2.dat' ;
```

```
data indata1 ;
```

```
set indata ;
```

```
file out2 ;
```

```
if hwresid = . then hwresid = -99 ;
```

```
if hw = . then hw = -99 ;
```

```
put (mm dd yy hr hw hwresid) (4*5.0 2*11.2) ;
```

```
run ;
```

APPENDIX E

**A SAMPLE PROGRAM FOR PERFORMING DATA-SCREENING OF
ENERGY USE IN COMMERCIAL BUILDINGS**

```

/*****
THIS PROGRAM WILL DEVELOP MODELS FOR TEMPERATURE AND
WEATHER DEPENDENT ENERGY USE FROM TRAINING DATA SET AND USE
THE PREDICTION LIMITS FOR SCREENING ANY TEST DATA SET.
MAXIMUM NUMBER OF OBSERVATIONS OF BOTH TRAIN AND TEST DATA
SET IS LIMITED BY THE VALUE OF MAXLINE DEFINED AT THE
BEGINNING OF THE PROGRAM.

```

```

*****/

```

```

#include <stdio.h>
#include <stdlib.h>
#include <math.h>
#include <float.h>

```

```

#define maxline 10000
#define col 15

```

```

main (int argc, char *argv[])
{
int i, j, k, ll, m, n, p, jj, ip1, kp1, nn, wdobs, weobs, indwd[maxline] ;
int wdobst, weobst, day, dow, line, lines, linest, indwe[maxline] ;
double decimal, in[maxline][col], wdin[maxline][col], wein[maxline][col] ;
double xwd[maxline][col], xwe[maxline][col], xtwd[col][maxline] ;
double xtwe[col][maxline], ywd[maxline], ywe[maxline], ytywd, ytywe ;
double xty[3], xtywd[col], xtywe[col], xtxwd[col][col], xtxwe[col][col] ;
double xtx[3][3], xtxinv[3][3], xtxinvwd[col][col], xtxinvwe[col][col] ;
double xtxdet, x[maxline][3], xt[3][maxline], y[maxline] ;
double yty, ssewd, ssewe, rmsewd, rmsewe, sse, rmse, btxywd, btxywe ;
double betawd[col], betawe[col], beta[3], tin[maxline][col] ;
double l[3], ltxtxinv[3], ltxxl, utl, ltl, lwd[maxline][col] ;
double lwe[maxline][col], predwe[maxline], ltwe[col][maxline] ;
double ltxtxwe[maxline][col], ltxxlwd[maxline], ltxxlwe[maxline] ;
double predwd[maxline], ltwd[col][maxline], ltxtxwd[maxline][col] ;

```

```

double test[maxline][col], wdtest[maxline][col], wetest[maxline][col] ;
int wdtest1, wdtest2, wdtest3, wdtest4, wdtest7 ;
int wetest1, wetest2, wetest3, wetest4, wetest7 ;
double uplwd, uplwe, lplwd, lplwe ;
double a[col][col], b[col][col], big, temp, quot, ab, sum ;

char s[100] ;

FILE *ifpi, *ifpt, *ofpwd, *ofpwe ;

if (argc != 5) {
    printf("\n\n Improper command !\n") ;
    printf("Proper format is:\n") ;
    printf("screen1 train_data_file test_data_file wd_outfile we_outfile\n") ;
    exit(1) ;
}

ifpi = fopen(argv[1], "r") ;
ifpt = fopen(argv[2], "r") ;
ofpwd = fopen(argv[3], "w") ;
ofpwe = fopen(argv[4], "w") ;

/* reads input training data and stores weekdays and weekends data
separately in wdin[][] and wein[][] respectively */

n = 1 ;
while((fgets(s, 100, ifpi) != NULL) && (n <= maxline)) {
    sscanf(s, "%lf%lf%lf%lf%lf%lf%lf%lf%lf%lf", &in[n][1], &in[n][2],
        &in[n][3], &in[n][4], &in[n][5], &in[n][6], &in[n][7], &in[n][8],
        &in[n][9], &in[n][10]) ;

    in[n][7] = in[n][7]/100 ;
    if ((in[n][8] > 0) && (in[n][9] > 0))
        n++ ;
}

printf("\n input data read\n") ;
lines = n - 1 ;

n = 1 ;
wdobs = 1 ;

```



```

weobs = 1 ;
while (n <= lines) {
    decimal = in[n][6] ;
    day = (int) (decimal + 3) ;
    dow = (day % 7) ;
    if ((dow == 1) || (dow == 0)) {
        for(i = 1; i <= 10; i++) wein[weobs][i] = in[n][i] ;
        weobs++ ;
    }
    else {
        for(i = 1; i <= 10; i++) wdin[wdots][i] = in[n][i] ;
        wdots++ ;
    }
    n++ ;
}

wdots = wdots - 1 ;
weobs = weobs - 1 ;
printf("\n no problem so far!\n") ;

/* Does regression to develop model for weekdays */

for(i = 1; i <= wdots; i++) {
    ywd[i] = wdin[i][8] ;
    xwd[i][1] = 1 ;
    xwd[i][2] = wdin[i][9] ;
    xwd[i][3] = sin((2*3.14/80)*(wdin[i][9]-20)) ;
    xwd[i][4] = xwd[i][3]*sin((2*3.14/24)*(wdin[i][7])) ;
    xwd[i][5] = wdin[i][9]*cos((2*3.14/24)*(wdin[i][7])) ;
    for (j = 1; j <= 5; j++) xtwd[j][i] = xwd[i][j] ;
}

for (j = 1; j <= 5; j++) {
    xtywd[j] = 0 ;
    for (k = 1; k <= 5; k++) xtxwd[j][k] = 0 ;
}

for (j = 1; j <= 5; j++) {
    for (k = 1; k <= 5; k++) {
        for(i = 1; i <= wdots; i++) xtxwd[j][k] += xtwd[j][i]*xwd[i][k] ;
    }
}

for (j = 1; j <= 5; j++) {

```

```

for(i = 1; i <= wdobs; i++) xtywd[j] += xtwd[j][i]*ywd[i] ;
}

```

```

ytywd = 0 ;
for(i = 1; i <= wdobs; i++) ytywd += ywd[i]*ywd[i] ;

```

```

/* INVERSE MATRIX CALCULATION */

```

```

n = 5 ;
m = n + n ;
ll = n - 1 ;

```

```

for (p = 1; p <= n; p++) {
    for (i = 1; i <= n; i++) {
        for (j = 1; j <= n; j++) a[i][j] = xtxwd[i][j] ;
    }

    for (i = 1; i <= n; i++) a[i][m] = 0 ;
    a[p][m] = 1 ;

    for (k = 1; k <= ll; k++) {
        jj = k;
        big = fabs(a[k][k]) ;
        kp1 = k + 1 ;
        for (i = kp1; i <= n; i++) {
            ab = fabs(a[i][k]) ;
            if (big < ab) {
                big = ab ;
                jj = i ;
            }
        }

        if (jj != k) {
            for (j = k; j <= m; j++) {
                temp = a[jj][j] ;
                a[jj][j] = a[k][j] ;
                a[k][j] = temp ;
            }
        }

        for (i = kp1; i <= n; i++) {
            quot = a[i][k] / a[k][k] ;

```

```

        for (j = kp1; j <= m; j++)
            a[i][j] = a[i][j] - quot*a[k][j];
        }

    for (i = kp1; i <= n; i++) a[i][k] = 0;

    }

b[n][p] = a[n][m] / a[n][n];

for (nn = 1; nn <= ll; nn++) {
    sum = 0;
    i = n - nn;
    ip1 = i + 1;
    for (j = ip1; j <= n; j++) sum += a[i][j]*b[j][p];
    b[i][p] = (a[i][m] - sum) / a[i][i];
}

}

for (i = 1; i <= n; i++) {
    for (j = 1; j <= n; j++) xtxinvwd[i][j] = b[i][j];
}

```

```

/* END OF INVERSE MATRIX CALCULATION */

```

```

for (i = 1; i <= 5; i++) betawd[i] = 0;

for (i = 1; i <= 5; i++) {
    for (j = 1; j <= 5; j++) betawd[i] += xtxinvwd[i][j]*xtywd[j];
}

for (i = 1; i <= 5; i++)
printf("\n betawd[%d] = %f", i, betawd[i]);

btxtywd = 0;
for (i = 1; i <= 5; i++) btxtywd += betawd[i]*xtywd[i];

ssewd = ytywd - btxtywd;
rmsewd = sqrt(ssewd/(wdobs - 4));

```

```

/* Does regression to develop model for weekends */

for(i = 1; i <= weobs; i++) {
    ywe[i] = wein[i][8];
    xwe[i][1] = 1;
    xwe[i][2] = wein[i][9];
    xwe[i][3] = cos((2*3.14/80)*(wein[i][9] - 20));
    xwe[i][4] = sin((2*3.14/80)*(wein[i][9] - 20))*sin((2*3.14/24)*(wein[i][7]));
    xwe[i][5] = wein[i][9]*sin((2*3.14/24)*(wein[i][7]));
    xwe[i][6] = wein[i][9]*cos((2*3.14/24)*(wein[i][7]));
    for (j = 1; j <= 6; j++) xtwe[j][i] = xwe[i][j];
}

for (j = 1; j <= 6; j++) {
    xtywe[j] = 0;
    for (k = 1; k <= 6; k++) xtxwe[j][k] = 0;
}

for (j = 1; j <= 6; j++) {
    for (k = 1; k <= 6; k++) {
        for(i = 1; i <= weobs; i++) xtxwe[j][k] += xtwe[j][i]*xwe[i][k];
    }
}

for (j = 1; j <= 6; j++) {
    for(i = 1; i <= weobs; i++) xtywe[j] += xtwe[j][i]*ywe[i];
}

ytywe = 0;
for(i = 1; i <= weobs; i++) ytywe += ywe[i]*ywe[i];

/* INVERSE MATRIX CALCULATION */

n = 6;
m = n + n;
ll = n - 1;

for (p = 1; p <= n; p++) {
    for (i = 1; i <= n; i++) {
        for (j = 1; j <= n; j++) a[i][j] = xtxwe[i][j];
    }
}

```

```

    }

for (i = 1; i <= n; i++) a[i][m] = 0 ;
a[p][m] = 1 ;

for (k = 1; k <= ll; k++) {
    jj = k;
    big = fabs(a[k][k]) ;
    kp1 = k + 1 ;
    for (i = kp1; i <= n; i++) {
        ab = fabs(a[i][k]) ;
        if (big < ab) {
            big = ab ;
            jj = i ;
        }
    }

    if (jj != k) {
        for (j = k; j <= m; j++) {
            temp = a[jj][j] ;
            a[jj][j] = a[k][j] ;
            a[k][j] = temp ;
        }
    }

    for (i = kp1; i <= n; i++) {
        quot = a[i][k] / a[k][k] ;
        for (j = kp1; j <= m; j++)
            a[i][j] = a[i][j] - quot*a[k][j] ;
    }

    for (i = kp1; i <= n; i++) a[i][k] = 0 ;

}

b[n][p] = a[n][m] / a[n][n] ;

for (nn = 1; nn <= ll; nn++) {
    sum = 0 ;
    i = n - nn ;
    ip1 = i + 1 ;
    for (j = ip1; j <= n; j++) sum += a[i][j]*b[j][p] ;
    b[i][p] = (a[i][m] - sum) / a[i][i] ;
}

```

```

        }

for (i = 1; i <= n; i++) {
    for (j = 1; j <= n; j++) xtxinvwe[i][j] = b[i][j];
}

/* END OF INVERSE MATRIX CALCULATION */

for (i = 1; i <= 6; i++) betawe[i] = 0;

for (i = 1; i <= 6; i++) {
    for (j = 1; j <= 6; j++) betawe[i] += xtxinvwe[i][j]*xtywe[j];
}
for (i = 1; i <= 6; i++)
printf("\n betawe[%d] = %f", i, betawe[i]);

btxtywe = 0;
for (i = 1; i <= 6; i++) btxtywe += betawe[i]*xtywe[i];

ssewe = ytywe - btxtywe;
rmsewe = sqrt(ssewe/(weobs - 6));

/* Creates temperature model from input training data */

yty = 0;

for (i = 1; i <= 2; i++) {
    xty[i] = 0;
    for (j = 1; j <= 2; j++) xtx[i][j] = 0;
}

rewind(ifpi);
n = 1;
while((fgets(s, 100, ifpi) != NULL) && (n <= maxline)) {
    sscanf(s, "%lf%lf%lf%lf%lf%lf%lf%lf%lf%lf", &tin[n][1], &tin[n][2],
&tin[n][3], &tin[n][4], &tin[n][5], &tin[n][6], &tin[n][7], &tin[n][8],
&tin[n][9], &tin[n][10]);

    if((tin[n][9] > 0) && (tin[n][10] > 0))

```

```

n++;

}

line = n - 1 ;
printf("\n line = %d", line) ;

for (n = 1; n <= line; n++) {
    y[n] = tin[n][9] ;
    x[n][1] = 1 ;
    x[n][2] = tin[n][10] ;
    xt[1][n] = x[n][1] ;
    xt[2][n] = x[n][2] ;
    xty[1] += xt[1][n]*y[n] ;
    xty[2] += xt[2][n]*y[n] ;
    yty += y[n]*y[n] ;
}

for (i = 1; i <= 2; i++) {
    for (j = 1; j <= 2; j++) {
        for (n = 1; n <= line; n++) xtx[i][j] += xt[i][n]*x[n][j] ;
    }
}

xtxdet = xtx[1][1]*xtx[2][2] - xtx[1][2]*xtx[2][1] ;
xtxinv[1][1] = xtx[2][2]/xtxdet ;
xtxinv[1][2] = -xtx[1][2]/xtxdet ;
xtxinv[2][1] = -xtx[2][1]/xtxdet ;
xtxinv[2][2] = xtx[1][1]/xtxdet ;

beta[1] = xtxinv[1][1]*xty[1] + xtxinv[1][2]*xty[2] ;
beta[2] = xtxinv[2][1]*xty[1] + xtxinv[2][2]*xty[2] ;

printf("\n beta[1] = %f, beta[2] = %f.", beta[1], beta[2]) ;

sse = yty - (beta[1]*xty[1]+beta[2]*xty[2]) ;
rmse = sqrt(sse/(line - 2)) ;

/* Reads test data set for screening */

n = 1 ;

```

```

while((fgets(s, 100, ifpt) != NULL) && (n <= maxline)) {
    sscanf(s, "%lf%lf%lf%lf%lf%lf%lf%lf%lf%lf", &test[n][1], &test[n][2],
        &test[n][3], &test[n][4], &test[n][5], &test[n][6], &test[n][7],
        &test[n][8], &test[n][9], &test[n][10]);
    test[n][7] = test[n][7]/100;
    n++;
}

```

```

linest = n - 1;

```

```

/* Performs screening of temperature data */

```

```

for (n = 1; n <= linest; n++) {
    if (test[n][10] > 0) {
        l[1] = 1;
        l[2] = test[n][10];
        ltxtxinv[1] = l[1]*xtxinv[1][1]+l[2]*xtxinv[2][1];
        ltxtxinv[2] = l[2]*xtxinv[1][2]+l[2]*xtxinv[2][2];
        lxtxl = ltxtxinv[1]*l[1] + ltxtxinv[2]*l[2];

        utl = (beta[1]+test[n][10]*beta[2])+3.09*rmse*sqrt(1+ lxtxl);
        ltl = (beta[1]+test[n][10]*beta[2])-3.09*rmse*sqrt(1+ lxtxl);
        if ((test[n][9] < ltl) || (test[n][9] > utl))
            test[n][9] = beta[1]+test[n][10]*beta[2];
    }
}

```

```

n = 1;
wdobst = 1;
weobst = 1;
while (n <= linest) {
    decimal = test[n][6];
    day = (int) (decimal + 3);
    dow = (day % 7);
    if ((dow == 1) || (dow == 0)) {
        for(i = 1; i <= 10; i++) wetest[weobst][i] = test[n][i];
        weobst++;
    }
    else {
        for(i = 1; i <= 10; i++) wdtest[wdobst][i] = test[n][i];
        wdobst++;
    }
}

```



```

    }
    n++;
  }

wdobst-- ;
weobst-- ;

/*****
*****
* DATA-SCREENING STARTS HERE ! FIRST, TEMPERATURE DATA IS
SCREENED AND *
* REPLACED, IF NECESSARY BY NWS DATA. THEN THE ENERGY DATA IS
SCREENED. *
*****
*****/

/* weekday energy data is screened now and printed to a file */

for(i = 1; i <= wdobst; i++) {
  lwd[i][1] = 1 ;
  lwd[i][2] = wdtest[i][9] ;
  lwd[i][3] = sin((2*3.14/80)*(wdtest[i][9]-20)) ;
  lwd[i][4] = lwd[i][3]*sin((2*3.14/24)*(wdtest[i][7])) ;
  lwd[i][5] = wdtest[i][9]*cos((2*3.14/24)*(wdtest[i][7])) ;

  predwd[i] = 0 ;
  for (j = 1; j <= 5; j++) {
    ltwd[j][i] = lwd[i][j] ;
    predwd[i] += betawd[j]*lwd[i][j] ;
    lttxwd[i][j] = 0 ;
    for (k = 1; k <= 5; k++) {
      lttxwd[i][j] += ltwd[k][i]*xtxinvw[k][j] ;
    }
  }

  lttxlwd[i] = 0 ;
  for (k = 1; k <= 5; k++) lttxlwd[i] += lttxwd[i][k]*ltwd[k][i] ;

```

```

    uplwd = predwd[i] + 3.09*rmsewd*sqrt(1+ltxtlwd[i]);
    lplwd = predwd[i] - 3.09*rmsewd*sqrt(1+ltxtlwd[i]);

    if ((wdtest[i][8] <= 0) || (wdtest[i][8] < lplwd) || (wdtest[i][8] > uplwd)) indwd[i]
= 1;
    else indwd[i] = 0;

wdtest1 = (int) wdtest[i][1];
wdtest2 = (int) wdtest[i][2];
wdtest3 = (int) wdtest[i][3];
wdtest4 = (int) wdtest[i][4];
wdtest7 = (int) wdtest[i][7];

fprintf(ofpwd, "%d %d %d %d %d %f %f %d\n",
        wdtest1, wdtest2, wdtest3, wdtest4, wdtest7, wdtest[i][8],
        wdtest[i][9], indwd[i]);
    }

/* weekend energy data is screened now and printed to a file */

for(i = 1; i <= weobst; i++) {

    lwe[i][1] = 1;
    lwe[i][2] = wetest[i][9];
    lwe[i][3] = cos((2*3.14/80)*(wetest[i][9] - 20));
    lwe[i][4] = sin((2*3.14/80)*(wetest[i][9] - 20))*sin((2*3.14/24)*(wetest[i][7]));
    lwe[i][5] = wetest[i][9]*sin((2*3.14/24)*(wetest[i][7]));
    lwe[i][6] = wetest[i][9]*cos((2*3.14/24)*(wetest[i][7]));

    predwe[i] = 0;
    for (j = 1; j <= 6; j++) {
        ltwe[j][i] = lwe[i][j];
        predwe[i] += betawe[j]*lwe[i][j];
        lttxwe[i][j] = 0;
        for (k = 1; k <= 6; k++) {
            lttxwe[i][j] += ltwe[k][i]*txinvwe[k][j];
        }
    }

    lttxlwe[i] = 0;
    for (k = 1; k <= 6; k++) lttxlwe[i] += lttxwe[i][k]*ltwe[k][i];

```

```
    uplwe = predwe[i] + 3.09*rmsewe*sqrt(1+ltxtxlwe[i]);
    lplwe = predwe[i] - 3.09*rmsewe*sqrt(1+ltxtxlwe[i]);

    if ((wetest[i][8] <= 0) || (wetest[i][8] < lplwe) || (wetest[i][8] > uplwe)) indwe[i]
= 1;
    else indwe[i] = 0 ;

wetest1 = (int) wetest[i][1];
wetest2 = (int) wetest[i][2];
wetest3 = (int) wetest[i][3];
wetest4 = (int) wetest[i][4];
wetest7 = (int) wetest[i][7];

fprintf (ofpwe, "%d %d %d %d %d %f %f %d\n",
        wetest1, wetest2, wetest3, wetest4, wetest7, wetest[i][8],
        wetest[i][9], indwe[i]);
        }

fclose(ifpi);
fclose(ifpt);
fclose(ofpwd);
fclose(ofpwe);

}
```

VITA

Amitava Dhar was born in Bagdah, India on March 2, 1964. He received a Bachelor of Mechanical Engineering degree from Jadavpur University at Calcutta, India in 1985, and an M.Tech. degree in Mechanical Engineering from Indian Institute of Technology, Kharagpur, India in 1986. He has worked in the fields of internal combustion engine, heating, ventilation, airconditioning and building energy analysis.

His permanent address is:

Amitava Dhar,
Motigunj, P.O. Bongaon,
24 Parganas (N), West Bengal, PIN 743 235,
India.